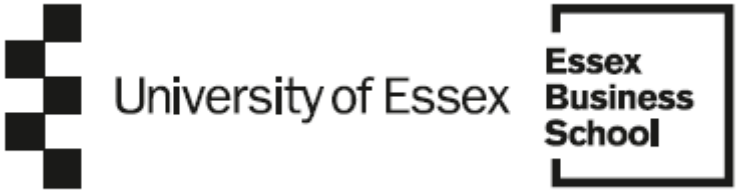

Essex Finance Centre

Working Paper Series

Working Paper No 87: 08-2024

"Bonferroni-Type Tests for Return Predictability with Possibly Trending Predictors"

"Sam Astill, David I. Harvey, Stephen J. Leybourne and A.M. Robert Taylor"

Essex Business School, University of Essex, Wivenhoe Park, Colchester, CO4 3SQ
Web site: http://www.essex.ac.uk/ebs/

Bonferroni-Type Tests for Return Predictability with Possibly Trending Predictors*

Sam Astill[a], David I. Harvey[b], Stephen J. Leybourne[b] and A.M. Robert Taylor[a]

[a] Essex Business School, University of Essex

[b] Granger Centre for Time Series Econometrics and School of Economics, University of Nottingham

August 7, 2024

Abstract

The Bonferroni Q test of Campbell and Yogo (2006) is widely used in empirical studies investigating predictability in asset returns by strongly persistent and endogenous predictors. Its formulation, however, only allows for a constant mean in the predictor, seemingly at odds with many of the predictors used in practice. We establish the asymptotic size and local power properties of the Q test, and the corresponding Bonferroni t-test of Cavanagh, Elliott and Stock (1995), as operationalised for the constant mean case by Campbell and Yogo (2006), under a local-to-zero specification for a linear trend in the predictor, revealing that size and power depends on the magnitude of the trend for both. To rectify this we develop with-trend variants of the operational Bonferroni Q and t tests. However, where a trend is not present in the predictor we show that these tests lose (both finite sample and asymptotic local) power relative to the extant constant-only versions of the tests. In practice uncertainty will necessarily exist over whether a linear trend is genuinely present in the predictor or not. To deal with this, we also develop hybrid tests based on union-of-rejections and switching mechanisms to capitalise on the relative power advantages of the constant-only tests when a trend is absent (or very weak) and the with-trend tests otherwise. A further extension allows use of a conventional t-test where the predictor appears to be weakly persistent. We show that, overall, our recommended hybrid test can offer excellent size and power properties regardless of whether or not a linear trend is present in the predictor, or the predictor's degrees of persistence and endogeneity. An empirical application to an updated Welch and Goyal (2008) dataset illustrates the practical relevance of our new approach.

Keywords: predictive regression; linear trend; unknown regressor persistence; Bonferroni tests; hybrid tests; union of rejections.

JEL Classifications: C22; C12; G14.

*We are grateful to the Editor, Barbara Rossi, and two anonymous referees for their helpful and constructive comments. We also thank Motohiro Yogo for making his Gauss programs to implement the constant-only Bonferroni Q and t tests publicly available on his website. We thank participants at the 2022 NBER-NSF Time Series Conference held at Boston University for helpful comments and feedback. Taylor gratefully acknowledges financial support provided by the Economic and Social Research Council of the United Kingdom under research grant ES/R00496X/1. Address correspondence to: Robert Taylor, Essex Business School, University of Essex, Wivenhoe Park, Colchester, CO4 3SQ, UK. Email: robert.taylor@essex.ac.uk.

1 Introduction and Motivation

The predictability of asset returns has received a great deal of attention in both the finance and economics literature, leading to a large number of published studies examining whether the lagged values of various financial and macroeconomic variables have predictive power for returns. Candidate predictor variables considered have included valuation ratios such as the dividend-price or earnings-price ratio, the dividend yield, various interest rate measures, inflation, and industrial production. For early contributions see, *inter alia*, Fama (1981), Keim and Stambaugh (1986), Campbell (1987), Campbell and Shiller (1988a,b), and Fama and French (1988,1989).

A common feature of many predictors used in empirical studies is that they are highly persistent and endogenous, with a strong negative correlation found between the innovations to the returns and those driving the predictor; see, eg, Campbell and Yogo (2006) [CY] and Welch and Goyal (2008). Basing inference on conventional tests for such predictors can be misleading. CY show that comparing a conventional regression t-statistic, obtained from the linear predictive regression model with a constant and lagged putative predictor, which we denote as x_{t-1}, with slope coefficient β, with standard normal critical values (as would be appropriate in large samples if x_t was weakly stationary) leads to right-tail tests for $\beta = 0$ that are asymptotically oversized, with this oversize becoming increasingly severe the stronger the persistence or endogeneity of the predictor, other things equal.

As a result, predictability tests have been developed that are valid for use with strongly persistent and endogenous regressors. These include likelihood-based tests developed by Cavanagh, Elliott and Stock (1995) [CES], Lewellen (2004), CY and Jansson and Moreira (2006). These approaches explicitly model the predictor series x_t, as an autoregressive process with the dominant root given by $\rho = 1 + cT^{-1}$ where c is a finite constant and T the sample size. Of these, the Bonferroni Q test of CY has been widely adopted in the empirical literature. Other approaches based on instrumental variable estimation have also been proposed, including contributions by Kostakis *et al.* (2015) and Breitung and Demetrescu (2015). Regardless of the approach taken, a common feature of all of these papers is that their primary (or even exclusive) focus is on the constant-only tests, and the properties of these tests in the presence of a (neglected) trend in the predictor remain unestablished.

Assuming that the predictor only contains a deterministic constant would seem justified for some of the candidate predictors considered in previous empirical studies. Few, for example, would argue that for developed countries macroeconomic variables such as inflation or interest rates would likely contain deterministic elements other than a constant.

However, the same is not true for other variables that have been considered in the literature, and in many instances one cannot discount the possibility that a predictor variable may contain a deterministic linear trend. A key aim of this paper is to examine the impact that an omitted trend can have on extant tests for predictability, and to consider predictability tests that explicitly allow for the potential presence of a trend.

To that end, we develop with-trend variants of the Bonferroni Q and t tests operationalised in CY. The Bonferroni approach underpinning these, developed in CES, constructs an initial confidence interval for the dominant autoregressive root, ρ, in the predictor, by inverting a unit root test, then bases a confidence interval for the predictive regression coefficient on this initial confidence interval for ρ. It is well known that an omitted deterministic trend impacts the asymptotic distribution of constant-only unit root tests, see, e.g., Harvey *et al.* (2009), and we will show in section 4 that not allowing for a trend in the predictive regression test stage also impacts the limit distribution of the constant-only regression statistics on which the Bonferroni Q and t tests are based when a trend is present in the predictor. When the correlation between the innovations to the predictor and returns is negative both of these effects combined will be shown to lead the constant-only Bonferroni Q and t-tests to exhibit substantial asymptotic undersize when testing in the right tail, with a subsequent loss of power, and substantial asymptotic oversize when testing in the left tail. The with-trend Bonferroni procedures we consider are based on an initial confidence interval for ρ that uses a trend-augmented unit root test statistic, and a secondary confidence interval for the coefficient on the predictor from a trend-augmented predictive regression. As a result, these belong to the class of invariant tests whose associated test statistics are numerically invariant to linear translations of the form $x_t \mapsto x_t + a_0 + a_1 t$, for arbitrary constants a_0 and a_1; equivalently, they do not depend on the value of the coefficients on the constant (level) and linear trend terms in the DGP for the predictor.

In practice, however, uncertainty will necessarily exist over whether a linear trend is present in the predictor or not and so practitioners will be faced with the dilemma of whether to use the extant tests that do not allow for a trend or the modifications we suggest that do. To illustrate the difficulties this poses for practitioners, we now discuss two brief motivating empirical examples of testing for the predictability of returns, which form part of our wider empirical application in section 7. Specifically, consider Figure 1, panel (a) of which graphs the quarterly log Dividend-Price Ratio, and panel (b) the monthly Book-to-Market Value Ratio series, in each case with the linear trend line fitted by OLS to the data added. The former is one of the most widely explored predictors in applications of predictive regression methods to returns. The data we use are from an updated version of the Welch and Goyal (2008) dataset; see section 7 for a detailed description of the data.

Figure 1: Time-Series Plots of Dividend-Price Ratio and Book-to-Market Value Ratio

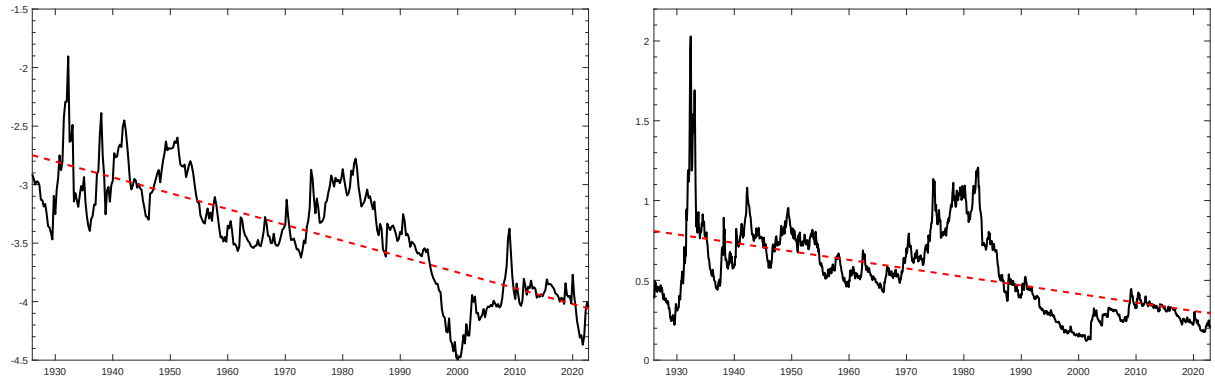

(a): Dividend-Price Ratio (b) Book-to-Market Value Ratio

Series: ——— , fitted trend: – –

Panels (a) and (b) in Figure 1 are both suggestive of a downward trend in the data, albeit rather weaker in the case of the Book-to-Market Value Ratio than the Dividend-Price Ratio. For the latter, the application of a variety of trend tests available in the literature that are designed to be robust to the order of integration of the series under test also uncovers some evidence of a trend. Of these tests (see Table 1 for details), the test of Perron and Yabu (2009) fails to reject the null hypothesis of no trend in the series, while the tests proposed in Harvey *et al.* (2007) and Bunzel and Vogelsang (2005) deliver statistically significant outcomes at either the 0.10- or 0.05-level. On balance, the evidence is suggestive of a linear trend in the Dividend-Price Ratio but it is by no means conclusive. For the Book-to-Market Value Ratio, only the Bunzel and Vogelsang (2005) test can reject the null hypothesis at the 0.10-level, suggesting that a trend may be present, but if so it is likely quite weak.

Using the lagged Dividend-Price Ratio as a predictor for the quarterly S&P500 value-weighted log-return, applying the standard constant-only Bonferroni Q test of CY, we find that the lower bound of the one-sided (upper tail) 95% confidence interval for β is -0.0134, such that we cannot reject the null hypothesis that $\beta = 0$ against the alternative of positive predictability, $\beta > 0$, at the 0.05-level. However, using the with-trend extension of the CY test that we propose in this paper yields a lower bound on the 95% confidence interval for β of 0.0117, thereby yielding statistically significant evidence at the 0.05-level that the Dividend-Price Ratio has positive predictive content for returns. When using the lagged Book-to-Market Value Ratio as a potential predictor for monthly returns, the standard constant-only Q test of CY gives a lower bound on the 95% confidence interval of 0.0017, while for the with-trend version of Q this lower bound is -0.0041. Consequently, the

constant-only CY test detects predictability at the 0.05-level while the with-trend version of the test fails to reject the null. Note that the estimated endogeneity correlation for the Dividend-Price Ratio is -0.951 and for the Book-to-Market Value Ratio it is -0.811, illustrating the strength of negative endogeneity correlation often observed with such predictors.

These two examples illustrate the dilemma the practitioner faces. In the first, by not allowing for the possibility of a trend in the price-dividend ratio one fails to find predictability that is otherwise found if the trend is accommodated. This outcome is consonant with our theoretical and numerical findings that an unmodelled trend in the predictor causes the right-tailed constant-only Q tests to exhibit much lower power than when no trend is present. The second example highlights a potential drawback of simply using a *conservative strategy*, whereby one always uses the with-trend version of the predictability test. In the unit root testing context it is known that while the inclusion of a trend in the unit root test regression renders inference invariant to linear translations of the data, doing so entails sizeable losses in (both asymptotic local and finite sample) power relative to their constant-only counterparts if no trend is present in the data generating process [DGP]; again, see Harvey *et al.* (2009). We observe a similar phenomenon in the predictive regression testing context, with the with-trend Bonferroni Q and t-tests displaying large power losses relative to the constant-only Bonferroni Q and t-tests when no trend is present in the predictor.

The examples also highlight that pre-testing for a trend (using a with-trend predictability test if the trend test rejected at a given significance level, and the constant-only version otherwise) would be unlikely to work well in practice, because in both examples the available trend tests are rather equivocal. Nonetheless, we show that, at least in the practically most interesting case of right-tailed testing with a negative endogeneity correlation (or, equivalently, left-tailed testing with a positive correlation), one can do better than the conservative approach discussed above. Here, exploiting the different tests' power rankings across no trend and trend environments, we discuss a union-of-rejections strategy that combines inference from both the constant-only and with-trend Bonferroni Q tests. This proposed union-of-rejections based procedure is asymptotically size controlled regardless of whether the predictor contains a trend or not, and is able to capitalise on the relative power advantages of the constant-only and with-trend tests in the no trend and trend scenarios, respectively, delivering attractive levels of power in both scenarios. For left (right) tailed testing when the correlation is negative (positive), the constant-only tests are over-sized (even asymptotically), and so a union-of-rejections approach would not deliver an asymptotically size-controlled procedure; here, we recommend simply using the with-trend Bonferroni Q test.

For right (left) tailed testing when the correlation is negative (positive), the basic union-of-rejections strategy is shown to be of most benefit when the predictor is strongly persistent

with $\rho = 1+cT^{-1}$ and c close to zero. For larger values of c the with-trend Bonferroni t-test displays higher power than the with-trend Bonferroni Q test and we therefore further develop our recommended hybrid test that switches into the with-trend Bonferroni t-test when there is evidence that c is not close to zero. Our final proposed hybrid procedure employs an additional switch, regardless of which tail is being tested in, into the conventional t-test when there is sufficient evidence that the predictor is weakly persistent. For the Dividend-Price Ratio and Book-to-Market Value Ratio, our recommended hybrid test gives lower bounds for the 95% confidence interval of 0.0066 and 0.0007, respectively, thereby rejecting the no predictability null in favour of positive predictability at the 0.05-level in both cases.

The paper is organised as follows. Section 2 outlines the predictive regression model we consider and the assumptions we will work under. Section 3 describes the constant-only Bonferroni Q and t-tests of CY and CES, respectively, and the modifications of these which allow for a trend in the predictor. Section 4 reports the limiting distributions of the predictive regression and unit root statistics used in the procedures outlined in this paper, and examines the relative local asymptotic power of the constant-only and with-trend Bonferroni type tests. Our proposed hybrid tests are outlined in section 5, and the local asymptotic power of these tests, as well as recommendations on which test to use in practice, are provided in section 6. An empirical exercise applying our new tests to an updated version of the Welch and Goyal (2008) dataset is discussed in section 7. Section 8 concludes. A supplementary appendix provides additional simulation and empirical results, together with mathematical proofs. In what follows "$\overset{w}{\to}$" and "$\overset{p}{\to}$" denote weak convergence of the associated probability measures and convergence in probability, respectively.

2 The Predictive Regression DGP

We consider the following predictive regression DGP

$$r_t = \alpha + \beta(x_{t-1} - \gamma(t-1)) + u_t, \qquad t = 2, ..., T \tag{1}$$

where r_t denotes the return on an asset in period t, and x_{t-1} denotes a putative predictor observed at time $t-1$. We assume the process for x_t is given by

$$x_t = \mu + \gamma t + w_t, \qquad t = 1, ..., T \tag{2}$$

$$w_t = \rho w_{t-1} + v_t, \qquad t = 2, ..., T \tag{3}$$

where w_1 is assumed to be an $O_p(1)$ random variable and where u_t and v_t are disturbances, formal assumptions on which are made below.

Remark 2.1. While we permit the potential presence of a linear trend in the predictor, x_t, through the parameter γ, note that (1) implies that only the detrended component of the predictor enters the DGP for returns, r_t. This assumption is made to rule out the possibility of a linear trend in r_t when $\beta \neq 0$ which is not empirically reasonable. ♢

We make the following assumptions concerning the disturbances u_t and v_t.

Assumption 1. *Assume that* $\psi(L)v_t = e_t$ *where* $\psi(L) := \sum_{i=0}^{p-1} \psi_i L^i$ *with* $\psi_0 = 1$ *and* $\psi(1) \neq 0$*, with the characteristic roots of* $\psi(L)$ *assumed to all be greater than one in absolute value. Assume that* $z_t := (u_t, e_t)'$ *is a bivariate martingale difference sequence [MDS] with respect to the natural filtration* $\mathcal{F}_t := \sigma\{z_s, s \leq t\}$ *satisfying the following conditions: (i)* $E[z_t z_t'] = \begin{bmatrix} \sigma_u^2 & \sigma_{ue} \\ \sigma_{ue} & \sigma_e^2 \end{bmatrix}$*, (ii)* $\sup_t E[u_t^4] < \infty$*, and (iii)* $\sup_t E[e_t^4] < \infty$*. For future reference, we define* $\omega_v^2 := \lim_{T\to\infty} T^{-1} E(\sum_{t=2}^{T} v_t)^2 = \sigma_e^2/\psi(1)^2$ *to be the long run variance of the error process* $\{v_t\}$*, and* $\delta := \sigma_{ue}/\sigma_u\sigma_e$ *as the correlation between the innovations* $\{u_t\}$ *and* $\{e_t\}$*.*

Remark 2.2. The conditions in Assumption 1 coincide with the most general set of assumptions considered by CY (see pages 56-57 of CY). The assumptions placed on z_t permit conditional heteroskedasticity in the innovations, but impose unconditional homoskedasticity. The MDS aspect of Assumption 1 implies the standard assumption made in this literature that the unpredictable component of returns, u_t, is serially uncorrelated. Assumption 1 allows the dynamics of the predictor variable to be captured by an $AR(p)$, with the degree of persistence of the predictor (strong or weak) controlled by the parameter ρ in (3), as will be formalised in Assumptions 2.1 and 2.2 below. ♢

As discussed in section 1, the focus of this paper is on testing the null hypothesis that $(r_t - \alpha)$ is a MDS and, hence, that r_t is not predictable by x_{t-1}; that is, $H_0 : \beta = 0$ in (1). We focus on developing tests that offer reliable levels of size and power regardless of whether a linear trend is present in the predictor variable x_t under different assumptions regarding the degree of persistence in the predictor. We therefore allow the predictor process $\{x_t\}$ in (2) to satisfy one of the following two assumptions.

Assumption 2. *The predictor* $\{x_t\}$ *in (2)-(3) satisfies one of the following conditions:*

1. $\{x_t\}$ *is strongly persistent, with* $\rho = \rho_T = 1 + cT^{-1}$*, where* c *is a finite constant.*
2. $\{x_t\}$ *is weakly persistent, with* ρ *fixed and bounded away from unity,* $|\rho| < 1$*.*

Remark 2.3. Under Assumption 2.1, x_t is a local-to-unity process whose persistence is controlled by the parameter c. For $c = 0$, x_t is a pure unit root process, while for $c < 0$, x_t is a near-integrated process. Finally, for $c > 0$, x_t is a (locally) explosive process. ♢

In order to facilitate an asymptotic power analysis in the strongly persistent case, we consider the following local-to-zero alternative hypothesis for β:

Assumption 3. *When the predictor $\{x_t\}$ is strongly persistent, the local alternative hypothesis is given by $H_b : \beta = \beta_T = b(\sigma_u/\omega_v)T^{-1}$, where b is a finite constant.*

Our analysis will consider both with-trend predictability tests that do not depend on the trend parameter γ, and also the corresponding constant-only versions of these tests that do depend on γ. To provide useful asymptotic theory for the latter in the case where the predictor x_t is strongly persistent (i.e. when Assumption 2.1 holds), at points below we will make use of a local-to-zero assumption for γ. We also consider in our analysis the impact of a fixed magnitude trend on the constant-only tests. We therefore assume that γ satisfies exactly one of the following two assumptions:

Assumption 4. *The trend coefficient γ in (1) and (2) is given by one of the following:*

1. *$\gamma = \gamma_T = \kappa\omega_v T^{-1/2}$, where κ is a finite constant.*
2. *$\gamma = \kappa\omega_v$, where κ is a finite non-zero constant.*

Remark 2.4. Under Assumptions 3 and 4.1, the scalings by T^{-1} and $T^{-1/2}$ in β_T and γ_T, respectively, provide the appropriate Pitman drifts when x_t is strongly persistent, while the scalings by σ_u/ω_v and ω_v are simply convenience measures to ensure that these nuisance parameters do not appear in the subsequent expressions for the limit distributions. For consistency, we also scale κ by ω_v in Assumption 4.2. ♢

3 Predictability Tests under Strong Persistence

In this section we outline the Bonferroni-based predictability Q and t-tests of CY and CES, respectively. We first review the extant constant-only versions of these, valid only if no trend is present in the predictor, x_t. We then discuss with-trend modifications of these tests which allow for the possibility that $\gamma \neq 0$, such that a trend might be present in x_t.

3.1 Bonferroni Q Tests

The Bonferroni Q test of CY makes use of an initial confidence interval for $\rho = 1 + cT^{-1}$, obtained by inverting a unit root test. CY consider only the possibility of a constant appearing in the predictor series; that is, they impose that $\gamma = 0$ in (2). For a given value of ρ, CY propose a confidence interval for β based on the following (infeasible) statistic

$$\begin{aligned} Q_\mu(\beta,\rho) &:= \frac{\sum_{t=2}^{T} x_{\mu,t-1}\left[r_t - \beta x_{t-1} - \frac{\sigma_{ue}}{\sigma_e\omega_v}(x_t - \rho x_{t-1})\right] + \frac{T}{2}\frac{\sigma_{ue}}{\sigma_e\omega_v}(\omega_v^2 - \sigma_v^2)}{\sqrt{\sigma_u^2(1-\delta^2)\sum_{t=2}^{T} x_{\mu,t-1}^2}} \\ &= Q_\mu(0,\rho) - \beta/(s_\mu\sqrt{1-\delta^2}) \end{aligned}$$

where $s_\mu^2 := \sigma_u^2 / \sum_{t=2}^T x_{\mu,t-1}^2$, σ_v^2 denotes the short run variance of v_t, and $x_{\mu,t-1}$, $t = 2, ..., T$, are the residuals from regressing x_{t-1} on a constant. The (infeasible) statistic $Q_\mu(0, \rho)$, hereafter denoted simply by $Q_\mu(\rho)$, represents a test statistic for the null hypothesis $\beta = 0$.

As we will quantify later, the behaviour of $Q_\mu(\rho)$, and the confidence interval based on this statistic, will depend on the trend coefficient γ when $\gamma \neq 0$. In view of this, we propose a variant of the Bonferroni Q test based on a statistic which does not depend on γ. To obtain such a variant, we replace $x_{\mu,t-1}$ with $x_{\tau,t-1}$, where $x_{\tau,t-1}$, $t = 2, ..., T$, denotes the residuals from a regression of x_{t-1} on a constant and linear trend. The modified statistic is then

$$\begin{aligned} Q_\tau(\beta, \rho) &:= \frac{\sum_{t=2}^T x_{\tau,t-1} \left[r_t - \beta x_{t-1} - \frac{\sigma_{ue}}{\sigma_e \omega_v}(x_t - \rho x_{t-1}) \right] + \frac{T}{2} \frac{\sigma_{ue}}{\sigma_e \omega_v}(\omega_v^2 - \sigma_v^2)}{\sqrt{\sigma_u^2 (1 - \delta^2) \sum_{t=2}^T x_{\tau,t-1}^2}} \\ &= Q_\tau(0, \rho) - \beta / (s_\tau \sqrt{1 - \delta^2}) \end{aligned}$$

where $s_\tau^2 := \sigma_u^2 / \sum_{t=2}^T x_{\tau,t-1}^2$. In what follows we denote $Q_\tau(0, \rho)$ simply by $Q_\tau(\rho)$.

Remark 3.1. As with equation (24) on page 57 of CY, the form of $Q_\mu(\rho)$ given above is, on omitting the serial correlation correction term, $\frac{T}{2} \frac{\sigma_{ue}}{\sigma_e \omega_v}(\omega_v^2 - \sigma_v^2)$, the (infeasible) t-ratio from regressing $r_t^* := r_t - (\sigma_{ue}/\sigma_e \omega_v)(x_t - \rho x_{t-1})$ on the de-meaned predictor $x_{\mu,t-1}$ (up to the factor of proportionality, $1/\sqrt{1 - \delta^2}$). Similarly, $Q_\tau(\rho)$ is (again omitting the serial correlation correction term) the t-ratio from regressing r_t^* on the de-trended predictor, $x_{\tau,t-1}$. Following the discussion on page 32 of CY, these t-ratios are, by the Frisch-Waugh Theorem, equivalent to the t-ratios on x_{t-1} obtained from the regression of r_t^* on: x_{t-1} and a constant, in the case of $Q_\mu(\rho)$; and on x_{t-1}, a constant, and linear trend, in the case of $Q_\tau(\rho)$. These two approaches to accounting for either the constant or the trend in the predictor therefore yield numerically identical statistics (noting that the serial correlation correction term added to the numerator is the same quantity in each case). ♢

Remark 3.2. The statistic $Q_\tau(\rho)$ is (exact) invariant to linear translations of the form $x_t \mapsto x_t + a_0 + a_1 t$ and $r_t \mapsto r_t + a_2 + a_3 t$, for arbitrary bounded constants a_i, $i = 0, ..., 3$. Equivalently, $Q_\tau(\rho)$ does not depend on the values of the nuisance parameters α, μ and γ in (1) and (2). Indeed, for the more general DGP $r_t = \alpha + \zeta t + \beta x_{t-1} + u_t$, $Q_\tau(\rho)$ would not depend on the values of α, μ, ζ or γ; cf. Remark 2.1. This invariance property can be straightforwardly established using standard properties of OLS estimators. In contrast, $Q_\mu(\rho)$ is invariant to additive translations of the form $x_t \mapsto x_t + a_0$ and $r_t \mapsto r_t + a_2$, but not to linear translations and so will depend on γ under DGP (1). ♢

Theorem 1 in section 4 establishes that, under Assumptions 1 and 2.1, $Q_\mu(\rho)$ admits a standard normal limiting distribution when $\beta = 0$, provided $\gamma = 0$. Theorem 1 also shows that the same holds for $Q_\tau(\rho)$ under these assumptions, but regardless of the value of γ. Therefore, when the predictor x_t is strongly persistent a $100(1-\alpha)\%$ confidence interval for β, $[\underline{\beta}_d^Q(\rho,\alpha), \overline{\beta}_d^Q(\rho,\alpha)]$ with $d = \mu$ denoting the constant-only case and $d = \tau$ the with-trend case, can be constructed as:

$$\underline{\beta}_d^Q(\rho,\alpha) = \{Q_d(\rho) - z_{\alpha/2}\} s_d \sqrt{1-\delta^2}, \quad \overline{\beta}_d^Q(\rho,\alpha) = \{Q_d(\rho) + z_{\alpha/2}\} s_d \sqrt{1-\delta^2} \tag{4}$$

with $z_{\alpha/2}$ denoting the $1-\alpha/2$ quantile of the standard normal distribution.

The confidence interval in (4), however, implicitly relies on knowledge of the value of $\rho = 1 + cT^{-1}$, where the parameter c cannot be consistently estimated. In the constant only case, $d = \mu$, CY propose obtaining a valid confidence interval for ρ by inverting the constant-only ADF-GLS test[1] of Elliott *et al.* (1996), denoted $DF\text{-}GLS_\mu$ henceforth, applied to the predictor x_t using pre-computed (asymptotic) confidence belts for the $DF\text{-}GLS_\mu$ test statistic. Denoting this confidence interval for ρ constructed at the α_1 level as $[\underline{\rho}_\mu(\alpha_1), \overline{\rho}_\mu(\alpha_1)]$ CY show that the confidence interval $[\underline{\beta}_\mu^Q(\overline{\rho}_\mu(\alpha_1),\alpha_2), \overline{\beta}_\mu^Q(\underline{\rho}_\mu(\alpha_1),\alpha_2)]$ has (asymptotic) coverage of at least $100(1-\alpha)\%$ where $\alpha = \alpha_1 + \alpha_2$.

In the case where $d = \tau$, such that a linear trend is permitted in the predictor, we use the obvious with-trend parallel of the approach taken in CY. Specifically, we obtain a confidence interval for ρ by inverting the with-trend ADF-GLS test of Elliott *et al.* (1996), henceforth denoted $DF\text{-}GLS_\tau$, applied to the predictor x_t using pre-computed (asymptotic) confidence belts for the $DF\text{-}GLS_\tau$ test statistic. Denoting this confidence interval for ρ constructed at the α_1 level as $[\underline{\rho}_\tau(\alpha_1), \overline{\rho}_\tau(\alpha_1)]$, the confidence interval $[\underline{\beta}_\tau^Q(\overline{\rho}_\tau(\alpha_1),\alpha_2), \overline{\beta}_\tau^Q(\underline{\rho}_\tau(\alpha_1),\alpha_2)]$ will have (asymptotic) coverage of at least $100(1-\alpha)\%$ where, again, $\alpha = \alpha_1 + \alpha_2$.

CY show that the confidence interval $[\underline{\beta}_\mu^Q(\overline{\rho}_\mu(\alpha_1),\alpha_2), \overline{\beta}_\mu^Q(\underline{\rho}_\mu(\alpha_1),\alpha_2)]$ suffers from over-coverage, with the asymptotic size of tests based on this confidence interval often well below $(\alpha/2)$, and we found the same for the confidence interval $[\underline{\beta}_\tau^Q(\overline{\rho}_\tau(\alpha_1),\alpha_2), \overline{\beta}_\tau^Q(\underline{\rho}_\tau(\alpha_1),\alpha_2)]$. Therefore, we follow CY and use a refinement where the significance level used to obtain the initial confidence interval for ρ is adapted to the upper and lower bounds separately, and also to the value of δ. Values of this significance level are chosen numerically to minimise over-coverage associated with the confidence interval for β, while ensuring that the asymptotic size of the overall Bonferroni test does not exceed a chosen level across

[1] In the context of both $DF\text{-}GLS_\mu$ and the $DF\text{-}GLS_\tau$ statistic defined below, denoting $\overline{c}$ as the parameter used for quasi-difference demeaning/detrending the data we follow Elliott *et al.* (1996) and set $\overline{c} = -7$ for $DF\text{-}GLS_\mu$ and $\overline{c} = -13.5$ for $DF\text{-}GLS_\tau$ in what follows. Owing to Assumption 1, the $DF\text{-}GLS_\mu$ and $DF\text{-}GLS_\tau$ unit root statistics will be calculated from ADF-type regressions which include $p-1$ lags.

a specified range of c. Denoting the chosen significance levels for the lower and upper confidence bounds for ρ by $\underline{\alpha}^{Q}_{1,d}$ and $\overline{\alpha}^{Q}_{1,d}$, respectively, the confidence interval for ρ can be written as $[\underline{\rho}_d(\underline{\alpha}^{Q}_{1,d}), \overline{\rho}_d(\overline{\alpha}^{Q}_{1,d})]$, and the resulting $100(1-\alpha_2)\%$ confidence interval for β is obtained as $[\underline{\beta}^{Q}_{d}(\overline{\rho}_d(\overline{\alpha}^{Q}_{1,d}), \alpha_2), \overline{\beta}^{Q}_{d}(\underline{\rho}_d(\underline{\alpha}^{Q}_{1,d}), \alpha_2)]$ where

$$\underline{\beta}^{Q}_{d}(\overline{\rho}_d(\overline{\alpha}^{Q}_{1,d}), \alpha_2) = \{Q_d(\overline{\rho}_d(\overline{\alpha}^{Q}_{1,d})) - z_{\alpha_2/2}\} s_d \sqrt{1-\delta^2}, \tag{5}$$

$$\overline{\beta}^{Q}_{d}(\underline{\rho}_d(\underline{\alpha}^{Q}_{1,d}), \alpha_2) = \{Q_d(\underline{\rho}_d(\underline{\alpha}^{Q}_{1,d})) + z_{\alpha_2/2}\} s_d \sqrt{1-\delta^2}. \tag{6}$$

For a given value of δ, CY propose selecting $\underline{\alpha}^{Q}_{1,d}$ and $\overline{\alpha}^{Q}_{1,d}$ such that one-sided tests for predictability constructed in this manner have an asymptotic size of exactly $\alpha_2/2$ for some value of c while remaining slightly undersized for other values of c. Consequently, two-sided tests will have size of at most α_2 across the specified range of c.

CY calibrate their constant-only test procedure by fixing $\alpha_2 = 0.1$ and considering $c \in [-50, 5]$ such that their resulting one-sided tests have a maximum (asymptotic) size of 0.05. The appropriate values of $\underline{\alpha}^{Q}_{1,\mu}$ and $\overline{\alpha}^{Q}_{1,\mu}$ are reported in Table 2 of CY, and are reproduced in Table S.1 in section S.3 of the supplementary appendix for convenience. We denote the predictability test based on this confidence interval as Q^{GLS}_{μ}. We follow the approach taken by CY for the trend-augmented version of the Bonferroni Q test, with the appropriate values of $\underline{\alpha}^{Q}_{1,\tau}$ and $\overline{\alpha}^{Q}_{1,\tau}$ chosen such that one-sided tests for predictability also have a maximum asymptotic size of 0.05 for $c \in [-50, 5]$, with the asymptotic size of the test computed using the limiting distributions we subsequently outline in section 4, and with these values of $\underline{\alpha}^{Q}_{1,\tau}$ and $\overline{\alpha}^{Q}_{1,\tau}$ also reported in Table S.1. We denote the predictability test based on this confidence interval as Q^{GLS}_{τ}.

Remark 3.3. The appropriate values of $\underline{\alpha}^{Q}_{1,d}$ and $\overline{\alpha}^{Q}_{1,d}$ reported in Table S.1 are only provided for $\delta < 0$. For $\delta > 0$, CY note that replacing x_t in (1) with $-x_t$ flips the sign of both β and δ (and, indeed, of γ). Therefore, an equivalent right (left) tailed test for predictability when $\delta > 0$ can be performed as a left (right) tailed test for predictability based on (1) with x_t replaced by $-x_t$ using the values of $\underline{\alpha}^{Q}_{1,d}$ and $\bar{\alpha}^{Q}_{1,d}$ appropriate for a negative value of δ. This also holds for the Bonferroni t test discussed below. ♢

3.2 Bonferroni t Tests

The second test procedure we consider is the Bonferroni t test based approach of CES. Where $\gamma = 0$ in (2), this is based on the following (infeasible) OLS statistic for testing the null $\beta = 0$, $t_\mu := \hat{\beta}_\mu / \sqrt{\sigma^2_u / \sum_{t=2}^{T} x^2_{\mu,t-1}}$, where $\hat{\beta}_\mu$ is obtained from the OLS estimated regression, $r_t = \hat{\alpha} + \hat{\beta}_\mu x_{t-1} + \hat{u}_t$. As with $Q_\mu(\beta, \rho)$, the behaviour of t_μ will be dependent

on the trend coefficient γ, when $\gamma \neq 0$. Accordingly, CES suggest a with-trend variant of the OLS t statistic that does not depend on γ, specifically

$$t_\tau := \frac{\hat{\beta}_\tau}{s.e.(\hat{\beta}_\tau)} \tag{7}$$

where $\hat{\beta}_\tau$ is obtained from the with-trend estimated OLS regression, $r_t = \hat{\alpha} + \hat{\gamma} t + \hat{\beta}_\tau x_{t-1} + \hat{u}_t$ and $s.e.(\hat{\beta}_\tau) = \sqrt{\sigma_u^2 / \sum_{t=2}^{T} x_{\tau,t-1}^2}$.

Under Assumptions 1 and 2.1 the limiting null distribution of t_d for $d = \mu$ or $d = \tau$ is a function of the unknown parameter c. CES overcome this issue by constructing a confidence interval for β based on an initial confidence interval for c, denoted $[\underline{c}(\alpha_1), \overline{c}(\alpha_1)]$ obtained by inverting the constant-only or with-trend ADF-OLS test (henceforth denoted $DF\text{-}OLS_\mu$ or $DF\text{-}OLS_\tau$ respectively) using pre-computed confidence belts.

Specifically, for a given value of δ, a $100(1-\alpha_2)\%$ confidence interval for β is obtained as $[\underline{\beta}_d^t(\overline{\alpha}_{1,d}^t, \alpha_2), \overline{\beta}_d^t(\underline{\alpha}_{1,d}^t, \alpha_2)]$, $d = \{\mu, \tau\}$, where

$$\underline{\beta}_d^t(\overline{\alpha}_1^{t,d}, \alpha_2) = \hat{\beta}_d - \left\{ \max_{\underline{c}(\overline{\alpha}_{1,d}^t) \leq c \leq \overline{c}(\overline{\alpha}_{1,d}^t)} cv_{1-\alpha_2/2,d}^c \right\} s_d, \tag{8}$$

$$\overline{\beta}_d^t(\underline{\alpha}_{1,d}^t, \alpha_2) = \hat{\beta}_d - \left\{ \min_{\underline{c}(\underline{\alpha}_{1,d}^t) \leq c \leq \overline{c}(\underline{\alpha}_{1,d}^t)} cv_{\alpha_2/2,d}^c \right\} s_d \tag{9}$$

and where $cv_{\eta,d}^c$ denotes the η-level critical value of the limiting null distribution of t_d for a given value of c. The significance levels $\underline{\alpha}_{1,d}^t$ and $\overline{\alpha}_{1,d}^t$ used to construct the one-sided confidence interval bounds for c, $\underline{c}(\overline{\alpha}_{1,d}^t)$, $\overline{c}(\overline{\alpha}_{1,d}^t)$, $\underline{c}(\underline{\alpha}_{1,d}^t)$ and $\overline{c}(\underline{\alpha}_{1,d}^t)$, are selected numerically to ensure that the implied one-sided tests for predictability constructed in this manner will have an asymptotic size of exactly $\alpha_2/2$ for some value of $c \in [-50, 5]$ while remaining slightly undersized for other values of c. For $\alpha_2 = 0.1$, the appropriate values of $\underline{\alpha}_{1,\mu}^t$ and $\overline{\alpha}_{1,\mu}^t$ are those given by CY, and are reported in Table S.1 in section S.3 of the supplementary appendix. We denote the predictability test based on this confidence interval as t_μ^{OLS}. The appropriate values of $\underline{\alpha}_{1,\tau}^t$ and $\overline{\alpha}_{1,\tau}^t$ in the with-trend case are also reported in Table S.1 and were found by directly simulating the limit distributions that we subsequently detail in section 4. We denote the predictability test based on this confidence interval as t_τ^{OLS}.

For full details on the practical implementation of the Q_μ^{GLS} and t_μ^{OLS} procedures, including OLS-based consistent estimation of the parameters σ_e, σ_u, σ_v, σ_{ue}, ω_v and δ, implementation of the $DF\text{-}GLS_\mu$ and $DF\text{-}OLS_\mu$ unit root tests, and the pre-computed confidence belts for the $DF\text{-}GLS_\mu$ and $DF\text{-}OLS_\mu$ test statistics, see CY, CES and the corre-

sponding supplementary material to CY.[2] In constructing our Q_τ^{GLS} and t_τ^{OLS} tests we follow exactly the same steps as CY outline for Q_μ^{GLS} and t_μ^{OLS}, augmenting any regression including only a constant with a linear trend, including the OLS regressions used to obtain estimates of the parameters σ_e, σ_u, σ_v, σ_{ue}, ω_v and δ. Pre-computed confidence belts for the $DF\text{-}GLS_\tau$ and $DF\text{-}OLS_\tau$ test statistics are included as part of the code used to implement all of the tests outlined in this paper which is available on request.

4 Asymptotic Behaviour of Tests under Strong Persistence

In this section we outline the asymptotic behaviour of the constant-only Q_μ^{GLS} and t_μ^{OLS} tests, and the with-trend Q_τ^{GLS} and t_τ^{OLS} tests, when Assumption 2.1 holds, i.e. the case where the predictor is a strongly persistent process and contains a trend. While the Q_τ^{GLS} and t_τ^{OLS} tests do not depend on the value of the trend coefficient γ, the Q_μ^{GLS} and t_μ^{OLS} tests do. For the latter statistics, in order to reflect in the asymptotic distribution theory the uncertainty that will exist in practice over whether the predictor contains a linear trend component, we will analyse their behaviour under the local-to-zero trend specified by Assumption 1. We will also report results for the case where γ is a fixed constant.

We begin by outlining the limiting distributions of the relevant test statistics under the local alternative $H_b : \beta = b(\sigma_u/\omega_v)T^{-1}$. We will then use these representations to numerically investigate the asymptotic size and power of the corresponding procedures both when a linear trend is present and when it is not. The following Theorem outlines the limiting distribution of the statistics, where in the context of Q_μ^{GLS} and Q_τ^{GLS}, $\tilde{\rho} = 1 + \tilde{c}T^{-1}$ for an arbitrary $\tilde{c}$.

Theorem 1. *Let data be generated according to (1)-(3). Let $W_1(s)$ and $W_2(s)$ be independent standard Brownian motion processes and let $W_{1c}(r) = \int_0^r e^{(r-s)c}dW_1(s)$. Under Assumptions 1 and 2.1, and under the local alternative specified in Assumption 3, the following large sample results hold, as $T \to \infty$:*

1. *Under Assumption 4.1:*

$$(i) \quad t_\mu \xrightarrow{w} \frac{b\left\{\kappa \int_0^1 rW_{1c}^\mu(r)dr + \int_0^1 W_{1c}^\mu(r)^2dr\right\} + \delta \int_0^1 W_{1c}^{\mu,\kappa}(r)dW_1(r)}{\sqrt{\int_0^1 W_{1c}^{\mu,\kappa}(r)^2dr}} + \sqrt{1-\delta^2}Z_\mu$$

$$(ii) \quad Q_\mu(\tilde{\rho}) \xrightarrow{w} \frac{b\left\{\kappa \int_0^1 rW_{1c}^\mu(r)dr + \int_0^1 W_{1c}^\mu(r)^2dr\right\} + \delta c\kappa \int_0^1 rW_{1c}^{\mu,\kappa}(r)dr + \delta(\tilde{c}-c)\int_0^1 W_{1c}^{\mu,\kappa}(r)^2dr}{\sqrt{1-\delta^2}\sqrt{\int_0^1 W_{1c}^{\mu,\kappa}(r)^2dr}} + Z_\mu$$

[2] The supplement to CY is available at https://scholar.harvard.edu/campbell/publications/implementing-econometric-methods-efficient-tests-stock-return-predictability-0. The confidence belts and also code for the procedures are available from Motohiro Yogo's personal website: https://sites.google.com/site/motohiroyogo/research/asset-pricing.

2. *Under Assumption 4.2:*

$$(i) \quad t_\mu \xrightarrow{w} b\sqrt{12}\int_0^1 rW_{1c}^\mu(r)dr + Z_\mu^* \qquad (ii) \quad T^{-1/2}Q_\mu(\tilde{\rho}) \xrightarrow{p} \frac{\delta\tilde{c}|\kappa|}{\sqrt{1-\delta^2}\sqrt{12}}$$

3. *Under Assumption 4.1 or 4.2:*

$$(i) \quad t_\tau \xrightarrow{w} b\sqrt{\int_0^1 W_{1c}^\tau(r)^2dr} + \delta\frac{\int_0^1 W_{1c}^\tau(r)dW_1(r)}{\sqrt{\int_0^1 W_{1c}^\tau(r)^2dr}} + \sqrt{1-\delta^2}Z_\tau$$

$$(ii) \quad Q_\tau(\tilde{\rho}) \xrightarrow{w} \frac{\{b+\delta(\tilde{c}-c)\}\sqrt{\int_0^1 W_{1c}^\tau(r)^2dr}}{\sqrt{1-\delta^2}} + Z_\tau$$

where $W_{1c}^\mu(r) := W_{1c}(r) - \int_0^1 W_{1c}(s)ds$, $W_{1c}^\tau(r) := W_{1c}^\mu(r) - 12(r-0.5)\int_0^1 (s-0.5)W_{1c}(s)ds$ *and* $W_{1c}^{\mu,\kappa}(r) := \kappa(r-0.5)+W_{1c}^\mu(r)$. *Finally,* $Z_\mu := \left(\int_0^1 W_{1c}^{\mu,\kappa}(r)^2dr\right)^{-1/2}\int_0^1 W_{1c}^{\mu,\kappa}(r)dW_2(r)$, $Z_\tau := \left(\int_0^1 W_{1c}^\tau(r)^2dr\right)^{-1/2}\int_0^1 W_{1c}^\tau(r)dW_2(r)$, *and* $Z_\mu^* := \sqrt{12}\left(\delta\int_0^1(r-0.5)dW_1(r) + \sqrt{1-\delta^2}\int_0^1(r-0.5)dW_2(r)\right)$, *are all standard normal random variables.*

Remark 4.1. Representations for the limiting null distributions of the statistics obtain on setting $b = 0$ in the expressions in Theorem 1. If $b = 0$ and $\tilde{c} = c$, then $Q_\tau(\tilde{\rho})$ is asymptotically distributed as a $N(0,1)$ random variable, as is t_τ if $b = \delta = 0$. Where Assumption 4.1 holds: if $\kappa = b = 0$ and $\tilde{c} = c$, then $Q_\mu(\tilde{\rho})$ is also asymptotically distributed as a $N(0,1)$ random variable; while if $\kappa = \delta = b = 0$ then t_μ is also asymptotically distributed as a $N(0,1)$ random variable. ♢

Remark 4.2. The representations in (i) and (ii) of Theorem 1.1 show that under Assumption 4.1 the limiting null and local alternative distributions of both t_μ and $Q_\mu(\tilde{\rho})$ depend on the value of the local trend parameter, κ. In the case where γ is a fixed non-zero constant, the representation in Theorem 1.2 (i) shows that t_μ has a well-defined limiting distribution that depends only on b, and which is standard normal when $b = 0$. In contrast, Theorem 1.2 (ii) shows that $Q_\mu(\tilde{\rho})$ will diverge to either plus or minus infinity (depending on the signs of δ and $\tilde{c}$) at rate $T^{1/2}$. In particular, if $\tilde{c}$ is positive then $Q_\mu(\tilde{\rho})$ will diverge to positive infinity if $\delta < 0$ and to negative infinity if $\delta > 0$. In contrast, from the representations in (i) and (ii) of Theorem 1.3 the limiting distributions of t_τ and $Q_\tau(\tilde{\rho})$ do not depend on the trend parameter γ, regardless of whether it is fixed or local-to-zero. ♢

Remark 4.3. It is straightforward but tedious to show that the representations in (i) and (ii) of Theorem 1.1 are unchanged on replacing κ with $-\kappa$. From Theorem 1.2, it is seen that the limiting distribution of $T^{-1/2}Q_\mu(\tilde{\rho})$ is also invariant to the sign of κ. ♢

Remark 4.4. While the results of Theorem 1 are given for the infeasible versions of t_μ, $Q_\mu(\tilde{\rho})$, t_τ and $Q_\tau(\tilde{\rho})$ that use the true values of σ_e, σ_u, σ_v, σ_{ue}, ω_v and δ, the same results obtain if these parameters are replaced by their estimated counterparts, using the estimates as described in the previous section. It is interesting to note that the estimates of these parameters used in the constant-only statistics t_μ and $Q_\mu(\tilde{\rho})$, which are based on OLS regressions that do not fit a trend term, remain consistent when a trend is present in the predictor. While this might be unsurprising in the case of a neglected local-to-zero trend, i.e. under Assumption 4.1, it is also true in the case of a neglected trend of fixed magnitude, i.e. under Assumption 4.2 - see section S.2 of the supplementary appendix for further details. In the case of the with-trend statistics t_τ and $Q_\tau(\tilde{\rho})$, the parameter estimates are obtained from regressions augmented with a trend term, and are therefore trivially seen to be consistent under both Assumptions 4.1 and 4.2. ♢

4.1 Local Asymptotic Power of t_d^{OLS} and Q_d^{GLS} tests

We now report results of a Monte Carlo simulation experiment examining the asymptotic power of the t_d^{OLS} and Q_d^{GLS} tests under the local alternative given in Assumption 3, when Assumptions 1 and 2.1 hold. For t_μ^{OLS} and Q_μ^{GLS}, Assumption 4.1 is also taken to hold. We will focus on testing for predictability when $\delta < 0$ as the size and power of right (left) tailed tests for predictability when $\delta > 0$ are identical to left (right) tailed tests for predictability when $\delta < 0$, for the reasons outlined in Remark 3.3.

Before proceeding we require the limiting distributions of the $DF\text{-}OLS_\mu$, $DF\text{-}GLS_\mu$, $DF\text{-}OLS_\tau$ and $DF\text{-}GLS_\tau$ test statistics used to construct the initial confidence interval for ρ for the t_μ^{OLS}, Q_μ^{GLS}, t_τ^{OLS} and Q_τ^{GLS} tests, respectively. Under the conditions of Theorem 1 (also imposing Assumption 4.1 in the case of $DF\text{-}OLS_\mu$ and $DF\text{-}GLS_\mu$), these limiting distributions are given by (see, for example, Harvey *et al.*, 2009):

$$DF\text{-}OLS_\mu \xrightarrow{w} \frac{(\kappa/2 + W_{1c}^\mu(1))^2 - (-\kappa/2 + W_{1c}^\mu(0))^2 - 1}{2\sqrt{\int_0^1 \{\kappa(r-1/2) + W_{1c}^\mu(r)\}^2 dr}} \tag{10}$$

$$DF\text{-}GLS_\mu \xrightarrow{w} \frac{(\kappa + W_{1c}(1))^2 - 1}{2\sqrt{\int_0^1 \{\kappa r + W_{1c}(r)\}^2 dr}} \tag{11}$$

$$DF\text{-}OLS_\tau \xrightarrow{w} \frac{W_{1c}^\tau(1)^2 - W_{1c}^\tau(0)^2 - 1}{2\sqrt{\int_0^1 W_{1c}^\tau(r)^2 dr}}, \qquad DF\text{-}GLS_\tau \xrightarrow{w} \frac{W_{1c}^{\tau,\bar{c}}(1)^2 - 1}{2\sqrt{\int_0^1 W_{1c}^{\tau,\bar{c}}(r)^2 dr}} \tag{12}$$

where $W_{1c}^{\tau,\bar{c}}(r) := W_{1c}(r) - r\left\{\bar{c}^* W_{1c}(1) + 3(1-\bar{c}^*)\int_0^1 r W_{1c}(r)dr\right\}$ and $\bar{c}^* := (1-\bar{c})/(1-\bar{c}+\bar{c}^2/3)$.

Remark 4.5. The representations in (10) and (11) show that under the local-to-zero trend specified by Assumption 4.1, the limiting distributions of $DF\text{-}OLS_\mu$ and $DF\text{-}GLS_\mu$ depend on κ. In contrast, (12) shows that the limiting distributions of $DF\text{-}OLS_\tau$ and $DF\text{-}GLS_\tau$ do not depend on the linear trend parameter γ, regardless of whether it is fixed or local-to-zero, i.e. under either of Assumptions 4.1 or 4.2. Harvey *et al.* (2009) show that the impact of a neglected local trend in $DF\text{-}OLS_\mu$ and $DF\text{-}GLS_\mu$ is to reduce both size and power of the unit root tests, implying a rightward shift in the tail of the distribution, resulting in a corresponding rightward shift in the confidence intervals for c. ♢

Remark 4.6. When a fixed magnitude trend is present in x_t, the result for t_μ given in Theorem 1.2 (i) implies that

$$\begin{aligned}
\frac{\underline{\beta}_\mu^t(\overline{\alpha}_1^{t,\mu},\alpha_2)}{s_\mu} &= b\sqrt{12}\int_0^1 rW_{1c}^\mu(r)dr + Z_\mu^* - \left\{\max_{\underline{c}(\overline{\alpha}_{1,\mu}^t)\le c\le\overline{c}(\overline{\alpha}_{1,\mu}^t)} cv_{1-\alpha_2/2,\mu}^c\right\} + o_p(1),\\
\frac{\overline{\beta}_\mu^t(\underline{\alpha}_{1,\mu}^t,\alpha_2)}{s_\mu} &= b\sqrt{12}\int_0^1 rW_{1c}^\mu(r)dr + Z_\mu^* - \left\{\min_{\underline{c}(\underline{\alpha}_{1,\mu}^t)\le c\le\overline{c}(\underline{\alpha}_{1,\mu}^t)} cv_{\alpha_2/2,\mu}^c\right\} + o_p(1).
\end{aligned}$$

Consequently, under the null H_0, where $b=0$, the confidence interval $[\underline{\beta}_\mu^t(\overline{\alpha}_{1,\mu}^t,\alpha_2), \overline{\beta}_\mu^t(\underline{\alpha}_{1,\mu}^t,\alpha_2)]$ will not have the desired asymptotic coverage. This arises because the critical value scaling terms $\max_{\underline{c}(\overline{\alpha}_{1,\mu}^t)\le c\le\overline{c}(\overline{\alpha}_{1,\mu}^t)} cv_{1-\alpha_2/2,\mu}^c$ and $\min_{\underline{c}(\underline{\alpha}_{1,\mu}^t)\le c\le\overline{c}(\underline{\alpha}_{1,\mu}^t)} cv_{\alpha_2/2,\mu}^c$, which depend on c and δ, are not appropriate for the standard normal distribution of Z_μ^*. Under the local alternative where $b\neq 0$, because $E(\int_0^1 rW_{1c}^\mu(r)dr)=0$, it is not possible to associate the upper or lower bound of the confidence interval with a particular sign of b. These two features render t_μ^{OLS} an unreliable procedure in the presence of a (neglected) fixed trend. ♢

Remark 4.7. Denoting $\overline{c}_\mu(\overline{\alpha}_{1,\mu}^Q) = T\{\overline{\rho}_\mu(\overline{\alpha}_{1,\mu}^Q)-1\}$ and $\underline{c}_\mu(\underline{\alpha}_{1,\mu}^Q) = T\{\underline{\rho}_\mu(\underline{\alpha}_{1,\mu}^Q)-1\}$, the result for $Q_\mu(\tilde{\rho})$ given in Theorem 1.2 (ii) implies that when a fixed trend is present in x_t and $\delta\neq 0$ then

$$\begin{aligned}
T^{-2}\underline{\beta}_\mu^Q(\overline{\rho}_\mu(\overline{\alpha}_{1,\mu}^Q),\alpha_2) &= T^{-1/2}Q_\mu(\overline{\rho}_\mu(\overline{\alpha}_{1,\mu}^Q))T^{-3/2}s_\mu\sqrt{1-\delta^2}+o_p(1)\\
&\xrightarrow{p} \delta\overline{c}_\mu(\overline{\alpha}_{1,\mu}^Q)|\kappa|/12,\\
T^{-2}\overline{\beta}_\mu^Q(\underline{\rho}_\mu(\underline{\alpha}_{1,\mu}^Q),\alpha_2) &= T^{-1/2}Q_\mu(\underline{\rho}_\mu(\underline{\alpha}_{1,\mu}^Q))T^{-3/2}s_\mu\sqrt{1-\delta^2}+o_p(1)\\
&\xrightarrow{p} \delta\underline{c}_\mu(\underline{\alpha}_{1,\mu}^Q)|\kappa|/12.
\end{aligned}$$

Harvey *et al.* (2009) show that, in the fixed trend case, $DF\text{-}GLS_\mu$ diverges to positive infinity at rate $T^{1/2}$. Inverting this test statistic results in the confidence interval bounds $\underline{c}_\mu(\underline{\alpha}^Q_{1,\mu})$ and $\overline{c}_\mu(\overline{\alpha}^Q_{1,\mu})$ being positive, and as a consequence, under the null or local alternative, both the lower and upper bounds of the confidence interval $[\underline{\beta}^Q_\mu(\overline{\rho}_\mu(\overline{\alpha}^Q_{1,\mu}),\alpha_2), \overline{\beta}^Q_\mu(\underline{\rho}_\mu(\underline{\alpha}^Q_{1,\mu}),\alpha_2)]$ will diverge to $+\infty$ when $\delta > 0$, and to $-\infty$ when $\delta < 0$. This implies that upper tailed Q^{GLS}_μ tests will have asymptotic size and local power of one (zero) when δ is positive (negative); similarly, lower tailed Q^{GLS}_μ tests will have asymptotic size and local power of one (zero) when δ is negative (positive). $\diamondsuit$

For clarity, we now outline how local asymptotic power is computed for the right-tailed tests. Left-tailed testing is handled similarly with obvious modifications. Here and throughout the paper, for the case of the constant-only tests we use the limiting representations that obtain under the local-to-zero trend specification imposed by Assumption 4.1.

For the Q^{GLS}_d, $d = \{\mu, \tau\}$, tests we first simulate draws from the limiting distribution of $DF\text{-}GLS_d$. These draws are then used to compute the upper bound of the confidence interval for c which we denote $\overline{c}(\overline{\alpha}^Q_{1,d})$ using pre-computed confidence belts implemented using the values of $\overline{\alpha}^Q_{1,d}$ appropriate for δ taken from Table S.1 in section S.3 of the supplementary appendix.[3] Note that this value of c also corresponds to the upper bound of the confidence interval for ρ, i.e. $\overline{\rho}^d(\bar{\alpha}^Q_{1,d}) = 1 + \overline{c}(\bar{\alpha}^Q_{1,d})T^{-1}$. Testing in the right tail is equivalent to determining whether $\underline{\beta}^Q_d(\overline{\rho}_d(\overline{\alpha}^Q_{1,d}),\alpha_2) > 0$, and the asymptotic local power function associated with $Q_d(\overline{\rho}_d(\bar{\alpha}^Q_{1,d}))$ is given by $E[\Phi(h_d(\overline{\alpha}^Q_{1,d},\alpha_2))]$ where $\Phi(.)$ denotes one minus the standard normal cdf and

$$h_d(\overline{\alpha}^Q_{1,d},\alpha_2) := z_{\alpha_2/2} - (Q^\infty_d - Z_d) \tag{13}$$

where Q^∞_d denotes the limiting distribution of $Q_d(\overline{\rho}_d(\bar{\alpha}^Q_{1,d}))$, and Z_d is as defined in Theorem 1. Next we simulate a draw from Q^∞_d and construct $h_d(\overline{\alpha}^Q_{1,d},\alpha_2)$ in (13). Finally, we evaluate whether a simulated draw from a Z_d exceeds this value of $h(\overline{\alpha}^Q_{1,d},\alpha_2)$. The limiting power is then obtained as the average of these exceedances across replications.

For t^{OLS}_d, in each simulation replication we first simulate a draw from the limiting distribution of $DF\text{-}OLS_d$, and then obtain $[\underline{c}(\overline{\alpha}^t_{1,d}), \overline{c}(\overline{\alpha}^t_{1,d})]$ using the corresponding pre-computed confidence belts for the values of $\overline{\alpha}^t_{1,d}$ appropriate for δ obtained from Table S.1. Then we simulate the limit of t_d using the results in Theorem 1, and compare this with the

[3]Here and throughout the paper results were obtained by direct simulation of the limiting distributions, with the Wiener processes approximated using NIID(0,1) random variates, and with the integrals approximated by normalized sums of 1,000 steps. All simulations were performed in Gauss 22.2 using 20,000 Monte Carlo replications. The confidence belts form part of the Gauss code used throughout the paper and are available on request.

critical value $\max_{\underline{c}(\overline{\alpha}^t_{1,d})\leq c\leq \overline{c}(\overline{\alpha}^t_{1,d})} cv^c_{1-\alpha_2/2,d}$. The limiting power is again calculated as the average of these exceedances across replications.

Asymptotic local power functions of infeasible versions of the t^{OLS}_d and Q^{GLS}_d tests, $d = \{\mu, \tau\}$, where the value of $\rho = 1 + cT^{-1}$ is assumed known to the practitioner, can also be computed. For these infeasible tests, no initial confidence interval for c is needed and the predictability statistics are computed using the true value of c. For the purposes of computing the asymptotic local power of these infeasible tests we simply need to replace the limit distribution of $Q_d(\overline{\rho}_d(\bar{\alpha}^Q_{1,d}))$ with the limit distribution $Q_d(\rho)$, where $\rho = 1 + cT^{-1}$, for the infeasible analogues of the Q^{GLS}_d tests, and to compare t_d to $cv^c_{\eta,d}$ for the infeasible analogues of the t^{OLS}_d tests. While these tests are infeasible in practice, even for large samples (c cannot be consistently estimated), they do provide a useful benchmark to compare the power of the feasible tests against. Figure S.1, which along with Figures S.2–S.15 can be found in section S.4 of the supplementary appendix, reports the asymptotic local power functions of feasible 0.05-level right-tailed t^{OLS}_μ and Q^{GLS}_μ tests together with their infeasible analogues for $\delta = -0.95$ (consonant with the estimated value of δ found for the dividend-price ratio in section 1) and $c = \{0, -2, -5, -10, -20, -50\}$ when there is no trend in the predictor, i.e. $\kappa = 0$. The results in this figure closely mirror those reported in Figure 3 on page 42 of CY. The feasible Bonferroni-based tests are shown to have reduced power relative to their infeasible counterparts. Examining the results for the with-trend tests in Figure S.2 we see a similar pattern, with the power of the feasible tests below their infeasible counterparts. We also observe by comparing the results in Figures S.1 and S.2 that the power of the infeasible constant-only tests is almost everywhere superior to their with-trend counterparts, other things held equal. Crucially, however, these results are for the case where there is no trend in the predictor, i.e. $\kappa = 0$. We will subsequently show that the power of right-tailed constant-only tests is severely diminished when the true value of κ is non-zero, with this drop in power more severe the larger is the value of κ. In contrast, the power of the with-trend versions of the tests do not depend on the value of κ. Therefore, if a practitioner is uncertain as to whether the predictor contains a linear trend no single deterministic specification for the tests is superior. Always performing constant-only tests would give superior power for κ close to or equal to zero, but far inferior power for larger values of κ. Likewise, while a conservative strategy where a trend is always accounted for would deliver excellent power for larger values of κ, this would be at the expense of far reduced power when κ is close to or equal to zero. This trade-off is the key motivation in our development of hybrid tests in section 5 designed to capture the power of constant-only tests when κ is close to zero and that of with-trend tests when κ is larger.

Figures S.3-S.10 report the local asymptotic power of right-tailed test for predictability for $c = \{0, -2, -5, -10, -20, -30, -40, -50\}$ for various values of the local trend parameter κ. We again consider the setting $\delta = -0.95$; corresponding results for $\delta = -0.75$ were found to be qualitatively similar, for both right-tailed and left-tailed tests, and can be found in section S.5 of the supplementary appendix. Note, these figures also include results for the hybrid U^{hyb} and S^{hyb} test procedures we propose in section 5 - these will be discussed later.

When $\kappa = 0$, so that no trend is present in the predictor (panel (a) of each figure), it is apparent that for small or moderate (negative) values of c the best power performance is offered by the Q_{μ}^{GLS} test, followed by the t_{μ}^{OLS} test. Also for this range of c, we observe that the Q_{τ}^{GLS} test has superior power to the t_{τ}^{OLS} test, although both have power that falls below the constant-only tests. These results when no trend is present are entirely expected, since the Q_{τ}^{GLS} and t_{τ}^{OLS} tests are based on regressions that unnecessarily include a trend.

As c becomes more negative, the Bonferroni t-tests start to display superior power to the Bonferroni Q tests, with t_{μ}^{OLS} displaying consistently superior power to Q_{μ}^{GLS} for $c \leq -30$. However, in this more negative c setting, the power differences between the competing tests are reduced compared to the small c cases, hence there is relatively little to choose between the constant-only procedures here. Overall, one would arguably wish to use the Q_{μ}^{GLS} test in the case of $\kappa = 0$ if allowing only for a constant in the predictor. For the trend-augmented tests there is little to choose between t_{τ}^{OLS} and Q_{τ}^{GLS} for $c = -30$, with t_{τ}^{OLS} offering superior power to Q_{τ}^{GLS} for lower values of b and vice-versa. For $c \leq -40$, however, t_{τ}^{OLS} clearly offers superior power to Q_{τ}^{GLS} across almost the full range of values of b. This relative power performance of the trend augmented tests is true for all values of κ given that the trend-augmented tests do not depend on the value of κ.

We now consider panels (b)-(f) of each figure, where κ is positive and increasing in magnitude. Here a different pattern emerges as the value of κ increases away from zero.[4] The asymptotic sizes of Q_{μ}^{GLS} and t_{μ}^{OLS} are now decreasing in κ, and as a consequence the powers of these tests are also decreasing in κ, with this effect more pronounced the more negative is the value of c. As previously discussed, the power functions of the Q_{τ}^{GLS} and t_{τ}^{OLS} tests do not depend on the value of κ, with the consequence that for larger values of κ these tests outperform their constant-only counterparts, with the Q_{τ}^{GLS} test becoming the best performing procedure for small or moderate c, and the t_{τ}^{OLS} test displaying the best power for the larger c. Hence for larger κ, one would wish to use the Q_{τ}^{GLS} test when the c values are small or moderate, and the t_{τ}^{OLS} test otherwise.

[4] We also generated results for negative values of κ and found them to be almost identical to those found for the corresponding positive values of κ, as would be expected from the discussion in Remark 4.3.

Figures S.11-S.15 report the local asymptotic power of left-tailed tests for predictability for $\delta = -0.95$ and $c = \{0, -2, -5, -10, -20\}$ for various values of κ. When $\kappa = 0$ the constant-only Q_{μ}^{GLS} and t_{μ}^{OLS} tests again outperform their with-trend Q_{τ}^{GLS} and t_{τ}^{OLS} counterparts for a given $d \in \{\mu, \tau\}$, as expected. In the left-tailed testing environment it can also be seen that the range of values of c over which the Q_{d}^{GLS} tests display superior power to the t_{d}^{OLS} tests is smaller for a given $d \in \{\mu, \kappa\}$. There is little to choose between the t_{μ}^{OLS} and Q_{μ}^{GLS} tests for $c = -5$, but for $c \leq -10$ the t_{μ}^{OLS} test has superior power to Q_{μ}^{GLS}. Likewise, there is little to choose between the t_{τ}^{OLS} and Q_{τ}^{GLS} tests for $c = -10$, but for $c = -20$ the t_{τ}^{OLS} test has superior power to Q_{τ}^{GLS}. Additional results reported in section S.5 in the supplementary appendix show that the t_{d}^{OLS} tests continue to display superior power over the Q_{d}^{GLS} tests for $c < -20$. For $\kappa > 0$, however, the Q_{μ}^{GLS} and t_{μ}^{OLS} tests can suffer from substantial oversize, with the degree of this oversize increasing in κ and also as c becomes more negative. As such, the Q_{μ}^{GLS} and t_{μ}^{OLS} tests are inappropriate for testing for predictability in the left tail when $\delta < 0$ when uncertainty exists over the possible presence of a linear trend, and reliable inference can only be made using Q_{τ}^{GLS} or t_{τ}^{OLS}. Here we would ideally use Q_{τ}^{GLS} for small or moderate c, and t_{τ}^{OLS} otherwise.

The results in Figures S.3-S.15 show that no single test is best suited to testing for predictability when uncertainty exists over both the values of c and κ. Instead, each of Q_{μ}^{GLS}, Q_{τ}^{GLS} and t_{τ}^{OLS} provides the best overall power for certain combinations of these parameters. Given that neither c nor κ can be consistently estimated, in the following section we propose hybrid tests for predictability that use combinations of the Q_{μ}^{GLS}, Q_{τ}^{GLS} and t_{τ}^{OLS} tests to deliver both controlled size and good power across the parameter space.

5 Hybrid Tests for Predictability

Based on the results in section 4.1 we now propose tests for predictability when uncertainty exists over the possible presence of a linear trend in the predictor. We start with tests that are designed for strongly persistent predictors generated according to Assumption 2.1, motivated by the results of the previous section, before outlining how these can be modified to also allow for weakly stationary predictors generated according to Assumption 2.2.

We will outline our hybrid tests in what follows only for the case where $\delta < 0$. For $\delta > 0$, from the result in Remark 3.3, we may simply replace the predictor x_t in (1) with $-x_t$, thereby flipping the sign of δ such that our recommended procedures for negative values of δ which follow can then be applied. Given that this also flips the sign of β, for a right (left) tailed test for predictability one should perform a left (right) tailed test for predictability in the transformed predictive regression based on the predictor $-x_{t-1}$. So, for example, the right-tailed tests appropriate for $\delta < 0$ outlined in section 5.1 are also

recommended, on replacing x_{t-1} by $-x_{t-1}$ throughout, for use in the case where one wishes to perform left-tailed tests with $\delta > 0$. In practice, the true value of δ will be unknown, but the appropriate approach can be determined according to the sign of a consistent estimator of δ. Here we propose using the estimate of δ from the with-trend Bonferroni type test procedures, i.e. the sample correlation between $\hat{u}_t$ and $\hat{e}_t$, where $\hat{u}_t$ are the residuals from a regression of r_t on a constant, trend and x_{t-1} and $\hat{e}_t$ are the residuals from estimating an $AR(p)$ for the predictor variable allowing for a constant and trend.

5.1 Right-Tailed Tests when $\delta < 0$

The results in section 4.1 suggest that for strongly persistent predictors, with $\delta < 0$, when $\kappa = 0$ the constant-only Q_{μ}^{GLS} test outperforms its with-trend counterpart Q_{τ}^{GLS}, while for larger κ the converse is true. As such, when testing in the right-tail the first test procedure we propose is a Union-of-Rejections strategy in which we reject the null of $\beta = 0$ in favour of the alternative that $\beta > 0$ when either the Q_{μ}^{GLS} or Q_{τ}^{GLS} tests reject, with the aim of capturing the relative power advantages of Q_{μ}^{GLS} and Q_{τ}^{GLS} for different magnitudes of κ. Taking a simple union-of-rejections in this manner, however, will inevitably result in an overall test with asymptotic size in excess of $\alpha_2/2$, given that inference from two tests is being combined, each individually calibrated to have a maximum asymptotic size of $\alpha_2/2$. To ensure that the union-of-rejections strategy has a maximum asymptotic size of $\alpha_2/2$ we modify the significance levels at which the confidence intervals for ρ are constructed for both the $DF\text{-}GLS_{\mu}$ and $DF\text{-}GLS_{\tau}$ tests, as well as the significance level used to construct the confidence interval for β for a given value of ρ. Recalling that the lower bound of the confidence interval for ρ used for right-tailed testing for the Q_{d}^{GLS} test is given by $\underline{\beta}_{d}^{Q}(\overline{\rho}_{d}(\overline{\alpha}_{1,d}^{Q}), \alpha_2)$ our proposed union-of-rejections test, U, is given by

$$U: \text{ Reject } H_0 \text{ if } \underline{U} > 0 \tag{14}$$

where

$$\underline{U} := \max\left(\underline{\beta}_{\mu}^{Q}(\overline{\rho}_{\mu}(\xi\overline{\alpha}_{1,\mu}^{Q}), \xi\alpha_2), \underline{\beta}_{\tau}^{Q}(\overline{\rho}_{\tau}(\xi\overline{\alpha}_{1,\tau}^{Q}), \xi\alpha_2)\right) \tag{15}$$

with $\xi < 1$ a scaling parameter chosen such that, for a given value of δ, the asymptotic size of U is no greater than $\alpha_2/2$ for the same grid of values of c considered by CY, i.e. $c \in [-50, 5]$. The appropriate values of ξ that lead to a right-tailed test with maximum asymptotic size of 0.05 are reported in Table S.1 in section S.3 of the supplementary appendix.[5]

While the union-of-rejections strategy outlined above will be shown to capture the superior power of Q_{μ}^{GLS} when κ is small, and that of Q_{τ}^{GLS} for larger values of κ when c

[5] An immediate consequence of Remark 4.7 is that the maximum asymptotic size of U will also be maintained at 0.05 in the case where the trend coefficient, γ, in (1) is a fixed constant.

is small or moderate, it is apparent from the results reported in Figures S.3-S.10 that for the more negative values of c the power of both the Q_{μ}^{GLS} and Q_{τ}^{GLS} tests lag behind that of t_{τ}^{OLS}. As such, we consider an extra layer to our test procedure where for right-tailed tests the union-of-rejections test is employed when c is estimated to be "small", and the t_{τ}^{OLS} test is employed when c is estimated to be "large". To do so we propose using an estimate of c to choose which test to perform in practice. Specifically, we propose computing an estimate, $\hat{c}$, that is equal to the with-trend ADF-GLS normalised bias unit root test statistic, henceforth denoted $NB\text{-}GLS_{\tau}$. Specifically, $\hat{c} = NB\text{-}GLS_{\tau} := T\tilde{\phi}/(1 - \sum_{i=1}^{p-1} \tilde{\psi}_i)$, where $\tilde{\phi}$ and $\tilde{\psi}_i$, $i = 1, ..., p-1$ are obtained by OLS estimation of

$$\Delta\tilde{x}_t = \phi\tilde{x}_{t-1} + \sum\nolimits_{i=1}^{p-1} \psi_i \Delta\tilde{x}_{t-i} + e_t$$

where, on setting $\bar{\rho}_T := 1 + \bar{c}T^{-1}$, $\tilde{x}_t := x_t - z_t'\tilde{\theta}$ with $\tilde{\theta}$ obtained from the quasi-differenced regression of $x_{\bar{c}} := (x_1, x_2 - \bar{\rho}_T x_1, ..., x_T - \bar{\rho}_T x_{T-1})'$ on $Z_{\bar{c}} := (z_1, z_2 - \bar{\rho}_T z_1, ..., z_T - \bar{\rho}_T z_{T-1})'$, where $z_t := (1, t)'$. The $NB\text{-}GLS_{\tau}$ statistic is closely related to $DF\text{-}GLS_{\tau}$, being obtained from the same regression, and in keeping with this link between the statistics, we use $\bar{c} = -13.5$; cf. footnote 1. Under Assumption 2.1, the limiting distribution of $\hat{c}$ is given by

$$\hat{c} \xrightarrow{w} \frac{W_{1c}^{\tau,\bar{c}}(1)^2 - 1}{2\int_0^1 W_{1c}^{\tau,\bar{c}}(r)^2 dr} \tag{16}$$

where $W_{1c}^{\tau,\bar{c}}$ is as previously defined under equation (12). While it is clear that $\hat{c}$ is not a consistent estimate of c, a near monotonic relationship nonetheless exists between the expected value of the limiting distribution of $\hat{c}$ and the true value of c. We therefore propose a cut-off rule where we employ the U test for $\hat{c} \geq c_R$, but switch to the t_{τ}^{OLS} test for $\hat{c} < c_R$ for some cut-off point c_R (R denoting right-tailed). Formally, our second proposed testing procedure, S, is therefore given by:

$$S: \text{ Reject } H_0 \text{ if } \underline{US} > 0 \tag{17}$$

where

$$\underline{US} := \mathbb{I}(\hat{c} \geq c_R)\underline{U} + \mathbb{I}(\hat{c} < c_R)\underline{\beta}_{\tau}^{t}(\overline{\alpha}_{1,\tau}^{t}, \alpha_2). \tag{18}$$

and where $\mathbb{I}(.)$ denotes the indicator function equal to 1 (0) when its argument is true (false). Our choice of the cut-off value c_R to use in practice is motivated by the asymptotic local power functions in Figures S.3-S.10 and the associated discussion in section 4.1. We found through extensive Monte Carlo simulation that the choice of $c_R = -35$ gave an overall test for predictability with the best overall power properties, tracking the power of U for small c and that of t_{τ}^{OLS} for large c. We also found that using the existing calibration

for U and t_τ^{OLS} led to S maintaining a maximum asymptotic size of 0.05 for $c \in [-50, 5]$, so no further calibration was required for this particular test.

5.2 Left-Tailed Tests when $\delta < 0$

We now turn our attention to left-tailed tests when $\delta < 0$ and Assumption 2.1 holds. We propose a simpler strategy for left-tailed tests as the asymptotic oversize of Q_μ^{GLS} and t_μ^{OLS} when $\kappa \neq 0$ prevents the implementation of an asymptotically size-controlled union-of-rejections procedure, such as that proposed in section 5.1, as this relies on the constituent tests being (asymptotically) correctly sized or undersized both when $\kappa = 0$ and when $\kappa \neq 0$. The appropriate simplification for the U procedure is then to just use Q_τ^{GLS}, which recalling section 3, entails rejecting the null of no predictability if $\overline{\beta}_d^Q(\underline{\rho}_d(\underline{\alpha}_{1,d}^Q), \alpha_2) < 0$.

Examining the relative power of Q_τ^{GLS} and t_τ^{OLS} in Figures S.11-S.15 it is immediately apparent that the Q_τ^{GLS} test only offers superior power to t_τ^{OLS} when c is small, with the power of t_τ^{OLS} above that of Q_τ^{GLS} for even modest values of c. As such, for the switching strategy S we propose a simpler version to that in section 5.1 where the Q_τ^{GLS} test is employed when $\hat{c} \geq c_L$ (L denoting left-tailed) and the t_τ^{OLS} test is used when $\hat{c} < c_L$. Specifically, for left-tailed tests the decision rule for our test procedure S is given by.

$$S: \text{ Reject } H_0 \text{ if } \overline{S} < 0 \tag{19}$$

where

$$\overline{S} := \mathbb{I}(\hat{c} \geq c_L)\overline{\beta}_\tau^Q(\underline{\rho}_\tau(\underline{\alpha}_{1,\tau}^Q), \alpha_2) + \mathbb{I}(\hat{c} < c_L)\overline{\beta}_\tau^t(\underline{\alpha}_{1,\tau}^t, \alpha_2). \tag{20}$$

Our choice of the cut-off value c_L to use in practice is, again, motivated by the local asymptotic power functions presented in Figures S.11-S.15 which, as discussed in section 4.1, show that the local asymptotic power of the Q_τ^{GLS} test is superior to that of t_τ^{OLS} for $c > -10$ but inferior for $c < -10$, with little to choose between the two tests for $c = -10$. We again used Monte Carlo simulation to determine an appropriate value for c_L and found a value of $c_L = -15$ led to a test with the best overall power properties. As was the case for right-tailed testing, we found that the maximum asymptotic size of S was still maximised at 0.05 for $c \in [-50, 5]$ when testing in the left tail, so no further calibration was required.

5.3 Dealing with Weakly Persistent Predictors

The U and S tests outlined in sections 5.1 and 5.2 are constructed under the assumption that the predictor is strongly persistent. When Assumption 2.2 holds, such that the predictor is weakly persistent, the Q_d^{GLS} and t_d^{OLS} tests, and hence the U and S tests, are asymptotically invalid. In contrast, under Assumption 2.2 a "conventional" OLS t-test, which

compares the OLS t-statistic t_τ of (7) with standard normal critical values, is asymptotically valid and is optimal (among feasible tests) under Gaussianity, regardless of the value of δ; see Jansson and Moreira (2006,p.704).[6]

Based on these considerations, we propose an approach similar to that followed by Elliott *et al.* (2015) and Harvey *et al.* (2021), whereby we switch from the use of the U and S tests to a conventional t-test which compares t_τ of (7) with standard normal critical values, when there is sufficient evidence that the predictor is weakly persistent. We will use the with-trend variant of the ADF-OLS normalised bias statistic, $NB\text{-}OLS_\tau := T\hat{\phi}/(1-\sum_{i=1}^{p-1}\hat{\psi}_i)$, where $\hat{\phi}$ and $\hat{\psi}_i$, $i=1,...,p-1$ are obtained by OLS estimation of

$$\Delta x_t = \pi_0 + \pi_1 t + \phi x_{t-1} + \sum_{i=1}^{p-1}\psi_i \Delta x_{t-i} + e_t,$$

to determine whether the predictor is weakly persistent. We use the OLS variant of the normalised bias unit root statistic, rather than the GLS variant used to estimate c in section 5.1, because of its superior power properties for non-local departures from a unit root.

Under Assumption 2.1, $NB\text{-}OLS_\tau = O_p(1)$, while under Assumption 2.2, $NB\text{-}OLS_\tau$ diverges to $-\infty$ at a rate faster than $T^{1/2}$. If we classify a predictor as weakly persistent when $NB\text{-}OLS_\tau < cv_{NB}$ then, for any fixed value of cv_{NB}, a predictor generated according to Assumption 2.2 will be classified as weakly persistent asymptotically with probability one. However, employing a fixed critical value can result in a strongly persistent predictor generated according to Assumption 2.1 being classified as weakly persistent with non-zero probability (the usual type I error). To address this issue we instead propose the use of a (sample size dependent) diverging critical value given by $cv_{NB} = -\upsilon T^{1/2}$ where $\upsilon > 0$ is a user-chosen tuning parameter, so that the conventional t-test is employed whenever $NB\text{-}OLS_\tau < -\upsilon T^{1/2}$. The divergence rate of $NB\text{-}OLS_\tau$ ensures that, in the limit, our Bonferroni-type U and S tests will always be performed when the predictor is strongly persistent, while the conventional t-test based on comparing t_τ of (7) with standard normal critical values will always be performed when the predictor is weakly persistent, regardless of the value of υ.

5.4 Overall Testing Approach

On the basis of sections 5.1-5.3 we are now in a position to present our overall hybrid testing procedures for predictability, which we denote by U^{hyb} and S^{hyb}. We outline these test

[6] In contrast to the case of strongly persistent predictors, for weakly stationary predictors there is no loss of asymptotic local power, relative to a test based on t_μ (where the trend regressor is omitted), from basing the conventional t-test on the with-trend t_τ statistic when the trend is irrelevant (see, e.g., Grenander and Rosenblatt, 1957). We therefore always base the conventional t-test on t_τ because, unlike t_μ, it does not depend on the linear trend coefficient, γ.

procedures for the case where $\delta < 0$. For $\delta > 0$, proceed as per the discussion at the start of section 5 substituting x_{t-1} for $-x_{t-1}$ throughout. The decision rules for one-sided tests performed at the $\alpha/2$ nominal asymptotic level can be written as follows, where we again denote the $(1-\alpha)$ quantile of the normal distribution as z_α. All confidence intervals are constructed so that the resultant one-sided tests for predictability have maximum asymptotic size of $\alpha/2$.

Decision Rule for Hybrid Test Procedures ($\delta < 0$)

- **Decision Rule for U^{hyb}:**
  - **Right-Tailed Tests:**
    - **If** $NB\text{-}OLS_\tau \geq -\upsilon T^{1/2}$**: Reject** H_0 **if** $\underline{U} > 0$
    - **If** $NB\text{-}OLS_\tau < -\upsilon T^{1/2}$**: Reject** H_0 **if** $\hat{\beta}_\tau - z_{\alpha/2} s.e.(\hat{\beta}_\tau) > 0$
  - **Left-Tailed Tests:**
    - **If** $NB\text{-}OLS_\tau \geq -\upsilon T^{1/2}$**: Reject** H_0 **if** $\overline{\beta}^Q_\tau(\underline{\rho}_\tau(\underline{\alpha}^Q_{1,\tau}), \alpha_2) < 0$
    - **If** $NB\text{-}OLS_\tau < -\upsilon T^{1/2}$**: Reject** H_0 **if** $\hat{\beta}_\tau + z_{\alpha/2} s.e.(\hat{\beta}_\tau) < 0$
- **Decision Rule for S^{hyb}:**
  - **Right-Tailed Tests:**
    - **If** $NB\text{-}OLS_\tau \geq -\upsilon T^{1/2}$**: Reject** H_0 **if** $\underline{US} > 0$
    - **If** $NB\text{-}OLS_\tau < -\upsilon T^{1/2}$**: Reject** H_0 **if** $\hat{\beta}_\tau - z_{\alpha/2} s.e.(\hat{\beta}_\tau) > 0$
  - **Left-Tailed Tests:**
    - **If** $NB\text{-}OLS_\tau \geq -\upsilon T^{1/2}$**: Reject** H_0 **if** $\overline{S} < 0$
    - **If** $NB\text{-}OLS_\tau < -\upsilon T^{1/2}$**: Reject** H_0 **if** $\hat{\beta}_\tau + z_{\alpha/2} s.e.(\hat{\beta}_\tau) < 0$

Remark 5.1. Although the definitions of the U^{hyb} and S^{hyb} procedures given above are framed in terms of one-sided tests for predictability, in principle each of these procedures can also be used to perform two-sided tests for predictability. For a given test, if the right tailed and left-tailed versions of the test are constructed such that they have asymptotic size no greater than $\alpha/2$, then combining inference from the two individual one-sided tests for predictability will lead to an overall two-sided test for predictability that will have asymptotic size no greater than α. ♢

6 Local Asymptotic Power of Hybrid Tests

We now return to Figures S.3-S.10 to assess the power of our proposed U^{hyb} and S^{hyb} test procedures, concentrating first on right-tailed tests for predictability.

On examining Figures S.3-S.7 we see that when c is small or moderate, the powers of our hybrid U^{hyb} and S^{hyb} tests essentially coincide with each other, as for such values of

c, drawings from the limit distribution of $\hat{c}$ in (16) rarely fall below c_R. For small κ, the powers of U^{hyb} and S^{hyb} lie between those of the Q_μ^{GLS} and Q_τ^{GLS} tests, as expected, but it can be seen that the U^{hyb} and S^{hyb} power profiles are reasonably close to that of the best performing Q_μ^{GLS} test and often well in excess of that for Q_τ^{GLS}. As κ increases, Q_τ^{GLS} becomes the most powerful individual test, and here we see that the U^{hyb} and S^{hyb} powers now move towards the Q_τ^{GLS} power profile. The consequence of this is that the hybrid tests are always among the best performing tests, having power close to that of Q_μ^{GLS} when κ is close to or equal to zero, and that of Q_τ^{GLS} for larger values of κ.

We next examine Figures S.8-S.10 where c is large. When κ is small the power of the U^{hyb} test still tracks the power of the Q_μ^{GLS} test reasonably well, and for larger values of κ the power of U^{hyb} continues to track the power of the Q_τ^{GLS} test. However, for the larger c values we see that the power of U^{hyb} can lag behind that of the t_τ^{OLS} test regardless of the value of κ. For these larger c cases we see that the power of the S^{hyb} test now diverges from that of U^{hyb} since $\hat{c}$ is here much more likely to take a value below -35, causing S^{hyb} to switch into the t_τ^{OLS} test, more so as c becomes increasingly negative. The consequence is that the power of S^{hyb} is far superior to that of U^{hyb} for these values of c, and is almost identical to that of the best performing t_τ^{OLS} test for $c = \{-40, -50\}$.

We now turn our attention to Figures S.11-S.15 which present the performance of S^{hyb} when testing in the left tail. (Here, we recall that the U^{hyb} test reduces to Q_τ^{GLS} in the left tail under strong persistence.) The results show that for small c, $\hat{c}$ is almost never less than -15, hence the power of S^{hyb} coincides almost perfectly with that of Q_τ^{GLS}, which is the most powerful test in these scenarios that maintains size control across κ. As c becomes more negative, $\hat{c}$ increasingly drops below -15, with the consequence that inference for S^{hyb} increasingly becomes based on t_τ^{OLS}. As such, for large c the power of S^{hyb} more closely tracks that of t_τ^{OLS}, which is the best performing size-controlled test. As a consequence, the S^{hyb} test displays one of the best power profiles among size-controlled tests across all values of c, having power close to that of the Q_τ^{GLS} test for smaller c and close to that of t_τ^{OLS} for larger c. We note also that, by virtue of being constructed using only the Q_τ^{GLS} and t_τ^{OLS} tests, the S^{hyb} test also does not depend on the value of κ when testing in the left tail.

An additional consideration in evaluating the local asymptotic size and power of the tests is their behaviour when $c > 0$, such that the predictor series is locally explosive. In section S.5 of the supplementary appendix, we report additional results for the case $c = 2$, for both right-tailed and left-tailed testing. We find that in the right-tailed testing context, the best performing individual tests are Q_μ^{GLS} and t_μ^{OLS}, even when a large local trend is present (i.e. large κ), and the U^{hyb} and S^{hyb} procedures (which coincide here) track Q_μ^{GLS} fairly well across the different κ values considered. In the left-tailed testing scenario, of

the two individual tests that achieve size control across c, i.e. Q_τ^{GLS} and t_τ^{OLS}, we find that Q_τ^{GLS} provides the better power profile, as in the case of $c = 0$ and small negative c. Here, the S^{hyb} test has a power profile that always follows this better performing Q_τ^{GLS} test, offering an attractive power profile across κ. Overall, the newly proposed hybrid tests also perform well in the locally explosive context.

In summary, our proposed hybrid test procedures display excellent asymptotic size and power properties regardless of the values of c and κ. The S^{hyb} test, in particular, has a power profile that is always close to the best performing size-controlled test in each scenario.

Finite sample simulation results reported in section S.6 of the supplementary appendix show that the Q_τ^{GLS}, t_τ^{OLS}, U^{hyb} and S^{hyb} test procedures display excellent size control across a range of values of c and κ both when v_t in (3) is i.i.d. or serially correlated, with the only exception being Q_τ^{GLS} and U^{hyb} which display significant oversize for larger negative values of c. The oversize for Q_τ^{GLS} for less persistent predictors is expected given that this test is asymptotically invalid for weakly stationary predictors, while the oversize for U^{hyb} in this region arises from use of Q_τ^{GLS} through the union-of-rejections approach. Aside from this case, the relative power of the tests in finite samples is almost identical to that observed in the asymptotic power simulations, with the S^{hyb} test in particular displaying excellent power across the large range of simulation DGPs considered.

On the basis of our simulation results, we recommend basing inference on our proposed S^{hyb} predictability testing procedure as it has controlled size, and is always among the most powerful tests, over the full range of parameter settings considered.

7 Empirical Application

We report results of an empirical exercise applying the tests for predictability outlined in this paper to the US equity series analysed in Welch and Goyal (2008), using updated data at the annual, quarterly and monthly frequencies for the period 1926-2022, yielding effective sample sizes $T = 96$, 387 and 1163, respectively. The data can be obtained from http://www.hec.unil.ch/agoyal/. The dependent variable, r_t, is the S&P500 value-weighted log-return. For x_t we consider thirteen candidate predictors: the log Dividend Payout Ratio, log Earnings-Price Ratio, log Dividend-Price Ratio, log Dividend Yield, Default Yield Spread, Long Term Yield, Default Return Spread, Net Equity Expansion, Inflation Rate, Treasury Bill Rate, Term Spread the Book-to-Market Value Ratio, and Stock Variance.

Data from the original Welch and Goyal (2008) dataset (and updates thereof) have been examined by many authors in the context of predictability testing; see, *inter alia*, Welch and Goyal (2008), Campbell and Thompson (2008), Neely *et al.* (2014), Kostakis *et al.* (2015), Breitung and Demetrescu (2015), Harvey *et al.* (2021) and Goyal *et al.* (2024), and

references therein. Overall these papers, all of which implicitly assume that the candidate predictors variables are free of any linear trend components, find only modest evidence in support of predictability. The first part of our empirical analysis is therefore to examine to what extent, if any, the presence of linear trends is a consideration for these predictors.

7.1 Robust Tests for a Linear Trend

For a given predictor, x_t, we do not take an *a priori* stance on whether its stochastic component, w_t in (3), is strongly persistent (as under Assumption 2.1) or weakly persistent (as under Assumption 2.2). Therefore, in trying to establish whether x_t contains a deterministic linear trend component, we need to employ trend detection tests that are valid under either strong or weak persistence, in the sense that they have robust size control under the null of no trend ($\gamma = 0$) and have non-trivial power against local trend alternatives. Several such tests are available in the literature. Here we consider the $t_\beta^{RQF}(MU)$ test of Perron and Yabu (2009) the z_λ, z_λ^{m1} and z_λ^{m2} tests of Harvey *et al.* (2007), and the *Dan-J* test of Bunzel and Vogelsang (2005). All of these tests are designed to have correct asymptotic size when x_t is either weakly persistent or follows an exact unit root process, while being conservative for local-to-unit root processes.[7]

We perform one-sided trend tests for all predictors using the recommended test settings, with the tail under test determined by the sign of the trend test statistic. Table 1 reports the p-value of the $t_\beta^{RQF}(MU)$ and z_λ tests (referenced to the standard normal distribution), as well as the significance level at which the remaining tests (which are designed to be performed only at discrete pre-assigned significance levels of their non-standard distributions) reject the no trend null hypothesis ($\gamma = 0$), for each predictor at each data frequency.

From the results reported in Table 1 it is seen that for each of six predictor series: Default Yield Spread, Long Term Yield, Default Return Spread, Inflation Rate, Treasury Bill Rate and Stock Variance, no trend is detected, regardless of data frequency. In contrast, for the four series: Dividend Payout Ratio, Dividend-Price Ratio, Dividend Yield and Net Equity Expansion, a significant linear trend is detected by one or more of the trend tests, regardless of the data frequency. Moreover, for each of these latter four series there appears

[7]By way of a brief description of these tests, the $t_\beta^{RQF}(MU)$ test is a quasi-feasible GLS test which employs a super-efficient estimate of ρ for the case when $\rho = 1$. The *Dan-J* trend test is based on a standard regression t-statistic for a linear trend multiplied by a scaling factor that allows the limit critical values to be the same in the $|\rho| < 1$ and $\rho = 1$ cases for a given significance level. The z_λ test takes a weighted average of a regression t-statistic for a linear trend from a regression of the data in levels and a t-statistic for a constant from a regression of the data in first differences. The weight is shifted between the two t-statistics according to whether $|\rho| < 1$ or $\rho = 1$ so that the asymptotic null distribution of z_λ is standard normal in either case. Here z_λ^{m1} and z_λ^{m2} are modifications of z_λ designed to improve size when ρ is local to unity and have non-standard limit distributions.

to be generally substantial levels of agreement between the outcomes of the different trend tests. For the remaining three predictor series: Earnings-Price Ratio, Term Spread and Book-to-Market Value Ratio, the results of the trend tests are mixed, with one or more of the trend tests indicating the presence of a trend at some, but not all, data frequencies. In summary, there is statistically significant evidence of a linear trend being present in seven of the thirteen predictors considered.

We next examine to what extent the confidence intervals for the autoregressive parameters are affected by what is assumed about the trend component in the ADF-GLS tests.

7.2 GLS-Based Confidence Intervals for the Autoregressive Parameter

Table 1 also reports the values of the constant-only $DF\text{-}GLS_\mu$ and with-trend $DF\text{-}GLS_\tau$ unit root tests for each predictor x_t. The underlying ADF-GLS regressions were estimated with the number of lagged difference terms selected using the Bayes Information Criterion (BIC) with a maximum number of lagged differences of 4. For each of $DF\text{-}GLS_\mu$ and $DF\text{-}GLS_\tau$ we present the associated 95% confidence intervals for c, denoted c_μ and c_τ in the table, and the associated 95% confidence intervals for the autoregressive coefficient ρ, denoted ρ_μ and ρ_τ in the table. The two sets of confidence intervals are related by $\rho_d = 1 + c_d T^{-1}$, $d = \{\mu, \tau\}$.

Taking the leading case of Dividend Payout Ratio with annual data, here we saw very convincing evidence for the presence of a linear trend from all of the robust trend tests. The confidence interval for c based on $DF\text{-}GLS_\mu$ is $[-64.5, -25.8]$, compared with $[-101.2, -49.3]$ when the confidence interval is based on $DF\text{-}GLS_\tau$. Therefore, failure to account for the trend causes a very substantial rightward shift in this confidence interval for c. Equivalently, this is also seen in the confidence interval for ρ whereby we see the without-trend interval $[0.328, 0.731]$ is rightward shifted compared to the with-trend version $[-0.054, 0.486]$. In contrast, examining, for example, the Book-to-Market Value Ratio at the same annual frequency, no significant evidence for a trend was uncovered. Here the confidence intervals for c and ρ associated with $DF\text{-}GLS_\mu$ and $DF\text{-}GLS_\tau$ are very similar. Overall, we see that those series for which marked rightward shifts in the confidence intervals for c and ρ associated with $DF\text{-}GLS_\mu$ are seen, relative to those associated with $DF\text{-}GLS_\tau$, are those where the strongest evidence of a trend was found, while often those series for which little such rightward shift is evident are those where no evidence of a trend was found. This is the kind of behaviour we would have anticipated in view of the discussion in Remarks 4.5 and 4.7. A notable exception to this pattern seen for the Dividend Payout Ratio with monthly data. The majority of the robust trend tests suggest a linear trend is

present, but there is very little difference between the confidence intervals from $DF\text{-}GLS_\mu$ and $DF\text{-}GLS_\tau$. However, this is pretty much the only substantive exception of this type.

Having found evidence for the presence of trends in the majority of our predictor series, and seen the subsequent effect of these on the confidence intervals for the autoregressive parameter, we now examine the extent to which what is assumed about the trend component affects inference arising from the tests for return predictability for these data.

7.3 Predictability Tests

We now discuss the results of applying all the predictability tests considered in the paper: t_μ^{OLS}, Q_μ^{GLS}, t_τ^{OLS}, Q_τ^{GLS} and the hybrid procedures U^{hyb} and S^{hyb}. Campbell and Thompson (2008) find that imposing positive predictability (so that the sign of the predictor is imposed to be positive under the alternative) almost always improves the out-of-sample predictability obtained for the predictors considered for equity returns in Welch and Goyal (2008). Consequently, for all of the putative predictors (each of which is lagged one period in the predictive regressions) we conduct right-tailed tests for $H_0 : \beta = 0$ against $H_1 : \beta > 0$, at the 0.05 nominal significance level. All of the unit root tests utilised in the test procedures are again performed using BIC with a maximum of 4 lagged differences.

In order to perform 0.05-level right-tailed tests we compute the lower bound of the 95% one-sided (upper-tail) confidence interval for β, generically denoted $\underline{\beta}$, when $\hat{\delta} < 0$ (where $\hat{\delta}$ denotes the appropriate with-trend or without-trend estimate of δ), or when $\hat{\delta} > 0$ we multiply the predictor by -1 and compute $\underline{\beta}$ as -1 times the upper bound of the 95% one-sided confidence interval for β from the transformed data (cf. Remark 3.3). For the Q_μ^{GLS} and Q_τ^{GLS} tests this involves inverting the $DF\text{-}GLS_\mu$ and $DF\text{-}GLS_\tau$ tests, respectively, and computing an initial confidence interval for c using the significance levels appropriate for the value of $\hat{\delta}$ found in Table S.1 in section S.3 of the supplementary appendix, as discussed in section 3.1, and then computing the confidence interval for β according to (5)-(6). For the t_μ^{OLS} and t_τ^{OLS} tests this involves inverting the $DF\text{-}OLS_\mu$ and $DF\text{-}OLS_\tau$ tests, respectively, and computing an initial confidence interval for c using the significance levels appropriate for the value of $\hat{\delta}$ found in Table S.1 as discussed in section 3.2, and then computing the confidence interval for β according to (8)-(9). For the hybrid U^{hyb} test, when $\hat{\delta} < 0$, $\underline{\beta}$ is computed as the maximum value of $\underline{\beta}$ implied by the Q_μ^{GLS} and Q_τ^{GLS} tests when the significance levels used to construct the initial confidence interval c in these tests is scaled by the appropriate value of ξ reported in Table S.1,[8] whereas when $\hat{\delta} > 0$, $\underline{\beta}$ is simply the value of $\underline{\beta}$ implied by the Q_τ^{GLS} test. The value of $\underline{\beta}$ for the hybrid S^{hyb} test

[8] A specific worked example detailing how $\underline{\beta}$ is calculated in the context of the U^{hyb} test for the case of the quarterly log Dividend-Price ratio predictor is given in section S.3 in the supplementary appendix.

is computed in exactly the same manner as the U^{hyb} test, but where the value of $\underline{\beta}$ implied by the U^{hyb} test is replaced by that computed using the t_τ^{OLS} test for $\hat{c} < -35$ ($\hat{c} < -15$) when $\hat{\delta} < 0$ ($\hat{\delta} > 0$), where $\hat{c}$ is computed as the value of the $NB\text{-}GLS_\tau$ statistic; see section 5.1. Finally, in the calculation of the diverging critical value $cv_{NB} = -\upsilon T^{1/2}$ we set $\upsilon = 10$ such that our hybrid procedures U^{hyb} and S^{hyb} compute $\underline{\beta}$ using a standard confidence interval using standard normal critical values whenever $NB\text{-}OLS_\tau < -10T^{1/2}$ as we found this choice of υ delivered good finite sample performance across a wide range of DGPs in the Monte Carlo simulation results reported in section S.6 of the supplementary appendix.

The results are reported in Table 2. The first column of Table 2 reports the estimate of the correlation δ from the with-trend Bonferroni type test procedures.[9] Then, for each test we report the lower bound of the associated 95% one-sided confidence interval for β, $\underline{\beta}$.[10] We highlight any instances where this lower bound is greater than zero in bold, these corresponding to cases where the null of $\beta = 0$ is rejected in favour of the alternative that $\beta > 0$ at the 0.05-level. Finally, for the lower bound of β from the U^{hyb} and S^{hyb} tests we use the superscript ‡ to identify instances where these tests have switched into the conventional t-test for predictability, and for S^{hyb} we use the superscript † to denote instances where this test is basing inference on the Bonferroni t_τ^{OLS} test.

For the eight predictor series: Dividend Payout Ratio, Default Yield Spread, Long Term Yield, Net Equity Expansion, Inflation Rate, Treasury Bill Rate, Term Spread and Stock Variance, no evidence of predictability is found by any of the tests at any data frequency and so we will not discuss results for these predictors further. For the other five predictors, one or more of the tests does infer predictability so we concentrate our discussion around these.

For the Earnings-Price Ratio, as noted above, evidence for a linear trend is mixed across the different frequencies and tests considered. Interestingly, evidence for predictability is also mixed if we focus on the constant-only tests, with t_μ^{OLS} rejecting the null of no predictability for all frequencies, but Q_μ^{GLS} failing to reject at any frequency. In contrast, the with-trend tests Q_τ^{GLS} and t_τ^{OLS} both reject the null for all frequencies, as do the hybrid tests U^{hyb} and S^{hyb}. This pattern of results is in line with what might be expected from our earlier theoretical and simulation results if a modest trend is present and right-tailed predictability testing is conducted when the correlation is negative. Note that at

[9] The corresponding constant-only correlation estimates are very similar and hence not reported.

[10] When reporting our confidence intervals for β we follow CY and scale this confidence interval by $(\hat{\sigma}_e/\hat{\sigma}_u)$. In other words, we report the confidence interval for $\tilde{\beta} = (\sigma_e/\sigma_u)\beta$ instead of β. As discussed in CY, this scaling does not affect inference, but is a more natural way to report results for two reasons. First, $\tilde{\beta}$ can be interpreted as the coefficient in (1) when the innovations are normalised to have unit variance. Secondly, $\tilde{\beta}$ can be interpreted as the standard deviation of the change in expected returns relative to the standard deviation of the innovations to returns.

the quarterly and monthly frequencies, the S^{hyb} procedure switches out of the union of rejections statistic $\underline{U}$ and into the t_τ^{OLS} statistic (with Bonferroni critical values).

For the Dividend-Price Ratio, the Q_τ^{GLS}, U^{hyb} and S^{hyb} tests all reject the null of no predictability for annual and quarterly data, with t_τ^{OLS} also rejecting in the case of annual data. Neither of the constant-only tests t_μ^{OLS} and Q_μ^{GLS} reject the null for either frequency, and given very credible evidence of a linear trend is present at both of these frequencies, together with a large negative correlation, this suggests that an unmodelled trend in the predictor may be negatively impacting the power of the constant-only tests, with the trend-augmented and hybrid tests retaining power to find significant evidence of predictability. For monthly data, no tests reject the null, indicating no evidence of predictability.

In the case of the Dividend Yield predictor, which exhibits evidence of a trend at all frequencies, we again find that the constant-only tests fail to reject the null of no predictability, whilst the with-trend and hybrid tests all reject at all frequencies (note again that here S^{hyb} switches into Bonferroni t_τ^{OLS}). Once again it appears that a neglected trend affects the ability of the constant-only tests to detect predictability.

For the Default Return Spread, very little evidence of predictability is detected by any of the tests across the different frequencies, with a sole rejection by Q_μ^{GLS} for monthly data. No trends were detected for this predictor at any frequency, and the unit root statistics suggest that this series is weakly persistent, with the hybrid procedures U^{hyb} and S^{hyb} switching into the conventional t-test t_τ, which uses standard normal critical values. Given the evidence that this predictor is likely to be weakly persistent, it may be the case that the rejection from Q_μ^{GLS} is simply an artefact reflecting the oversize of this test for weakly persistent predictors.

Results for the Book-to-Market Value Ratio are mixed. At the annual frequency no evidence of a trend is found and the only test to reject is Q_μ^{GLS}, as might be expected if no trend is present and the predictive power of this series is weak. For quarterly data, again there is no evidence for a trend, and now both constant-only tests display evidence of predictability. In contrast, only one of the with-trend tests, t_τ^{OLS}, rejects, which could be indicative of with-trend tests having reduced power when accounting for a trend is not necessary. It is interesting to note that both hybrid tests reject the null of no predictability, again demonstrating their ability to reject when there is disagreement between the constituent tests. For monthly data, some weak evidence of a trend is now detected by one of the tests, and Q_μ^{GLS} rejects the null of no predictability, while t_μ^{OLS}, t_τ^{OLS} and Q_τ^{GLS} do not. Reassuringly, this more limited evidence for predictability, arising from just one of the constant-only tests, still translates into rejections by both hybrid procedures.

Overall, we conclude from our empirical application that where trends are identified in these predictor series, there is a distinct tendency for this to be associated with compro-

mised ability of the constant-only Bonferroni tests to infer predictability. In contrast, our proposed hybrid tests find evidence of predictability in many of these cases, highlighting the value of our procedures in detecting predictability when uncertainty exists regarding the presence of a linear trend in the predictor.

8 Conclusions

In this paper we have developed operational trend-augmented versions of the Bonferroni Q test of CY and the Bonferroni t-test of CES. We have shown that in the presence of an omitted trend in the predictor, when the endogeneity correlation $\delta < 0$ ($\delta > 0$) the constant-only Bonferroni Q and t-tests can be severely undersized when testing in the right (left) tail, displaying a subsequent lack of power, and severely oversized when testing in the left (right) tail. The trend augmented Bonferroni Q and t-tests, while displaying power below their constant-only counterparts when no trend is present, do not depend on whether or not a trend is present in the predictor. We subsequently proposed union-of-rejections type hybrid testing procedures that are able to capture the power of the constant-only Bonferroni Q test when the predictor admits only a deterministic constant, and the power of the trend-augmented Bonferroni Q and t-tests when a trend is present in the predictor, with S^{hyb} being our recommended testing procedure given that it has controlled size, and is always among the most powerful tests, over the full range of parameter settings considered. An empirical illustration using an updated version of the dataset of Welch and Goyal (2008) demonstrated that our proposed approach finds evidence of predictability in several instances where a trend appears to be present in the predictor where the constant-only Bonferroni Q and t-tests fail to reject, indicating that the presence of omitted trends may be negatively impacting the power of the constant-only tests in this commonly used dataset.

References

Breitung, J. and Demetrescu, M. (2015). Instrumental variable and variable addition based inference in predictive regressions. Journal of Econometrics 187, 358-375.

Bunzel, H. and Vogelsang, T.J. (2015). Powerful trend function tests that are robust to strong serial correlation, with an application to the Prebisch: Singer hypothesis. Journal of Business and Economic Statistics 23, 381-394.

Campbell, J. Y (1987). Stock returns and the term structure. Journal of Financial Economics 18, 373-399.

Campbell, J. Y. and Shiller, R.J. (1988a). Stock prices, earnings, and expected dividends. Journal of Finance 43, 661-676.

Campbell, J. Y. and Shiller, R.J. (1988b). The dividend-price ratio and expectations of future dividends and discount factors. Review of Financial Studies 1, 195-228.

Campbell, J. Y., and Thompson, S. B. (2008). Predicting excess stock returns out of sample: Can anything beat the historical average? Review of Financial Studies, 21, 1509–1531.

Campbell, J. Y. and Yogo, M. (2006). Efficient tests of stock return predictability. Journal of Financial Economics 81, 27-60.

Cavanagh, C. L., Elliott, G. and Stock, J.H. (1995). Inference in models with nearly integrated regressors. Econometric Theory 11, 1131-1147.

Elliott, G., Müller, U.K. and Watson, M.W. (2015). Nearly optimal tests when a nuisance parameter is present under the null hypothesis. Econometrica 83, 771-811.

Elliott, G., Rothenberg, T.J. and Stock, J.H. (1996). Efficient tests for an autoregressive unit root. Econometrica 64, 813-836.

Fama, E.F. (1981). Stock returns, real activity, inflation, and money. American Economic Review 71, 545-565.

Fama, E.F. and French (1988). Dividend yields and expected stock returns. Journal of Financial Economics 22, 3-24.

Fama, E.F. and French (1989). Business conditions and expected returns on stocks and bonds. Journal of Financial Economics 25, 23-49.

Goyal, A., Welch, I. and Zafirov, A. (2024). A comprehensive look at the empirical performance of equity premium prediction II. Forthcoming in Review of Financial Studies.

Grenander, U. and Rosenblatt, M. (1957). Statistical Analysis of Stationary Time Series. New York: Wiley.

Harvey, D.I., Leybourne, S.J. and Taylor, A.M.R. (2007). A simple, robust and powerful test of the trend hypothesis. Journal of Econometrics 141, 1302-1330.

Harvey, D.I., Leybourne, S.J. and Taylor, A.M.R. (2009). Unit root testing in practice: Dealing with uncertainty over the trend and initial condition. Econometric Theory 14, 587-636.

Harvey, D.I., Leybourne, S.J. and Taylor, A.M.R. (2021). Simple tests for stock return predictability with good size and power properties. Journal of Econometrics 224, 198-214.

Jansson, M. and M. J. Moreira (2006). Optimal inference in regression models with nearly integrated regressors. Econometrica 74, 681-714.

Keim, D.B. and Stambaugh, R.F. (1986). Predicting returns in the stock and bond markets. Journal of Financial Economics 17, 357-390.

Kostakis, A., Magdalinos, T. and Stamatogiannis, M.P. (2015). Robust econometric inference for stock return predictability. Review of Financial Studies 28, 1506-1553.

Lewellen, J. (2004). Predicting returns with financial ratios. Journal of Financial Economics 74, 209-235.

Neely, C. J., Rapach, D. E., Tu, J., and Zhou, G. (2014). Forecasting the equity risk premium: The role of technical indicators. Management Science, 60, 1772–1791.

Perron, P. and Yabu, T. (2009). Estimating deterministic trends with an integrated or stationary noise component. Journal of Econometrics 151, 56-69.

Welch, I. and Goyal, A. (2008). A comprehensive look at the empirical performance of equity premium prediction. Review of Financial Studies 21, 1455-1508.

Table 1: Trend Tests and Persistence Measures for Updated Welch and Goyal (2008) Dataset

Annual Data

Predictor	$p(t_\beta^{RQF})$	$p(Z_\lambda)$	Z_λ^{m1}	Z_λ^{m2}	$DAN\text{-}J$	$DF\text{-}GLS_\mu$	$DF\text{-}GLS_\tau$	95% CI: c_μ	95% CI: c_τ	95% CI: ρ_μ	95% CI: ρ_τ
Dividend Payout Ratio	**0.000**	**0.000**	***	***	***	-4.845	-6.085	[-64.5 , -25.8]	[-101.2 , -49.3]	[0.328 , 0.731]	[-0.054 , 0.486]
Earnings-Price Ratio	0.083	0.234				-3.130	-4.292	[-32.0 , -6.2]	[-53.6 , -16.5]	[0.667 , 0.936]	[0.442 , 0.828]
Dividend-Price Ratio	**0.000**	**0.010**	**	**	*	-1.669	-3.734	[-12.8 , 2.3]	[-41.7 , -8.9]	[0.867 , 1.024]	[0.565 , 0.907]
Dividend Yield	0.176	**0.026**	**	**	*	-0.610	-2.557	[-4.8 , 4.3]	[-21.7 , 2.9]	[0.950 , 1.044]	[0.774 , 1.030]
Default Yield Spread	0.358	0.457				-4.000	-4.086	[-47.2 , -15.0]	[-49.0 , -13.6]	[0.508 , 0.844]	[0.489 , 0.858]
Long Term Yield	0.495	0.493				-1.433	-1.459	[-10.5 , 3.0]	[-8.6 , 4.6]	[0.891 , 1.032]	[0.910 , 1.048]
Default Return Spread	0.398	0.202				-9.365	-9.688	[-187.0 , -115.6]	[-246.0 , -165.4]	[-0.968 , -0.217]	[-1.589 , -0.741]
Net Equity Expansion	**0.000**	**0.000**	**	**	**	-1.772	-5.792	[-13.9 , 2.0]	[-92.3 , -42.9]	[0.853 , 1.021]	[0.028 , 0.548]
Inflation Rate	0.275	0.272				-2.007	-2.146	[-16.5 , 1.1]	[-16.1 , 3.7]	[0.823 , 1.011]	[0.827 , 1.040]
Treasury Bill Rate	0.451	0.447				-2.329	-2.368	[-20.4 , -0.6]	[-19.0 , 3.2]	[0.788 , 0.994]	[0.802 , 1.033]
Term Spread	0.350	0.423				-4.043	-4.584	[-48.0 , -15.4]	[-60.3 , -20.9]	[0.500 , 0.839]	[0.372 , 0.782]
Book-to-Market Value Ratio	0.201	0.291				-2.420	-2.832	[-21.6 , -1.1]	[-25.8 , 2.3]	[0.775 , 0.988]	[0.731 , 1.024]
Stock Variance	0.249	0.468				-4.639	-4.709	[-60.0 , -22.9]	[-63.2 , -23.0]	[0.375 , 0.761]	[0.341 , 0.761]

Quarterly Data

Predictor	$p(t_\beta^{RQF})$	$p(Z_\lambda)$	Z_λ^{m1}	Z_λ^{m2}	$DAN\text{-}J$	$DF\text{-}GLS_\mu$	$DF\text{-}GLS_\tau$	95% CI: c_μ	95% CI: c_τ	95% CI: ρ_μ	95% CI: ρ_τ
Dividend Payout Ratio	**0.000**	**0.050**	**	**	***	-4.551	-7.015	[-58.2 , -21.8]	[-132.8 , -72.1]	[0.849 , 0.943]	[0.656 , 0.813]
Earnings-Price Ratio	**0.000**	0.260			*	-2.960	-4.844	[-29.3 , -4.9]	[-66.5 , -25.2]	[0.924 , 0.987]	[0.828 , 0.935]
Dividend-Price Ratio	0.224	**0.098**	**	**	**	-1.275	-3.608	[-9.2 , 3.4]	[-39.3 , -7.3]	[0.976 , 1.009]	[0.899 , 0.981]
Dividend Yield	0.259	0.131	*	*	*	-1.445	-3.394	[-10.6 , 3.0]	[-35.3 , -4.7]	[0.973 , 1.008]	[0.909 , 0.988]
Default Yield Spread	0.236	0.454				-3.500	-3.609	[-38.1 , -9.6]	[-39.3 , -7.3]	[0.901 , 0.975]	[0.898 , 0.981]
Long Term Yield	0.495	0.496				-1.491	-1.564	[-11.1 , 2.9]	[-9.6 , 4.5]	[0.971 , 1.007]	[0.975 , 1.012]
Default Return Spread	0.419	0.220				-21.091	-21.249	[-554.9 , -426.7]	[-750.3 , -677.7]	[-0.434 , -0.103]	[-0.939 , -0.751]
Net Equity Expansion	**0.000**	**0.002**	***	***	**	-1.329	-4.988	[-9.6 , 3.3]	[-70.2 , -27.7]	[0.975 , 1.009]	[0.815 , 0.927]
Inflation Rate	0.177	0.446				-4.239	-4.070	[-51.9 , -17.8]	[-48.7 , -13.4]	[0.865 , 0.954]	[0.873 , 0.965]
Treasury Bill Rate	0.463	0.468				-2.457	-2.501	[-22.1 , -1.3]	[-20.9 , 3.0]	[0.942 , 0.997]	[0.946 , 1.008]
Term Spread	0.110	0.454			*	-3.453	-4.389	[-37.3 , -9.1]	[-55.8 , -18.0]	[0.903 , 0.976]	[0.855 , 0.953]
Book-to-Market Value Ratio	0.409	0.376				-3.153	-3.491	[-32.4 , -6.4]	[-37.1 , -5.9]	[0.916 , 0.983]	[0.903 , 0.985]
Stock Variance	0.266	0.499				-6.450	-6.981	[-102.9 , -52.3]	[-131.6 , -71.2]	[0.733 , 0.865]	[0.659 , 0.816]

Monthly Data

Predictor	$p(t_\beta^{RQF})$	$p(Z_\lambda)$	Z_λ^{m1}	Z_λ^{m2}	$DAN\text{-}J$	$DF\text{-}GLS_\mu$	$DF\text{-}GLS_\tau$	95% CI: c_μ	95% CI: c_τ	95% CI: ρ_μ	95% CI: ρ_τ
Dividend Payout Ratio	0.456	**0.064**	**	***	***	-5.782	-5.743	[-86.2 , -40.4]	[-90.9 , -41.9]	[0.926 , 0.965]	[0.922 , 0.964]
Earnings-Price Ratio	0.361	0.370		**		-2.271	-4.410	[-19.6 , -0.2]	[-56.2 , -18.3]	[0.983 , 1.000]	[0.952 , 0.984]
Dividend-Price Ratio	0.259	0.241	*	**	*	-1.242	-3.209	[-8.9 , 3.5]	[-32.0 , -2.5]	[0.992 , 1.003]	[0.973 , 0.998]
Dividend Yield	0.240	0.229	*	**	*	-1.284	-3.249	[-9.3 , 3.4]	[-32.7 , -3.0]	[0.992 , 1.003]	[0.972 , 0.997]
Default Yield Spread	0.489	0.474				-3.650	-3.813	[-40.8 , -11.1]	[-43.3 , -10.0]	[0.965 , 0.990]	[0.963 , 0.991]
Long Term Yield	0.493	0.494				-1.347	-1.415	[-9.8 , 3.3]	[-8.2 , 4.7]	[0.992 , 1.003]	[0.993 , 1.004]
Default Return Spread	0.498	0.472				-30.547	-35.294	[-851.5 , -680.0]	[-1363.0 , -1300.0]	[0.268 , 0.415]	[-0.172 , -0.118]
Net Equity Expansion	**0.000**	**0.011**	***	***	**	-1.979	-4.173	[-16.1 , 1.2]	[-50.9 , -14.9]	[0.986 , 1.001]	[0.956 , 0.987]
Inflation Rate	0.188	0.484				-7.657	-9.595	[-135.8 , -76.4]	[-241.9 , -161.4]	[0.883 , 0.934]	[0.791 , 0.861]
Treasury Bill Rate	0.476	0.479				-2.357	-2.368	[-20.8 , -0.7]	[-19.0 , 3.2]	[0.982 , 0.999]	[0.984 , 1.003]
Term Spread	**0.005**	0.476				-3.997	-4.730	[-47.2 , -14.9]	[-63.8 , -23.3]	[0.959 , 0.987]	[0.945 , 0.980]
Book-to-Market Value Ratio	0.449	0.443			*	-2.254	-2.083	[-19.4 , -0.2]	[-15.4 , 3.8]	[0.983 , 1.000]	[0.987 , 1.003]
Stock Variance	0.221	0.498				-7.562	-7.998	[-133.2 , -74.6]	[-172.3 , -101.5]	[0.885 , 0.936]	[0.851 , 0.912]

Notes:
(i) The entries in the columns headed $p(t_\beta^{RQF})$ and $p(Z_\lambda)$ denote p-values for the t_β^{RQF} and Z_λ tests. Bold entries highlight p-values below 0.1.
(ii) For Z_λ^{m1}, Z_λ^{m2} and $DAN\text{-}J$, $*$ denotes rejection at the 0.10-level, $**$ denotes rejection at the 0.05-level, and $***$ denotes rejection at the 0.01-level.
(iii) $\rho_d = 1 + c_d T^{-1}$, $d = \{\mu, \tau\}$, represents the leading autoregressive parameter driving the predictor.

Table 2: Correlation Estimates, Lower Bounds of One-Sided 95% Confidence Intervals for β, and Normalised-Bias Statistics for Updated Welch and Goyal (2008) Dataset

Annual Data

		$\underline{\beta}$							
Predictor	$\hat{\delta}$	t_μ^{OLS}	Q_μ^{GLS}	t_τ^{OLS}	Q_τ^{GLS}	U^{hyb}	S^{hyb}	$NB\text{-}GLS_\tau$	$NB\text{-}OLS_\tau$
Dividend Payout Ratio	-0.366	-0.1693	-0.1416	-0.1676	-0.1315	-0.1556	-0.1676†	**-54.363**	-60.435
Earnings-Price Ratio	-0.261	**0.0036**	-0.0037	**0.0328**	**0.0486**	**0.0291**	**0.0291**	-31.513	-31.549
Dividend-Price Ratio	-0.843	-0.0628	-0.0454	**0.0092**	**0.0532**	**0.0381**	**0.0381**	-24.801	-26.528
Dividend Yield	0.118	-0.0001	-0.0003	**0.0985**	**0.0907**	**0.0907**	**0.0907**	-12.913	-13.522
Default Yield Spread	-0.646	-0.1379	-0.1105	-0.1844	-0.1389	-0.1290	-0.1290	-28.986	-30.718
Long Term Yield	-0.061	-0.0372	-0.0357	-0.0446	-0.0449	-0.0443	-0.0443	-4.530	-4.412
Default Return Spread	0.272	-0.2007	-0.2159	-0.1953	-0.3159	-0.2043‡	-0.2043‡	**-198.824**	**-245.534**
Net Equity Expansion	0.135	-0.3699	-0.3378	-0.3634	-0.3812	-0.3812	-0.3634†	**-68.659**	-73.124
Inflation Rate	-0.013	-0.0597	-0.0585	-0.0716	-0.0692	-0.0781	-0.0781	-11.231	-13.492
Treasury Bill Rate	0.053	-0.0684	-0.0719	-0.0728	-0.0753	-0.0753	-0.0753	-10.817	-10.868
Term Spread	-0.085	-0.0814	-0.0844	-0.0950	-0.0941	-0.1065	-0.0950†	**-36.378**	-38.281
Book-to-Market Value Ratio	-0.807	-0.0357	**0.0065**	-0.0228	-0.0152	-0.0057	-0.0057	-15.136	-20.757
Stock Variance	-0.448	-0.1428	-0.1205	-0.1500	-0.1369	-0.1413	-0.1500†	**-36.799**	-39.521

Quarterly Data

		$\underline{\beta}$							
Predictor	$\hat{\delta}$	t_μ^{OLS}	Q_μ^{GLS}	t_τ^{OLS}	Q_τ^{GLS}	U^{hyb}	S^{hyb}	$NB\text{-}GLS_\tau$	$NB\text{-}OLS_\tau$
Dividend Payout Ratio	-0.154	-0.0350	-0.0357	-0.0375	-0.0442	-0.0397	-0.0375†	**-99.545**	-139.120
Earnings-Price Ratio	-0.596	**0.0056**	-0.0145	**0.0124**	**0.0105**	**0.0063**	**0.0124**†	**-47.414**	-50.125
Dividend-Price Ratio	-0.951	-0.0146	-0.0134	-0.0059	**0.0117**	**0.0066**	**0.0066**	-25.323	-27.086
Dividend Yield	0.073	-0.0015	-0.0015	**0.0241**	**0.0230**	**0.0230**	**0.0241**†	**-22.500**	-26.390
Default Yield Spread	-0.507	-0.0281	-0.0253	-0.0438	-0.0323	-0.0308	-0.0308	-26.348	-26.832
Long Term Yield	-0.056	-0.0128	-0.0124	-0.0146	-0.0145	-0.0146	-0.0146	-5.160	-5.049
Default Return Spread	0.303	-0.1004	-0.1520	-0.0987	-0.3237	-0.1039‡	-0.1039‡	**-418.736**	**-430.409**
Net Equity Expansion	0.094	-0.0716	-0.0651	-0.0815	-0.0806	-0.0806	-0.0815†	**-62.271**	-72.145
Inflation Rate	0.013	-0.0732	-0.0709	-0.0767	-0.0744	-0.0744	-0.0767†	**-36.998**	-46.726
Treasury Bill Rate	-0.046	-0.0220	-0.0213	-0.0241	-0.0240	-0.0247	-0.0247	-13.245	-13.449
Term Spread	0.005	-0.0327	-0.0326	-0.0354	-0.0357	-0.0357	-0.0354†	**-45.802**	-53.015
Book-to-Market Value Ratio	-0.796	**0.0084**	**0.0058**	**0.0256**	-0.0013	**0.0025**	**0.0025**	-26.775	-43.187
Stock Variance	-0.384	-0.0643	-0.1039	-0.0643	-0.0874	-0.0971	-0.0643†	**-98.537**	-102.249

Monthly Data

		$\underline{\beta}$							
Predictor	$\hat{\delta}$	t_μ^{OLS}	Q_μ^{GLS}	t_τ^{OLS}	Q_τ^{GLS}	U^{hyb}	S^{hyb}	$NB\text{-}GLS_\tau$	$NB\text{-}OLS_\tau$
Dividend Payout Ratio	-0.057	-0.0064	-0.0065	-0.0073	-0.0080	-0.0071	-0.0073†	**-72.853**	-120.237
Earnings-Price Ratio	-0.798	**0.0015**	-0.0056	**0.0026**	**0.0028**	**0.0016**	**0.0026**†	**-39.697**	-40.377
Dividend-Price Ratio	-0.976	-0.0052	-0.0045	-0.0035	-0.0012	-0.0029	-0.0029	-20.699	-26.126
Dividend Yield	-0.062	-0.0003	-0.0002	**0.0088**	**0.0087**	**0.0073**	**0.0073**	-21.307	-26.552
Default Yield Spread	-0.249	-0.0094	-0.0090	-0.0118	-0.0098	-0.0106	-0.0106	-30.098	-30.531
Long Term Yield	-0.093	-0.0043	-0.0041	-0.0050	-0.0049	-0.0048	-0.0048	-4.308	-4.179
Default Return Spread	0.179	-0.0141	**0.0647**	-0.0138	-0.0235	-0.0155‡	-0.0155‡	**-1204.471**	**-1275.306**
Net Equity Expansion	-0.036	-0.0208	-0.0212	-0.0243	-0.0245	-0.0227	-0.0243†	**-35.012**	-37.824
Inflation Rate	0.033	-0.0648	-0.0560	-0.0667	-0.0626	-0.0626	-0.0667†	**-221.076**	-240.319
Treasury Bill Rate	-0.047	-0.0060	-0.0058	-0.0065	-0.0065	-0.0067	-0.0067	-11.334	-11.693
Term Spread	-0.005	-0.0089	-0.0089	-0.0100	-0.0098	-0.0110	-0.0100†	**-46.721**	-56.723
Book-to-Market Value Ratio	-0.811	-0.0019	**0.0017**	-0.0011	-0.0041	**0.0007**	**0.0007**	-9.055	-19.037
Stock Variance	-0.299	-0.0580	-0.1119	-0.0582	-0.1039	-0.1098	-0.0582†	**-154.848**	-181.770

Notes:
(i) $\hat{\delta} := \hat{\sigma}_{ue}/\hat{\sigma}_u\hat{\sigma}_e$ represents the estimated correlation between the innovations to returns, u_t, and the innovations to the predictor, e_t, when allowing for a linear trend in the predictor.
(ii) Bold entries in the $\underline{\beta}$ columns highlight cases where the null hypothesis of no predictability can be rejected at the 0.05-level in favour of positive predictability.
(iii) Bold entries in the $NB\text{-}GLS_\tau$ column highlight cases where $NB\text{-}GLS_\tau < -35$ when $\hat{\delta} < 0$ or $NB\text{-}GLS_\tau < -15$ when $\hat{\delta} > 0$ such that S^{hyb} switches into the t_τ^{OLS} test. Commensurately, for entries in the S^{hyb} columns, a † superscript denotes that $\underline{\beta}$ is computed using the Bonferroni-based t_τ^{OLS} test.
(iv) Bold entries in the $NB\text{-}OLS_\tau$ column highlight cases where $NB\text{-}OLS_\tau < -10T^{1/2}$. Commensurately, for entries in the U^{hyb} and S^{hyb} columns, a ‡ superscript denotes that $\underline{\beta}$ is computed using a conventional confidence interval based on standard normal critical values.

On-Line Supplementary Appendix - Bonferroni Type Tests for Return Predictability with Possibly Trending Predictors

Sam Astill[a], David I. Harvey[b], Stephen J. Leybourne[b] and A.M. Robert Taylor[a]

[a] Essex Business School, University of Essex

[b] Granger Centre for Time Series Econometrics and School of Economics, University of Nottingham

August 7, 2024

Abstract

The outline of this supplementary paper is as follows. Section S.1 provides a proof of Theorem 1 in the paper. Section S.2 establishes consistency of the nuisance parameter estimates used to construct the t_{μ}^{OLS} and Q_{μ}^{GLS} test statistics in the presence of a fixed magnitude trend in the predictor. Section S.3 shows numerically how the lower bound of the confidence interval for β is computed for the U^{hyb} procedure for one of the returns/predictor pairings considered in the empirical application of the main paper. Section S.4 reports Figures S.1–S.15 discussed in section 4.1 of the paper. Section S.5 reports the local asymptotic power of our proposed tests across additional scenarios to those considered in the main paper. Finally, section S.6 reports results from a Monte Carlo simulation exercise examining the finite sample size and power performance of our proposed tests.

S.1 Proof of Theorem 1

It is useful to use the Cholesky decomposition to write

$$\begin{aligned} e_t &= \sigma_e \varepsilon_{1t} \\ u_t &= \sigma_u \{\delta \varepsilon_{1t} + (1-\delta^2)^{1/2} \varepsilon_{2t}\} \end{aligned}$$

where e_t denotes the innovation to v_t, and ε_{1t} and ε_{2t} are independent martingale difference sequences each with unit (unconditional) variance. Also, note that we can write as

$$r_t = \alpha^* + \beta_T w_{t-1} + u_t \tag{S.1}$$

with $\alpha^* = \alpha + \beta_T \mu$. Since a constant term is fitted in the regression, for the purposes of the theory we can set $\alpha = \mu = 0$ (and therefore $\alpha^* = 0$) without loss of generality. In what follows we make use of the following weak convergence results:

$$\begin{aligned} T^{-1/2} \sum_{t=2}^{\lfloor rT \rfloor} \varepsilon_{1t} &\xrightarrow{w} W_1(r) \\ T^{-1/2} \sum_{t=2}^{\lfloor rT \rfloor} \varepsilon_{2t} &\xrightarrow{w} W_2(r) \end{aligned}$$

where $W_1(r)$ and $W_2(r)$, $r \in [0,1]$, are independent standard Brownian motions, and where $\lfloor \cdot \rfloor$ denotes the integer part of its argument.

S.1.1 Proof of Theorem 1.1 (i)

The t_μ statistic can be written as

$$t_\mu = \frac{T^{-1} \sum_{t=2}^{T} x_{t-1}(r_t - \bar{r})}{\sqrt{\sigma_u^2 T^{-2} \sum_{t=2}^{T} (x_{t-1} - \bar{x}_{-1})^2}}.$$

Consider first the numerator of t_μ. Using (S.1),

$$\begin{aligned} T^{-1}\sum_{t=2}^{T} x_{t-1}(r_t - \bar{r}) &= \beta_T T^{-1}\sum_{t=2}^{T} x_{t-1}(w_{t-1} - \bar{w}_{-1}) + T^{-1}\sum_{t=2}^{T} x_{t-1}(u_t - \bar{u}) \\ &= b(\sigma_u/\omega_v)T^{-2}\sum_{t=2}^{T} x_{t-1}(w_{t-1} - \bar{w}_{-1}) + T^{-1}\sum_{t=2}^{T} x_{t-1}(u_t - \bar{u}). \end{aligned}$$

Here,

$$\begin{aligned} T^{-2}\sum_{t=2}^{T} x_{t-1}(w_{t-1} - \bar{w}_{-1}) &= T^{-2}\sum_{t=2}^{T}\{\gamma_T(t-1) + w_{t-1}\}(w_{t-1} - \bar{w}_{-1}) \\ &= \kappa\omega_v T^{-5/2}\sum_{t=2}^{T}(t-1)(w_{t-1} - \bar{w}_{-1}) + T^{-2}\sum_{t=2}^{T}(w_{t-1} - \bar{w}_{-1})^2 \\ &\xrightarrow{w} \kappa\omega_v^2\int_0^1 rW_{1c}^{\mu}(r)dr + \omega_v^2\int_0^1 W_{1c}^{\mu}(r)^2 dr. \end{aligned}$$

Also,

$$\begin{aligned} T^{-1}\sum_{t=2}^{T} x_{t-1}(u_t - \bar{u}) &= T^{-1}\sum_{t=2}^{T}(x_{t-1} - \bar{x}_{-1})u_t \\ &= \kappa\omega_v T^{-3/2}\sum_{t=2}^{T}\{(t-1) - \overline{t-1}\}u_t + T^{-1}\sum_{t=2}^{T}(w_{t-1} - \bar{w}_{-1})u_t \\ &= \kappa\omega_v\sigma_u T^{-3/2}\sum_{t=2}^{T}\{(t-1) - \overline{t-1}\}\{\delta\varepsilon_{1t} + (1-\delta^2)^{1/2}\varepsilon_{2t}\} \\ &\quad +\sigma_u T^{-1}\sum_{t=2}^{T}(w_{t-1} - \bar{w}_{-1})\{\delta\varepsilon_{1t} + (1-\delta^2)^{1/2}\varepsilon_{2t}\} \\ &\xrightarrow{w} \kappa\omega_v\sigma_u\{\delta\int_0^1 (r-0.5)dW_1(r) + (1-\delta^2)^{1/2}\int_0^1 (r-0.5)dW_2(r)\} \\ &\quad +\omega_v\sigma_u\{\delta\int_0^1 W_{1c}^{\mu}(r)dW_1(r) + (1-\delta^2)^{1/2}\int_0^1 W_{1c}^{\mu}(r)dW_2(r)\} \\ &= \omega_v\sigma_u\int_0^1 W_{1c}^{\mu,\kappa}(r)\{\delta dW_1(r) + (1-\delta^2)^{1/2}dW_2(r)\}. \end{aligned}$$

So,

$$T^{-1}\sum_{t=2}^{T} x_{t-1}(r_t-\bar{r}) \xrightarrow{w} \sigma_u\omega_v b\{\kappa\int_0^1 rW_{1c}^{\mu}(r)dr+\int_0^1 W_{1c}^{\mu}(r)^2dr\}+\sigma_u\omega_v\{\delta\int_0^1 W_{1c}^{\mu,\kappa}(r)dW_1(r) +(1-\delta^2)^{1/2}\int_0^1 W_{1c}^{\mu,\kappa}dW_2(r)\}.$$

Next consider the denominator of t_μ

$$\begin{aligned}
T^{-2}\sum_{t=2}^{T}(x_{t-1}-\bar{x}_{-1})^2 &= T^{-2}\sum_{t=2}^{T}\{\gamma_T(t-1-\overline{t-1})+(w_{t-1}-\bar{w}_{-1})\}^2 \\
&= \kappa^2\omega_v^2T^{-3}\sum_{t=2}^{T}(t-1-\overline{t-1})^2+T^{-2}\sum_{t=2}^{T}(w_{t-1}-\bar{w}_{-1})^2 \\
&\quad +2\kappa\omega_vT^{-5/2}\sum_{t=2}^{T}(t-1-\overline{t-1})(w_{t-1}-\bar{w}_{-1}) \\
&\xrightarrow{w} \kappa^2\omega_v^2/12+\omega_v^2\int_0^1 W_{1c}^{\mu}(r)^2dr+2\kappa\omega_v^2\int_0^1 rW_{1c}^{\mu}(r)dr \\
&= \omega_v^2\int_0^1\{\kappa(r-0.5)+W_{1c}^{\mu}(r)\}^2dr \\
&= \omega_v^2\int_0^1 W_{1c}^{\mu,\kappa}(r)^2dr.
\end{aligned}$$

Hence we obtain

$$\begin{aligned}
t_\mu &= \frac{T^{-1}\sum_{t=2}^{T}x_{t-1}(r_t-\bar{r})}{\sqrt{\sigma_u^2T^{-2}\sum_{t=2}^{T}(x_{t-1}-\bar{x}_{-1})^2}} \\
&\xrightarrow{w} \frac{b\{\kappa\int_0^1 rW_{1c}^{\mu}(r)dr+\int_0^1 W_{1c}^{\mu}(r)^2dr\}+\delta\int_0^1 W_{1c}^{\mu,\kappa}(r)dW_1(r)+(1-\delta^2)^{1/2}\int_0^1 W_{1c}^{\mu,\kappa}dW_2(r)}{\sqrt{\int_0^1 W_{1c}^{\mu,\kappa}(r)^2dr}} \\
&= \frac{b\{\kappa\int_0^1 rW_{1c}^{\mu}(r)dr+\int_0^1 W_{1c}^{\mu}(r)^2dr\}+\delta\int_0^1 W_{1c}^{\mu,\kappa}(r)dW_1(r)}{\sqrt{\int_0^1 W_{1c}^{\mu,\kappa}(r)^2dr}}+(1-\delta^2)^{1/2}Z_\mu.
\end{aligned}$$

S.1.2 Proof of Theorem 1.1 (ii)

Assuming $\tilde{\rho}_T = 1 + \tilde{c}/T$ and letting $y_t := (r_t - (\sigma_{ue}/\sigma_e\omega_v)(x_t - \tilde{\rho}x_{t-1}))$, we can write $Q_\mu(\tilde{\rho})$ as

$$Q_\mu(\tilde{\rho}) = \frac{\sum_{t=2}^{T}(x_{t-1} - \bar{x}_{-1})y_t + \frac{T}{2}(\sigma_{ue}/\sigma_e\omega_v)(\omega_v^2 - \sigma_v^2)}{(1-\delta^2)^{1/2}\sigma_u\sqrt{\sum_{t=2}^{T}(x_{t-1} - \bar{x}_{-1})^2}}. \tag{S.2}$$

Turning first to the numerator of (S.2) first note that we can write

$$\begin{aligned}
y_t &= \beta_T w_{t-1} + u_t - (\sigma_{ue}/\sigma_e\omega_v)(x_t - \tilde{\rho}x_{t-1}) \\
&= \beta_T w_{t-1} + u_t - (\sigma_{ue}/\sigma_e\omega_v)(x_t - \rho x_{t-1}) \\
&\quad + (\sigma_{ue}/\sigma_e\omega_v)T^{-1}(\tilde{c} - c)x_{t-1} \\
&= \beta_T w_{t-1} + u_t - (\sigma_{ue}/\sigma_e\omega_v)\{v_t - \gamma_T\{cT^{-1}(t-1) - 1\} \\
&\quad + (\sigma_{ue}/\sigma_e\omega_v)T^{-1}(\tilde{c} - c)x_{t-1}
\end{aligned}$$

using

$$\begin{aligned}
x_t - \rho x_{t-1} &= \gamma_T t + w_t - \rho w_{t-1} - \rho\gamma_T(t-1) \\
&= v_t + \gamma_T\{t - (1 + cT^{-1})(t-1)\} \\
&= v_t - \gamma_T\{cT^{-1}(t-1) - 1\}.
\end{aligned}$$

So,

$$\begin{aligned}
y_t &= \beta_T w_{t-1} + \{u_t - (\sigma_{ue}/\sigma_e\omega_v)v_t\} + (\sigma_{ue}/\sigma_e\omega_v)\gamma_T\{cT^{-1}(t-1) - 1\} \\
&\quad + (\sigma_{ue}/\sigma_e\omega_v)\{T^{-1}(\tilde{c} - c)x_{t-1}\}
\end{aligned}$$

Hence we find

$$Q_\mu(\tilde{\rho}) = \frac{\beta_T \sum_{t=2}^T (x_{t-1}-\bar{x}_{-1})w_{t-1}}{(1-\delta^2)^{1/2}\sigma_u\sqrt{\sum_{t=2}^T (x_{t-1}-\bar{x}_{-1})^2}} \tag{S.3}$$

$$+\frac{\sum_{t=2}^T (x_{t-1}-\bar{x}_{-1})(u_t-(\sigma_{ue}/\sigma_e\omega_v)v_t)+\frac{T}{2}(\sigma_{ue}/\sigma_e\omega_v)(\omega_v^2-\sigma_v^2)}{(1-\delta^2)^{1/2}\sigma_u\sqrt{\sum_{t=2}^T (x_{t-1}-\bar{x}_{-1})^2}} \tag{S.4}$$

$$+\frac{(\sigma_{ue}/\sigma_e\omega_v)\gamma_T c T^{-1}\sum_{t=2}^T (x_{t-1}-\bar{x}_{-1})(t-1)}{(1-\delta^2)^{1/2}\sigma_u\sqrt{\sum_{t=2}^T (x_{t-1}-\bar{x}_{-1})^2}} \tag{S.5}$$

$$+\frac{(\sigma_{ue}/\sigma_e\omega_v)T^{-1}(\tilde{c}-c)\sum_{t=2}^T (x_{t-1}-\bar{x}_{-1})^2}{(1-\delta^2)^{1/2}\sigma_u\sqrt{\sum_{t=2}^T (x_{t-1}-\bar{x}_{-1})^2}}. \tag{S.6}$$

We now examine the limit of each of the terms (S.3)-(S.6) in turn. Beginning with (S.3), we can write it as

$$\frac{(b\sigma_u/\omega_v)T^{-2}\sum_{t=2}^T x_{t-1}(w_t-\bar{w}_{-1})}{(1-\delta^2)^{1/2}\sigma_u\sqrt{T^{-2}\sum_{t=2}^T (x_{t-1}-\bar{x}_{-1})^2}} \xrightarrow{w} \frac{(b\sigma_u/\omega_v)\{\kappa\omega_v^2\int_0^1 rW_{1c}^\mu(r)dr+\omega_v^2\int_0^1 W_{1c}^\mu(r)^2dr\}}{(1-\delta^2)^{1/2}\sigma_u\sqrt{\omega_v^2\int_0^1 W_{1c}^{\mu,\kappa}(r)^2dr}}$$

$$= \frac{b\{\kappa\int_0^1 rW_{1c}^\mu(r)dr+\int_0^1 W_{1c}^\mu(r)^2dr\}}{(1-\delta^2)^{1/2}\sqrt{\int_0^1 W_{1c}^{\mu,\kappa}(r)^2dr}}.$$

For (S.4) we note that

$$T^{-1}\sum_{t=2}^T (x_{t-1}-\bar{x}_{-1})v_t \xrightarrow{w} \omega_v^2\int_0^1 W_{1c}^{\mu,\kappa}(r)dW_1(r)+\frac{1}{2}(\omega_v^2-\sigma_v^2).$$

Then,

$$
\begin{aligned}
& \frac{T^{-1}\sum_{t=2}^{T}(x_{t-1}-\bar{x}_{-1})(u_t-\frac{\sigma_{ue}}{\sigma_e\omega_v}v_t)+\frac{1}{2}\frac{\sigma_{ue}}{\sigma_e\omega_v}(\omega_v^2-\sigma_v^2)}{\sigma_u(1-\delta^2)^{1/2}(T^{-2}\sum_{t=2}^{T}(x_{t-1}-\bar{x}_{-1})^2)^{1/2}} \\
= & \frac{T^{-1}\sum_{t=2}^{T}(x_{t-1}-\bar{x}_{-1})u_t-\frac{\sigma_{ue}}{\sigma_e\omega_v}T^{-1}\sum_{t=2}^{T}(x_{t-1}-\bar{x}_{-1})v_t+\frac{1}{2}\frac{\sigma_{ue}}{\sigma_e\omega_v}(\omega_v^2-\sigma_v^2)}{\sigma_u(1-\delta^2)^{1/2}(T^{-2}\sum_{t=2}^{T}(x_{t-1}-\bar{x}_{-1})^2)^{1/2}} \\
\xrightarrow{w} & \frac{\omega_v\sigma_u\int_0^1 W_{1c}^{\mu,\kappa}(r)\{\delta dW_1(r)+(1-\delta^2)^{1/2}dW_2(r)\}-\frac{\sigma_{ue}}{\sigma_e\omega_v}\omega_v^2\int_0^1 W_{1c}^{\mu,\kappa}(r)dW_1(r)}{\sigma_u(1-\delta^2)^{1/2}\omega_v\sqrt{\int_0^1 W_{1c}^{\mu,\kappa}(r)^2dr}} \\
& +\frac{-\frac{1}{2}\frac{\sigma_{ue}}{\sigma_e\omega_v}(\omega_v^2-\sigma_v^2)+\frac{1}{2}\frac{\sigma_{ue}}{\sigma_e\omega_v}(\omega_v^2-\sigma_v^2)}{\sigma_u(1-\delta^2)^{1/2}\omega_v\sqrt{\int_0^1 W_{1c}^{\mu,\kappa}(r)^2dr}} \\
= & \frac{\delta\int_0^1 W_{1c}^{\mu,\kappa}(r)dW_1(r)+(1-\delta^2)^{1/2}\int_0^1 W_{1c}^{\mu,\kappa}dW_2(r)-\delta\int_0^1 W_{1c}^{\mu,\kappa}(r)dW_1(r)}{(1-\delta^2)^{1/2}\sqrt{\int_0^1 W_{1c}^{\mu,\kappa}(r)^2dr}} \\
= & \frac{\int_0^1 W_{1c}^{\mu,\kappa}(r)dW_2(r)}{\sqrt{\int_0^1 W_{1c}^{\mu,\kappa}(r)^2dr}} \\
= & Z_\mu.
\end{aligned}
$$

For (S.5),

$$
\begin{aligned}
\frac{(\sigma_{ue}/\sigma_e\omega_v)\gamma_T cT^{-1}\sum_{t=2}^{T}(x_{t-1}-\bar{x}_{-1})(t-1)}{(1-\delta^2)^{1/2}\sigma_u\sqrt{\sum_{t=2}^{T}(x_{t-1}-\bar{x}_{-1})^2}} &= \frac{(\sigma_{ue}/\sigma_e\omega_v)c\kappa\omega_v T^{-3/2}\sum_{t=2}^{T}(x_{t-1}-\bar{x}_{-1})(t-1)}{(1-\delta^2)^{1/2}\sigma_u\sqrt{\sum_{t=2}^{T}(x_{t-1}-\bar{x}_{-1})^2}} \\
&= \frac{\delta c\kappa T^{-5/2}\sum_{t=2}^{T}(x_{t-1}-\bar{x}_{-1})(t-1)}{(1-\delta^2)^{1/2}\sqrt{T^{-2}\sum_{t=2}^{T}(x_{t-1}-\bar{x}_{-1})^2}} \\
&\xrightarrow{w} \frac{\delta c\kappa\omega_v\int_0^1 rW_{1c}^{\mu,\kappa}(r)dr}{(1-\delta^2)^{1/2}\omega_v\sqrt{\int_0^1 W_{1c}^{\mu,\kappa}(r)^2dr}} \\
&= \frac{\delta c\kappa\int_0^1 rW_{1c}^{\mu,\kappa}(r)dr}{(1-\delta^2)^{1/2}\sqrt{\int_0^1 W_{1c}^{\mu,\kappa}(r)^2dr}}.
\end{aligned}
$$

Finally, for (S.6),

$$\begin{aligned}\frac{(\sigma_{ue}/\sigma_e\omega_v)T^{-1}(\tilde{c}-c)\sum_{t=2}^{T}(x_{t-1}-\bar{x}_{-1})^2}{(1-\delta^2)^{1/2}\sigma_u\sqrt{\sum_{t=2}^{T}(x_{t-1}-\bar{x}_{-1})^2}} &= \frac{\delta\omega_v^{-1}(\tilde{c}-c)T^{-2}\sum_{t=2}^{T}(x_{t-1}-\bar{x}_{-1})^2}{(1-\delta^2)^{1/2}\sqrt{T^{-2}\sum_{t=2}^{T}(x_{t-1}-\bar{x}_{-1})^2}} \\ &\xrightarrow{w} \frac{\delta\omega_v^{-1}(\tilde{c}-c)\omega_v^2\int_0^1 W_{1c}^{\mu,\kappa}(r)^2dr}{(1-\hat{\delta}^2)^{1/2}\omega_v\sqrt{\int_0^1 W_{1c}^{\mu,\kappa}(r)^2dr}} \\ &= \frac{\delta(\tilde{c}-c)\int_0^1 W_{1c}^{\mu,\kappa}(r)^2dr}{(1-\delta^2)^{1/2}\sqrt{\int_0^1 W_{1c}^{\mu,\kappa}(r)^2dr}}.\end{aligned}$$

Combining results we therefore have that

$$Q_\mu(\tilde{\rho}) \xrightarrow{w} \frac{b\{\kappa\int_0^1 rW_{1c}^{\mu}(r)dr+\int_0^1 W_{1c}^{\mu}(r)^2dr\}+\delta c\kappa\int_0^1 rW_{1c}^{\mu,\kappa}(r)dr+\delta(\tilde{c}-c)\int_0^1 W_{1c}^{\mu,\kappa}(r)^2dr}{(1-\delta^2)^{1/2}\{\int_0^1 W_{1c}^{\mu,\kappa}(r)^2dr\}^{1/2}}+Z_\mu.$$

S.1.3 Proof of Theorem 1.2 (i)

The t_μ statistic can be written as

$$t_\mu = \frac{T^{-3/2}\sum_{t=2}^{T}x_{t-1}(r_t-\bar{r})}{\sqrt{\sigma_u^2T^{-3}\sum_{t=2}^{T}(x_{t-1}-\bar{x}_{-1})^2}}.$$

Using (S.1), the numerator can be expressed as

$$T^{-3/2}\sum_{t=2}^{T}x_{t-1}(r_t-\bar{r}) = b(\sigma_u/\omega_v)T^{-5/2}\sum_{t=2}^{T}x_{t-1}(w_{t-1}-\bar{w}_{-1})+T^{-3/2}\sum_{t=2}^{T}x_{t-1}(u_t-\bar{u}).$$

Here,

$$\begin{aligned}T^{-5/2}\sum_{t=2}^{T}x_{t-1}(w_{t-1}-\bar{w}_{-1}) &= T^{-5/2}\sum_{t=2}^{T}\{\gamma(t-1)+w_{t-1}\}(w_{t-1}-\bar{w}_{-1}) \\ &= \kappa\omega_vT^{-5/2}\sum_{t=2}^{T}(t-1)(w_{t-1}-\bar{w}_{-1})+o_p(1) \\ &\xrightarrow{w} \kappa\omega_v^2\int_0^1 rW_{1c}^{\mu}(r)dr.\end{aligned}$$

Also,

$$\begin{aligned} T^{-3/2}\sum_{t=2}^{T} x_{t-1}(u_t-\bar{u}) &= T^{-3/2}\sum_{t=2}^{T}(x_{t-1}-\bar{x}_{-1})u_t \\ &= \kappa\omega_v T^{-3/2}\sum_{t=2}^{T}\{(t-1)-\overline{t-1}\}u_t + T^{-3/2}\sum_{t=2}^{T}(w_{t-1}-\bar{w}_{-1})u_t \\ &= \kappa\omega_v\sigma_u T^{-3/2}\sum_{t=2}^{T}\{(t-1)-\overline{t-1}\}\{\delta\varepsilon_{1t}+(1-\delta^2)^{1/2}\varepsilon_{2t}\}+o_p(1) \\ &\xrightarrow{w} \kappa\omega_v\sigma_u\left\{\delta\int_0^1(r-0.5)dW_1(r)+(1-\delta^2)^{1/2}\int_0^1(r-0.5)dW_2(r)\right\}. \end{aligned}$$

So,

$$\begin{aligned} T^{-3/2}\sum_{t=2}^{T} x_{t-1}(r_t-\bar{r}) &\xrightarrow{w} \sigma_u\omega_v b\kappa\int_0^1 rW_{1c}^{\mu}(r)dr+\kappa\sigma_u\omega_v\{\delta\int_0^1(r-0.5)dW_1(r) \\ &\quad +(1-\delta^2)^{1/2}\int_0^1(r-0.5)dW_2(r)\}. \end{aligned} \tag{S.7}$$

Next consider the denominator of t_μ

$$\begin{aligned} T^{-3}\sum_{t=2}^{T}(x_{t-1}-\bar{x}_{-1})^2 &= T^{-3}\sum_{t=2}^{T}\{\gamma(t-1-\overline{t-1})+(w_{t-1}-\bar{w}_{-1})\}^2 \\ &= \kappa^2\omega_v^2 T^{-3}\sum_{t=2}^{T}(t-1-\overline{t-1})^2+o_p(1) \\ &\xrightarrow{p} \kappa^2\omega_v^2/12. \end{aligned} \tag{S.8}$$

Hence we obtain

$$\begin{aligned} t_\mu &\xrightarrow{w} \frac{\sigma_u\omega_v b\kappa\int_0^1 rW_{1c}^{\mu}(r)dr+\kappa\sigma_u\omega_v\left\{\delta\int_0^1(r-0.5)dW_1(r)+(1-\delta^2)^{1/2}\int_0^1(r-0.5)dW_2(r)\right\}}{\sqrt{\sigma_u^2\kappa^2\omega_v^2/12}} \\ &= \sqrt{12}\left\{b\int_0^1 rW_{1c}^{\mu}(r)dr+\delta\int_0^1(r-0.5)dW_1(r)+(1-\delta^2)^{1/2}\int_0^1(r-0.5)dW_2(r)\right\} \\ &= b\sqrt{12}\int_0^1 rW_{1c}^{\mu}(r)dr+Z_\mu^*. \end{aligned}$$

S.1.4 Proof of Theorem 1.2 (ii)

The $Q_\mu(\tilde{\rho})$ statistic can again be written as in (S.3)-(S.6), but with γ_T replaced by γ in (S.5). Introducing the appropriate scalings we can write

$$T^{-1/2}Q_\mu(\tilde{\rho}) = T^{-1/2}\frac{(b\sigma_u/\omega_v)T^{-5/2}\sum_{t=2}^{T}(x_{t-1}-\bar{x}_{-1})w_{t-1}}{(1-\delta^2)^{1/2}\sigma_u\sqrt{T^{-3}\sum_{t=2}^{T}(x_{t-1}-\bar{x}_{-1})^2}} \tag{S.9}$$

$$+T^{-1/2}\frac{T^{-3/2}\sum_{t=2}^{T}(x_{t-1}-\bar{x}_{-1})(u_t-(\sigma_{u,e}/\sigma_e\omega_v)v_t)+T^{-3/2}\frac{T}{2}(\sigma_{u,e}/\sigma_e\omega_v)(\omega_v^2-\sigma_v^2)}{(1-\delta^2)^{1/2}\sigma_u\sqrt{T^{-3}\sum_{t=2}^{T}(x_{t-1}-\bar{x}_{-1})^2}} \tag{S.10}$$

$$+\frac{(\sigma_{u,e}/\sigma_e\omega_v)\gamma cT^{-3}\sum_{t=2}^{T}(x_{t-1}-\bar{x}_{-1})(t-1)}{(1-\delta^2)^{1/2}\sigma_u\sqrt{T^{-3}\sum_{t=2}^{T}(x_{t-1}-\bar{x}_{-1})^2}} \tag{S.11}$$

$$+\frac{(\sigma_{u,e}/\sigma_e\omega_v)(\tilde{c}-c)T^{-3}\sum_{t=2}^{T}(x_{t-1}-\bar{x}_{-1})^2}{(1-\delta^2)^{1/2}\sigma_u\sqrt{T^{-3}\sum_{t=2}^{T}(x_{t-1}-\bar{x}_{-1})^2}}. \tag{S.12}$$

Notice that terms (S.9) and (S.10) are $o_p(1)$. Examining the limits of (S.11) and (S.12), we find

$$\begin{aligned} T^{-3}\sum_{t=2}^{T}(x_{t-1}-\bar{x}_{-1})(t-1) &= \sum_{t=2}^{T}\{\gamma(t-1-\overline{t-1})+(w_{t-1}-\bar{w}_{-1})\}(t-1) \\ &= \kappa\omega_v T^{-3}\sum_{t=2}^{T}(t-1-\overline{t-1})^2+T^{-3}\sum_{t=2}^{T}(w_{t-1}-\bar{w}_{-1})(t-1) \\ &\xrightarrow{p} \kappa\omega_v/12 \end{aligned}$$

which together with (S.8) results in

$$\begin{aligned} \frac{(\sigma_{u,e}/\sigma_e\omega_v)\gamma cT^{-3}\sum_{t=2}^{T}(x_{t-1}-\bar{x}_{-1})(t-1)}{(1-\delta^2)^{1/2}\sigma_u\sqrt{T^{-3}\sum_{t=2}^{T}(x_{t-1}-\bar{x}_{-1})^2}} &\xrightarrow{p} \frac{(\sigma_{u,e}/\sigma_e)\kappa^2 c/12}{(1-\delta^2)^{1/2}\sigma_u\sqrt{\kappa^2/12}} \\ &= \frac{\delta c\,|\kappa|}{(1-\delta^2)^{1/2}\sqrt{12}} \end{aligned}$$

and

$$\frac{(\sigma_{u,e}/\sigma_e\omega_v)(\tilde{c}-c)T^{-3}\sum_{t=2}^{T}(x_{t-1}-\bar{x}_{-1})^2}{(1-\delta^2)^{1/2}\sigma_u\sqrt{T^{-3}\sum_{t=2}^{T}(x_{t-1}-\bar{x}_{-1})^2}} \xrightarrow{p} \frac{(\sigma_{u,e}/\sigma_e)(\tilde{c}-c)\kappa^2/12}{(1-\delta^2)^{1/2}\sigma_u\sqrt{\kappa^2/12}}$$
$$= \frac{\delta(\tilde{c}-c)\,|\kappa|}{(1-\delta^2)^{1/2}\sqrt{12}}.$$

Combining results we therefore have that

$$T^{-1/2}Q_\mu(\tilde{\rho}) \xrightarrow{p} \frac{\delta c\,|\kappa|}{(1-\delta^2)^{1/2}\sqrt{12}} + \frac{\delta(\tilde{c}-c)\,|\kappa|}{(1-\delta^2)^{1/2}\sqrt{12}}$$
$$= \frac{\delta\tilde{c}\,|\kappa|}{(1-\delta^2)^{1/2}\sqrt{12}}.$$

S.1.5 Proof of Theorem 1.3 (i)

We can write the t_τ statistic as

$$t^\tau = \frac{b\sigma_u\omega_v^{-1}(T^{-2}\sum_{t=2}^{T}x_{\tau,t-1}^2)^{1/2}}{\sigma_u} + \frac{T^{-1}\sum_{t=2}^{T}x_{\tau,t-1}u_t}{\sigma_u\sqrt{T^{-2}\sum_{t=2}^{T}x_{\tau,t-1}^2}}$$
$$\xrightarrow{w} b\Big(\int_0^1 W_{1c}^\tau(r)^2dr\Big)^{1/2} + \frac{\delta\int_0^1 W_{1c}^\tau(r)dW_1(r) + (1-\delta^2)^{1/2}\int_0^1 W_{1c}^\tau(r)dW_2(r)}{\sqrt{\int_0^1 W_{1c}^\tau(r)^2dr}}$$
$$= b\Big(\int_0^1 W_{1c}^\tau(r)^2dr\Big)^{1/2} + \delta\frac{\int_0^1 W_{1c}^\tau(r)dW_1(r)}{\sqrt{\int_0^1 W_{1c}^\tau(r)^2dr}} + (1-\delta^2)^{1/2}Z_\tau.$$

S.1.6 Proof of Theorem 1.3 (ii)

The $Q_\tau(\tilde{\rho})$ statistic can be written as

$$Q_\tau(\tilde{\rho}) = \frac{b\omega_v^{-1}(T^{-2}\sum_{t=2}^{T}x_{\tau,t-1}^2)^{1/2}}{(1-\delta^2)^{1/2}} + \frac{\delta(\tilde{c}-c)(T^{-2}\sum_{t=2}^{T}x_{\tau,t-1}^2)^{1/2}}{\omega_v(1-\delta^2)^{1/2}}$$
$$+\frac{T^{-1}\sum_{t=2}^{T}x_{\tau,t-1}(u_t-\frac{\sigma_{ue}}{\sigma_e\omega_v}v_t)+\frac{1}{2}\frac{\sigma_{ue}}{\sigma_e\omega_v}(\omega_v^2-\sigma_v^2)}{\sigma_u(1-\delta^2)^{1/2}\sqrt{T^{-2}\sum_{t=2}^{T}x_{\tau,t-1}^2}}. \tag{S.13}$$

We will derive limiting expressions for each of the three terms on the right hand side of (S.13). Here

$$\frac{b\omega_v^{-1}(T^{-2}\sum_{t=2}^{T}x_{\tau,t-1}^2)^{1/2}}{(1-\delta^2)^{1/2}} \xrightarrow{w} \frac{b\{\int_0^1 W_{1c}^\tau(r)^2dr\}^{1/2}}{(1-\delta^2)^{1/2}}$$

and

$$\frac{\delta(\tilde{c}-c)(T^{-2}\sum_{t=2}^{T}x_{\tau,t-1}^{2})^{1/2}}{\omega_v(1-\delta^2)^{1/2}} \xrightarrow{w} \frac{\delta(\tilde{c}-c)\left(\int_0^1 W_{1c}^{\tau}(r)^2dr\right)^{1/2}}{(1-\delta^2)^{1/2}}.$$

Finally,

$$\begin{aligned}
& \frac{T^{-1}\sum_{t=2}^{T}x_{\tau,t-1}(u_t-\frac{\sigma_{ue}}{\sigma_e\omega_v}v_t)+\frac{1}{2}\frac{\sigma_{ue}}{\sigma_e\omega_v}(\omega_v^2-\sigma_v^2)}{\sigma_u(1-\delta^2)^{1/2}\sqrt{T^{-2}\sum_{t=2}^{T}x_{\tau,t-1}^2}} \\
= & \frac{T^{-1}\sum_{t=2}^{T}x_{\tau,t-1}u_t-\frac{\sigma_{ue}}{\sigma_e\omega_v}T^{-1}\sum_{t=2}^{T}x_{\tau,t-1}v_t+\frac{1}{2}\frac{\sigma_{ue}}{\sigma_e\omega_v}(\omega_v^2-\sigma_v^2)}{\sigma_u(1-\delta^2)^{1/2}\sqrt{T^{-2}\sum_{t=2}^{T}x_{\tau,t-1}^2}} \\
\xrightarrow{w} & \frac{\sigma_u\omega_v\int_0^1 W_{1c}^{\tau}(s)\{\delta dW_1(r)+(1-\delta^2)^{1/2}dW_2(r)\}-\frac{\sigma_{ue}}{\sigma_e\omega_v}\omega_v^2\int_0^1 W_{1c}^{\tau}(s)dW_1(s)}{\sigma_u(1-\delta^2)^{1/2}\omega_v\sqrt{\int_0^1 W_{1c}^{\tau}(r)^2dr}} \\
+ & \frac{-\frac{1}{2}\frac{\sigma_{ue}}{\sigma_e\omega_v}(\omega_v^2-\sigma_v^2)+\frac{1}{2}\frac{\sigma_{ue}}{\sigma_e\omega_v}(\omega_v^2-\sigma_v^2)}{\sigma_u(1-\delta^2)^{1/2}\omega_v\sqrt{\int_0^1 W_{1c}^{\tau}(r)^2dr}} \\
= & \frac{\int_0^1 W_{1c}^{\tau}(s)dW_2(s)}{\sqrt{\int_0^1 W_{1c}^{\tau}(r)^2dr}} \\
= & Z_\tau.
\end{aligned}$$

Combining results we obtain

$$Q_\tau(\tilde{\rho}) \xrightarrow{w} \frac{\{b+\delta(\tilde{c}-c)\}\{\int_0^1 W_{1c}^{\tau}(r)^2dr)^{1/2}\}}{(1-\delta^2)^{1/2}}+Z_\tau.$$

S.2 Consistency of Parameter Estimates with Neglected Fixed Trend

In this section we demonstrate that the parameter estimates used in t_μ and $Q_\mu(\tilde{\rho})$ remain consistent in the presence of a neglected fixed trend, i.e. under Assumption 4.2. For simplicity, we consider the case where $p = 1$ in Assumption 1, i.e. where $v_t = e_t$ and $\omega_v = \sigma_v = \sigma_e$. Given that $\delta = \sigma_{ue}/\sigma_u\sigma_e$, consistency of the estimator of δ follows directly from consistency of the estimators of σ_e, σ_u and σ_{ue}.

S.2.1 Consistency of σ_e^2 estimator

First consider $\hat{\sigma}_e^2 := T^{-1}\sum_{t=2}^{T}\hat{e}_t^2$ with $\hat{e}_t$ the residuals from the fitted OLS regression

$$\Delta x_t = \hat{a} + \hat{\phi} x_{t-1} + \hat{e}_t.$$

Here,

$$\begin{aligned}
\hat{\sigma}_e^2 &= T^{-1}\sum_{t=2}^{T}\{(\Delta x_t - \overline{\Delta x}) - \hat{\phi}(x_{t-1} - \bar{x}_{-1})\}^2 \\
&= T^{-1}\sum_{t=2}^{T}(\Delta x_t - \overline{\Delta x})^2 + \hat{\phi}^2 T^{-1}\sum_{t=2}^{T}(x_{t-1} - \bar{x}_{-1})^2 - 2\hat{\phi}T^{-1}\sum_{t=2}^{T}\Delta x_t(x_{t-1} - \bar{x}_{-1})
\end{aligned}$$

where

$$\hat{\phi} = \frac{\sum_{t=2}^{T}\Delta x_t(x_{t-1} - \bar{x}_{-1})}{\sum_{t=2}^{T}(x_{t-1} - \bar{x}_{-1})^2}.$$

As regards the numerator,

$$\begin{aligned}
\sum_{t=2}^{T}\Delta x_t(x_{t-1} - \bar{x}_{-1}) &= \sum_{t=2}^{T}(\gamma + \Delta w_t)(x_{t-1} - \bar{x}_{-1}) \\
&= \sum_{t=2}^{T}\Delta w_t(x_{t-1} - \bar{x}_{-1}) \\
&= \sum_{t=2}^{T}\Delta w_t\{\gamma(t - 1 - \overline{t-1}) + (w_{t-1} - \bar{w}_{-1})\} \\
&= \gamma\sum_{t=2}^{T}(t - 1 - \overline{t-1})\Delta w_t + \sum_{t=2}^{T}\Delta w_t(w_{t-1} - \bar{w}_{-1}) \\
T^{-3/2}\sum_{t=2}^{T}\Delta x_t(x_{t-1} - \bar{x}_{-1}) &= \kappa\omega_v T^{-3/2}\sum_{t=2}^{T}(t - 1 - \overline{t-1})\Delta w_t + o_p(1) \\
&= O_p(1)
\end{aligned}$$

and, together with the result for the denominator given in (S.8), we obtain $\hat{\phi} = O_p(T^{-3/2})$. It then follows that

$$\begin{aligned}\hat{\sigma}_e^2 &= T^{-1}\sum_{t=2}^{T}(\Delta w_t - \overline{\Delta w})^2 + (T^{3/2}\hat{\phi})^2 T^{-4}\sum_{t=2}^{T}(x_{t-1} - \bar{x}_{-1})^2 - 2(T^{3/2}\hat{\phi})T^{-5/2}\sum_{t=2}^{T}\Delta x_t(x_{t-1} - \bar{x}_{-1}) \\ &= T^{-1}\sum_{t=2}^{T}(\Delta w_t - \overline{\Delta w})^2 + o_p(1).\end{aligned}$$

Finally,

$$\begin{aligned}T^{-1}\sum_{t=2}^{T}(\Delta w_t - \overline{\Delta w})^2 &= T^{-1}\sum_{t=2}^{T}\{(\rho-1)(w_{t-1} - \bar{w}_{-1}) + (v_t - \bar{v})\}^2 \\ &= T^{-1}\sum_{t=2}^{T}\{cT^{-1}(w_{t-1} - \bar{w}_{-1}) + (v_t - \bar{v})\}^2 \\ &= c^2T^{-3}\sum_{t=2}^{T}(w_{t-1} - \bar{w}_{-1})^2 + T^{-1}\sum_{t=2}^{T}(v_t - \bar{v})^2 + 2cT^{-2}\sum_{t=2}^{T}(w_{t-1} - \bar{w}_{-1})(v_t - \bar{v}) \\ &= T^{-1}\sum_{t=2}^{T}(v_t - \bar{v})^2 + o_p(1) \\ &\xrightarrow{p} \sigma_e^2\end{aligned}$$

and so $\hat{\sigma}_e^2 \xrightarrow{p} \sigma_e^2$.

S.2.2 Consistency of σ_u^2 estimator

Next consider $\hat{\sigma}_u^2 := T^{-1}\sum_{t=2}^{T}\hat{u}_t^2$ with $\hat{u}_t$ the residuals from the fitted OLS regression

$$r_t = \hat{\alpha}^* + \hat{\beta}^* x_{t-1} + \hat{u}_t.$$

Here,

$$\begin{aligned}\hat{\sigma}_u^2 &= T^{-1}\sum_{t=2}^{T}\left\{(r_t - \bar{r}) - \frac{\sum_{t=2}^{T}x_{t-1}(r_t - \bar{r})}{\sum_{t=2}^{T}(x_{t-1} - \bar{x}_{-1})^2}(x_{t-1} - \bar{x}_{-1})\right\}^2 \\ &= T^{-1}\sum_{t=2}^{T}(r_t - \bar{r})^2 - T^{-1}\frac{\{T^{-3/2}\sum_{t=2}^{T}x_{t-1}(r_t - \bar{r})\}^2}{T^{-3}\sum_{t=2}^{T}(x_{t-1} - \bar{x}_{-1})^2} \\ &= T^{-1}\sum_{t=2}^{T}(r_t - \bar{r})^2 + o_p(1)\end{aligned}$$

given (S.7) and (S.8). Next,

$$\begin{aligned}
\sum_{t=2}^{T}(r_t-\bar{r})^2 &= \beta_T^2\sum_{t=2}^{T}(w_{t-1}-\bar{w}_{-1})^2+\sum_{t=2}^{T}(u_t-\bar{u})^2+2\beta_T\sum_{t=2}^{T}(w_{t-1}-\bar{w}_{-1})(u_t-\bar{u}) \\
T^{-1}\sum_{t=2}^{T}(r_t-\bar{r})^2 &= \sigma_u^2\omega_v^{-2}b^2T^{-3}\sum_{t=2}^{T}(w_{t-1}-\bar{w}_{-1})^2+T^{-1}\sum_{t=2}^{T}(u_t-\bar{u})^2 \\
&\quad +2\sigma_u\omega_v^{-1}bT^{-2}\sum_{t=2}^{T}(w_{t-1}-\bar{w}_{-1})(u_t-\bar{u}) \\
&= T^{-1}\sum_{t=2}^{T}(u_t-\bar{u})^2+o_p(1) \\
&\xrightarrow{p} \sigma_u^2
\end{aligned}$$

and therefore $\hat{\sigma}_u^2 \xrightarrow{p} \sigma_u^2$.

S.2.3 Consistency of σ_{ue} estimator

Finally consider $\hat{\sigma}_{ue} = T^{-1}\sum_{t=2}^{T}\hat{u}_t\hat{e}_t$. Here,

$$\begin{aligned}
\hat{\sigma}_{ue} &= T^{-1}\sum_{t=2}^{T}\left\{(r_t-\bar{r})-\hat{\beta}^*(x_{t-1}-\bar{x}_{-1})\right\}\{(\Delta x_t-\overline{\Delta x})-\hat{\phi}(x_{t-1}-\bar{x}_{-1})\} \\
&= T^{-1}\sum_{t=2}^{T}(\Delta x_t-\overline{\Delta x})(r_t-\bar{r})+(T^{3/2}\hat{\phi})(T^{3/2}\hat{\beta})T^{-4}\sum_{t=2}^{T}(x_{t-1}-\bar{x}_{-1})^2 \\
&\quad -(T^{3/2}\hat{\phi})T^{-5/2}\sum_{t=2}^{T}(x_{t-1}-\bar{x}_{-1})(r_t-\bar{r})-(T^{3/2}\hat{\beta})T^{-5/2}\sum_{t=2}^{T}(\Delta x_t-\overline{\Delta x})(x_{t-1}-\bar{x}_{-1}) \\
&= T^{-1}\sum_{t=2}^{T}(\Delta x_t-\overline{\Delta x})(r_t-\bar{r})+o_p(1)
\end{aligned}$$

since $\hat{\phi}=O_p(T^{-3/2})$ and $\hat{\beta}^*=O_p(T^{-3/2})$ given that

$$\begin{aligned}
T^{3/2}\hat{\beta}^* &= \frac{T^{-3/2}\sum_{t=2}^{T}x_{t-1}(r_t-\bar{r})}{T^{-3}\sum_{t=2}^{T}(x_{t-1}-\bar{x}_{-1})^2} \\
&= O_p(1).
\end{aligned}$$

Now

$$\begin{aligned}
T^{-1}\sum_{t=2}^{T}(\Delta x_t - \overline{\Delta x})(r_t - \bar{r}) &= T^{-1}\sum_{t=2}^{T}(\Delta w_t - \overline{\Delta w})\{\beta_T(w_{t-1} - \bar{w}_{-1}) + (u_t - \bar{u})\} \\
&= (b\sigma_u/\omega_v)T^{-2}\sum_{t=2}^{T}(\Delta w_t - \overline{\Delta w})(w_{t-1} - \bar{w}_{-1}) \\
&\quad + T^{-1}\sum_{t=2}^{T}(\Delta w_t - \overline{\Delta w})(u_t - \bar{u}) \\
&= T^{-1}\sum_{t=2}^{T}(\Delta w_t - \overline{\Delta w})(u_t - \bar{u}) + o_p(1) \\
&= T^{-1}\sum_{t=2}^{T}\{cT^{-1}(w_{t-1} - \bar{w}_{-1}) + (v_t - \bar{v})\}(u_t - \bar{u}) + o_p(1) \\
&= T^{-1}\sum_{t=2}^{T}(e_t - \bar{e})(u_t - \bar{u}) + o_p(1) \\
&\xrightarrow{p} \sigma_{ue}
\end{aligned}$$

and hence $\hat{\sigma}_{ue} \xrightarrow{p} \sigma_{ue}$.

S.3 Empirical Implementation Example

In this section we outline how $\underline{\beta}$, the lower bound of the confidence interval for β, is obtained for the U^{hyb} procedure in one of the empirical returns/predictor pairings, namely the predictability of quarterly log returns using the log Dividend-Price ratio. In this case the BIC selects $p = 1$ when allowing for either a constant or constant and linear trend in the DGP for x_t, and so no correction for serial correlation is required.

The lower bound of the confidence interval for β from U^{hyb} is given by the maximum of the lower bound of the confidence interval for β obtained from the Q_{μ}^{GLS} and Q_{τ}^{GLS} procedures where the significance levels used to construct the initial confidence interval for c, $\bar{\alpha}_{1,\mu}^{Q}$ and $\bar{\alpha}_{1,\tau}^{Q}$, as well as the significance level used to construct the subsequent confidence interval for β, are scaled by ξ, with the values of $\bar{\alpha}_{1,\mu}^{Q}$, $\bar{\alpha}_{1,\tau}^{Q}$ and ξ determined by using an estimate of the value of δ.

S.3.1 Lower Bound from Q_{μ}^{GLS}

The regression model is given by

$$r_t = \alpha + \beta x_{t-1} + u_t \tag{S.14}$$

$$x_t = \mu + \rho x_{t-1} + e_t \tag{S.15}$$

1. We first run regressions (S.14) and (S.15) and obtain the residuals $\hat{u}_t$ and $\hat{e}_t$. Using these residuals we compute $\hat{\sigma}_u^2 = 0.0108$, $\hat{\sigma}_e^2 = \hat{\omega}_v^2 = 0.0117$, $\hat{\sigma}_{ue} = -0.0107$, $\hat{\delta} = -0.952$ and the standard error of $\hat{\beta}$, denoted $SE(\hat{\beta}) = 0.0111$.

2. We then compute the $DF\text{-}GLS_{\mu}$ statistic applied to the predictor x_t which takes a value of -1.275.

3. Given $\hat{\delta} = -0.952$, from Table S.1 below the appropriate values of $\bar{\alpha}_{1,\mu}^{Q}$ and ξ are 10% and 0.66, respectively. Inverting the $DF\text{-}GLS_{\mu}$ test at the 10%×0.66=6.6% level gives us an upper bound on the confidence interval for c of 1.83.

4. We then construct r_t^* as defined in Remark 3.1 using $\rho = 1 + 1.83/T$, setting σ_{ue} and $\sigma_e = \omega_v$ to their estimated values obtained in step 1. We then run regression (S.14), replacing r_t with r_t^*, and denote the estimated coefficient on x_{t-1} as $\hat{\beta}(\rho)$.

5. Given that $\xi = 0.66$ the significance level used for the confidence interval for β is 5%×0.66=3.3%. This implies a lower bound on the confidence interval for β from this test of

$$\underline{\beta} = \hat{\beta}(\rho) - z_{0.033}(1-\delta^2)^{1/2} SE(\hat{\beta}) \tag{S.16}$$

$$= -0.0087 - 1.84(1-(-0.952)^2)^{1/2} 0.0111 = -0.01495 \tag{S.17}$$

6. Finally we scale this lower bound for β by $\hat{\sigma}_e/\hat{\sigma}_u = 1.0433$ to give a final value of $\underline{\beta} = -0.0156$

S.3.2 Lower Bound from Q_τ^{GLS}

The regression model is given by

$$r_t = \alpha + \theta t + \beta x_{t-1} + u_t \tag{S.18}$$

$$x_t = \mu + \gamma t + \rho x_{t-1} + e_t \tag{S.19}$$

1. We first run regressions (S.14) and (S.15) and obtain the residuals $\hat{u}_t$ and $\hat{e}_t$. Using these residuals we compute $\hat{\sigma}_u^2 = 0.0106$, $\hat{\sigma}_e^2 = \hat{\omega}_v^2 = 0.0115$, $\hat{\sigma}_{ue} = -0.0105$, $\hat{\delta} = -0.951$ and the standard error of $\hat{\beta}$, denoted $SE(\hat{\beta}) = 0.0179$.

2. We then compute the $DF\text{-}GLS_\tau$ statistic applied to the predictor x_t which takes a value of -3.608.

3. Given $\hat{\delta} = -0.951$, from Table S.1 below the appropriate values of $\bar{\alpha}_{1,\tau}^{Q}$ and ξ are 6.5% and 0.66, respectively. Inverting the $DF\text{-}GLS_\tau$ test at the 6.5%×0.66=4.3% level gives us an upper bound on the confidence interval for c of -9.79.

4. We then construct r_t^* as defined in Remark 3.1 using $\rho = 1 - 9.79/T$, setting σ_{ue} and $\sigma_e = \omega_v$ to their estimated values obtained in step 1. We then run regression (S.18), replacing r_t with r_t^*, and denote the estimated coefficient on x_{t-1} as $\hat{\beta}(\rho)$.

5. Given that $\xi = 0.66$ the significance level used for the confidence interval for β is 5%×0.66=3.3%. This implies a lower bound on the confidence interval for β from this test of

$$\underline{\beta} = \hat{\beta}(\rho) - z_{0.033}(1-\delta^2)^{1/2} SE(\hat{\beta}) \tag{S.20}$$

$$= 0.0165 - 1.84(1-(-0.951)^2)^{1/2} 0.0179 = 0.0063 \tag{S.21}$$

6. Finally we scale this lower bound for β by $\hat{\sigma}_e/\hat{\sigma}_u = 1.0410$ to give a final value of $\underline{\beta} = 0.0066$

The lower bound for the U^{hyb} procedure is therefore given by $\max\{-0.0156, 0.0066\} = 0.0066$.

Table S.1: Parameters to Deliver One-Sided Tests with Maximum 0.05 Asymptotic Size.

	Q_μ^{GLS}		t_μ^{OLS}		Q_τ^{GLS}		t_τ^{OLS}		U
δ	$\underline{\alpha}_{1,\mu}^{Q}$	$\bar{\alpha}_{1,\mu}^{Q}$	$\underline{\alpha}_{1,\mu}^{t}$	$\bar{\alpha}_{1,\mu}^{t}$	$\underline{\alpha}_{1,\tau}^{Q}$	$\bar{\alpha}_{1,\tau}^{Q}$	$\underline{\alpha}_{1,\tau}^{t}$	$\bar{\alpha}_{1,\tau}^{t}$	ξ
-0.999	0.050	0.055	0.020	0.035	0.050	0.050	0.040	0.035	0.500
-0.975	0.055	0.080	0.025	0.035	0.055	0.055	0.040	0.025	0.630
-0.950	0.055	0.100	0.025	0.040	0.060	0.065	0.040	0.020	0.660
-0.925	0.055	0.115	0.025	0.040	0.065	0.070	0.035	0.020	0.710
-0.900	0.060	0.130	0.025	0.035	0.070	0.075	0.050	0.020	0.730
-0.875	0.060	0.140	0.025	0.035	0.070	0.085	0.050	0.015	0.710
-0.850	0.060	0.150	0.025	0.035	0.075	0.090	0.050	0.015	0.730
-0.825	0.060	0.160	0.025	0.035	0.075	0.095	0.055	0.010	0.740
-0.800	0.065	0.170	0.025	0.035	0.080	0.100	0.060	0.010	0.750
-0.775	0.065	0.180	0.030	0.035	0.080	0.105	0.065	0.010	0.760
-0.750	0.065	0.190	0.025	0.035	0.085	0.110	0.065	0.010	0.760
-0.725	0.065	0.195	0.025	0.035	0.085	0.115	0.065	0.010	0.760
-0.700	0.070	0.205	0.025	0.035	0.090	0.120	0.065	0.010	0.750
-0.675	0.070	0.215	0.025	0.035	0.090	0.125	0.065	0.005	0.750
-0.650	0.070	0.225	0.025	0.035	0.095	0.130	0.080	0.005	0.740
-0.625	0.075	0.230	0.025	0.035	0.095	0.135	0.080	0.005	0.740
-0.600	0.075	0.240	0.030	0.035	0.100	0.140	0.085	0.005	0.740
-0.575	0.075	0.250	0.035	0.035	0.100	0.140	0.085	0.005	0.740
-0.550	0.080	0.260	0.035	0.035	0.105	0.145	0.090	0.005	0.730
-0.525	0.080	0.270	0.045	0.035	0.110	0.150	0.095	0.005	0.730
-0.500	0.080	0.280	0.060	0.035	0.115	0.150	0.095	0.010	0.730
-0.475	0.085	0.285	0.050	0.035	0.120	0.150	0.095	0.010	0.730
-0.450	0.085	0.295	0.055	0.040	0.120	0.155	0.095	0.010	0.730
-0.425	0.090	0.310	0.035	0.040	0.125	0.165	0.095	0.010	0.710
-0.400	0.090	0.320	0.060	0.040	0.130	0.165	0.150	0.010	0.710
-0.375	0.095	0.330	0.040	0.040	0.135	0.165	0.150	0.010	0.710
-0.350	0.100	0.345	0.030	0.040	0.140	0.170	0.150	0.010	0.690
-0.325	0.100	0.355	0.015	0.045	0.145	0.170	0.150	0.010	0.690
-0.300	0.105	0.360	0.010	0.050	0.150	0.175	0.150	0.010	0.680
-0.275	0.110	0.370	0.005	0.040	0.155	0.175	0.200	0.010	0.680
-0.250	0.115	0.375	0.005	0.035	0.165	0.175	0.200	0.010	0.680
-0.225	0.125	0.380	0.005	0.025	0.170	0.175	0.200	0.010	0.680
-0.200	0.130	0.390	0.005	0.025	0.175	0.175	0.200	0.005	0.670
-0.175	0.140	0.395	0.005	0.010	0.185	0.175	0.200	0.005	0.650
-0.150	0.150	0.400	0.005	0.010	0.200	0.175	0.200	0.005	0.650
-0.125	0.160	0.405	0.005	0.010	0.200	0.165	0.200	0.005	0.630
-0.100	0.175	0.415	0.005	0.005	0.210	0.145	0.200	0.005	0.610
-0.075	0.190	0.420	0.005	0.005	0.220	0.130	0.200	0.005	0.610
-0.050	0.215	0.425	0.005	0.005	0.225	0.100	0.150	0.005	0.590
-0.025	0.250	0.435	0.005	0.005	0.185	0.035	0.150	0.005	0.570

S.4 Figures S.1–S.15

Figure S.1: Local Asymptotic Power of Right-Tailed Bonferroni and Infeasible t_μ and Q_μ tests. DGP (1)-(3) with $\delta = -0.95$ and $\kappa = 0$, where c, κ and δ are the local-to-unity AR, trend, and endogeneity correlation parameters, respectively.

(a) $c = 0$

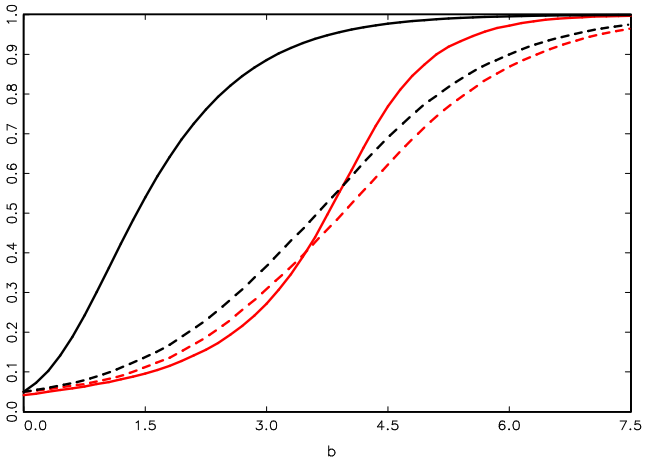

(b) $c = -2$

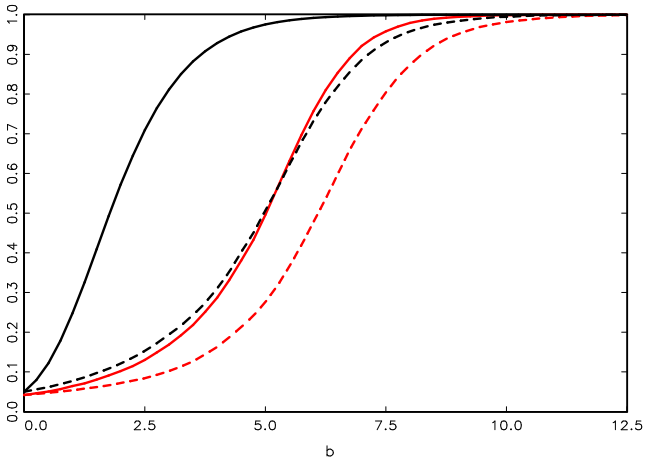

(c) $c = -5$

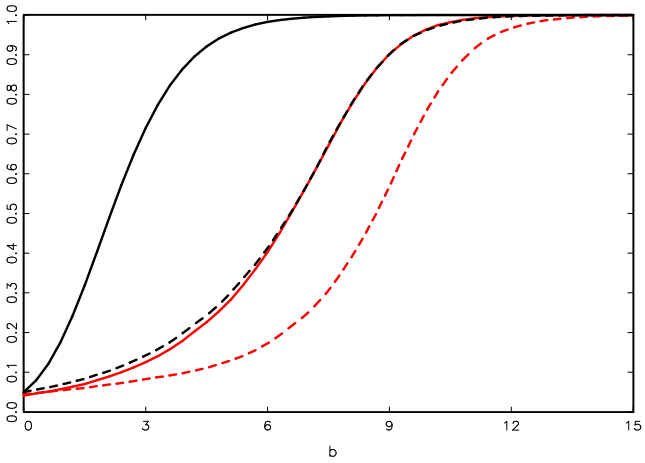

(d) $c = -10$

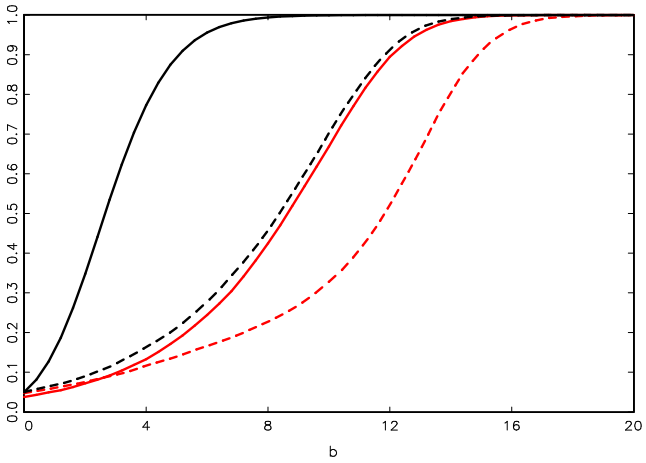

(e) $c = -20$

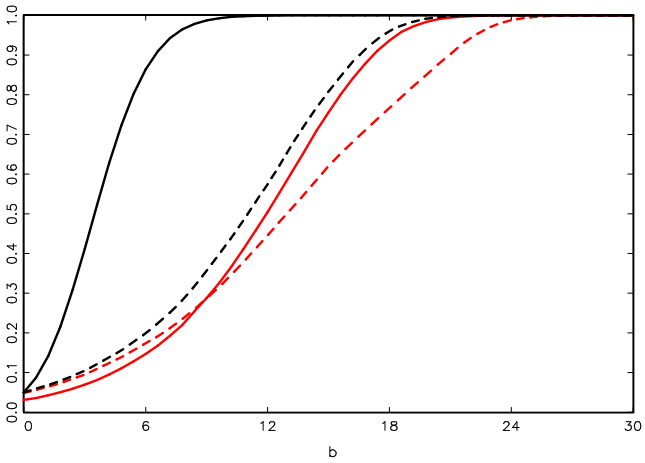

(f) $c = -50$

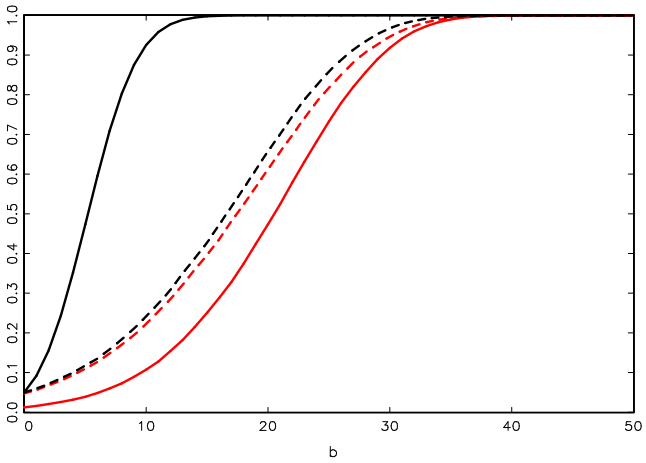

t_μ^{OLS}: – – , Q_μ^{GLS}: ——, Infeasible t_μ: – – , Infeasible Q_μ: ——

Figure S.2: Local Asymptotic Power of Right-Tailed Bonferroni and Infeasible t_τ and Q_τ tests. DGP (1)-(3) with $\delta = -0.95$, where c and δ are the local-to-unity AR and endogeneity correlation parameters, respectively.

(a) $c = 0$

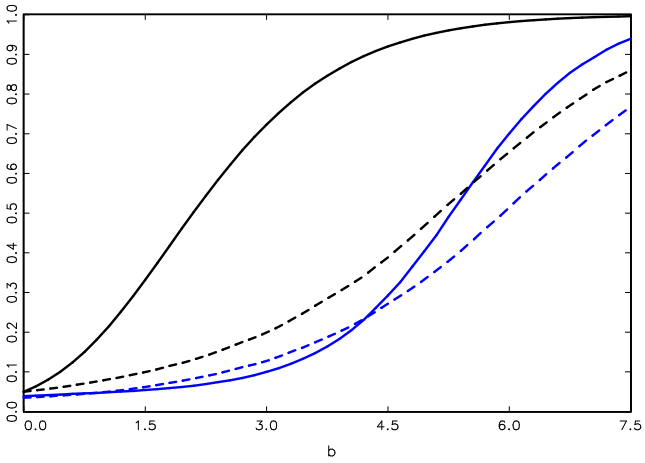

(b) $c = -2$

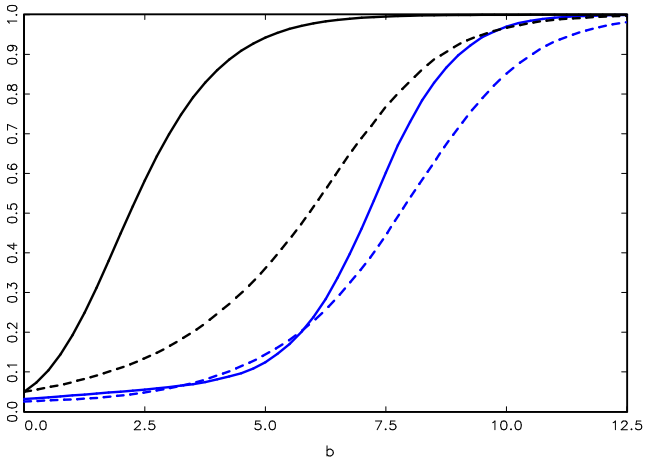

(c) $c = -5$

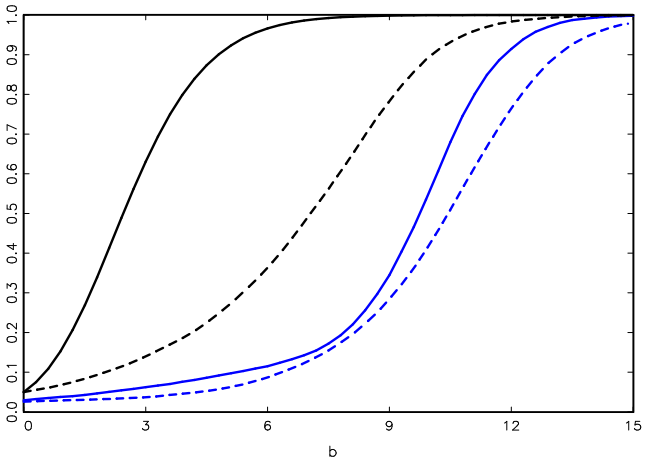

(d) $c = -10$

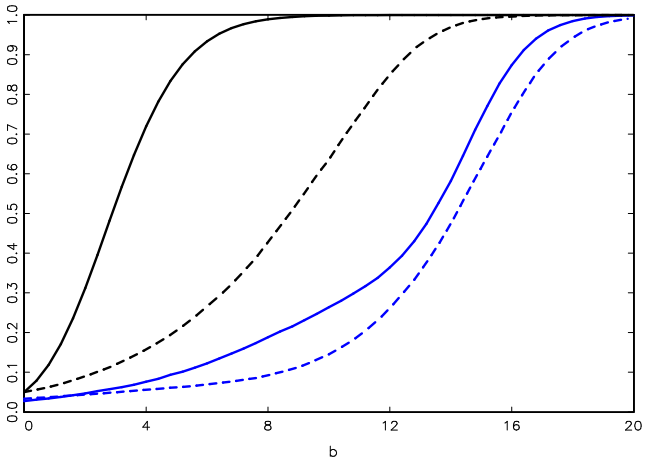

(e) $c = -20$

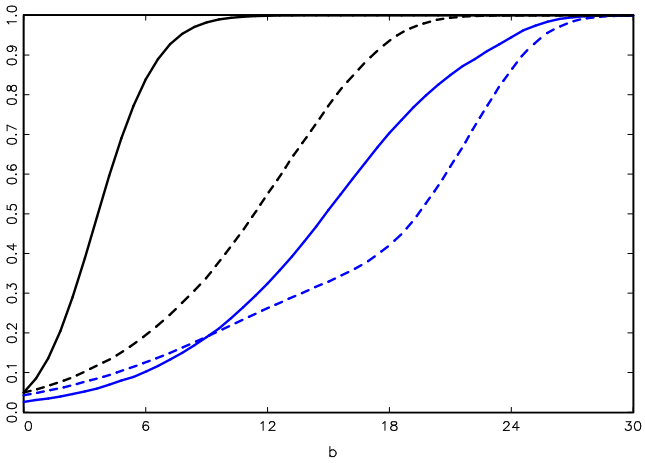

(f) $c = -50$

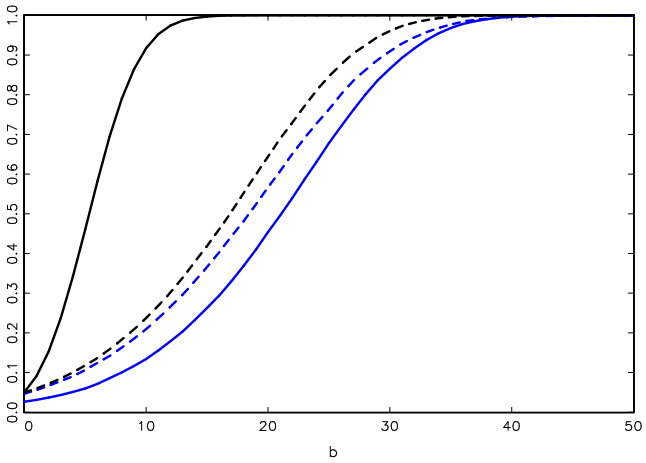

t_τ^{OLS}: – – , Q_τ^{GLS}: ——, Infeasible t_τ: – – , Infeasible Q_τ: ——

Figure S.3: Local Asymptotic Power of Right-Tailed Tests. DGP (1)-(3) with $c = 0$, $\delta = -0.95$ and $\kappa = \{0.0, 0.2, 0.4, 0.6, 0.8, 1.0\}$, where c, κ and δ are the local-to-unity AR, local-to-zero trend, and endogeneity correlation parameters, respectively.

(a) $\kappa = 0.0$

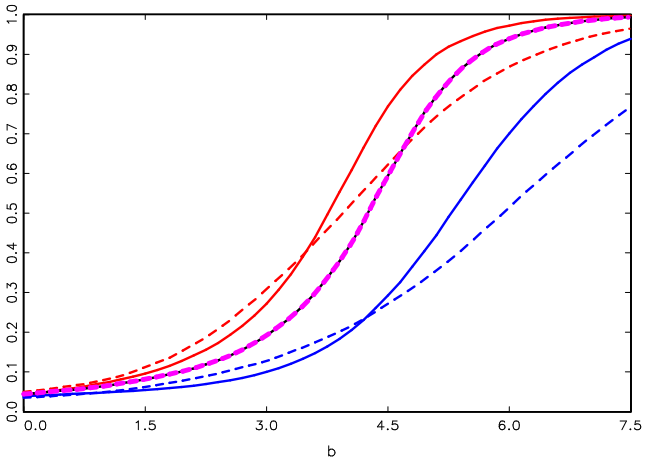

(b) $\kappa = 0.2$

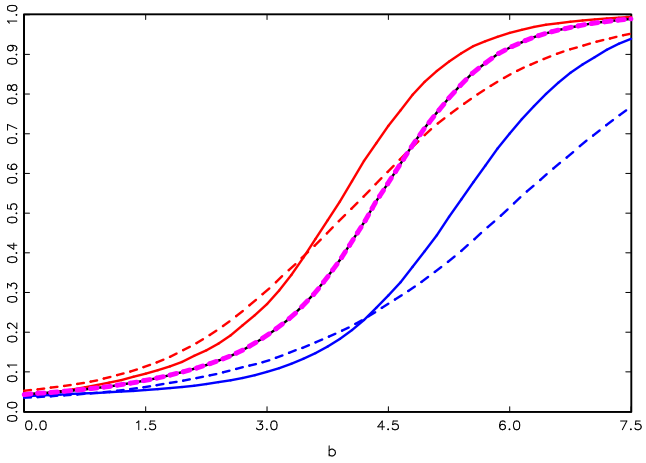

(c) $\kappa = 0.4$

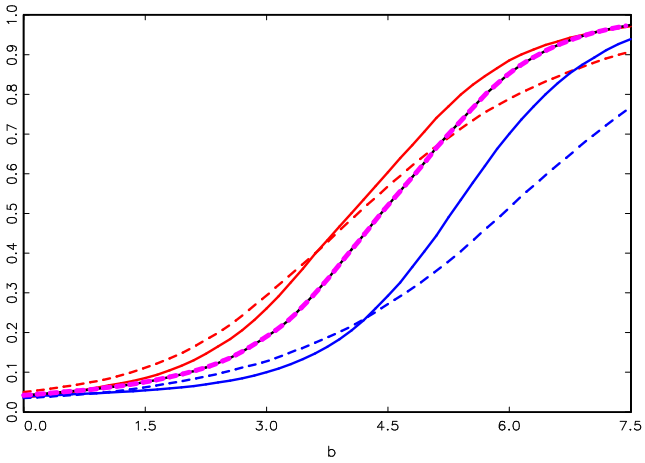

(d) $\kappa = 0.6$

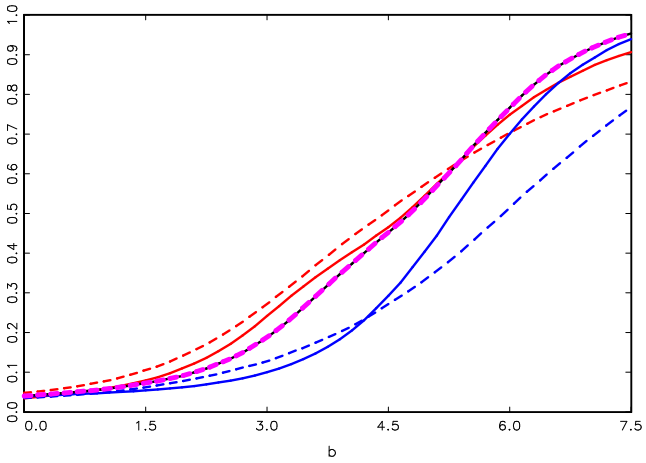

(e) $\kappa = 0.8$

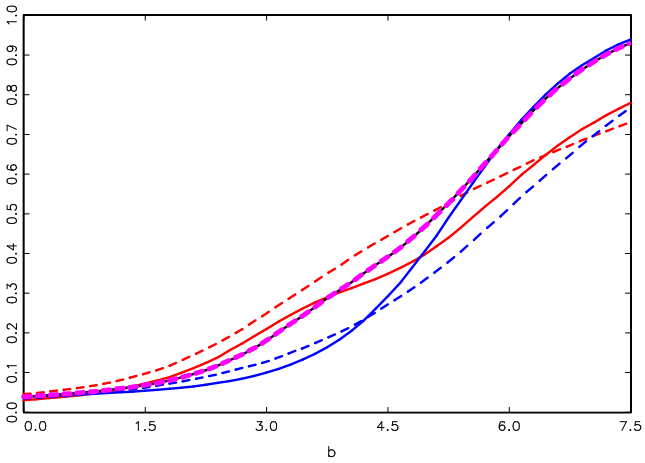

(f) $\kappa = 1.0$

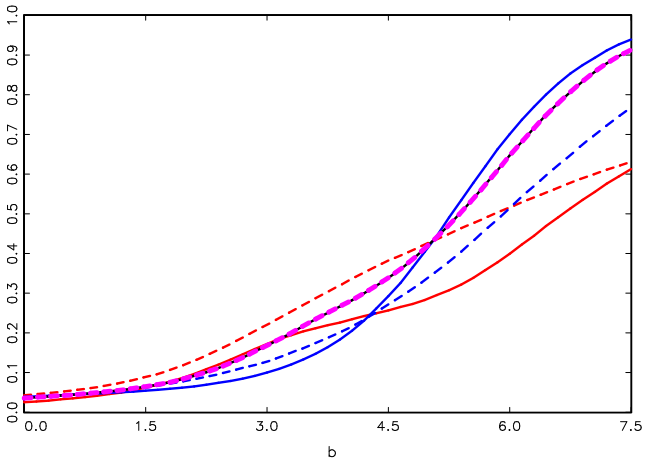

t_μ^{OLS}: – –, Q_μ^{GLS}: ——, t_τ^{OLS}: – –, Q_τ^{GLS}: ——, U^{hyb}: ——, S^{hyb}: – –

Figure S.4: Local Asymptotic Power of Right-Tailed Tests. DGP (1)-(3) with $c = -2$, $\delta = -0.95$ and $\kappa = \{0.0, 0.2, 0.4, 0.6, 0.8, 1.0\}$, where c, κ and δ are the local-to-unity AR, local-to-zero trend, and endogeneity correlation parameters, respectively.

(a) $\kappa = 0.0$

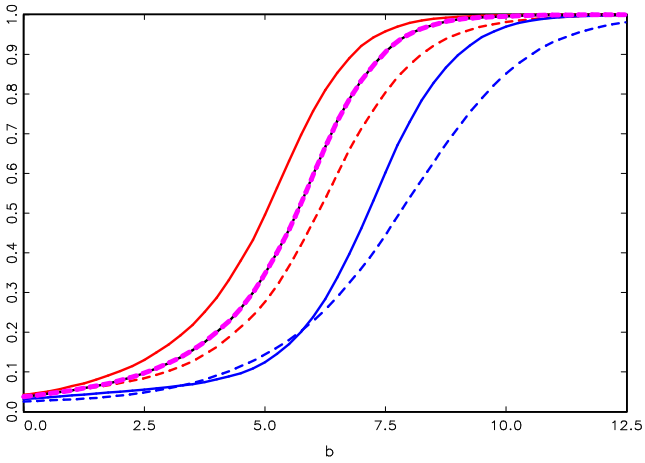

(b) $\kappa = 0.2$

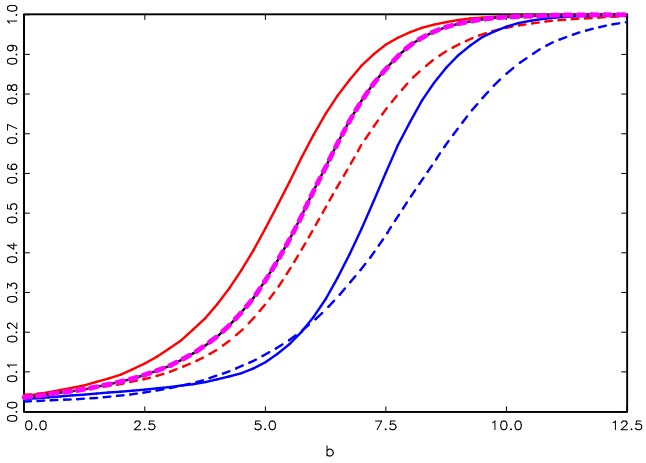

(c) $\kappa = 0.4$

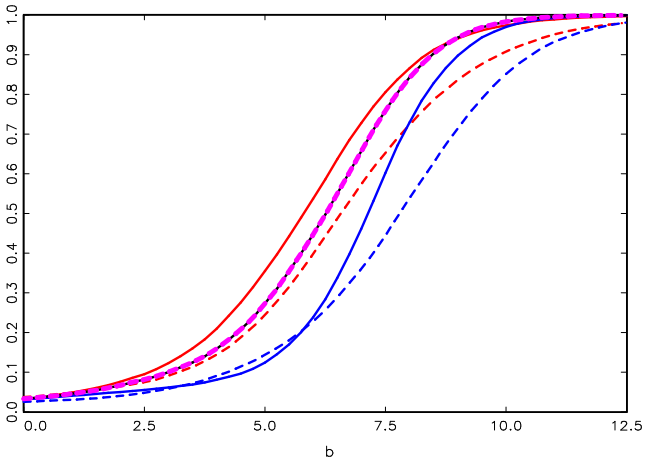

(d) $\kappa = 0.6$

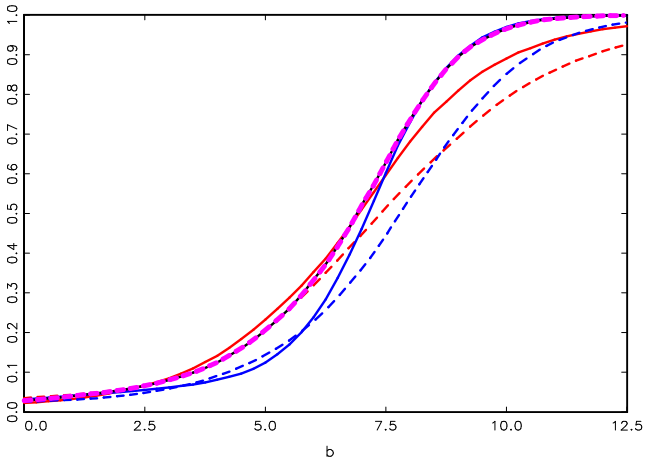

(e) $\kappa = 0.8$

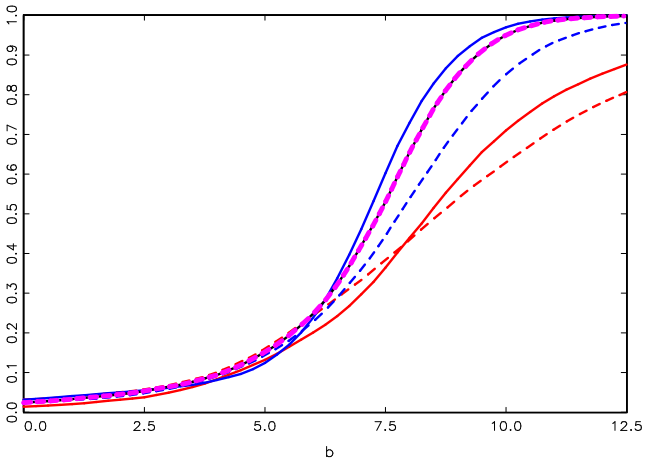

(f) $\kappa = 1.0$

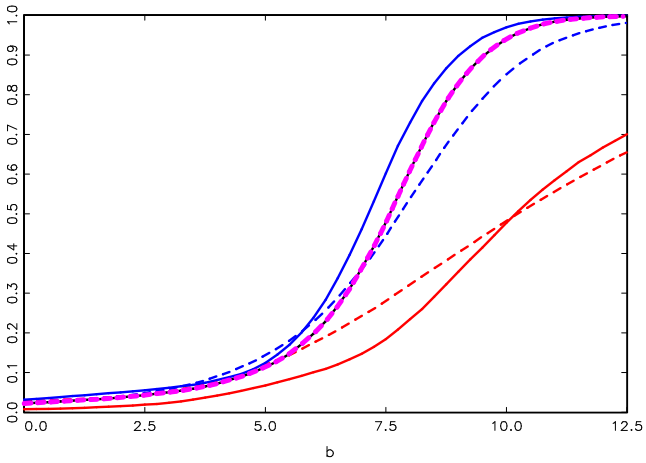

t_μ^{OLS}: – – , Q_μ^{GLS}: ——— , t_τ^{OLS}: – –, Q_τ^{GLS}: ———, U^{hyb}: ———, S^{hyb}: – –

Figure S.5: Local Asymptotic Power of Right-Tailed Tests. DGP (1)-(3) with $c = -5$, $\delta = -0.95$ and $\kappa = \{0.0, 0.2, 0.4, 0.6, 0.8, 1.0\}$, where c, κ and δ are the local-to-unity AR, local-to-zero trend, and endogeneity correlation parameters, respectively.

(a) $\kappa = 0.0$

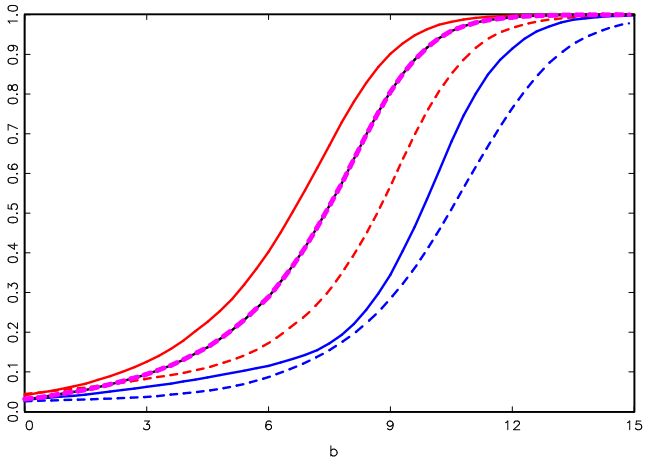

(b) $\kappa = 0.2$

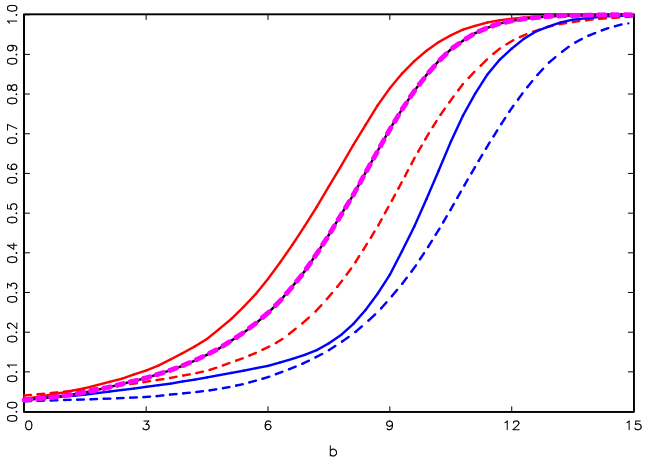

(c) $\kappa = 0.4$

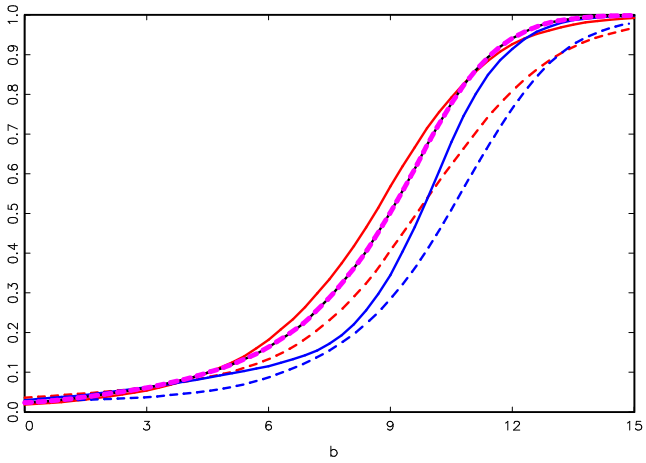

(d) $\kappa = 0.6$

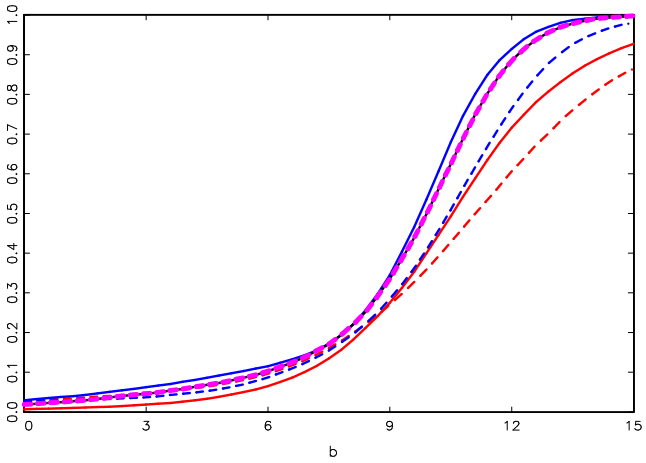

(e) $\kappa = 0.8$

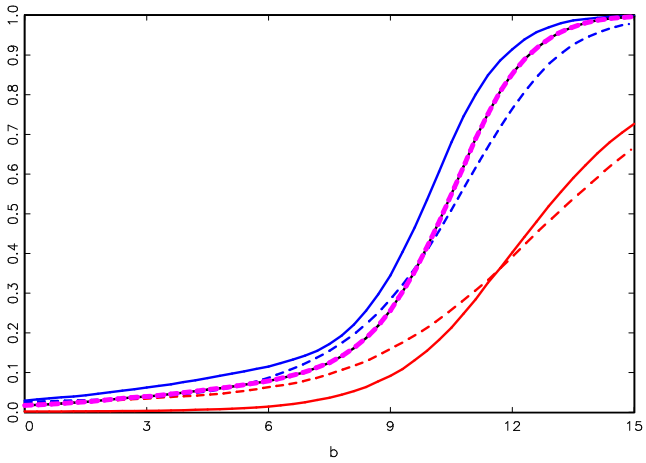

(f) $\kappa = 1.0$

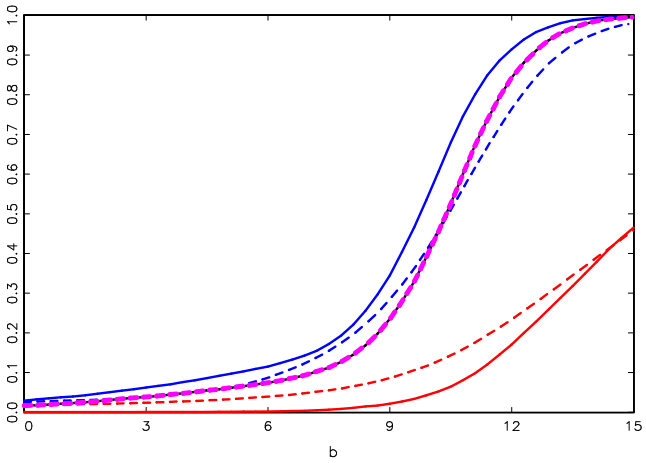

t_μ^{OLS}: – –, Q_μ^{GLS}: ——, t_τ^{OLS}: – –, Q_τ^{GLS}: ——, U^{hyb}: ——, S^{hyb}: – –

Figure S.6: Local Asymptotic Power of Right-Tailed Tests. DGP (1)-(3) with $c = -10$, $\delta = -0.95$ and $\kappa = \{0.0, 0.2, 0.4, 0.6, 0.8, 1.0\}$, where c, κ and δ are the local-to-unity AR, local-to-zero trend, and endogeneity correlation parameters, respectively.

(a) $\kappa = 0.0$

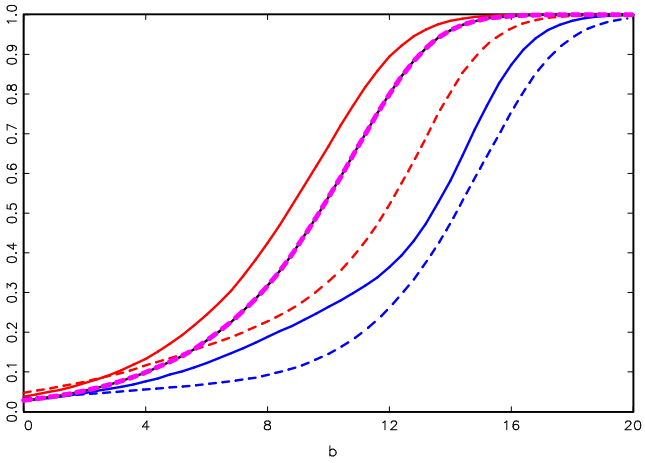

(b) $\kappa = 0.2$

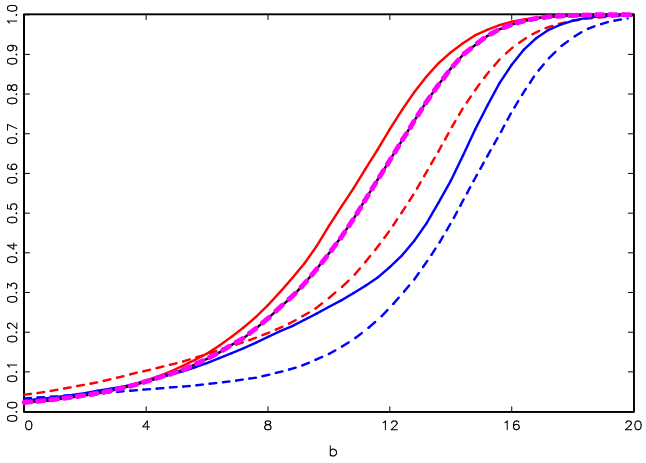

(c) $\kappa = 0.4$

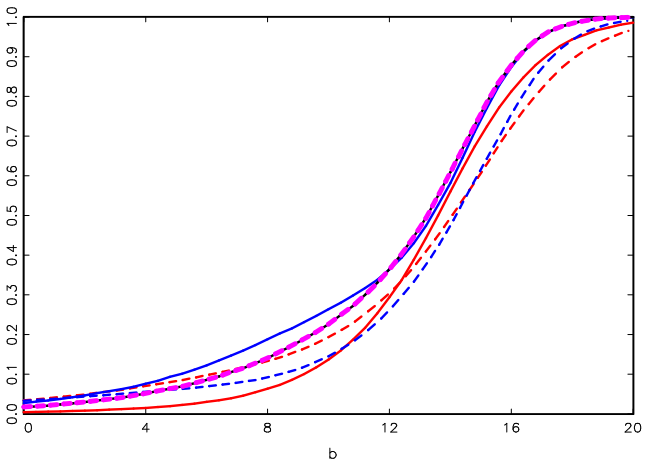

(d) $\kappa = 0.6$

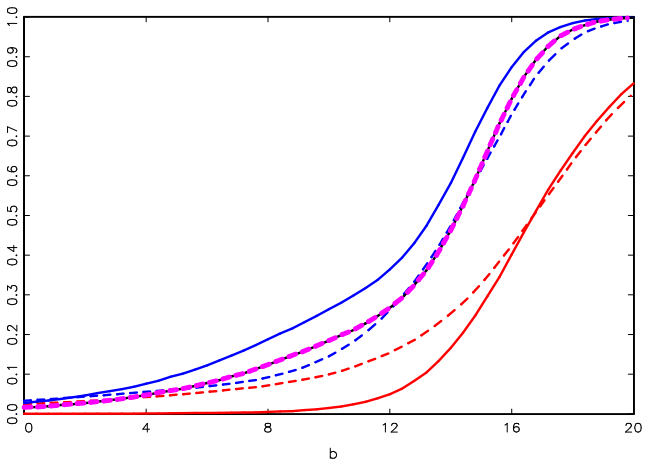

(e) $\kappa = 0.8$

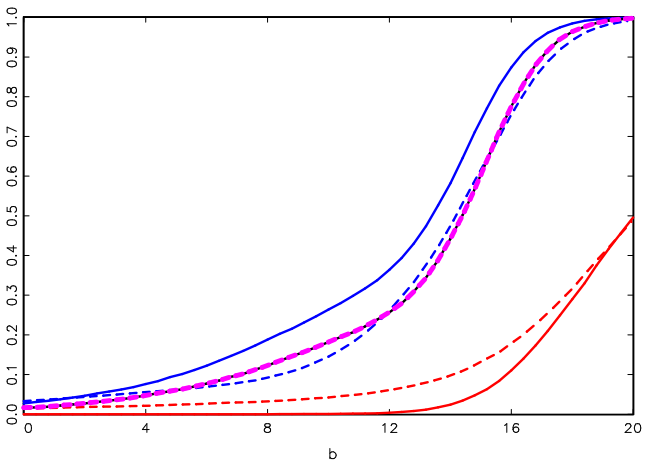

(f) $\kappa = 1.0$

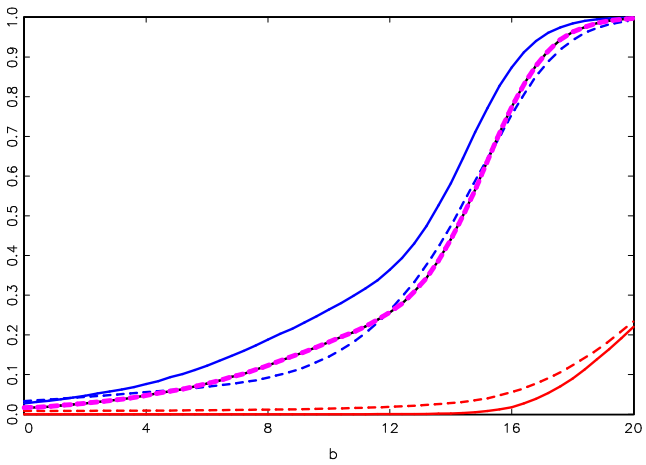

t_μ^{OLS}: – – , Q_μ^{GLS}: ——— , t_τ^{OLS}: – –, Q_τ^{GLS}: ———, U^{hyb}: ———, S^{hyb}: – –

Figure S.7: Local Asymptotic Power of Right-Tailed Tests. DGP (1)-(3) with $c = -20$, $\delta = -0.95$ and $\kappa = \{0.0, 0.1, 0.2, 0.3, 0.4, 0.5\}$, where c, κ and δ are the local-to-unity AR, local-to-zero trend, and endogeneity correlation parameters, respectively.

(a) $\kappa = 0.0$

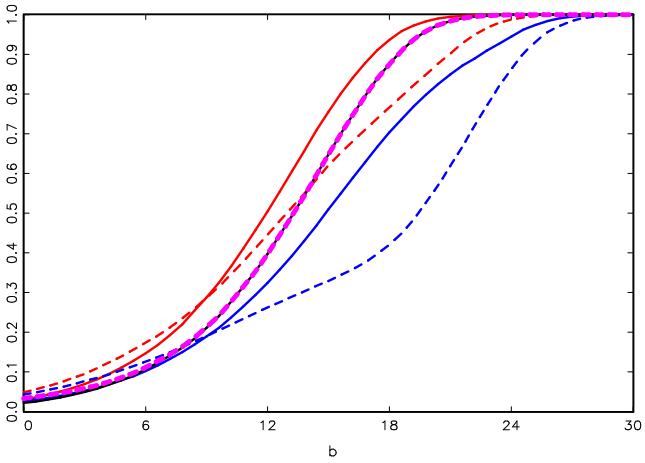

(b) $\kappa = 0.1$

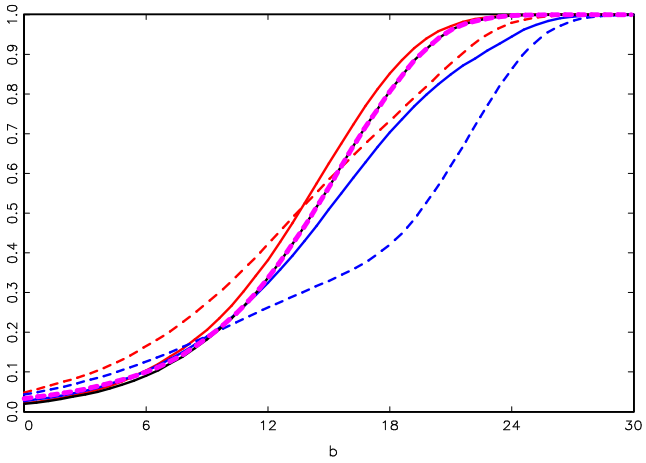

(c) $\kappa = 0.2$

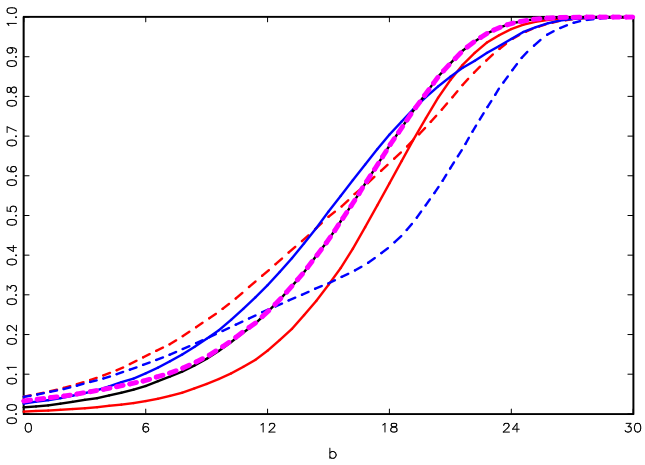

(d) $\kappa = 0.3$

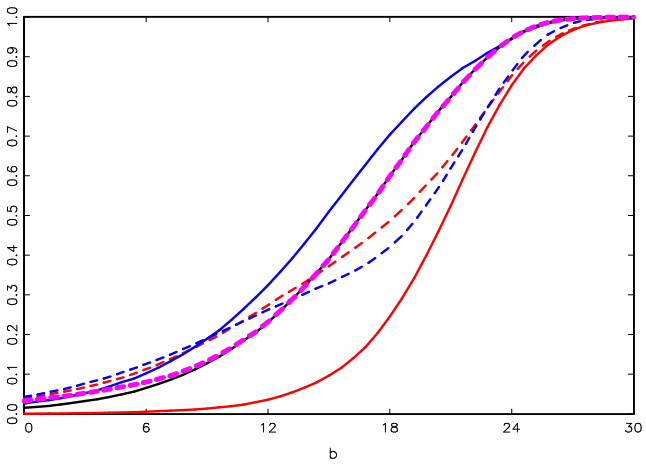

(e) $\kappa = 0.4$

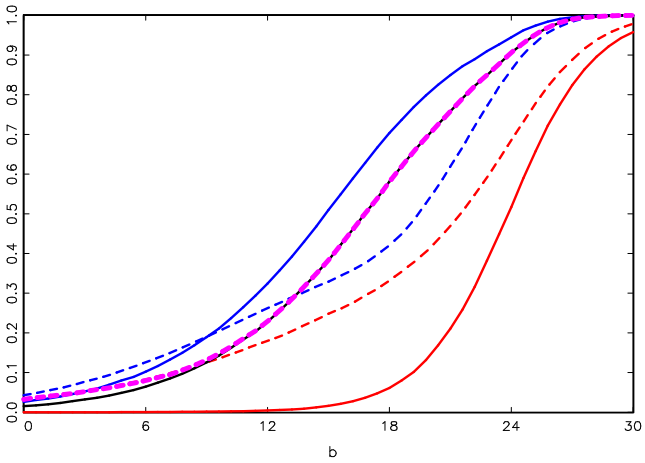

(f) $\kappa = 0.5$

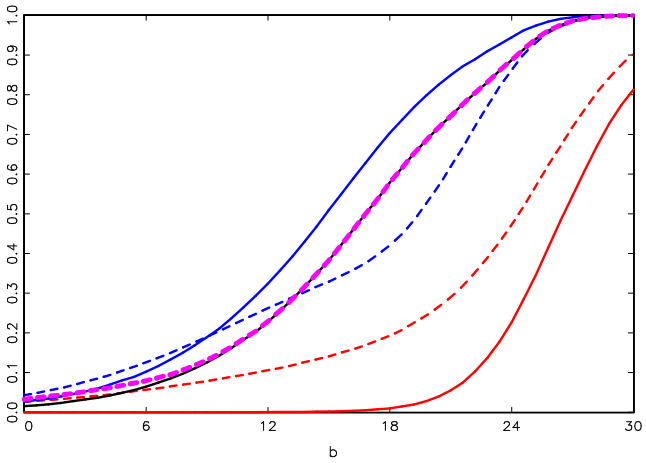

t_{μ}^{OLS}: – –, Q_{μ}^{GLS}: ——, t_{τ}^{OLS}: – –, Q_{τ}^{GLS}: ——, U^{hyb}: ——, S^{hyb}: – –

Figure S.8: Local Asymptotic Power of Right-Tailed Tests. DGP (1)-(3) with $c = -30$, $\delta = -0.95$ and $\kappa = \{0.0, 0.1, 0.2, 0.3, 0.4, 0.5\}$, where c, κ and δ are the local-to-unity AR, local-to-zero trend, and endogeneity correlation parameters, respectively.

(a) $\kappa = 0.0$

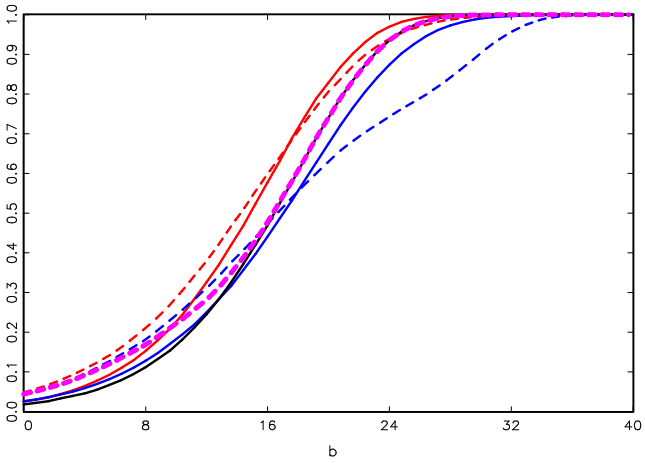

(b) $\kappa = 0.1$

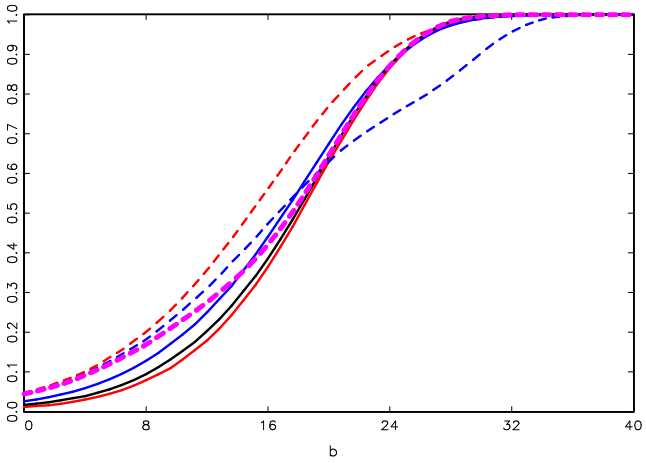

(c) $\kappa = 0.2$

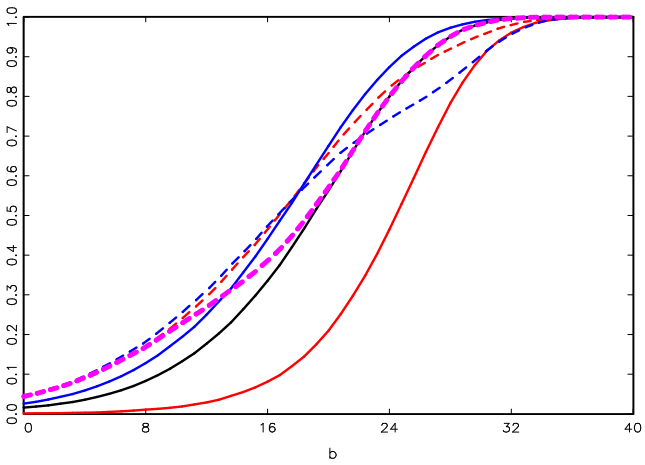

(d) $\kappa = 0.3$

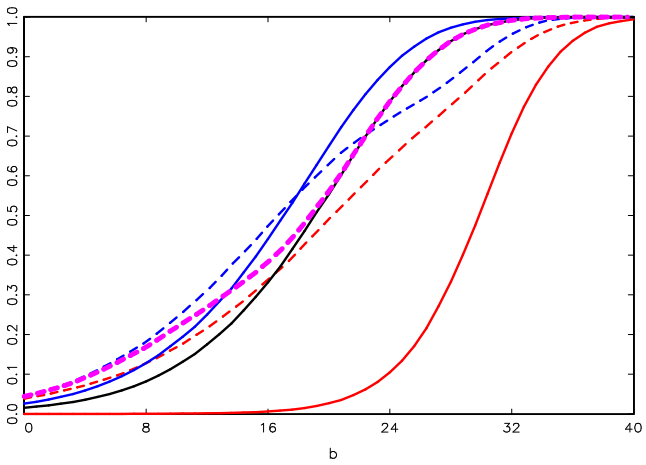

(e) $\kappa = 0.4$

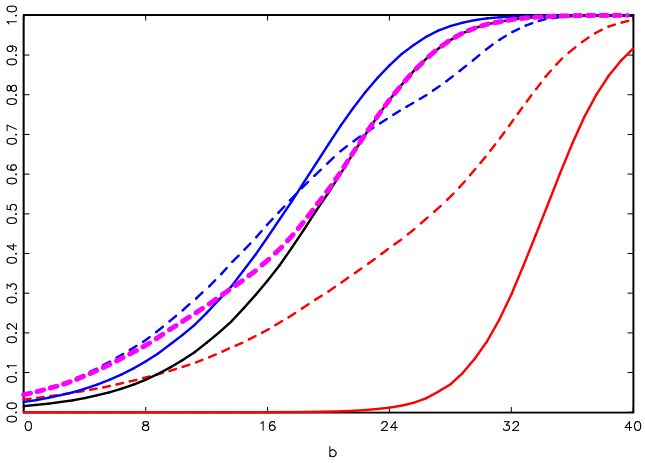

(f) $\kappa = 0.5$

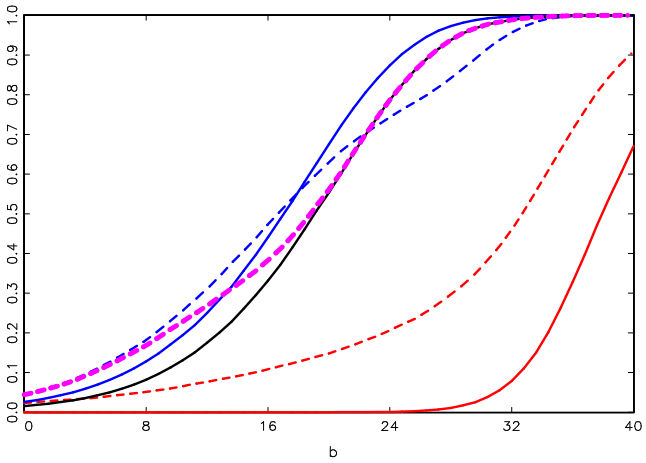

t_μ^{OLS}: – –, Q_μ^{GLS}: ——, t_τ^{OLS}: – –, Q_τ^{GLS}: ——, U^{hyb}: ——, S^{hyb}: – –

Figure S.9: Local Asymptotic Power of Right-Tailed Tests. DGP (1)-(3) with $c = -40$, $\delta = -0.95$ and $\kappa = \{0.0, 0.1, 0.2, 0.3, 0.4, 0.5\}$, where c, κ and δ are the local-to-unity AR, local-to-zero trend, and endogeneity correlation parameters, respectively.

(a) $\kappa = 0.0$

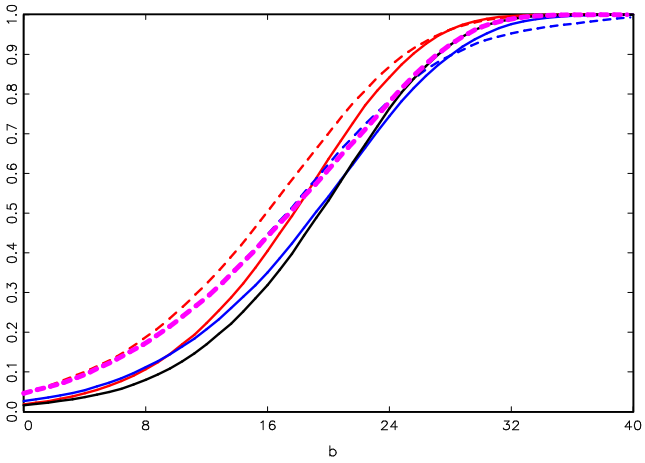

(b) $\kappa = 0.1$

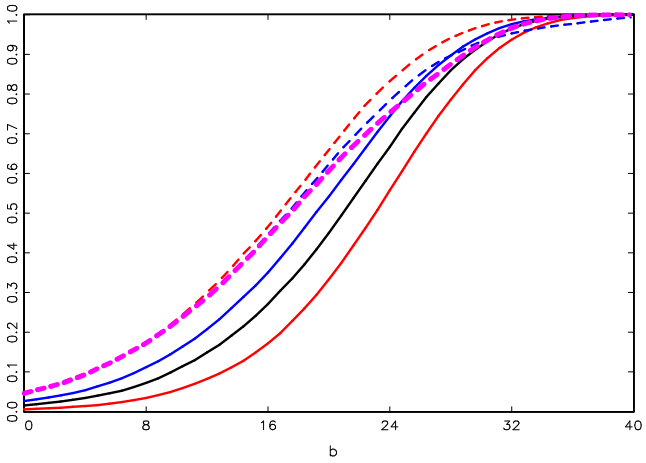

(c) $\kappa = 0.2$

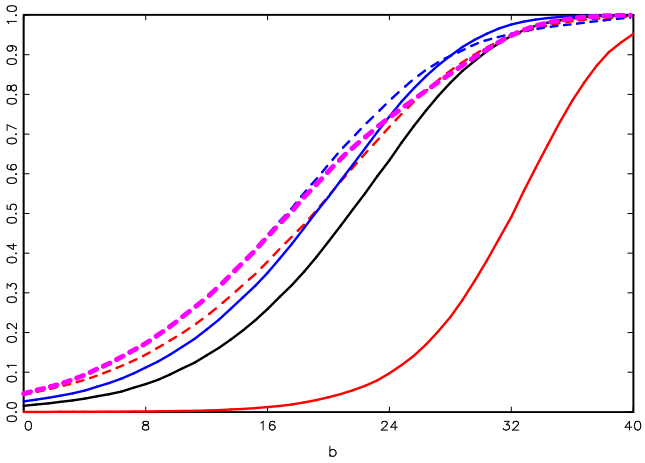

(d) $\kappa = 0.3$

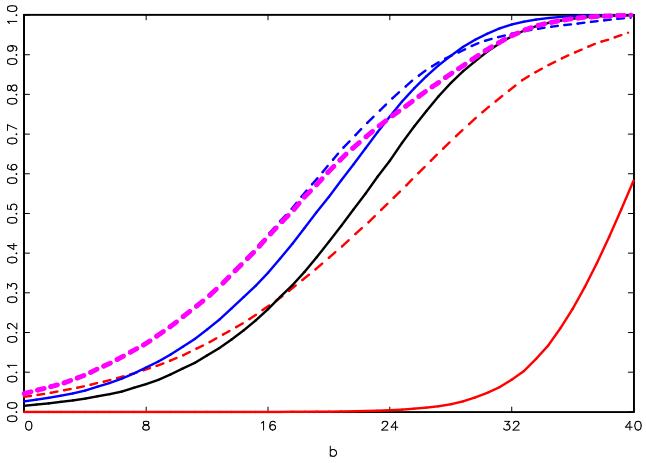

(e) $\kappa = 0.4$

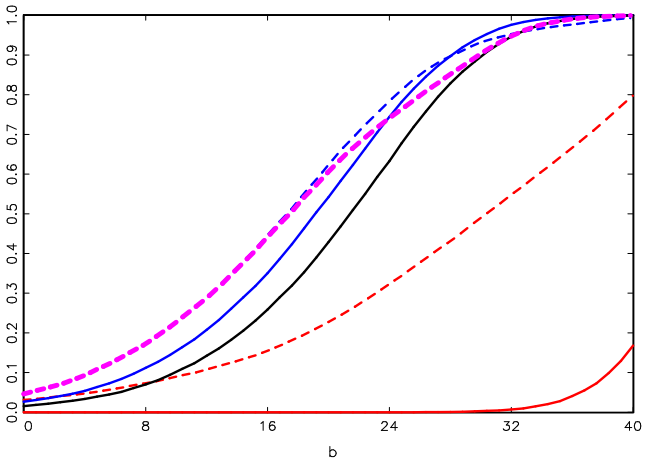

(f) $\kappa = 0.5$

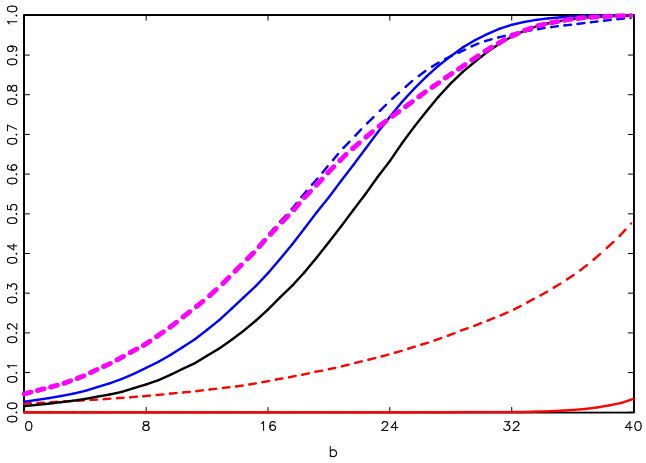

t_μ^{OLS}: – – , Q_μ^{GLS}: ——— , t_τ^{OLS}: – –, Q_τ^{GLS}: ———, U^{hyb}: ———, S^{hyb}: – –

Figure S.10: Local Asymptotic Power of Right-Tailed Tests. DGP (1)-(3) with $c = -50$, $\delta = -0.95$ and $\kappa = \{0.0, 0.1, 0.2, 0.3, 0.4, 0.5\}$, where c, κ and δ are the local-to-unity AR, local-to-zero trend, and endogeneity correlation parameters, respectively.

(a) $\kappa = 0.0$

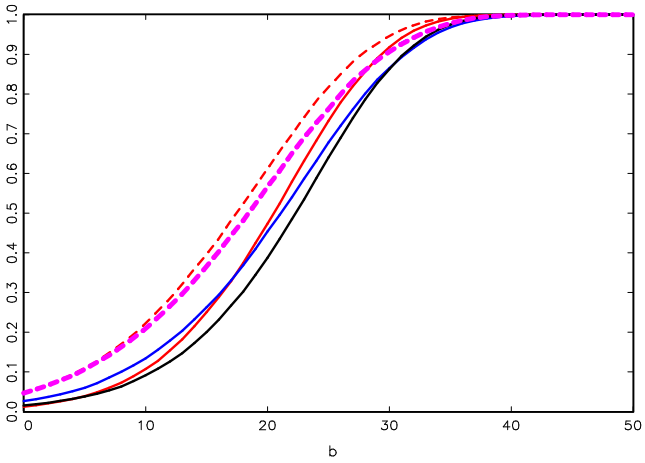

(b) $\kappa = 0.1$

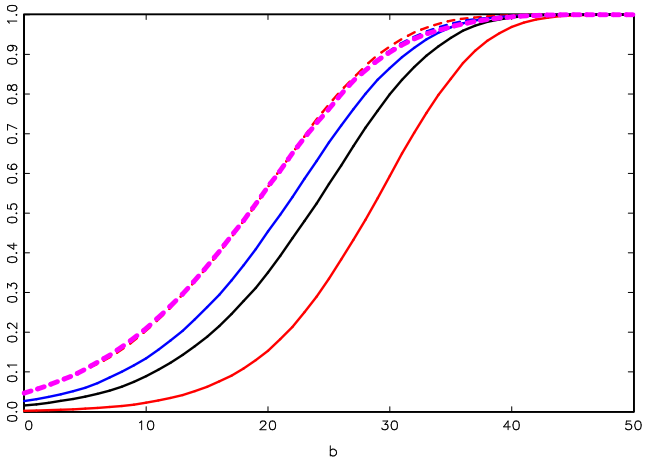

(c) $\kappa = 0.2$

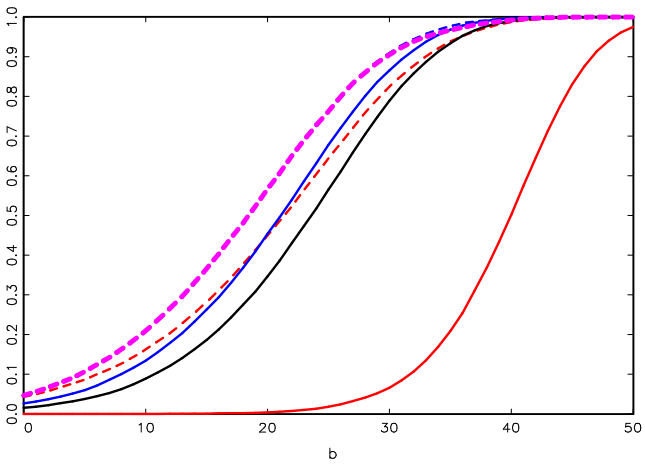

(d) $\kappa = 0.3$

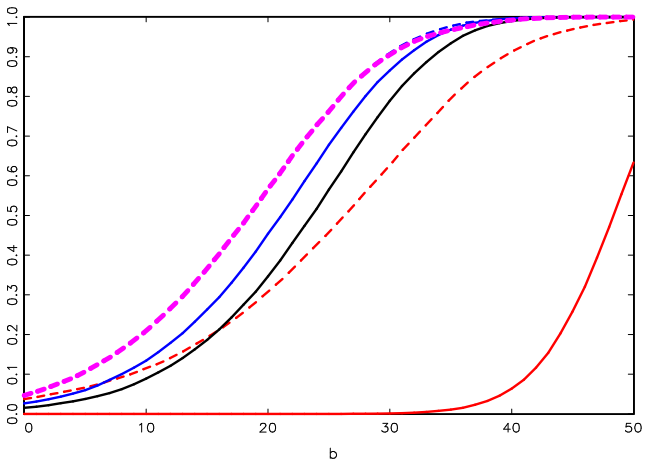

(e) $\kappa = 0.4$

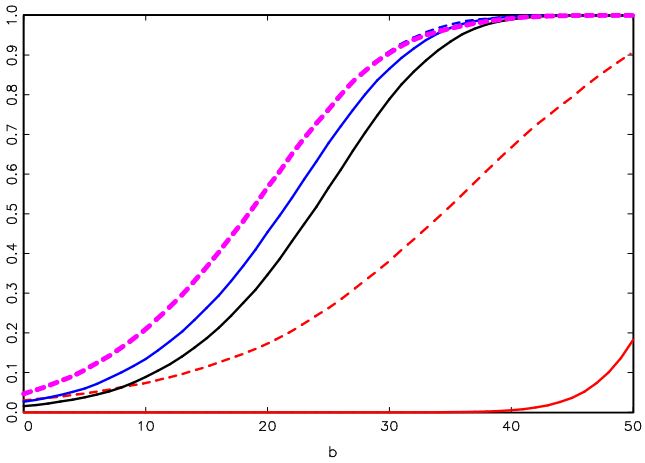

(f) $\kappa = 0.5$

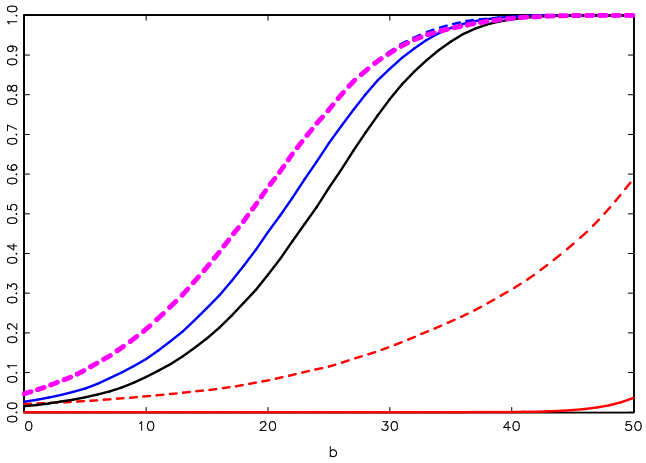

t_μ^{OLS}: – – , Q_μ^{GLS}: ——— , t_τ^{OLS}: – –, Q_τ^{GLS}: ———, U^{hyb}: ———, S^{hyb}: – –

Figure S.11: Local Asymptotic Power of Left-Tailed Tests. DGP (1)-(3) with $c = 0$, $\delta = -0.95$ and $\kappa = \{0.0, 0.2, 0.4, 0.6, 0.8, 1.0\}$, where c, κ and δ are the local-to-unity AR, local-to-zero trend, and endogeneity correlation parameters, respectively.

(a) $\kappa = 0.0$

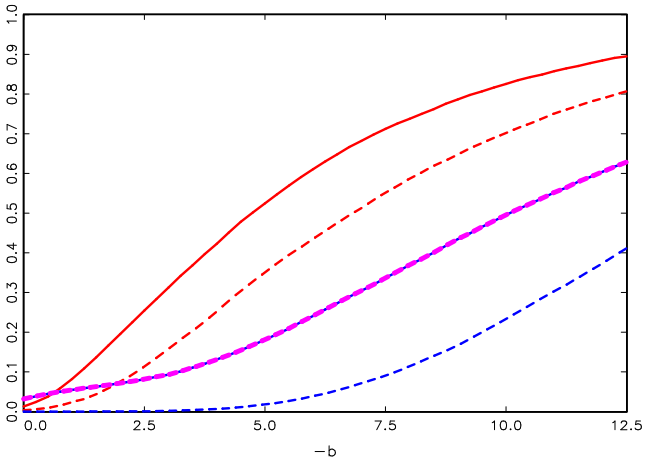

(b) $\kappa = 0.2$

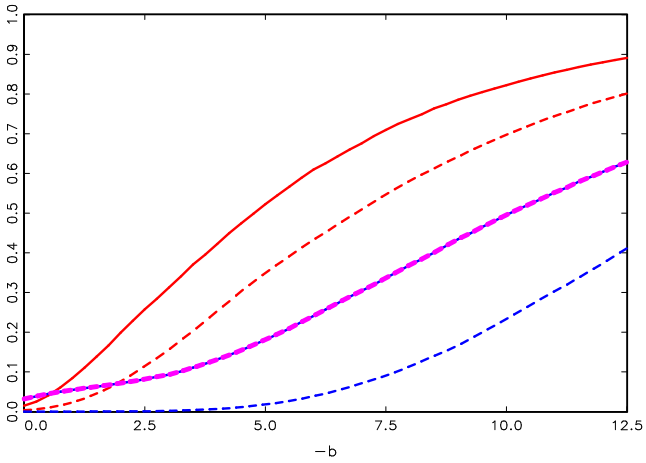

(c) $\kappa = 0.4$

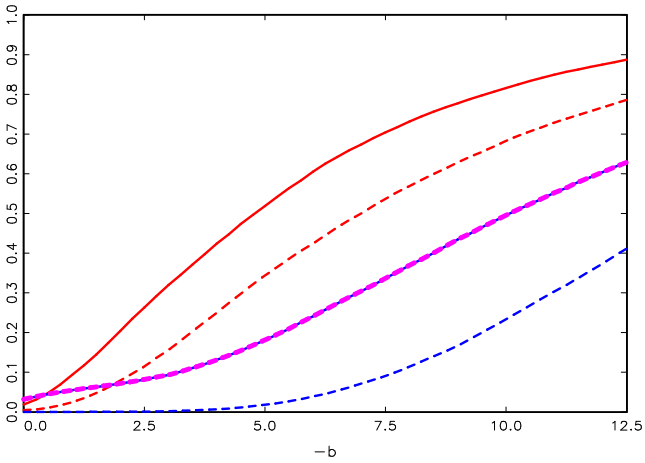

(d) $\kappa = 0.6$

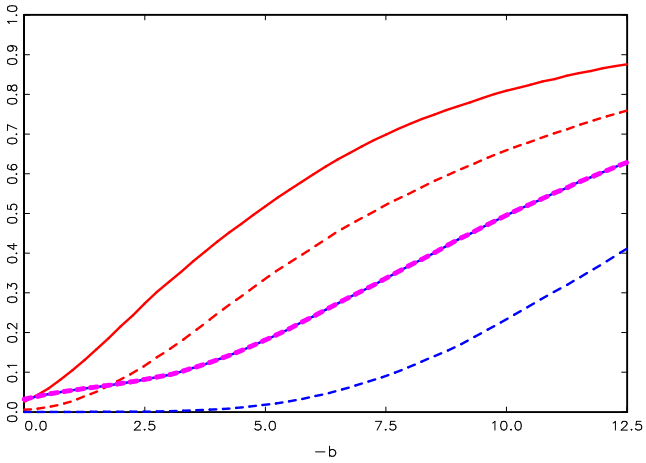

(e) $\kappa = 0.8$

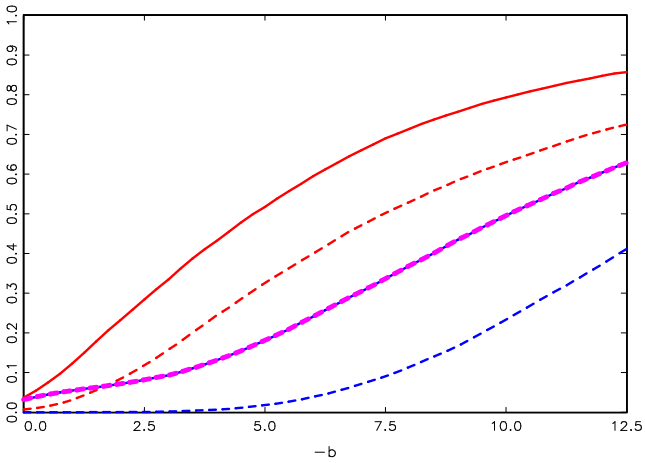

(f) $\kappa = 1.0$

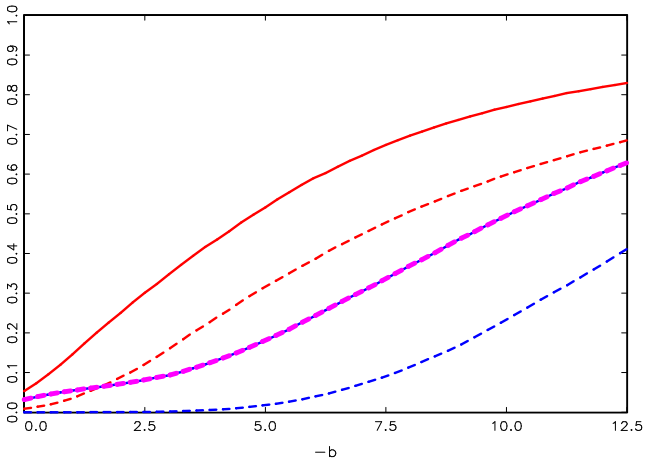

t_μ^{OLS}: – –, Q_μ^{GLS}: ——, t_τ^{OLS}: – –, Q_τ^{GLS}: ——, S^{hyb}: – –

Figure S.12: Local Asymptotic Power of Left-Tailed Tests. DGP (1)-(3) with $c = -2$, $\delta = -0.95$ and $\kappa = \{0.0, 0.2, 0.4, 0.6, 0.8, 1.0\}$, where c, κ and δ are the local-to-unity AR, local-to-zero trend, and endogeneity correlation parameters, respectively.

(a) $\kappa = 0.0$

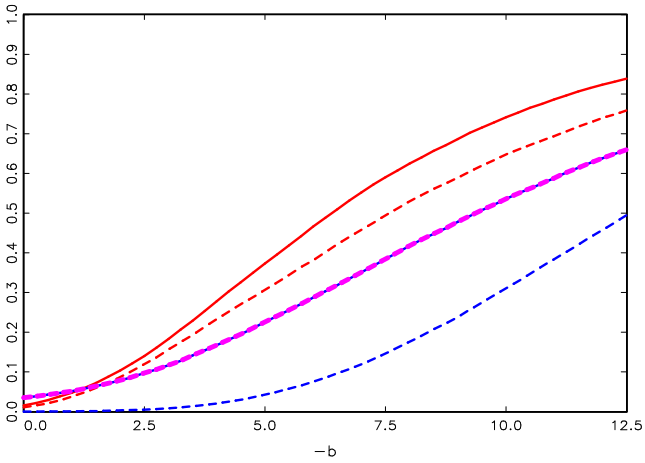

(b) $\kappa = 0.2$

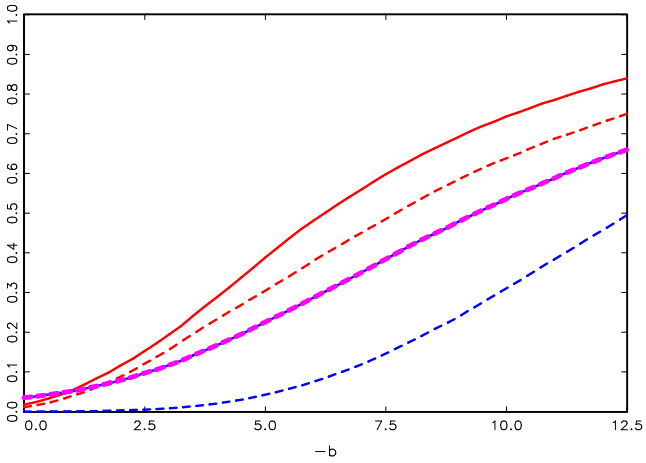

(c) $\kappa = 0.4$

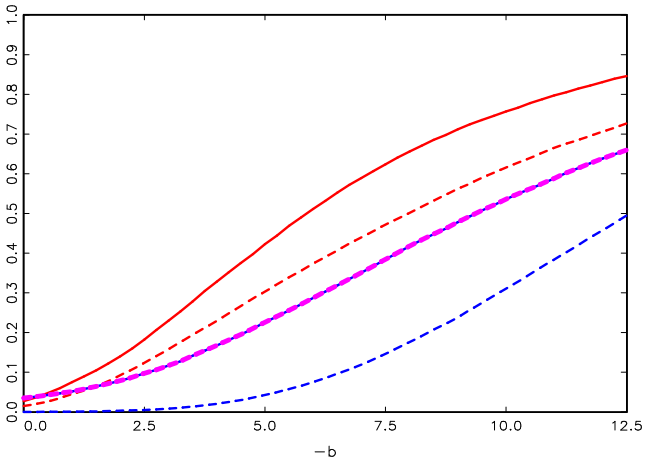

(d) $\kappa = 0.6$

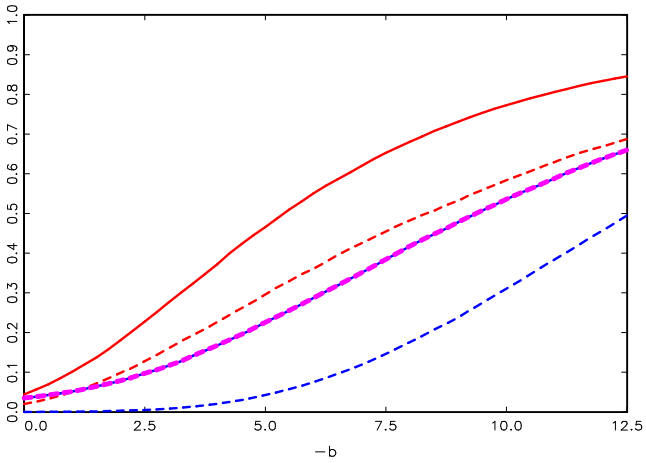

(e) $\kappa = 0.8$

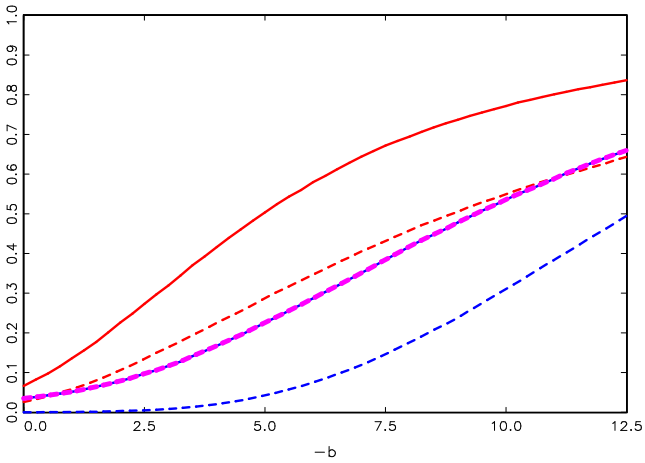

(f) $\kappa = 1.0$

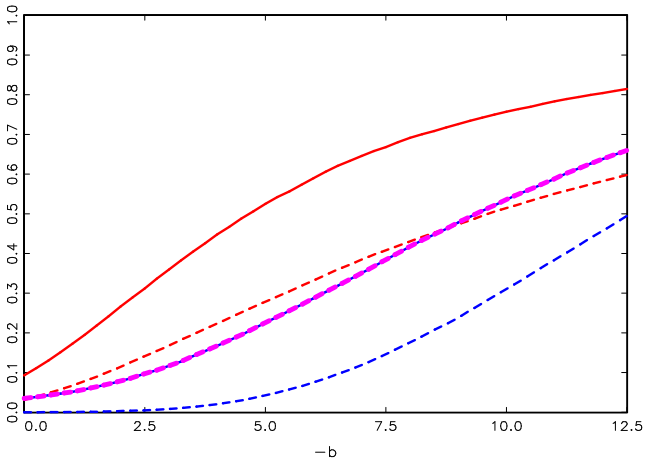

t_{μ}^{OLS}: – –, Q_{μ}^{GLS}: ——, t_{τ}^{OLS}: – –, Q_{τ}^{GLS}: ——, S^{hyb}: – –

Figure S.13: Local Asymptotic Power of Left-Tailed Tests. DGP (1)-(3) with $c = -5$, $\delta = -0.95$ and $\kappa = \{0.0, 0.2, 0.4, 0.6, 0.8, 1.0\}$, where c, κ and δ are the local-to-unity AR, local-to-zero trend, and endogeneity correlation parameters, respectively.

(a) $\kappa = 0.0$

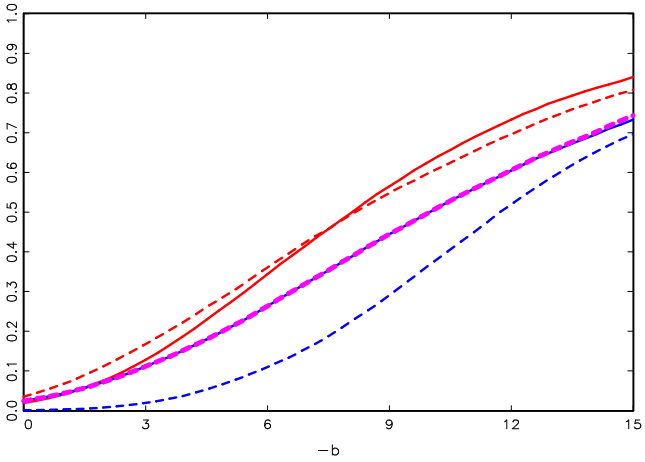

(b) $\kappa = 0.2$

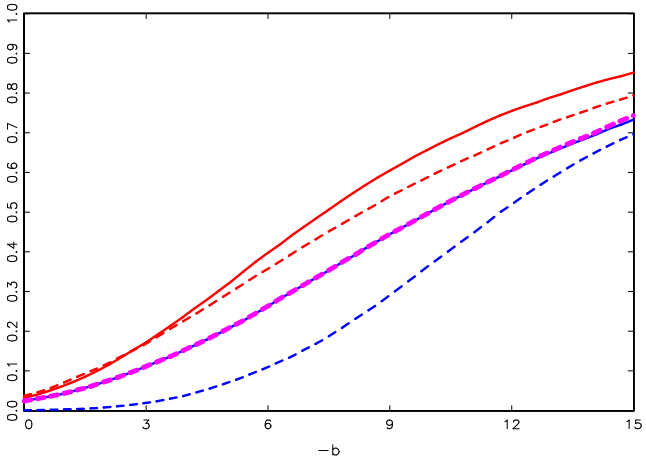

(c) $\kappa = 0.4$

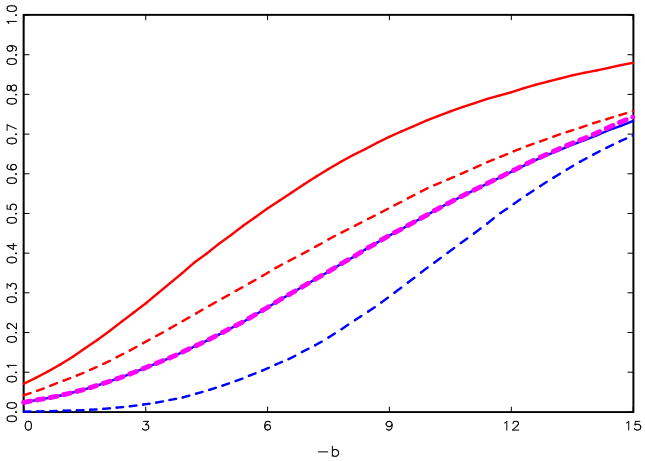

(d) $\kappa = 0.6$

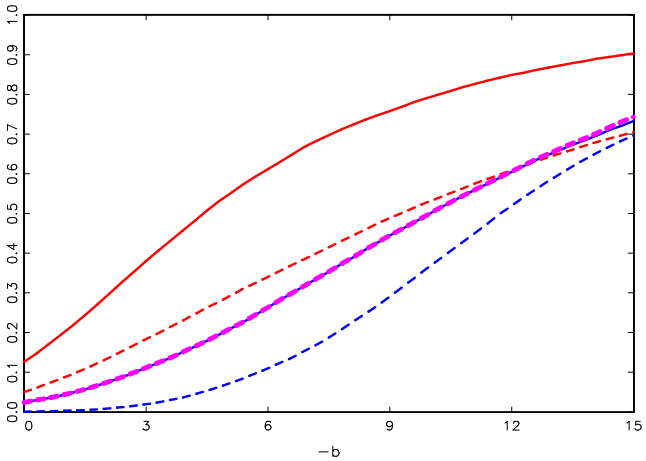

(e) $\kappa = 0.8$

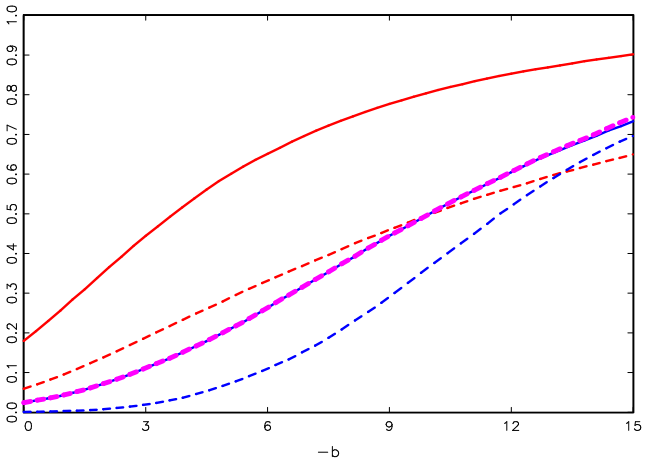

(f) $\kappa = 1.0$

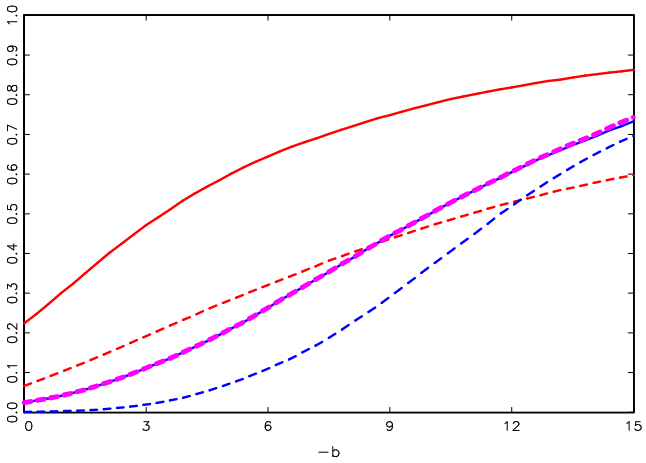

t_μ^{OLS}: – –, Q_μ^{GLS}: ——, t_τ^{OLS}: – –, Q_τ^{GLS}: ——, S^{hyb}: – –

Figure S.14: Local Asymptotic Power of Left-Tailed Tests. DGP (1)-(3) with $c = -10$, $\delta = -0.95$ and $\kappa = \{0.0, 0.2, 0.4, 0.6, 0.8, 1.0\}$, where c, κ and δ are the local-to-unity AR, local-to-zero trend, and endogeneity correlation parameters, respectively.

(a) $\kappa = 0.0$

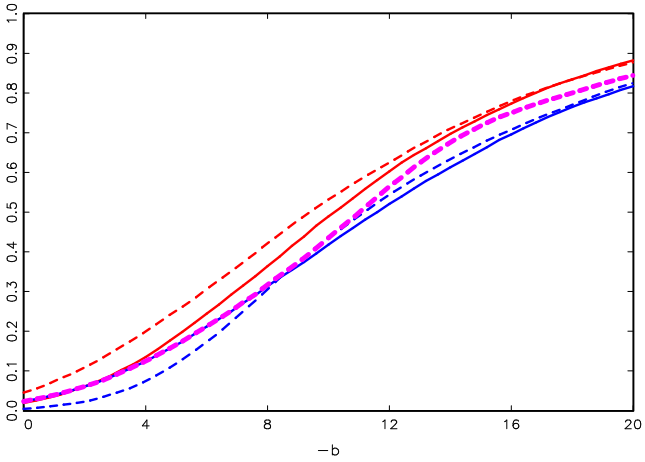

(b) $\kappa = 0.2$

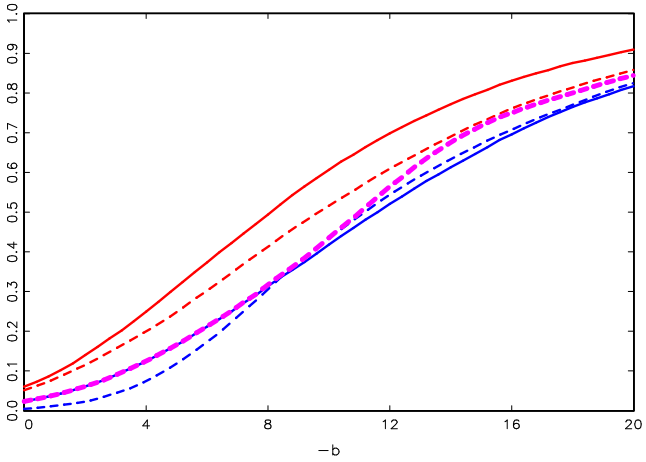

(c) $\kappa = 0.4$

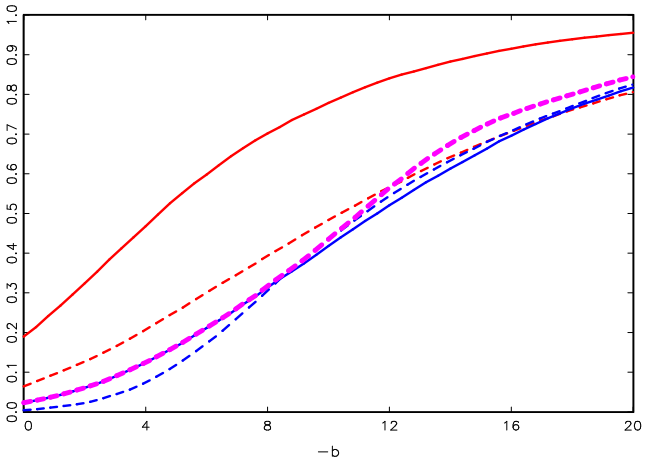

(d) $\kappa = 0.6$

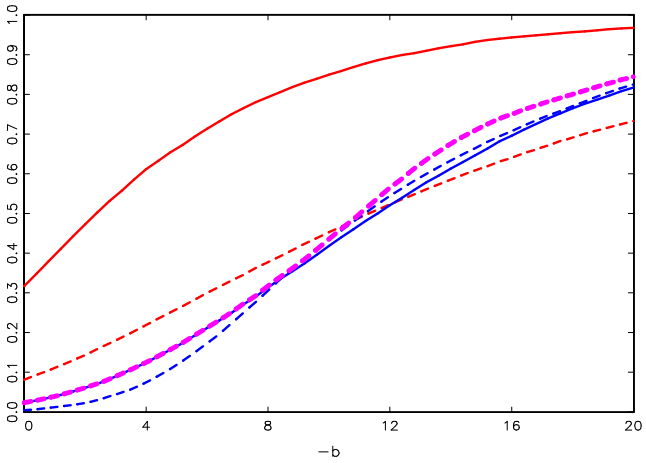

(e) $\kappa = 0.8$

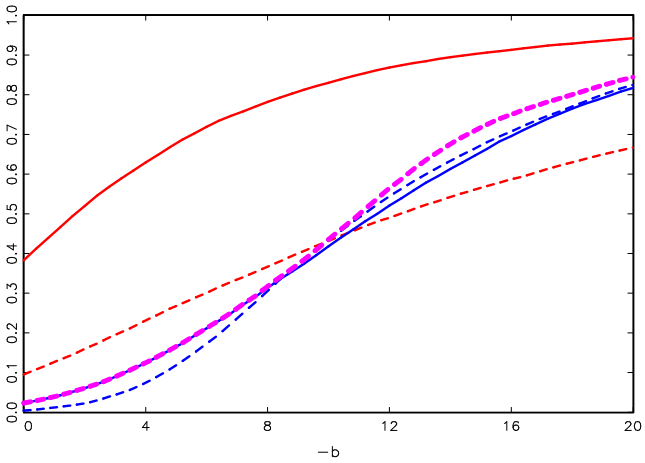

(f) $\kappa = 1.0$

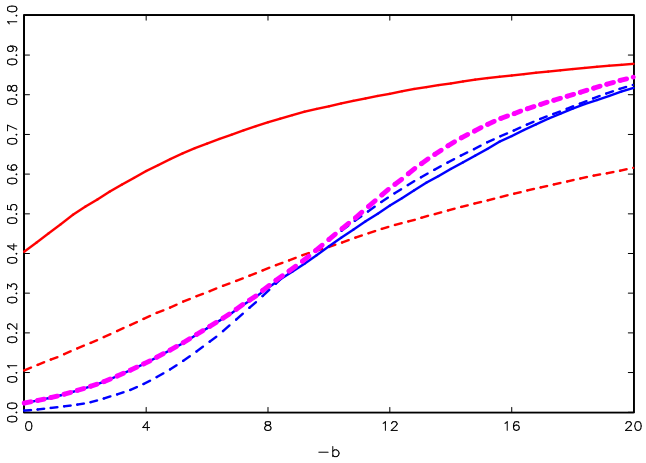

t_μ^{OLS}: – –, Q_μ^{GLS}: ——, t_τ^{OLS}: – –, Q_τ^{GLS}: ——, S^{hyb}: – –

Figure S.15: Local Asymptotic Power of Left-Tailed Tests. DGP (1)-(3) with $c = -20$, $\delta = -0.95$ and $\kappa = \{0.0, 0.1, 0.2, 0.3, 0.4, 0.5\}$, where c, κ and δ are the local-to-unity AR, local-to-zero trend, and endogeneity correlation parameters, respectively.

(a) $\kappa = 0.0$

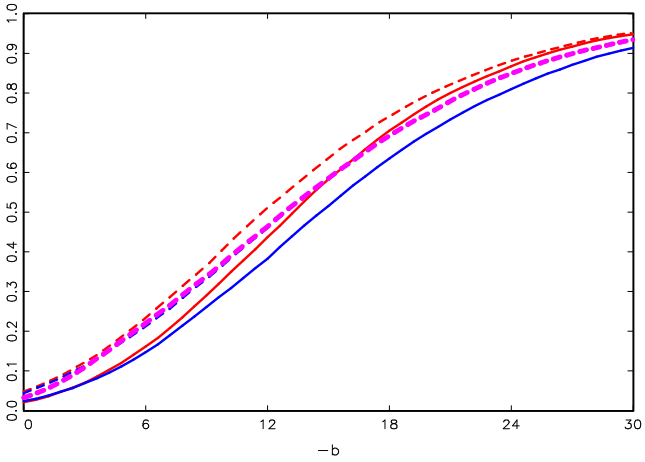

(b) $\kappa = 0.1$

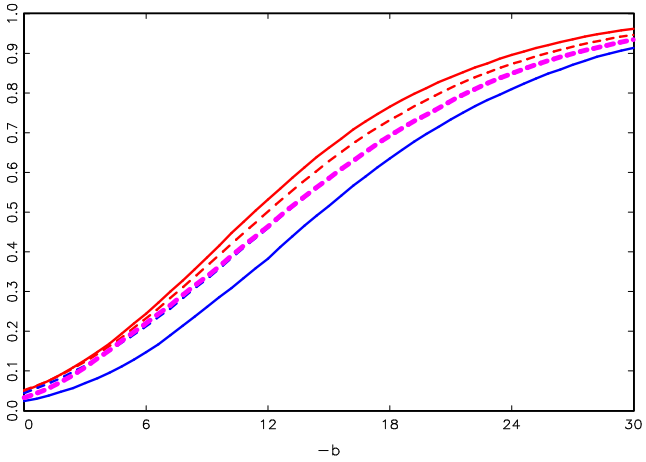

(c) $\kappa = 0.2$

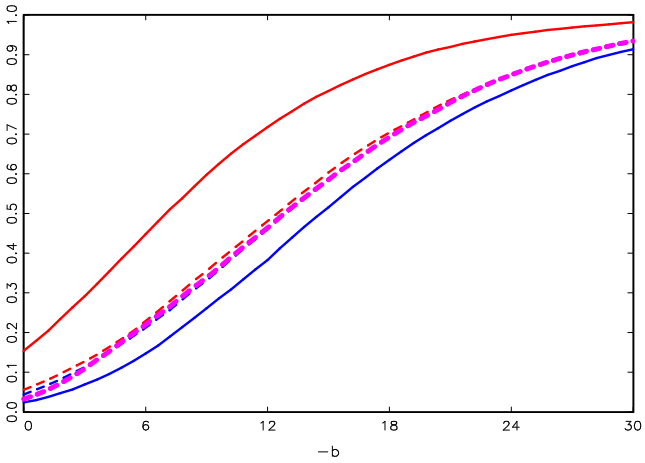

(d) $\kappa = 0.3$

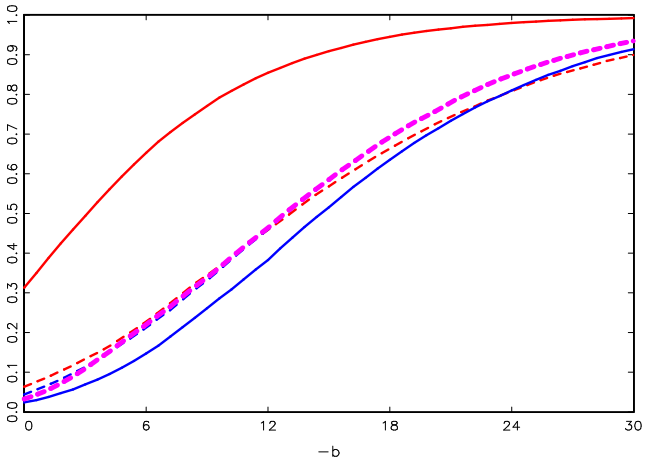

(e) $\kappa = 0.4$

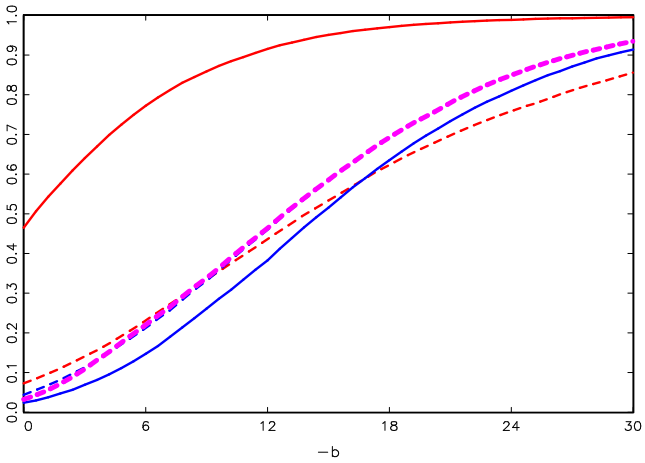

(f) $\kappa = 0.5$

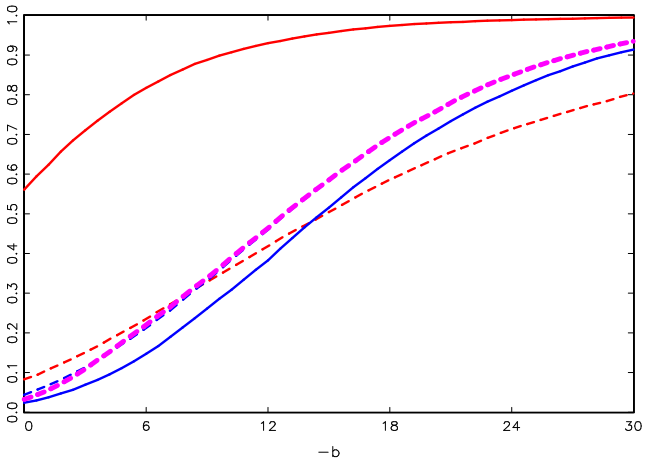

t_{μ}^{OLS}: – –, Q_{μ}^{GLS}: ——, t_{τ}^{OLS}: – –, Q_{τ}^{GLS}: ——, S^{hyb}: – –

S.5 Additional Local Asymptotic Power Simulations

In this section we report additional asymptotic simulation results to those reported in the main paper. Figures S.16 - S.23 report the local asymptotic power of right-tailed tests for predictability for $\delta = -0.75$ over the same grid of values of c considered for $\delta = -0.95$ in the main paper. Figures S.24 - S.26 report local asymptotic power for left-tailed tests for predictability with $\delta = -0.95$ and $c = -30, -40, -50$. Figures S.27 - S.34 report local asymptotic power for left-tailed tests for predictability with $\delta = -0.75$ and $c = 0, -2, -5, -10, -20, -30, -40, -50$. The local asymptotic power of the tests for predictability for an explosive predictor with $c = 2$ are reported in Figures S.35 - S.38, with Figures S.35 and S.36 reporting the power of right-tailed tests for $\delta = -0.95, -0.75$, respectively, and Figures S.37 and S.38 reporting the power of left-tailed tests for $\delta = -0.95, -0.75$, respectively. Finally, Figure S.39 reports the local asymptotic power of right-tailed versions of the infeasible t_μ and Q_μ tests compared to the feasible t_μ^{OLS} and Q_μ^{GLS} tests, and Figure S.40 reports the local asymptotic power of right-tailed versions of the infeasible t_τ and Q_τ tests compared to the feasible t_τ^{OLS} and Q_τ^{GLS} tests, in both cases where $\delta = -0.75$.

Figure S.16: Local Asymptotic Power of Right-Tailed Tests. DGP (1)-(3) with $c = 0$, $\delta = -0.75$ and $\kappa = \{0.0, 0.2, 0.4, 0.6, 0.8, 1.0\}$, where c, κ and δ are the local-to-unity AR, local-to-zero trend, and endogeneity correlation parameters, respectively.

(a) $\kappa = 0.0$

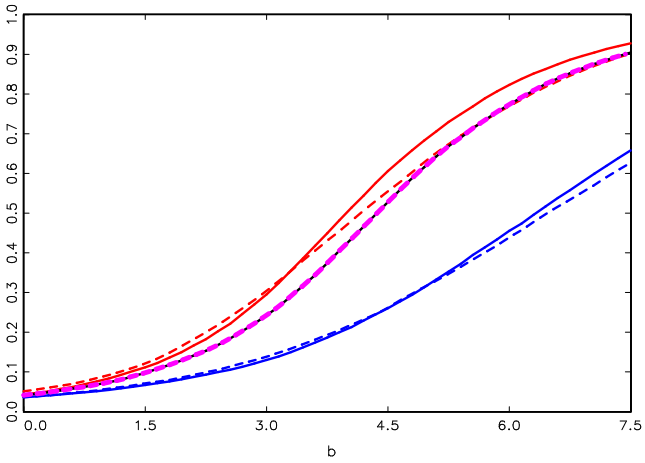

(b) $\kappa = 0.2$

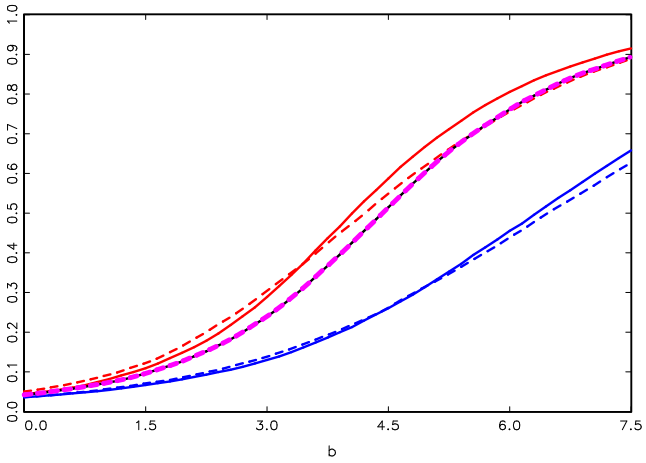

(c) $\kappa = 0.4$

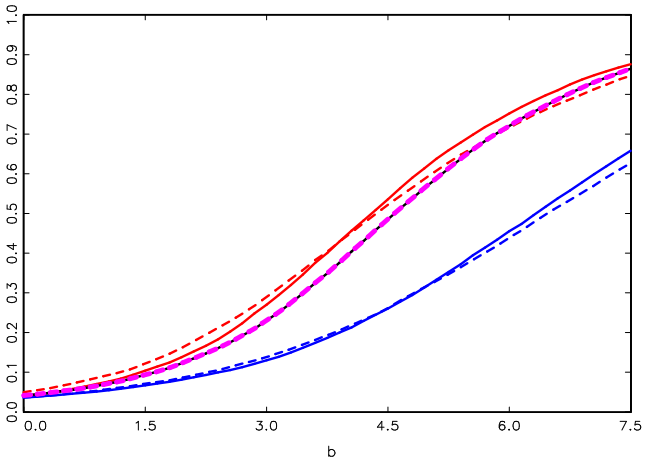

(d) $\kappa = 0.6$

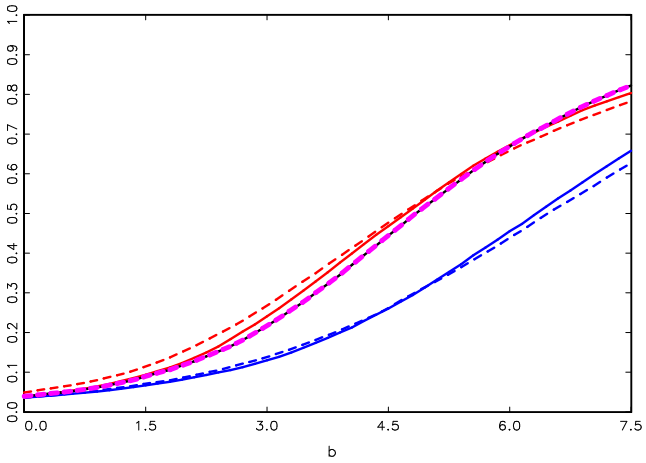

(e) $\kappa = 0.8$

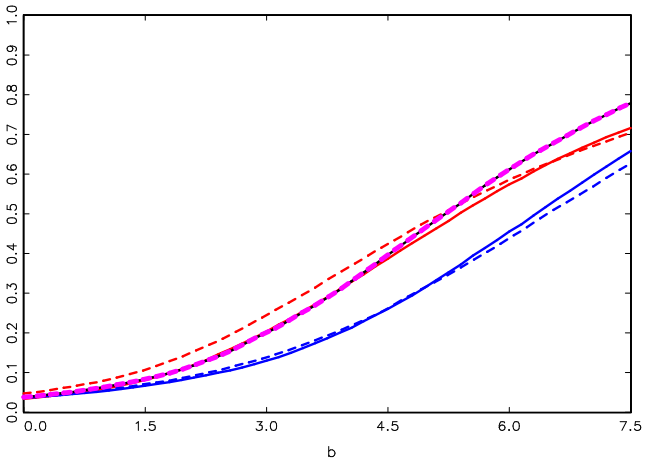

(f) $\kappa = 1.0$

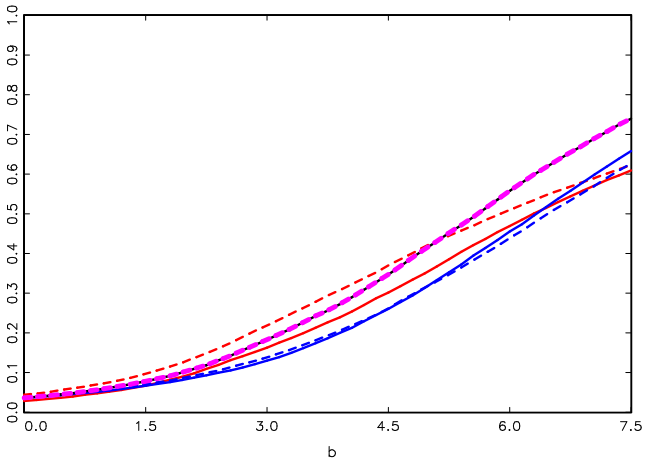

t_μ^{OLS}: – –, Q_μ^{GLS}: ——, t_τ^{OLS}: – –, Q_τ^{GLS}: ——, U^{hyb}: ——, S^{hyb}: – –

Figure S.17: Local Asymptotic Power of Right-Tailed Tests. DGP (1)-(3) with $c = -2$, $\delta = -0.75$ and $\kappa = \{0.0, 0.2, 0.4, 0.6, 0.8, 1.0\}$, where c, κ and δ are the local-to-unity AR, local-to-zero trend, and endogeneity correlation parameters, respectively.

(a) $\kappa = 0.0$

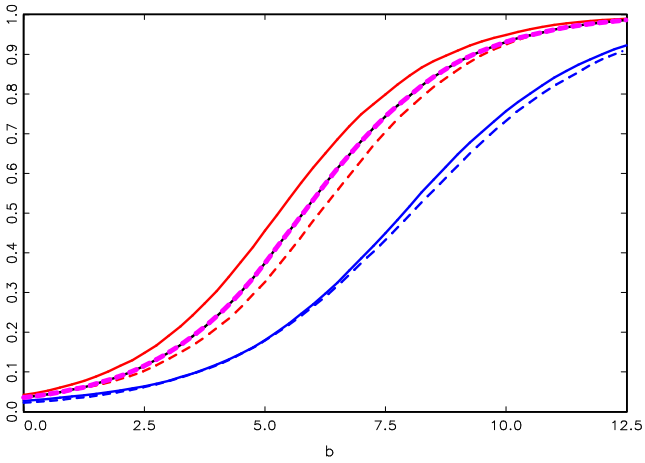

(b) $\kappa = 0.2$

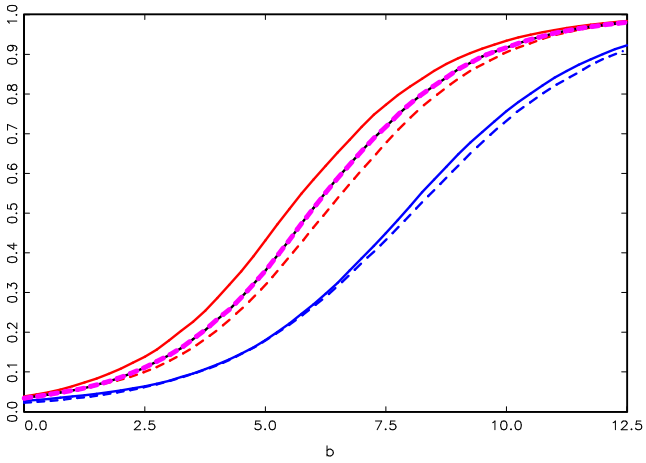

(c) $\kappa = 0.4$

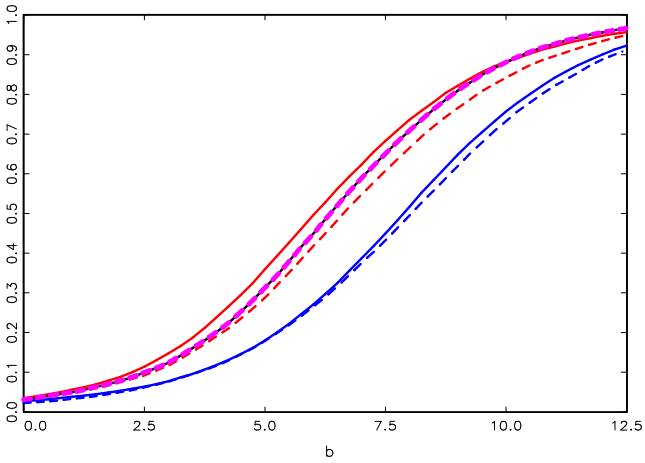

(d) $\kappa = 0.6$

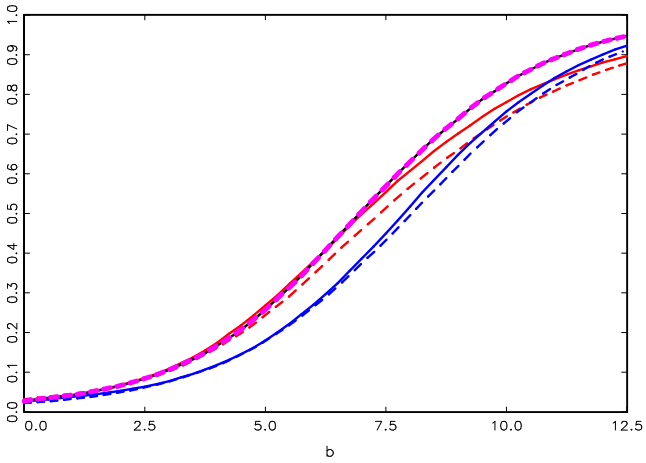

(e) $\kappa = 0.8$

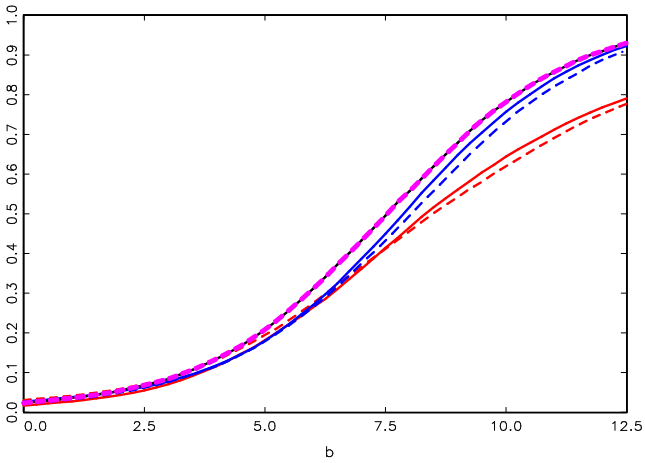

(f) $\kappa = 1.0$

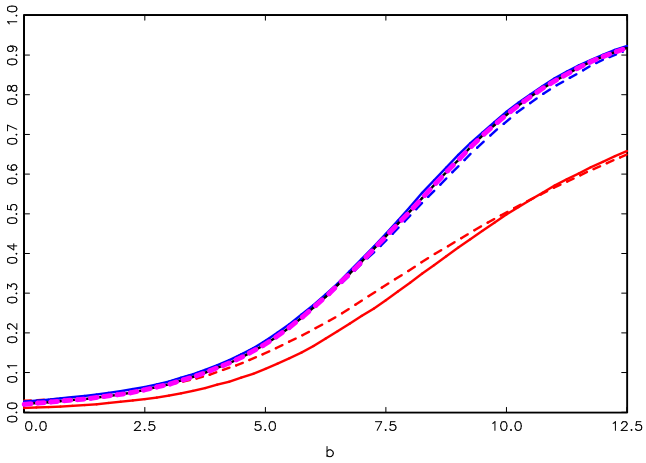

t_μ^{OLS}: – –, Q_μ^{GLS}: ——, t_τ^{OLS}: – –, Q_τ^{GLS}: ——, U^{hyb}: ——, S^{hyb}: – –

Figure S.18: Local Asymptotic Power of Right-Tailed Tests. DGP (1)-(3) with $c = -5$, $\delta = -0.75$ and $\kappa = \{0.0, 0.2, 0.4, 0.6, 0.8, 1.0\}$, where c, κ and δ are the local-to-unity AR, local-to-zero trend, and endogeneity correlation parameters, respectively.

(a) $\kappa = 0.0$

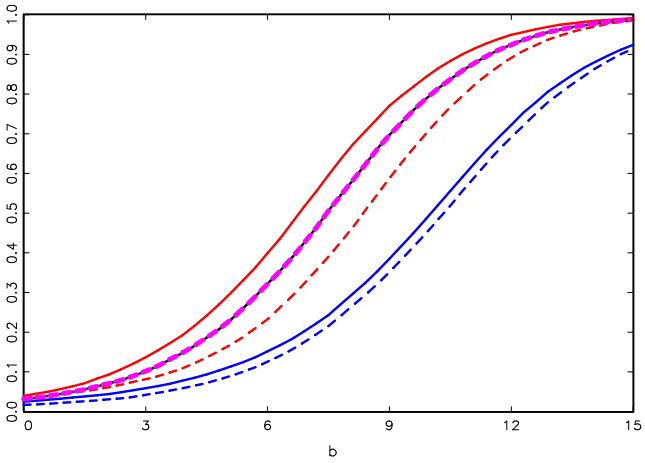

(b) $\kappa = 0.2$

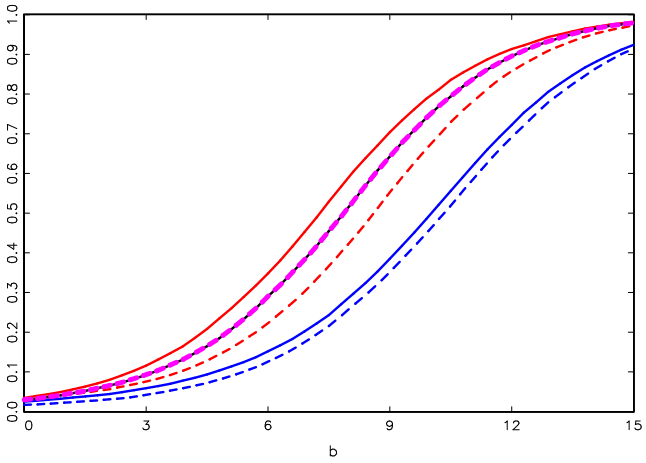

(c) $\kappa = 0.4$

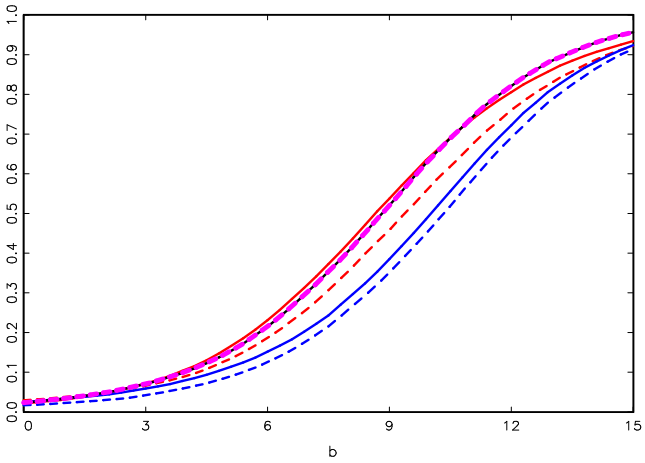

(d) $\kappa = 0.6$

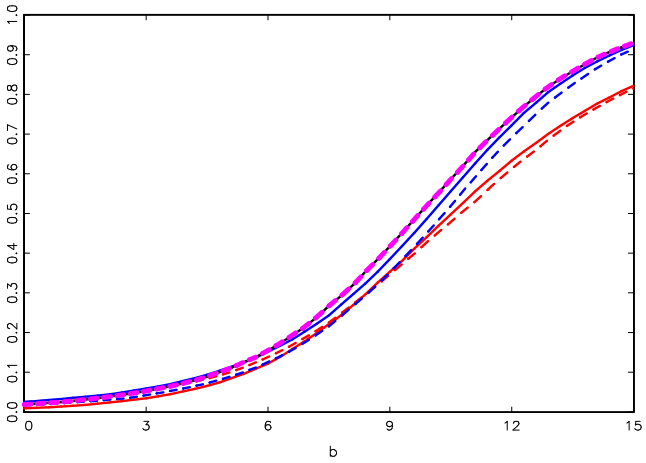

(e) $\kappa = 0.8$

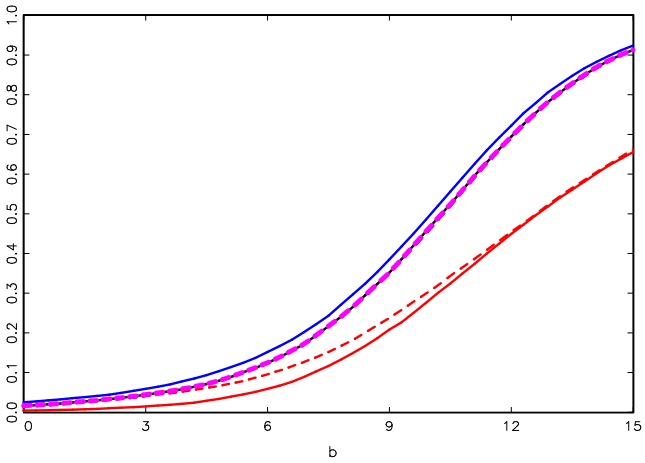

(f) $\kappa = 1.0$

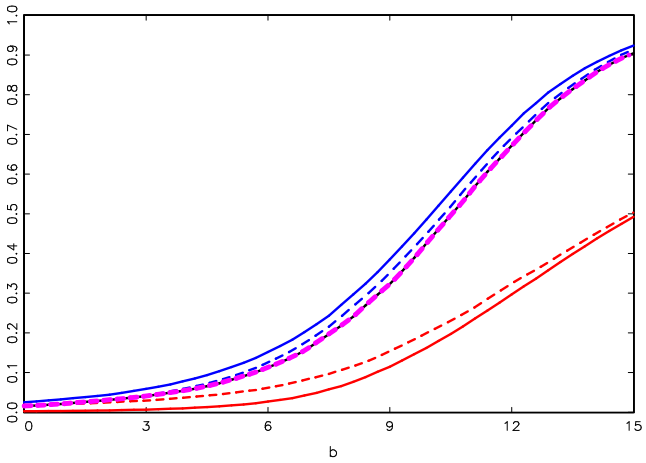

t_μ^{OLS}: – – , Q_μ^{GLS}: ——— , t_τ^{OLS}: – –, Q_τ^{GLS}: ———, U^{hyb}: ———, S^{hyb}: – –

Figure S.19: Local Asymptotic Power of Right-Tailed Tests. DGP (1)-(3) with $c = -10$, $\delta = -0.75$ and $\kappa = \{0.0, 0.2, 0.4, 0.6, 0.8, 1.0\}$, where c, κ and δ are the local-to-unity AR, local-to-zero trend, and endogeneity correlation parameters, respectively.

(a) $\kappa = 0.0$

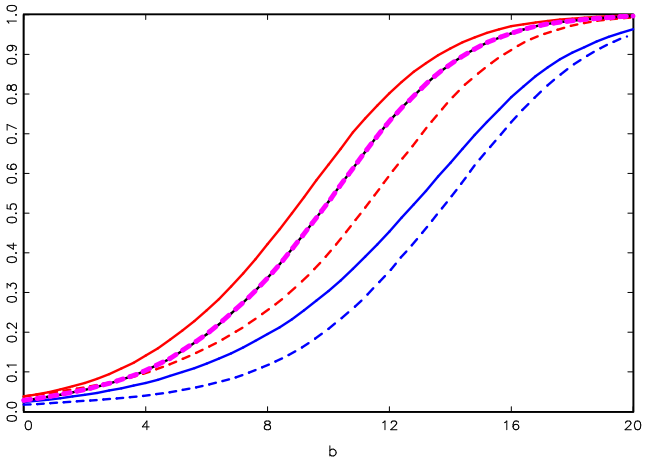

(b) $\kappa = 0.2$

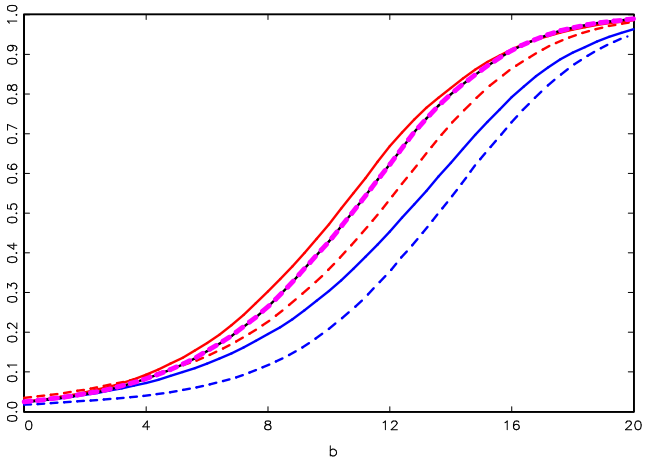

(c) $\kappa = 0.4$

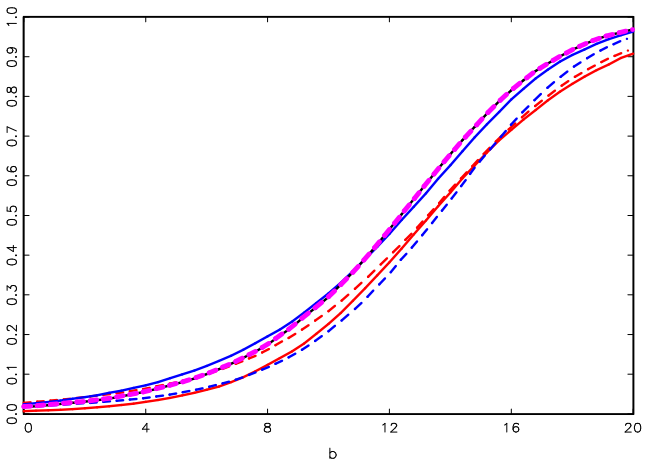

(d) $\kappa = 0.6$

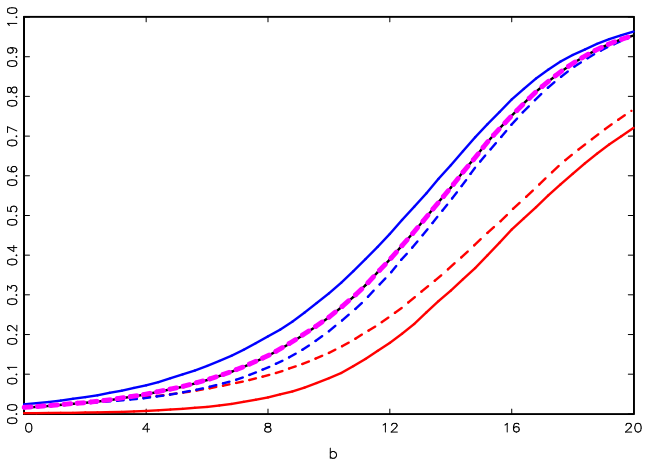

(e) $\kappa = 0.8$

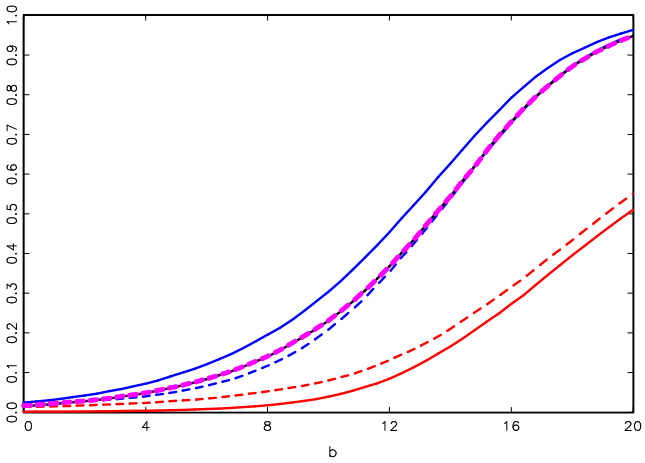

(f) $\kappa = 1.0$

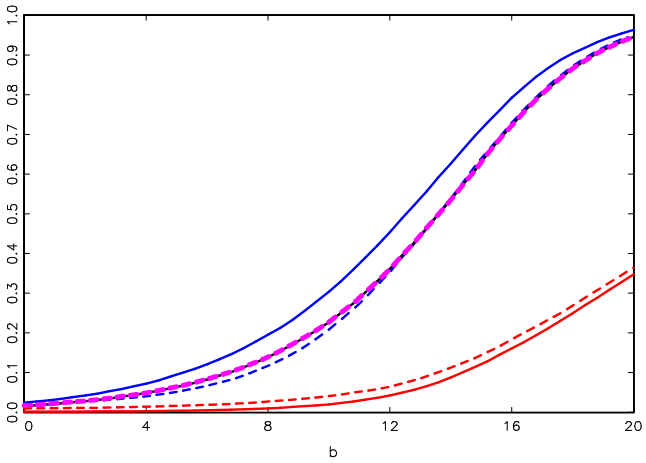

t_μ^{OLS}: – –, Q_μ^{GLS}: ——, t_τ^{OLS}: – –, Q_τ^{GLS}: ——, U^{hyb}: ——, S^{hyb}: – –

Figure S.20: Local Asymptotic Power of Right-Tailed Tests. DGP (1)-(3) with $c = -20$, $\delta = -0.75$ and $\kappa = \{0.0, 0.1, 0.2, 0.3, 0.4, 0.5\}$, where c, κ and δ are the local-to-unity AR, local-to-zero trend, and endogeneity correlation parameters, respectively.

(a) $\kappa = 0.0$

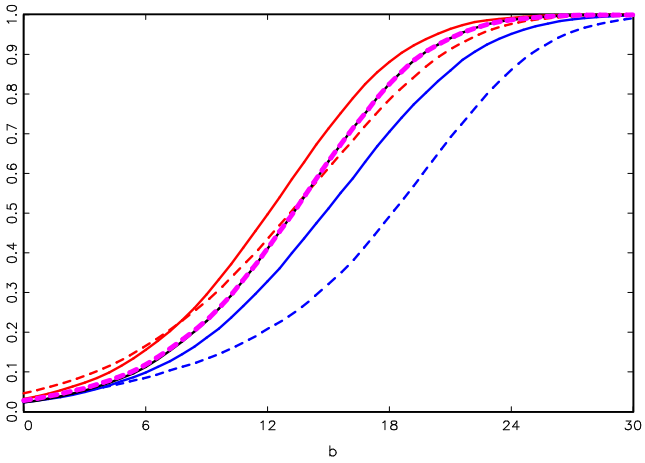

(b) $\kappa = 0.1$

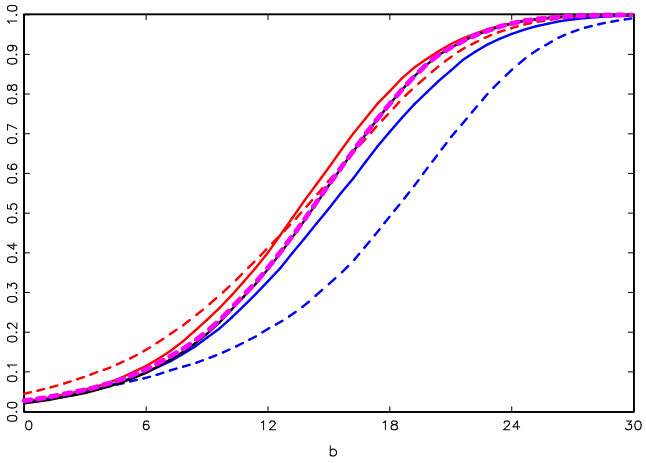

(c) $\kappa = 0.2$

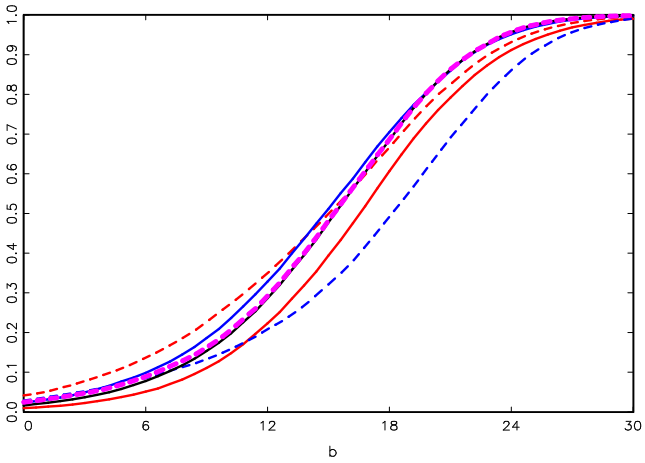

(d) $\kappa = 0.3$

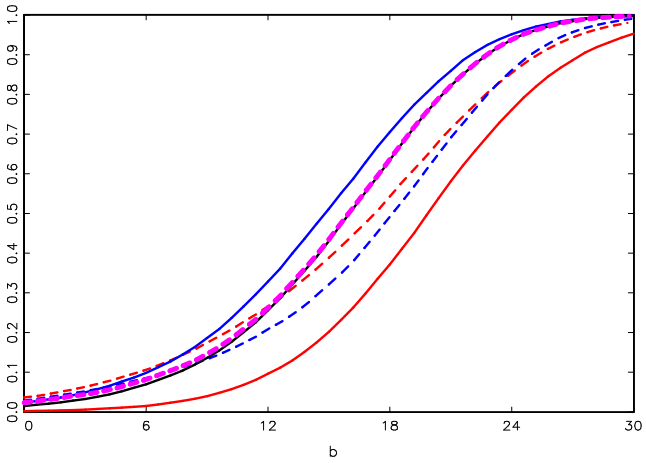

(e) $\kappa = 0.4$

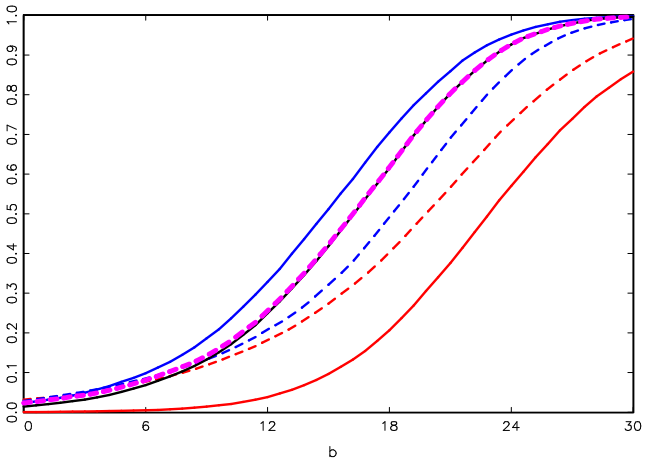

(f) $\kappa = 0.5$

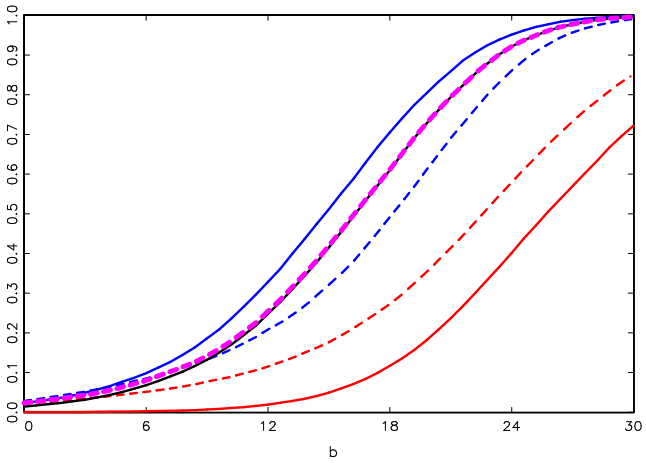

t_μ^{OLS}: – –, Q_μ^{GLS}: ——, t_τ^{OLS}: – –, Q_τ^{GLS}: ——, U^{hyb}: ——, S^{hyb}: – –

Figure S.21: Local Asymptotic Power of Right-Tailed Tests. DGP (1)-(3) with $c = -30$, $\delta = -0.75$ and $\kappa = \{0.0, 0.1, 0.2, 0.3, 0.4, 0.5\}$, where c, κ and δ are the local-to-unity AR, local-to-zero trend, and endogeneity correlation parameters, respectively.

(a) $\kappa = 0.0$

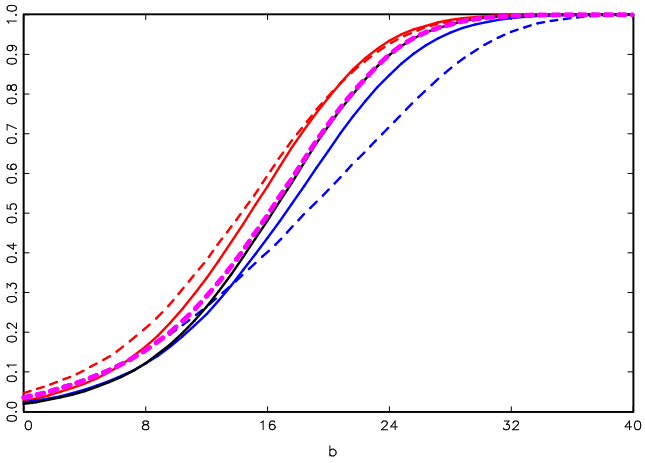

(b) $\kappa = 0.1$

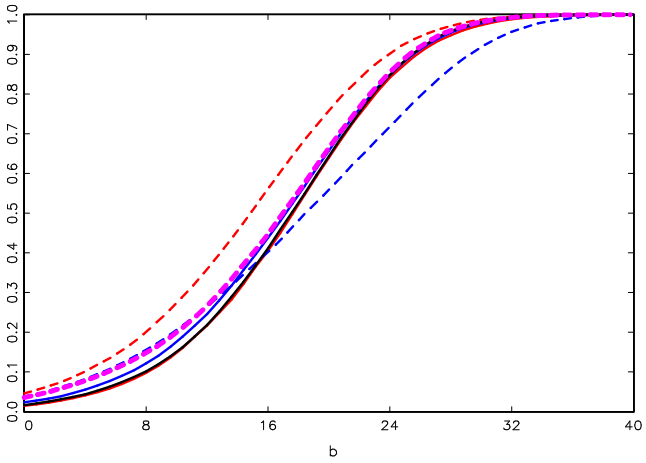

(c) $\kappa = 0.2$

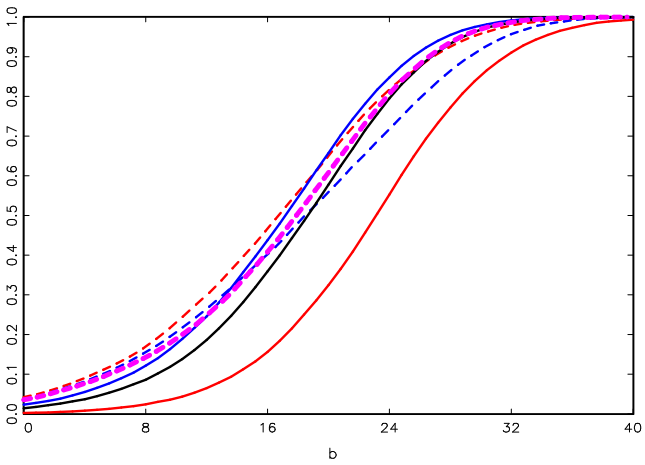

(d) $\kappa = 0.3$

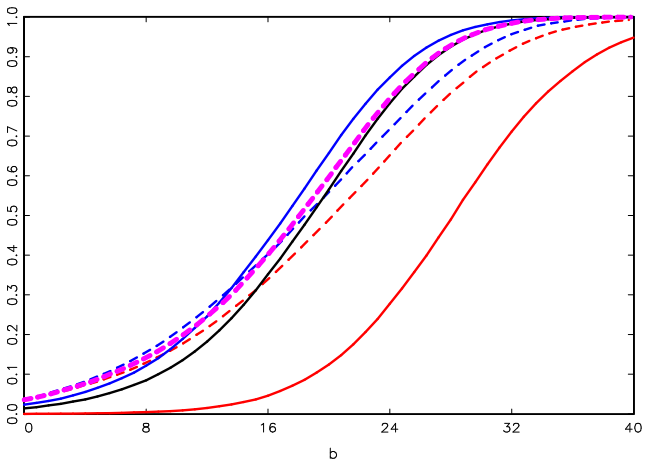

(e) $\kappa = 0.4$

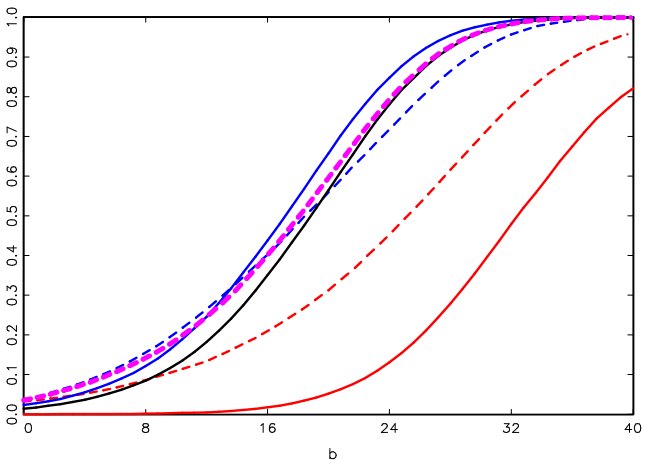

(f) $\kappa = 0.5$

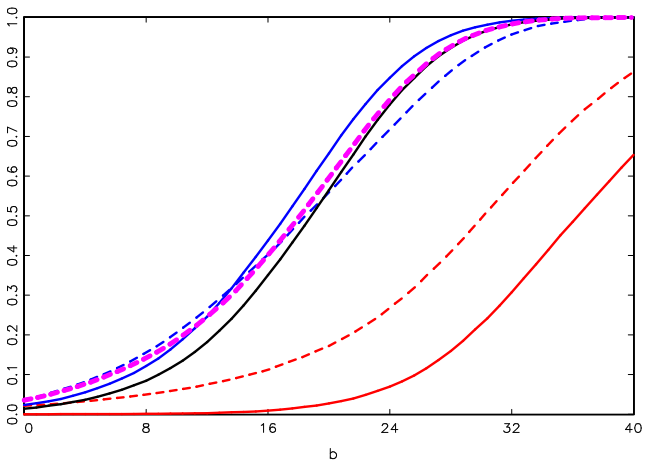

t_μ^{OLS}: – –, Q_μ^{GLS}: ——, t_τ^{OLS}: – –, Q_τ^{GLS}: ——, U^{hyb}: ——, S^{hyb}: – –

Figure S.22: Local Asymptotic Power of Right-Tailed Tests. DGP (1)-(3) with $c = -40$, $\delta = -0.75$ and $\kappa = \{0.0, 0.1, 0.2, 0.3, 0.4, 0.5\}$, where c, κ and δ are the local-to-unity AR, local-to-zero trend, and endogeneity correlation parameters, respectively.

(a) $\kappa = 0.0$

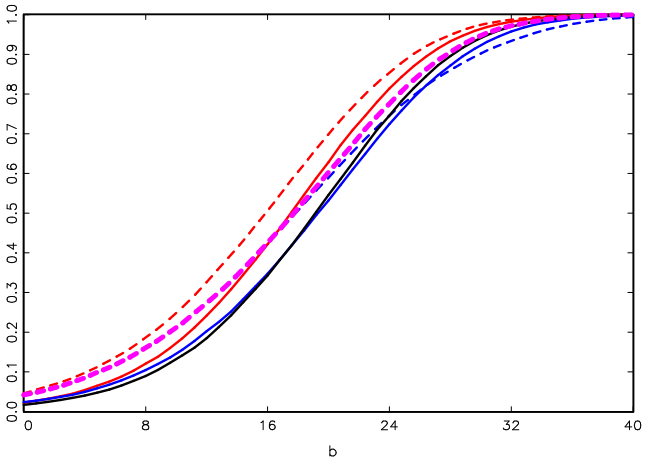

(b) $\kappa = 0.1$

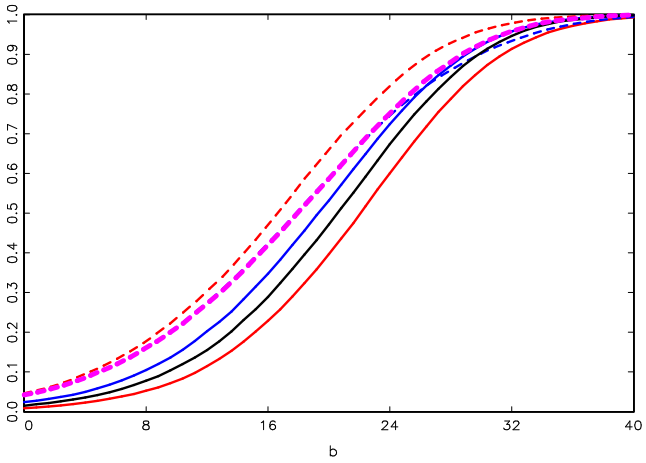

(c) $\kappa = 0.2$

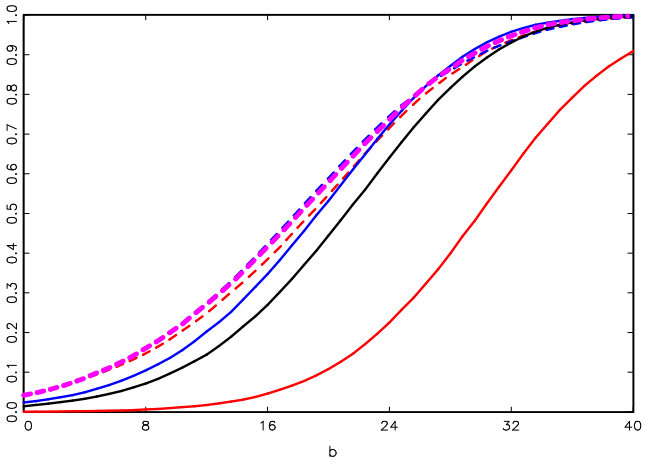

(d) $\kappa = 0.3$

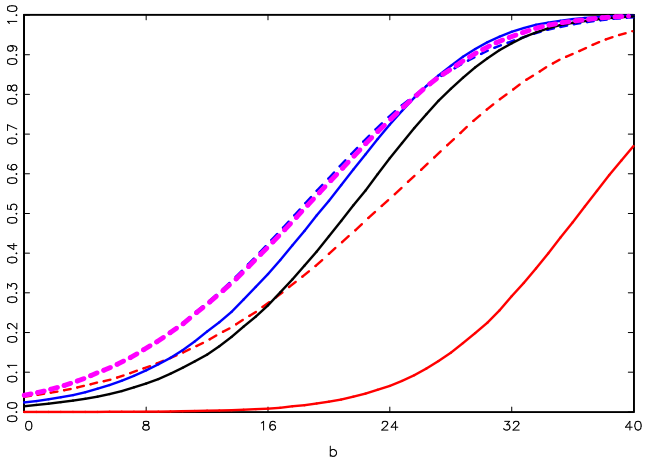

(e) $\kappa = 0.4$

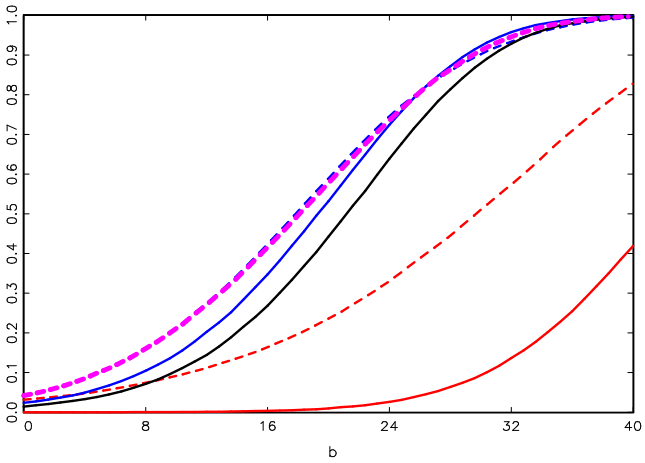

(f) $\kappa = 0.5$

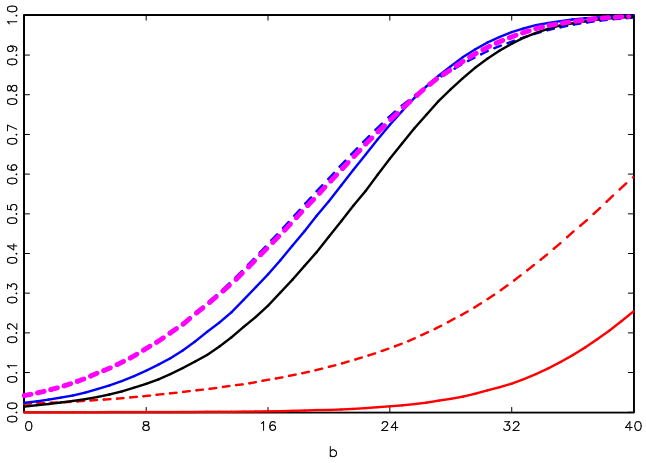

t_{μ}^{OLS}: – – , Q_{μ}^{GLS}: ——— , t_{τ}^{OLS}: – –, Q_{τ}^{GLS}: ———, U^{hyb}: ———, S^{hyb}: – –

Figure S.23: Local Asymptotic Power of Right-Tailed Tests. DGP (1)-(3) with $c = -50$, $\delta = -0.75$ and $\kappa = \{0.0, 0.1, 0.2, 0.3, 0.4, 0.5\}$, where c, κ and δ are the local-to-unity AR, local-to-zero trend, and endogeneity correlation parameters, respectively.

(a) $\kappa = 0.0$

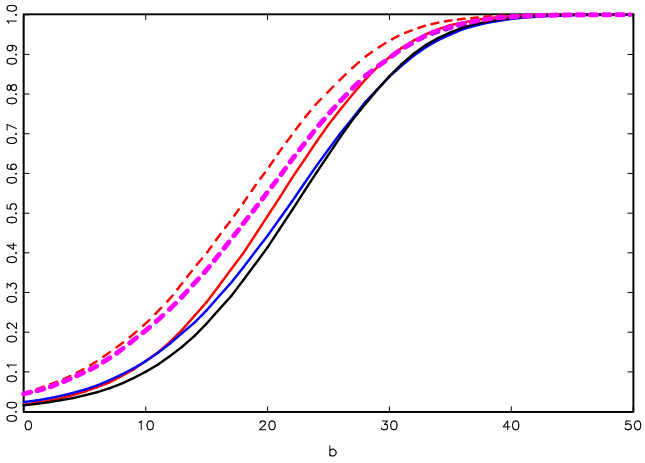

(b) $\kappa = 0.1$

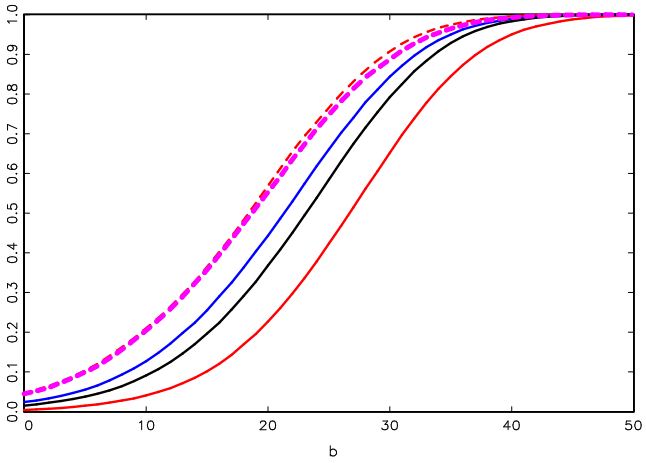

(c) $\kappa = 0.2$

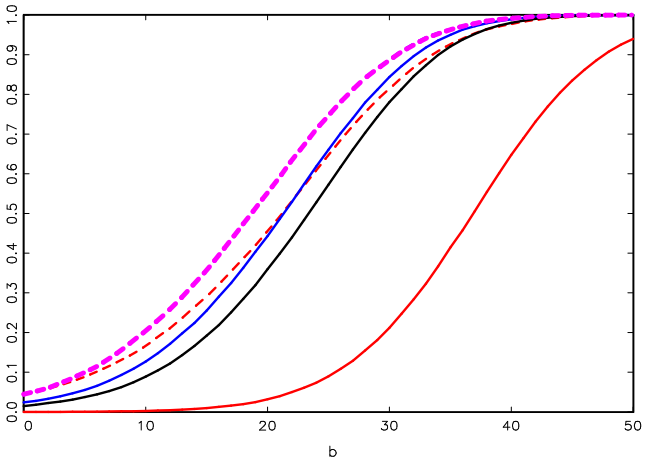

(d) $\kappa = 0.3$

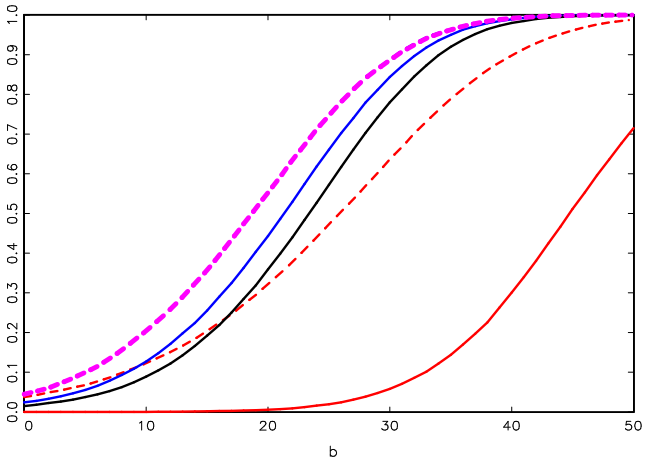

(e) $\kappa = 0.4$

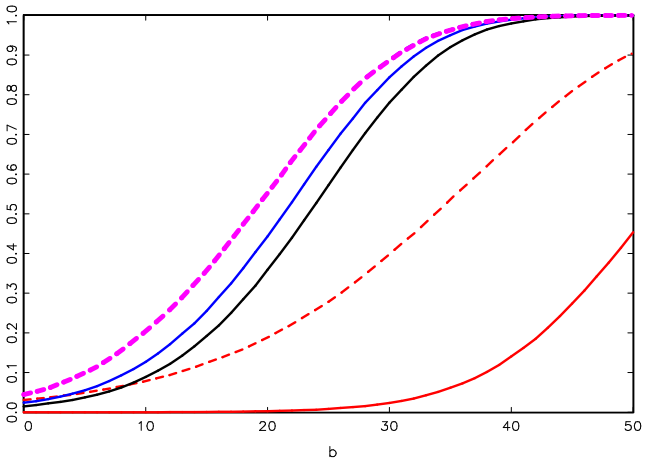

(f) $\kappa = 0.5$

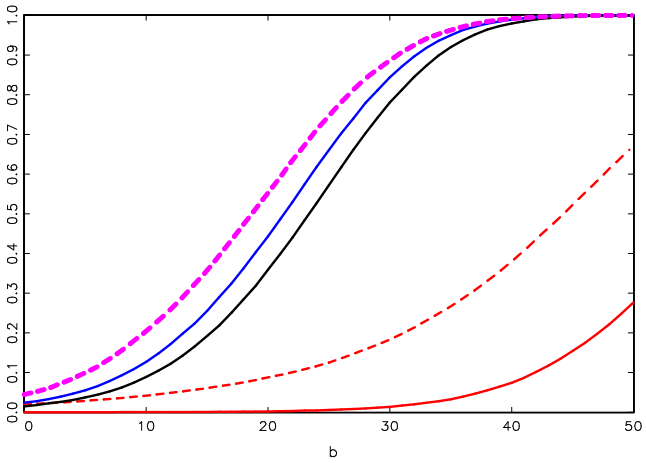

t_{μ}^{OLS}: – – , Q_{μ}^{GLS}: ——— , t_{τ}^{OLS}: – –, Q_{τ}^{GLS}: ———, U^{hyb}: ———, S^{hyb}: – –

Figure S.24: Local Asymptotic Power of Left-Tailed Tests. DGP (1)-(3) with $c = -30$, $\delta = -0.95$ and $\kappa = \{0.0, 0.1, 0.2, 0.3, 0.4, 0.5\}$, where c, κ and δ are the local-to-unity AR, local-to-zero trend, and endogeneity correlation parameters, respectively.

(a) $\kappa = 0.0$

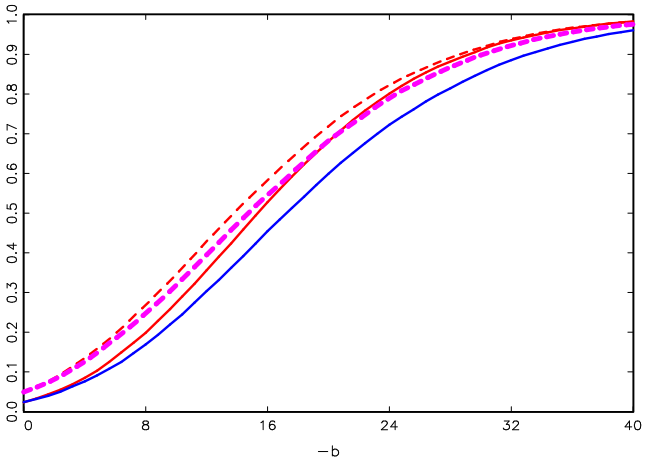

(b) $\kappa = 0.1$

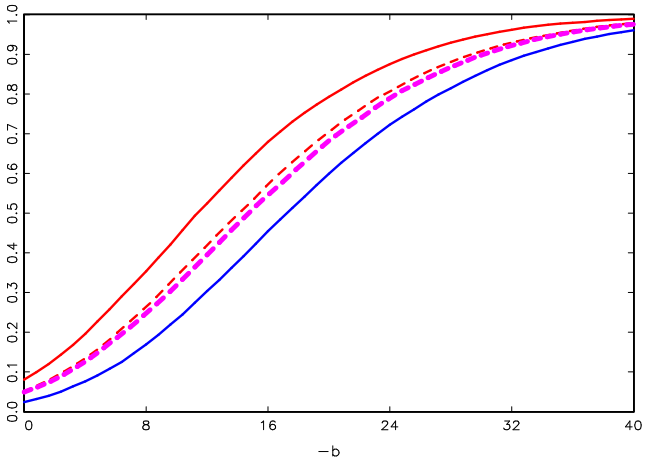

(c) $\kappa = 0.2$

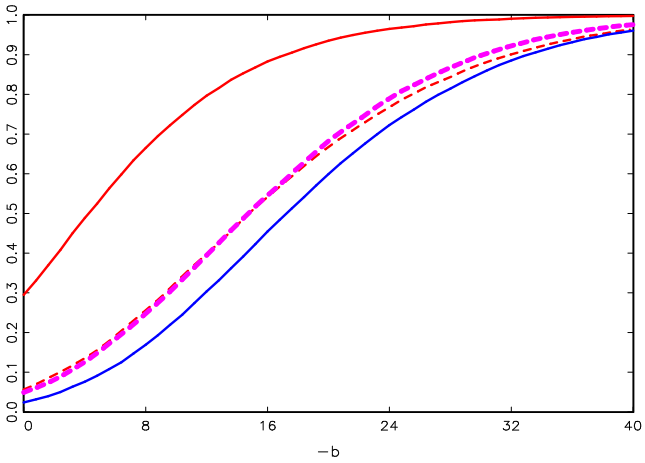

(d) $\kappa = 0.3$

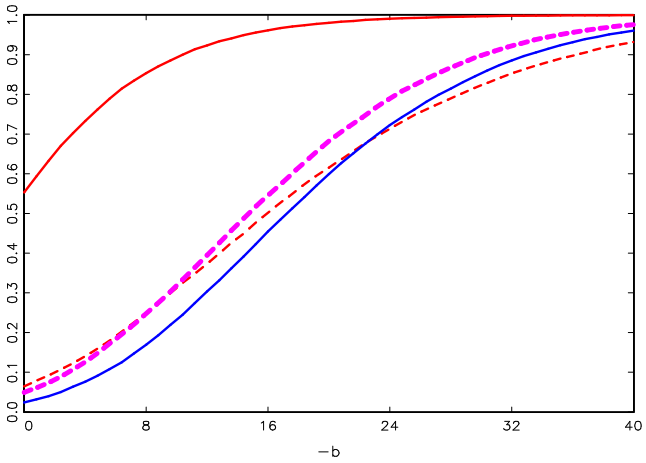

(e) $\kappa = 0.4$

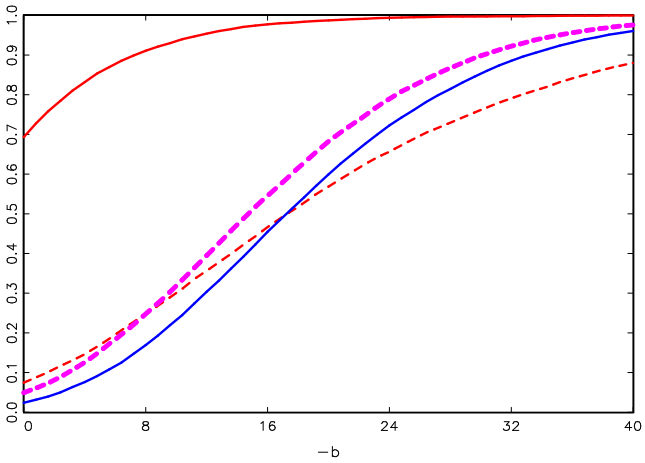

(f) $\kappa = 0.5$

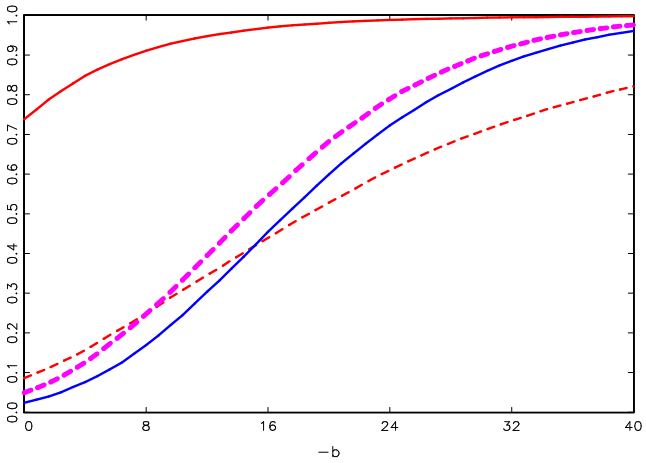

t_{μ}^{OLS}: – –, Q_{μ}^{GLS}: ——, t_{τ}^{OLS}: – –, Q_{τ}^{GLS}: ——, S^{hyb}: – –

Figure S.25: Local Asymptotic Power of Left-Tailed Tests. DGP (1)-(3) with $c = -40$, $\delta = -0.95$ and $\kappa = \{0.0, 0.1, 0.2, 0.3, 0.4, 0.5\}$, where c, κ and δ are the local-to-unity AR, local-to-zero trend, and endogeneity correlation parameters, respectively.

(a) $\kappa = 0.0$

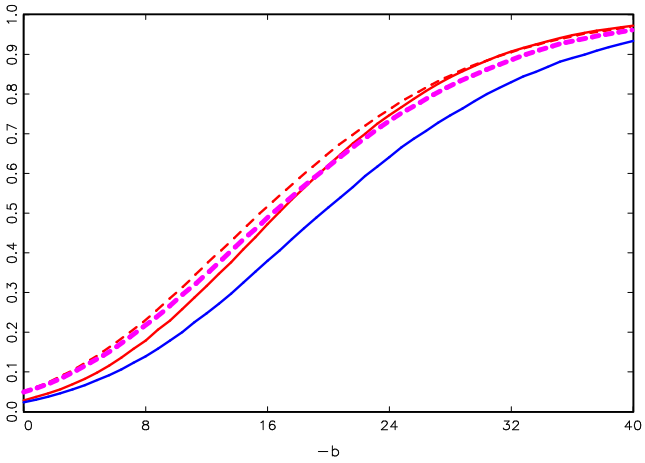

(b) $\kappa = 0.1$

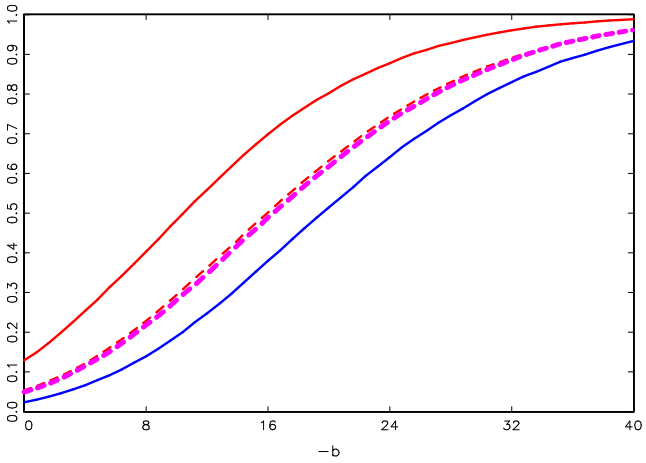

(c) $\kappa = 0.2$

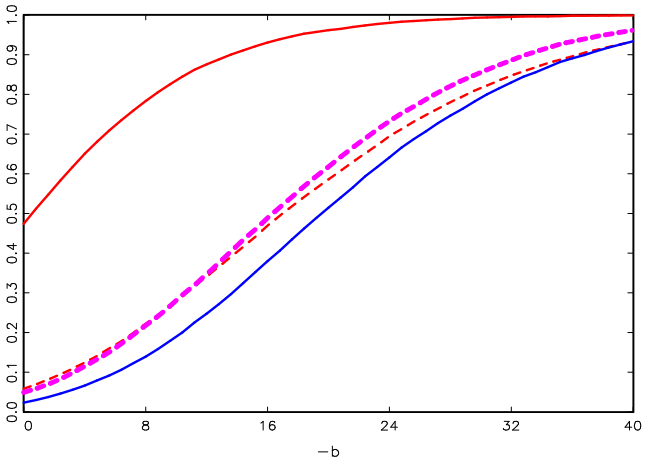

(d) $\kappa = 0.3$

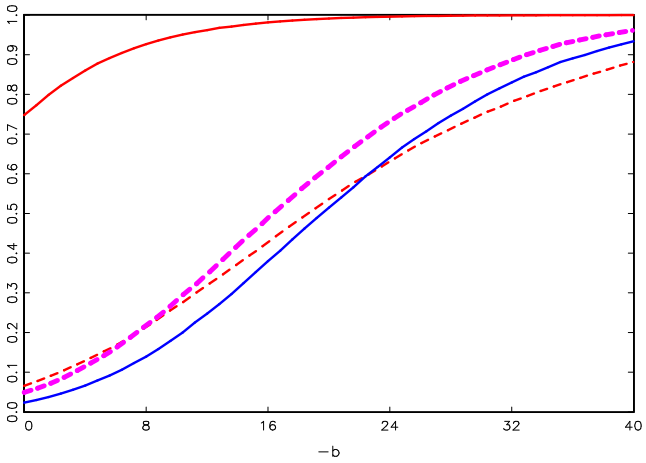

(e) $\kappa = 0.4$

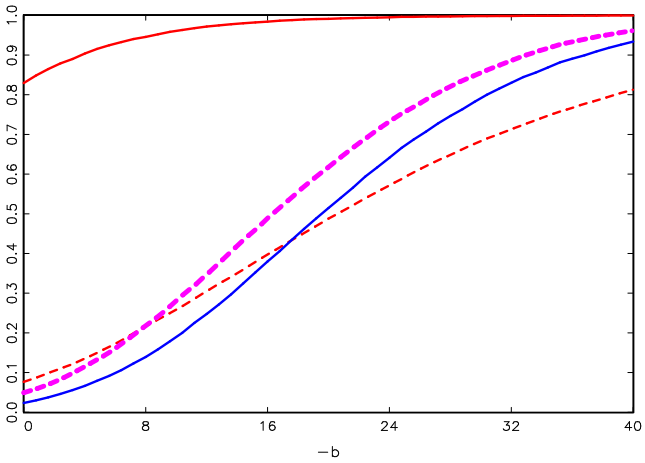

(f) $\kappa = 0.5$

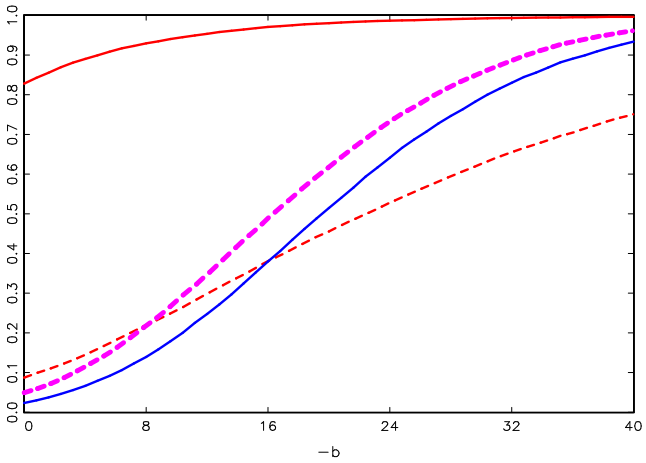

t_{μ}^{OLS}: – – , Q_{μ}^{GLS}: ——— , t_{τ}^{OLS}: – –, Q_{τ}^{GLS}: ———, S^{hyb}: – –

Figure S.26: Local Asymptotic Power of Left-Tailed Tests. DGP (1)-(3) with $c = -50$, $\delta = -0.95$ and $\kappa = \{0.0, 0.1, 0.2, 0.3, 0.4, 0.5\}$, where c, κ and δ are the local-to-unity AR, local-to-zero trend, and endogeneity correlation parameters, respectively.

(a) $\kappa = 0.0$

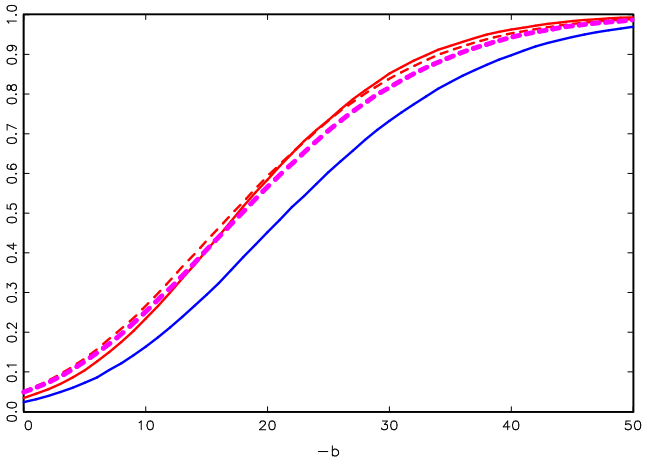

(b) $\kappa = 0.1$

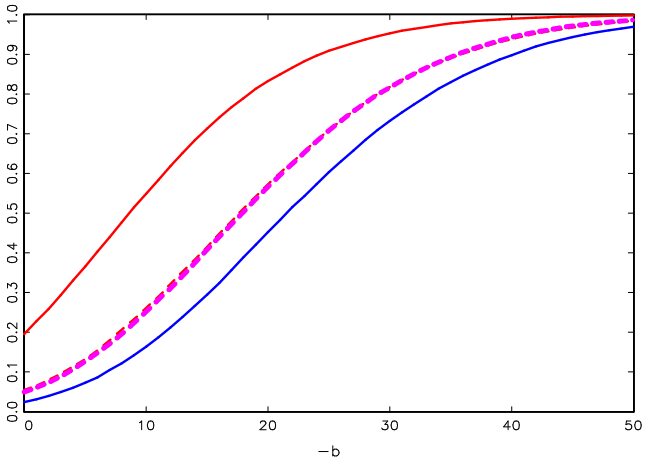

(c) $\kappa = 0.2$

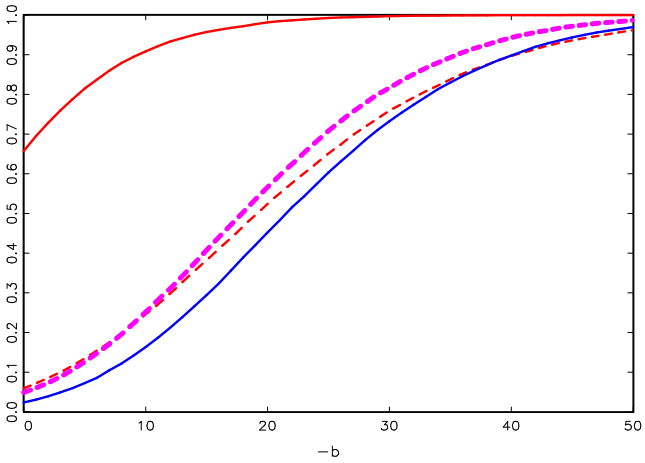

(d) $\kappa = 0.3$

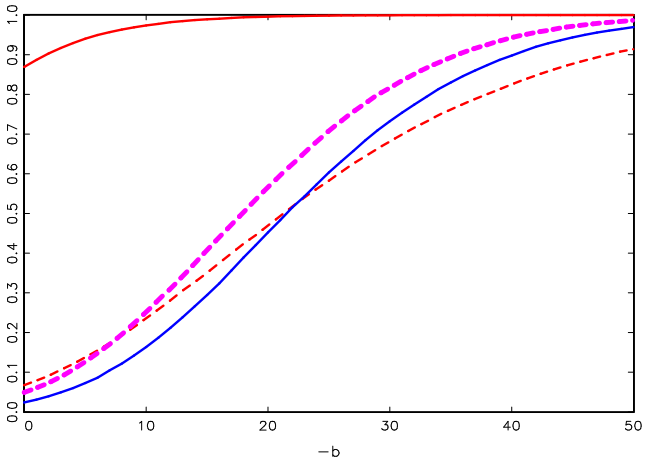

(e) $\kappa = 0.4$

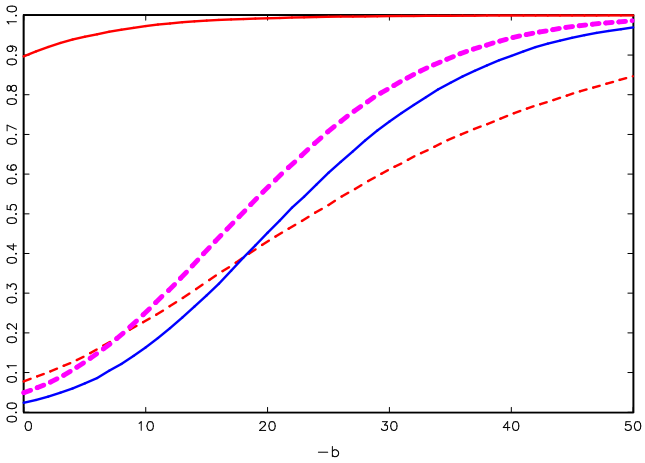

(f) $\kappa = 0.5$

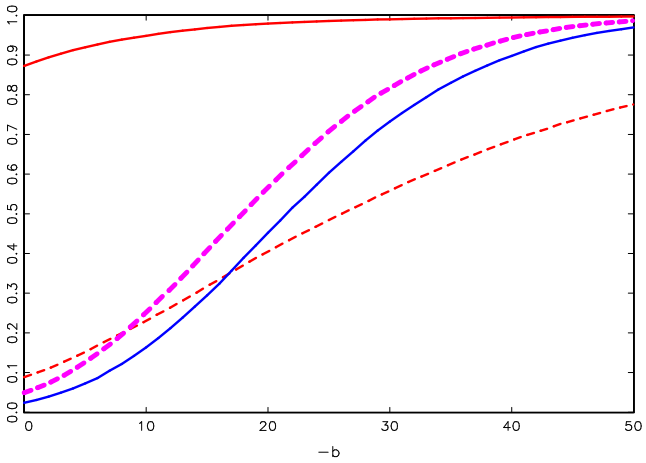

t_{μ}^{OLS}: – –, Q_{μ}^{GLS}: ——, t_{τ}^{OLS}: – –, Q_{τ}^{GLS}: ——, S^{hyb}: – –

Figure S.27: Local Asymptotic Power of Left-Tailed Tests. DGP (1)-(3) with $c = -0$, $\delta = -0.75$ and $\kappa = \{0.0, 0.2, 0.4, 0.6, 0.8, 1.0\}$, where c, κ and δ are the local-to-unity AR, local-to-zero trend, and endogeneity correlation parameters, respectively.

(a) $\kappa = 0.0$

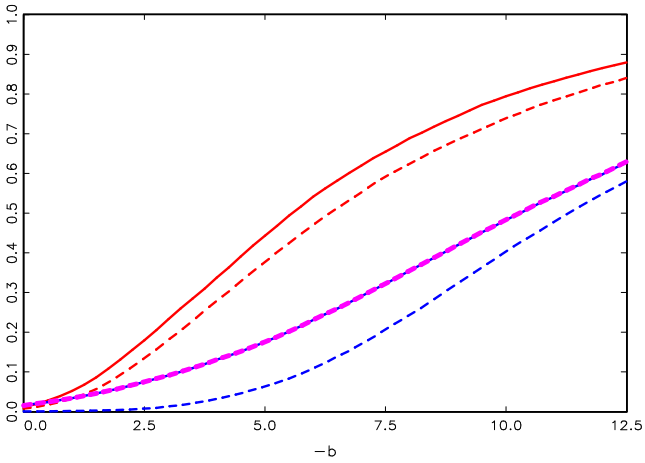

(b) $\kappa = 0.2$

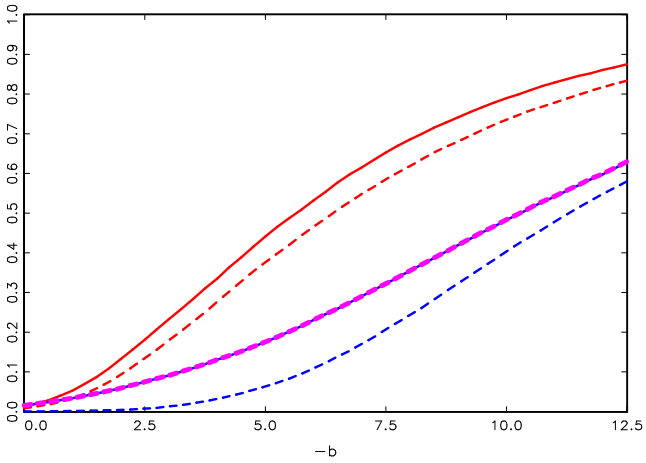

(c) $\kappa = 0.4$

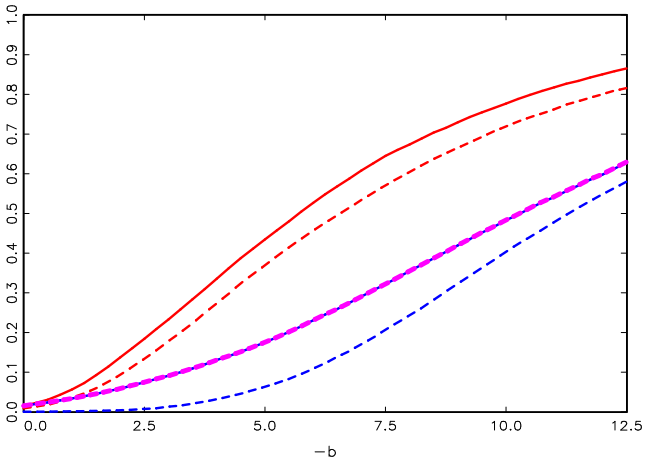

(d) $\kappa = 0.6$

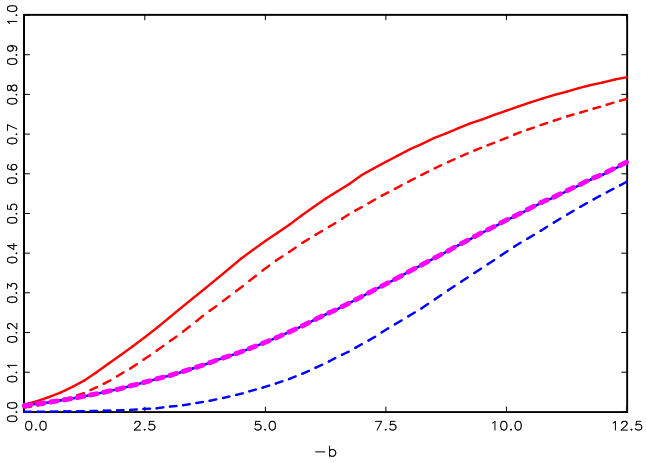

(e) $\kappa = 0.8$

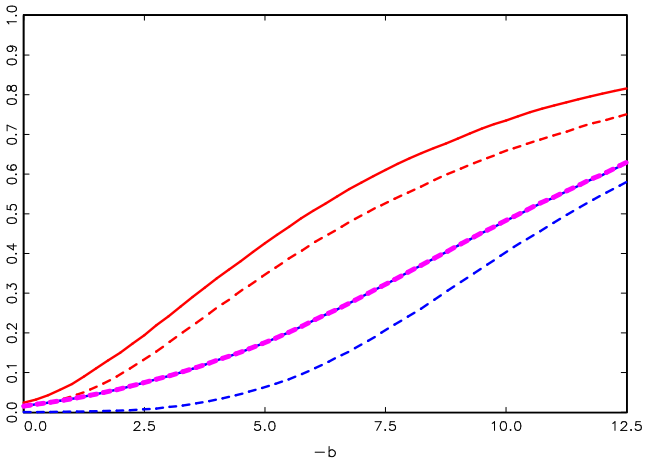

(f) $\kappa = 1.0$

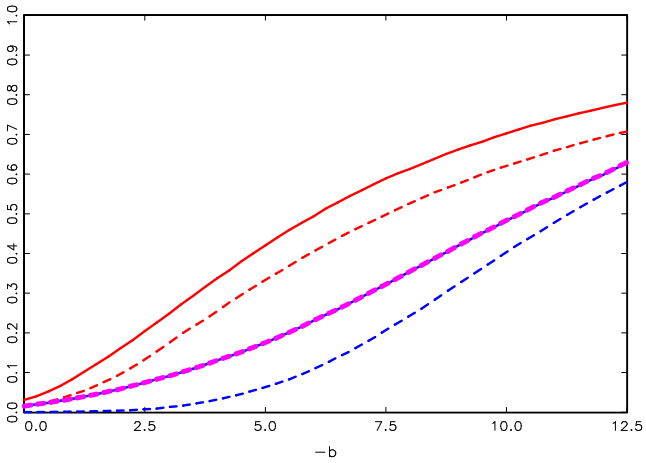

t_{μ}^{OLS}: – –, Q_{μ}^{GLS}: ——, t_{τ}^{OLS}: – –, Q_{τ}^{GLS}: ——, S^{hyb}: – –

Figure S.28: Local Asymptotic Power of Left-Tailed Tests. DGP (1)-(3) with $c = -2$, $\delta = -0.75$ and $\kappa = \{0.0, 0.2, 0.4, 0.6, 0.8, 1.0\}$, where c, κ and δ are the local-to-unity AR, local-to-zero trend, and endogeneity correlation parameters, respectively.

(a) $\kappa = 0.0$

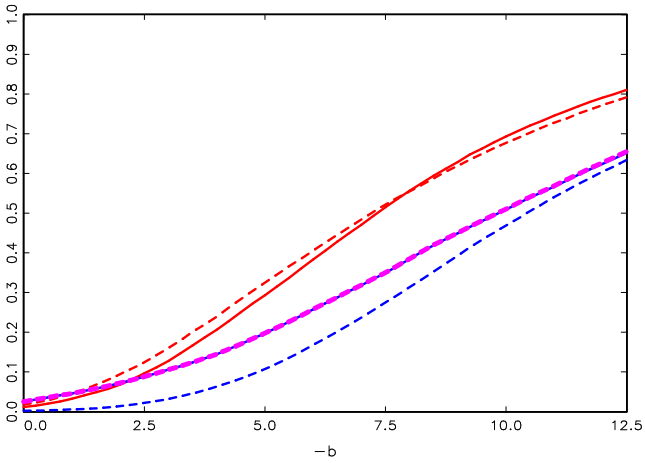

(b) $\kappa = 0.2$

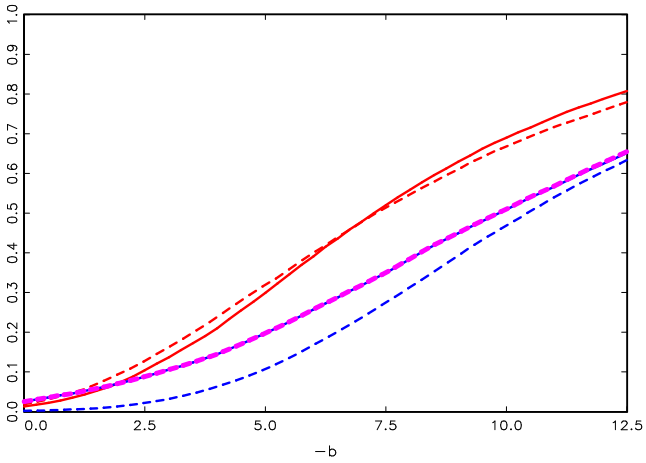

(c) $\kappa = 0.4$

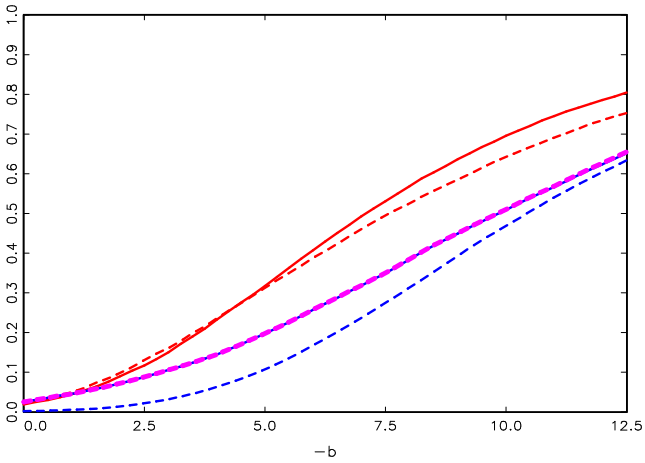

(d) $\kappa = 0.6$

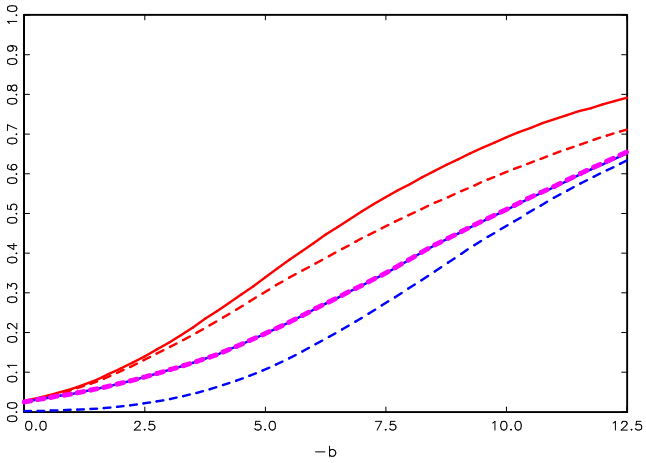

(e) $\kappa = 0.8$

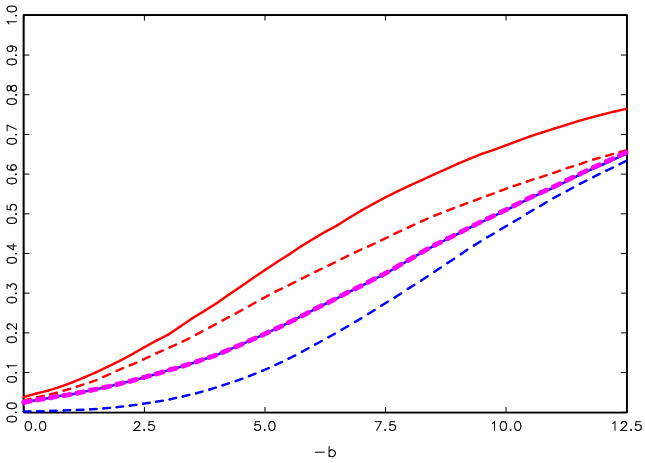

(f) $\kappa = 1.0$

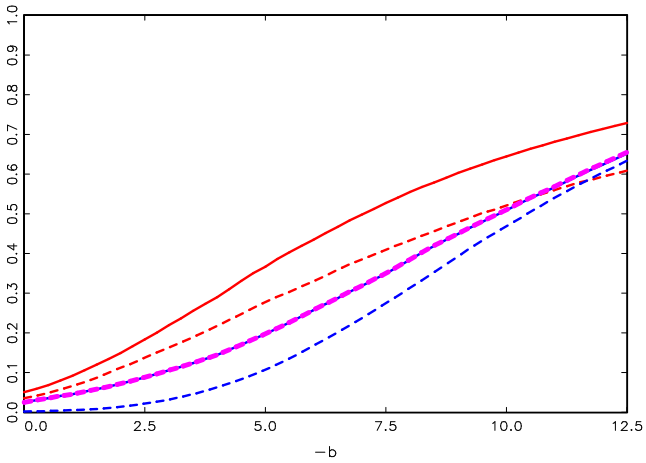

t_{μ}^{OLS}: – –, Q_{μ}^{GLS}: ——, t_{τ}^{OLS}: – –, Q_{τ}^{GLS}: ——, S^{hyb}: – –

Figure S.29: Local Asymptotic Power of Left-Tailed Tests. DGP (1)-(3) with $c = -5$, $\delta = -0.75$ and $\kappa = \{0.0, 0.2, 0.4, 0.6, 0.8, 1.0\}$, where c, κ and δ are the local-to-unity AR, local-to-zero trend, and endogeneity correlation parameters, respectively.

(a) $\kappa = 0.0$

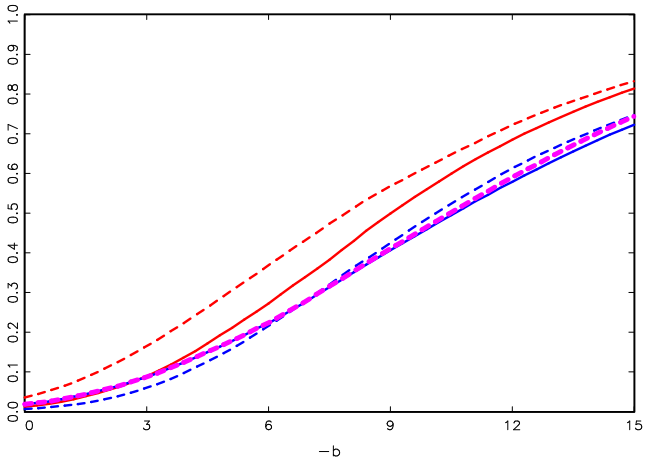

(b) $\kappa = 0.2$

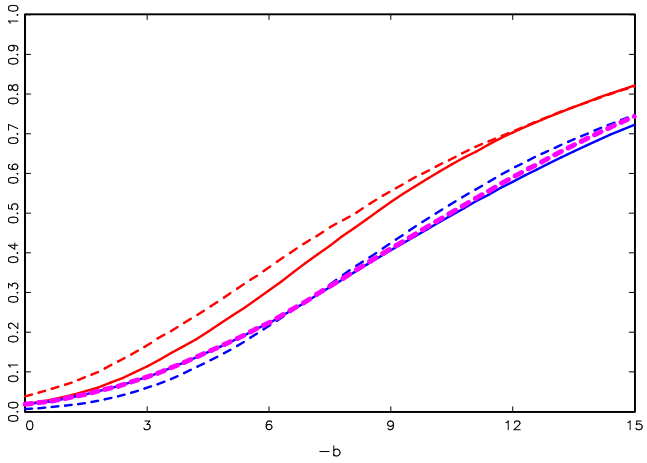

(c) $\kappa = 0.4$

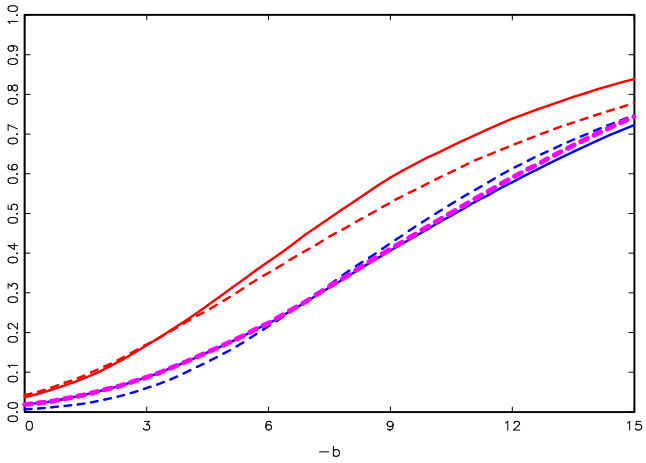

(d) $\kappa = 0.6$

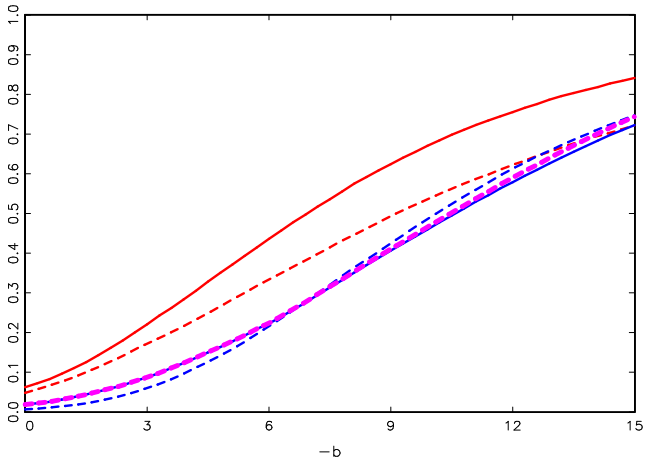

(e) $\kappa = 0.8$

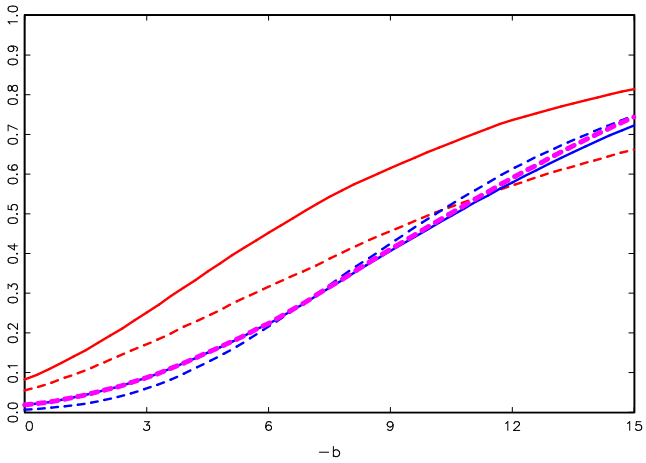

(f) $\kappa = 1.0$

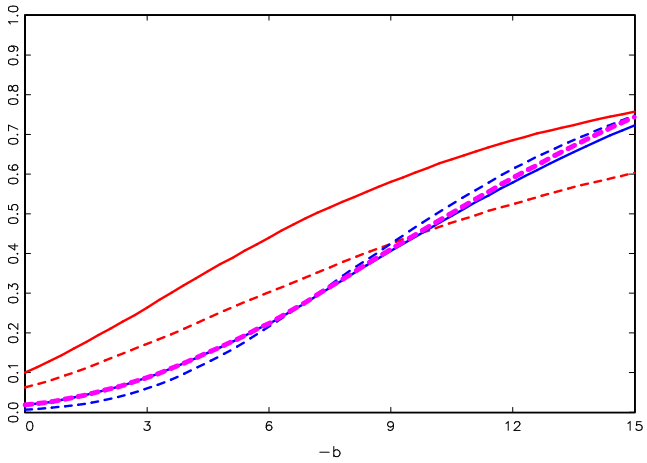

t_μ^{OLS}: – –, Q_μ^{GLS}: ——, t_τ^{OLS}: – –, Q_τ^{GLS}: ——, S^{hyb}: – –

Figure S.30: Local Asymptotic Power of Left-Tailed Tests. DGP (1)-(3) with $c = -10$, $\delta = -0.75$ and $\kappa = \{0.0, 0.2, 0.4, 0.6, 0.8, 1.0\}$, where c, κ and δ are the local-to-unity AR, local-to-zero trend, and endogeneity correlation parameters, respectively.

(a) $\kappa = 0.0$

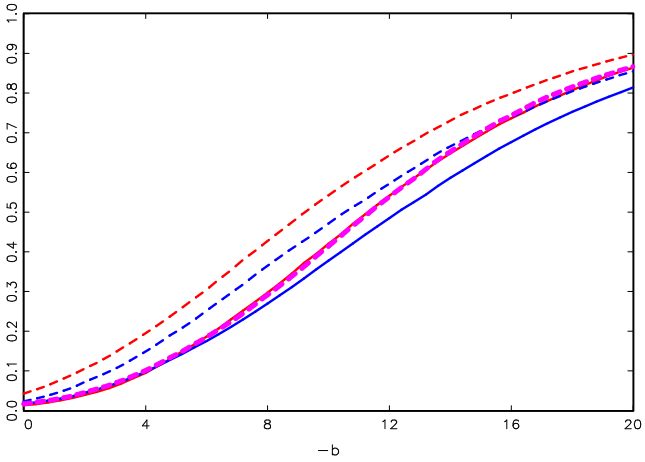

(b) $\kappa = 0.2$

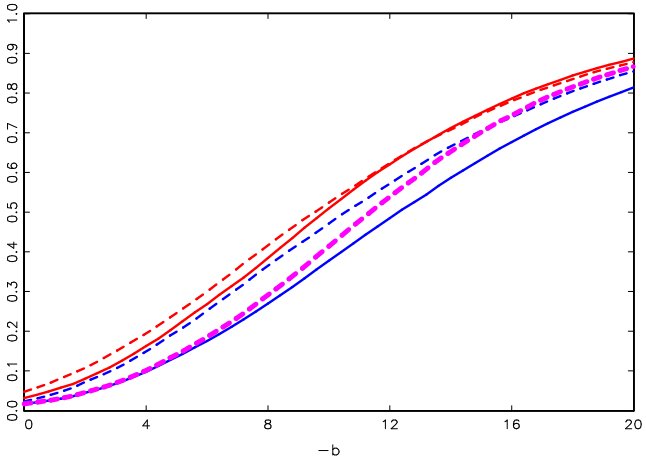

(c) $\kappa = 0.4$

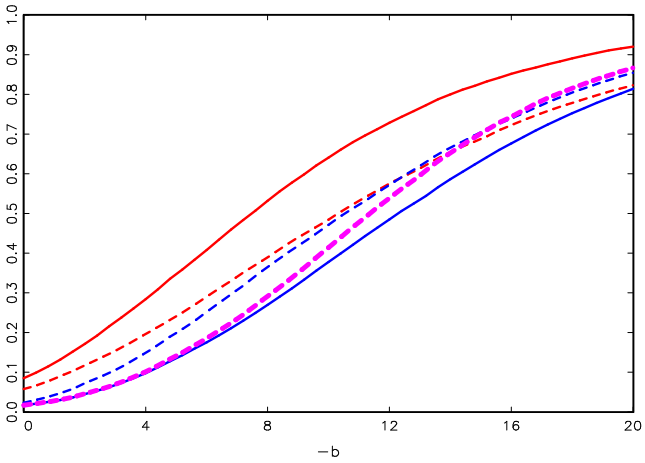

(d) $\kappa = 0.6$

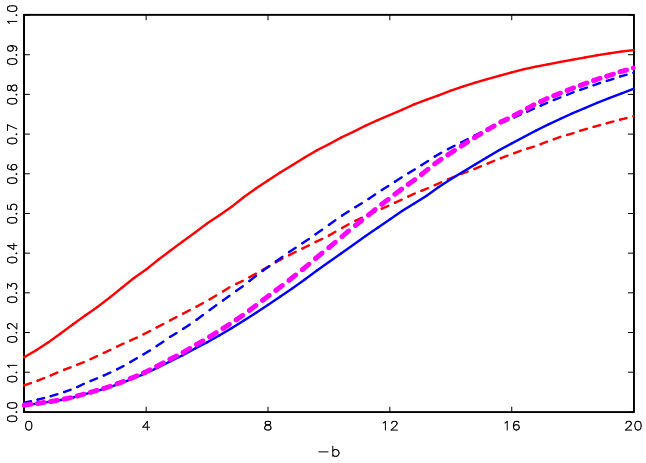

(e) $\kappa = 0.8$

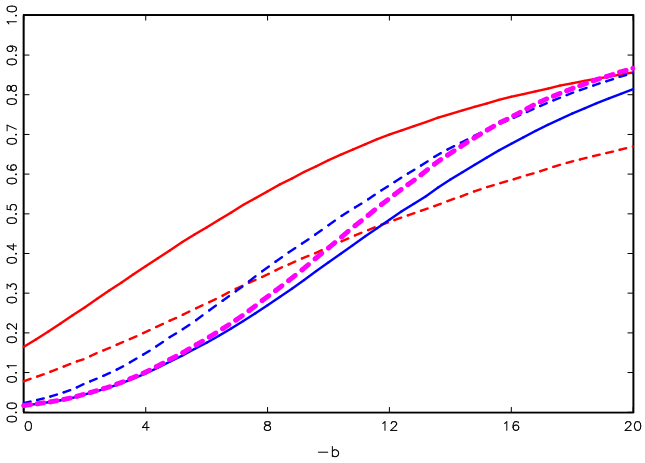

(f) $\kappa = 1.0$

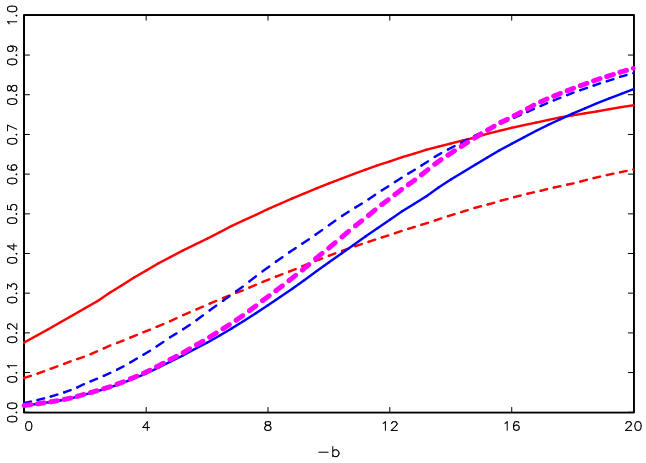

t_{μ}^{OLS}: – –, Q_{μ}^{GLS}: ——, t_{τ}^{OLS}: – –, Q_{τ}^{GLS}: ——, S^{hyb}: – –

Figure S.31: Local Asymptotic Power of Left-Tailed Tests. DGP (1)-(3) with $c = -20$, $\delta = -0.75$ and $\kappa = \{0.0, 0.1, 0.2, 0.3, 0.4, 0.5\}$, where c, κ and δ are the local-to-unity AR, local-to-zero trend, and endogeneity correlation parameters, respectively.

(a) $\kappa = 0.0$

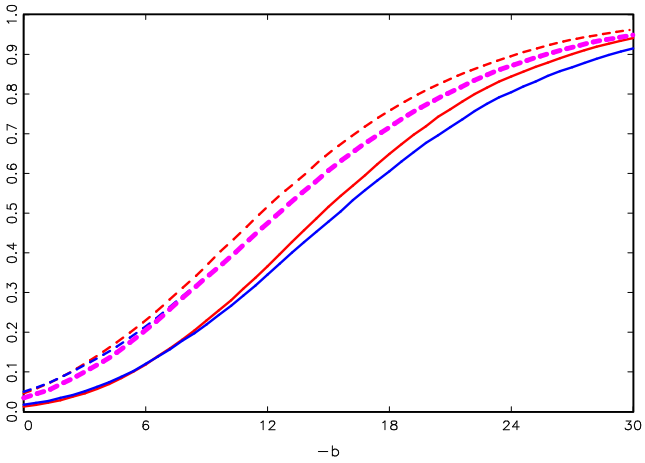

(b) $\kappa = 0.1$

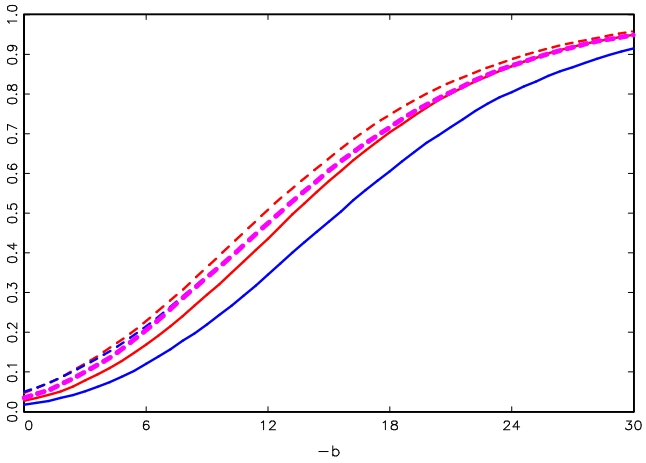

(c) $\kappa = 0.2$

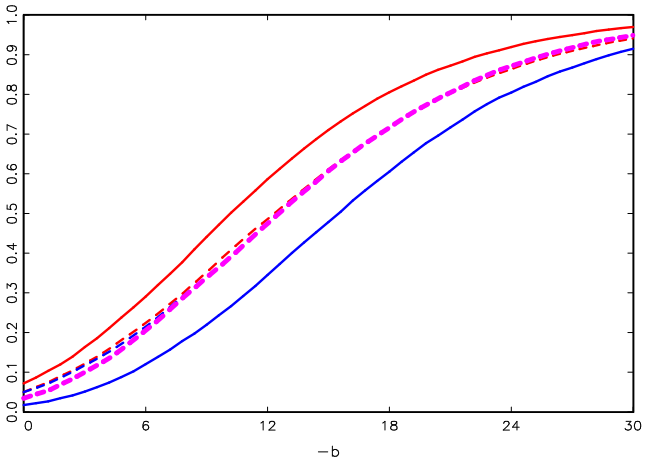

(d) $\kappa = 0.3$

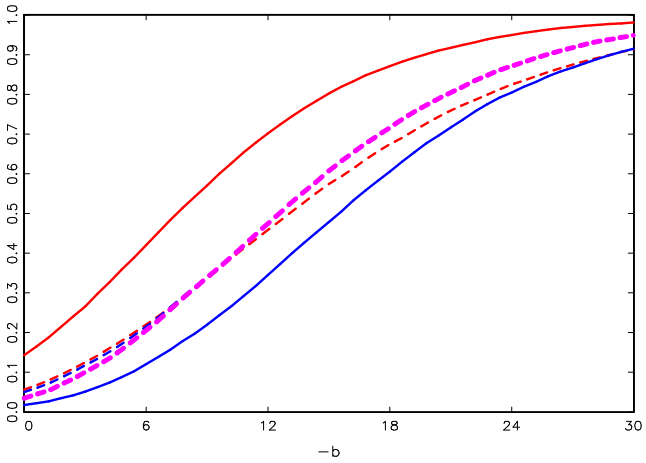

(e) $\kappa = 0.4$

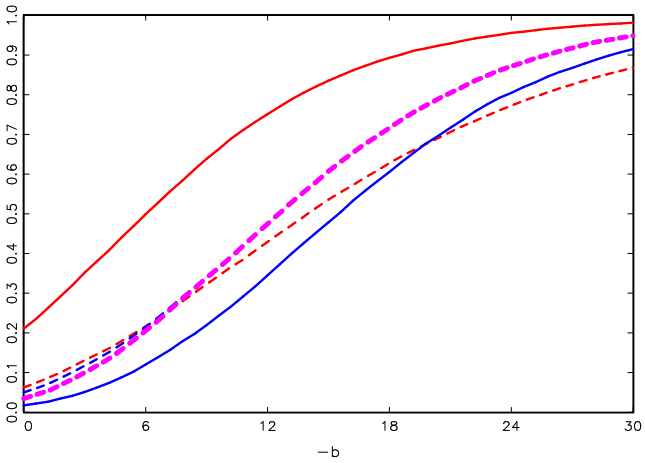

(f) $\kappa = 0.5$

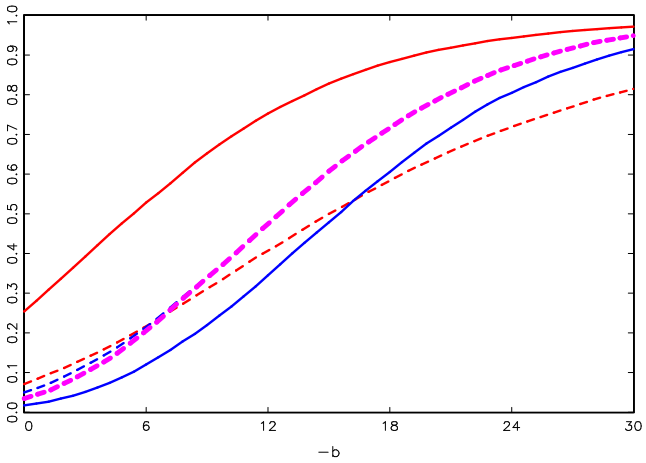

t_{μ}^{OLS}: – –, Q_{μ}^{GLS}: ——, t_{τ}^{OLS}: – –, Q_{τ}^{GLS}: ——, S^{hyb}: – –

Figure S.32: Local Asymptotic Power of Left-Tailed Tests. DGP (1)-(3) with $c = -30$, $\delta = -0.75$ and $\kappa = \{0.0, 0.1, 0.2, 0.3, 0.4, 0.5\}$, where c, κ and δ are the local-to-unity AR, local-to-zero trend, and endogeneity correlation parameters, respectively.

(a) $\kappa = 0.0$

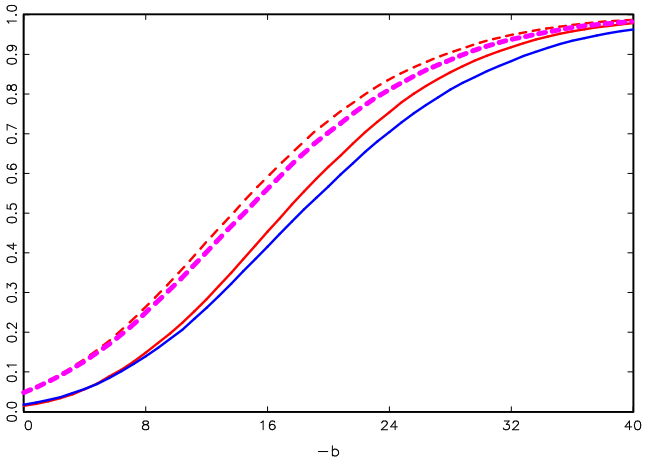

(b) $\kappa = 0.1$

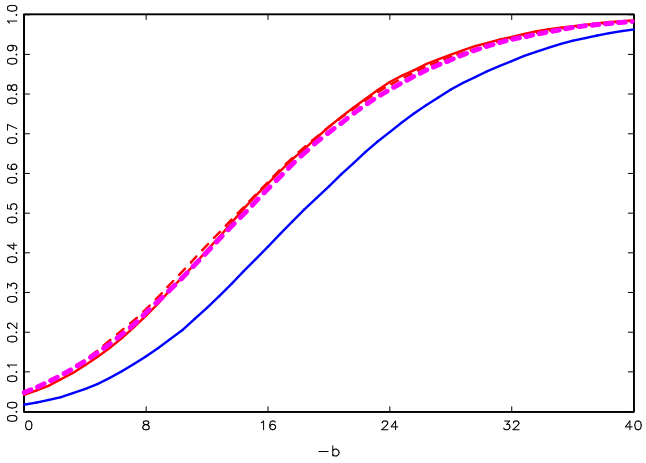

(c) $\kappa = 0.2$

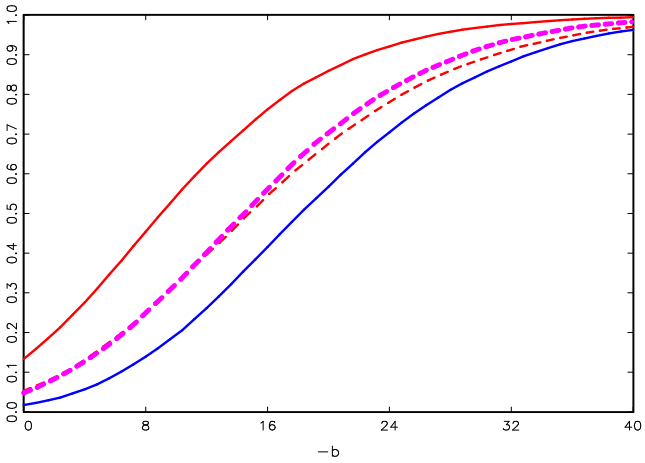

(d) $\kappa = 0.3$

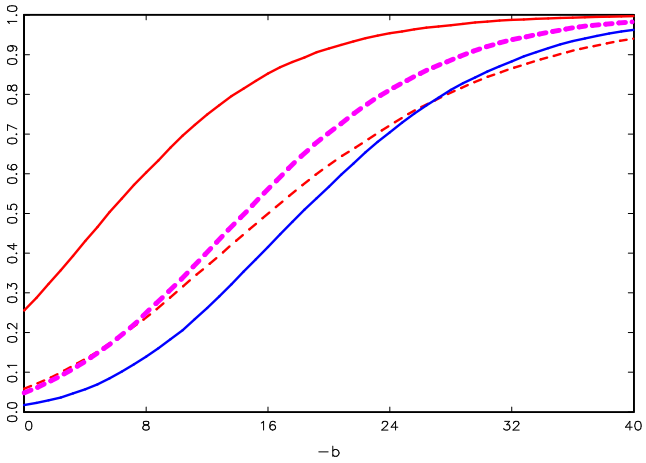

(e) $\kappa = 0.4$

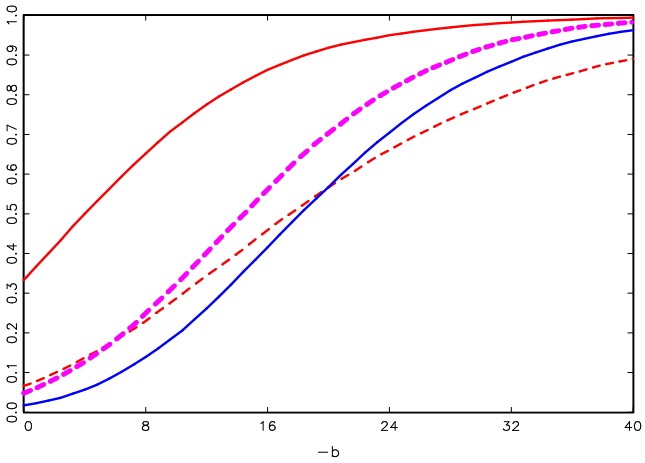

(f) $\kappa = 0.5$

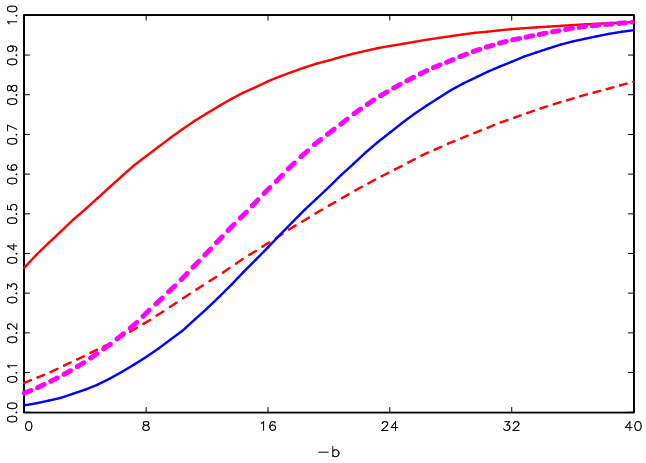

t_{μ}^{OLS}: – –, Q_{μ}^{GLS}: ——, t_{τ}^{OLS}: – –, Q_{τ}^{GLS}: ——, S^{hyb}: – –

Figure S.33: Local Asymptotic Power of Left-Tailed Tests. DGP (1)-(3) with $c = -40$, $\delta = -0.75$ and $\kappa = \{0.0, 0.1, 0.2, 0.3, 0.4, 0.5\}$, where c, κ and δ are the local-to-unity AR, local-to-zero trend, and endogeneity correlation parameters, respectively.

(a) $\kappa = 0.0$

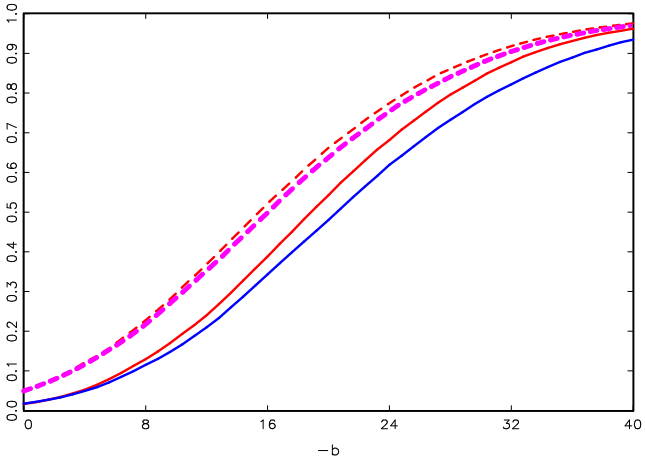

(b) $\kappa = 0.1$

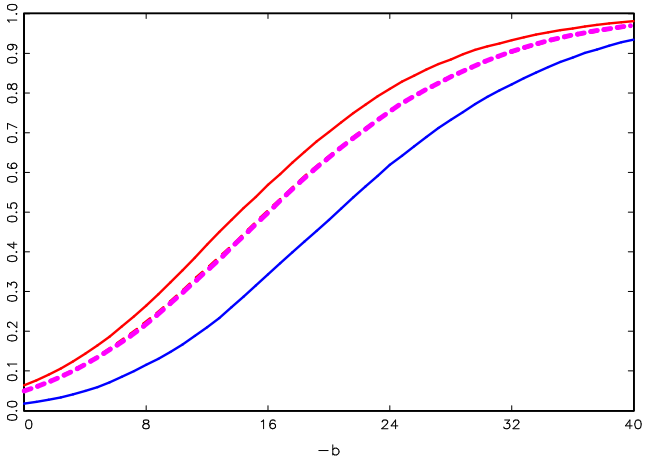

(c) $\kappa = 0.2$

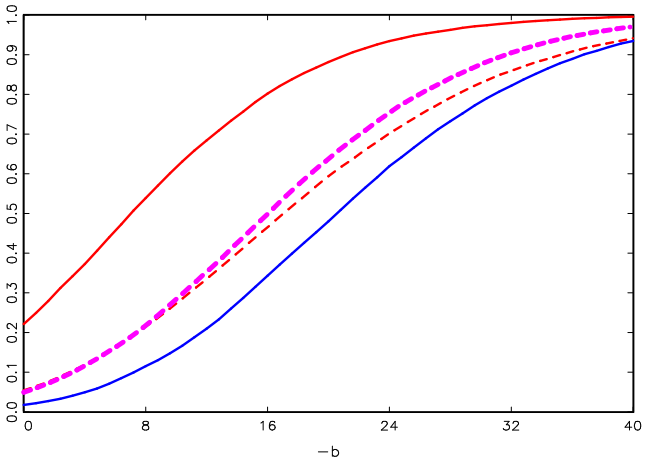

(d) $\kappa = 0.3$

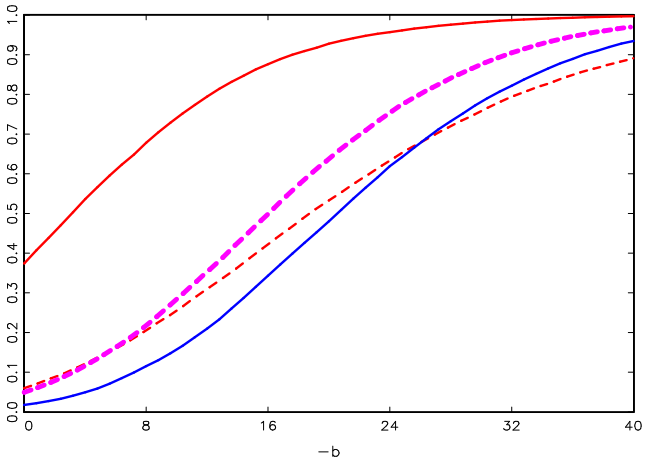

(e) $\kappa = 0.4$

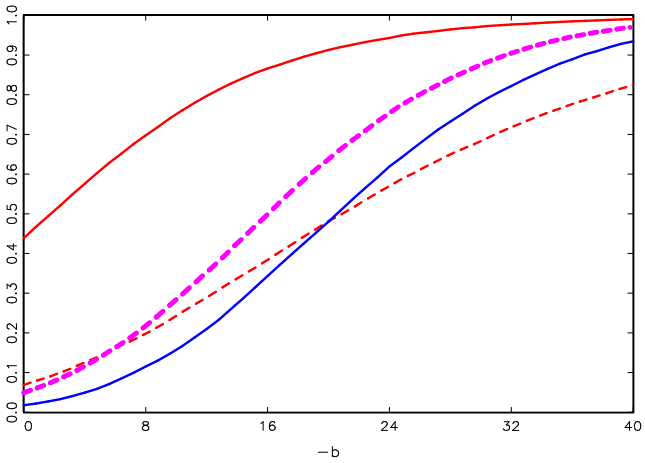

(f) $\kappa = 0.5$

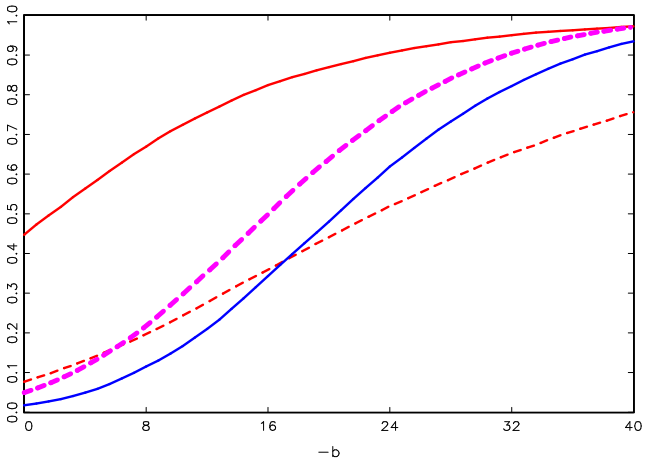

t_μ^{OLS}: – –, Q_μ^{GLS}: ——, t_τ^{OLS}: – –, Q_τ^{GLS}: ——, S^{hyb}: – –

Figure S.34: Local Asymptotic Power of Left-Tailed Tests. DGP (1)-(3) with $c = -50$, $\delta = -0.75$ and $\kappa = \{0.0, 0.1, 0.2, 0.3, 0.4, 0.5\}$, where c, κ and δ are the local-to-unity AR, local-to-zero trend, and endogeneity correlation parameters, respectively.

(a) $\kappa = 0.0$

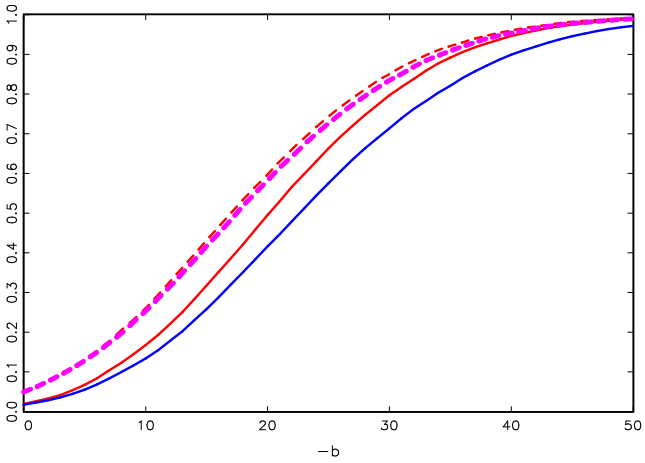

(b) $\kappa = 0.1$

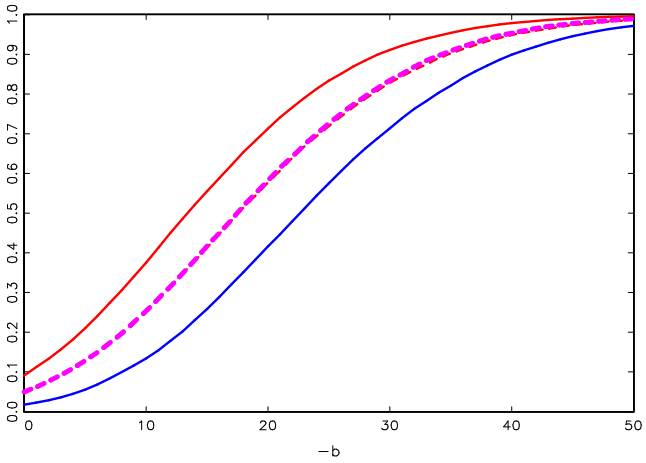

(c) $\kappa = 0.2$

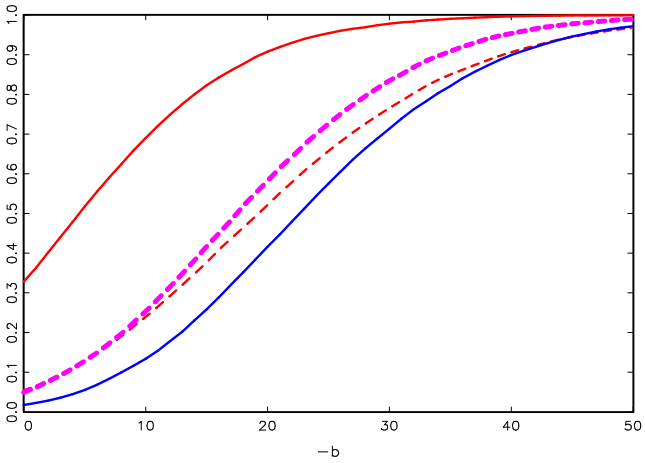

(d) $\kappa = 0.3$

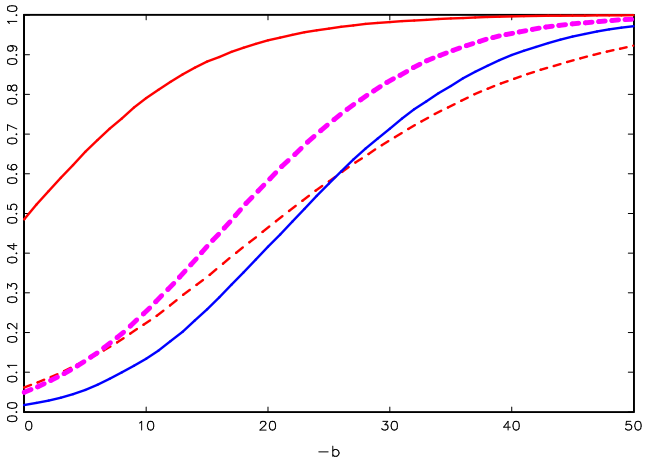

(e) $\kappa = 0.4$

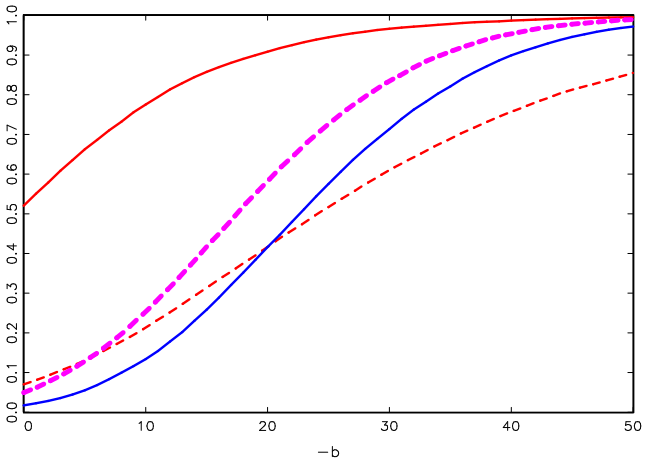

(f) $\kappa = 0.5$

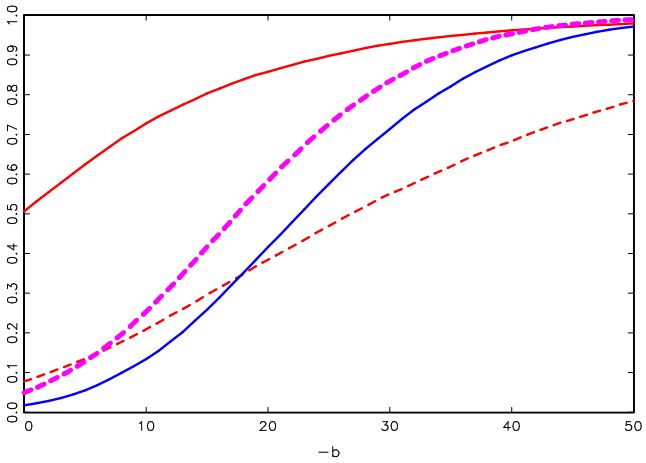

t_μ^{OLS}: – –, Q_μ^{GLS}: ——, t_τ^{OLS}: – –, Q_τ^{GLS}: ——, S^{hyb}: – –

Figure S.35: Local Asymptotic Power of Right-Tailed Tests. DGP (1)-(3) with $c = 2$, $\delta = -0.95$ and $\kappa = \{0.0, 0.2, 0.4, 0.6, 0.8, 1.0\}$, where c, κ and δ are the local-to-unity AR, local-to-zero trend, and endogeneity correlation parameters, respectively.

(a) $\kappa = 0.0$

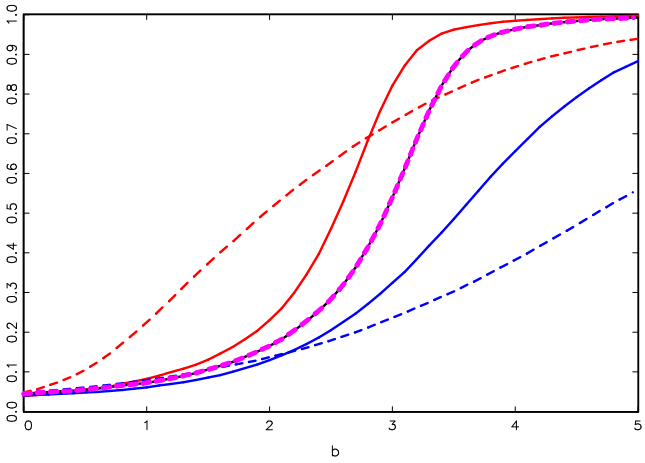

(b) $\kappa = 0.2$

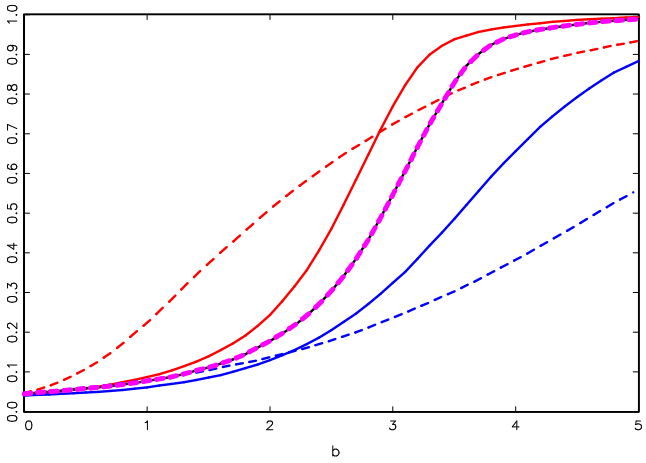

(c) $\kappa = 0.4$

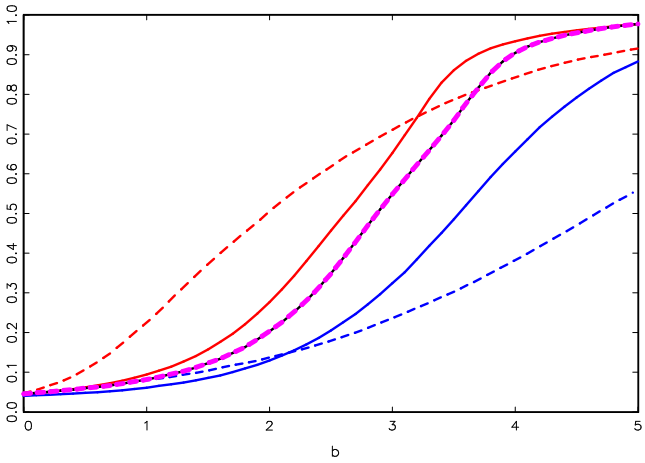

(d) $\kappa = 0.6$

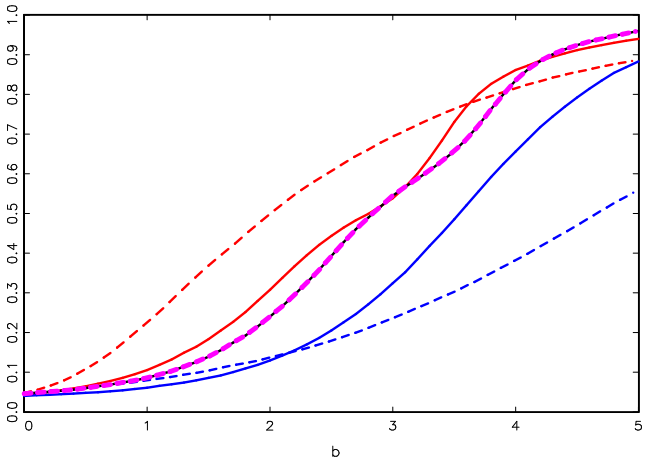

(e) $\kappa = 0.8$

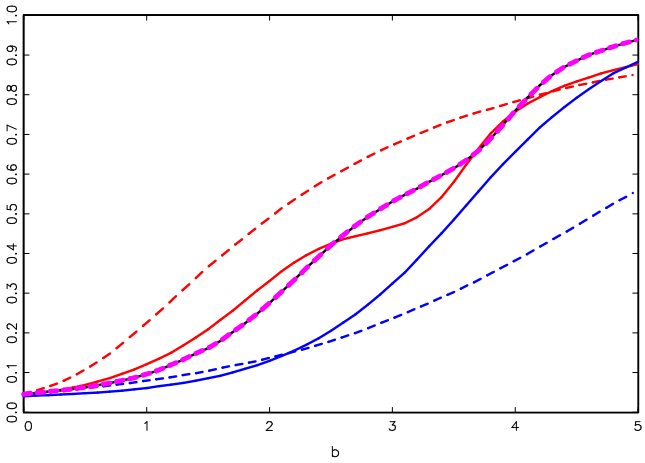

(f) $\kappa = 1.0$

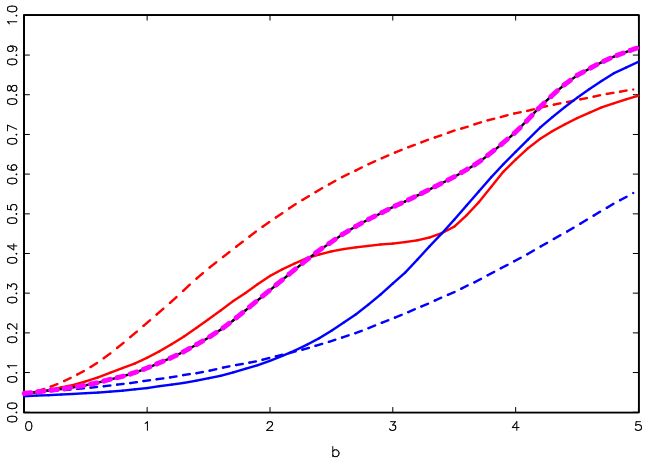

t_{μ}^{OLS}: – –, Q_{μ}^{GLS}: ——, t_{τ}^{OLS}: – –, Q_{τ}^{GLS}: ——, U^{hyb}: ——, S^{hyb}: – –

Figure S.36: Local Asymptotic Power of Right-Tailed Tests. DGP (1)-(3) with $c = 2$, $\delta = -0.75$ and $\kappa = \{0.0, 0.2, 0.4, 0.6, 0.8, 1.0\}$, where c, κ and δ are the local-to-unity AR, local-to-zero trend, and endogeneity correlation parameters, respectively.

(a) $\kappa = 0.0$

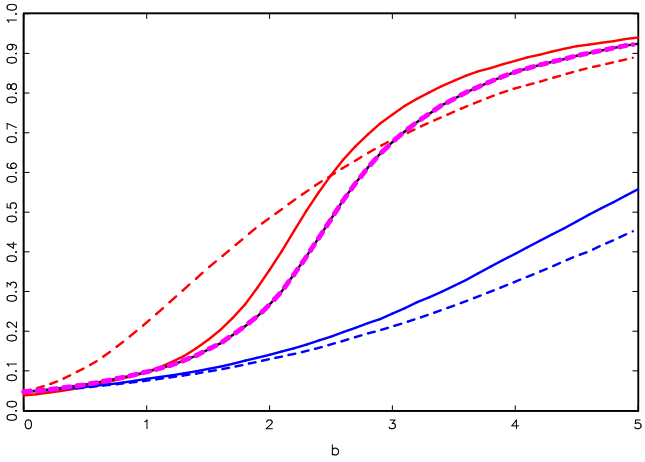

(b) $\kappa = 0.2$

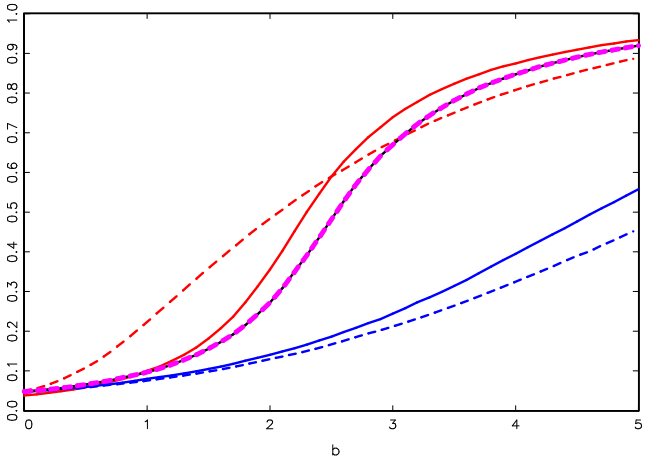

(c) $\kappa = 0.4$

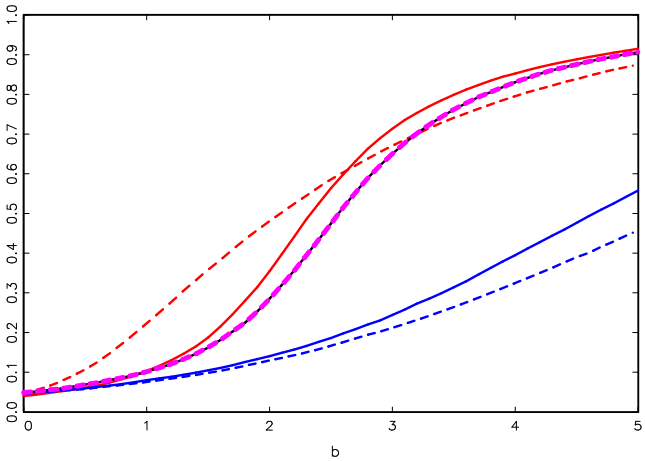

(d) $\kappa = 0.6$

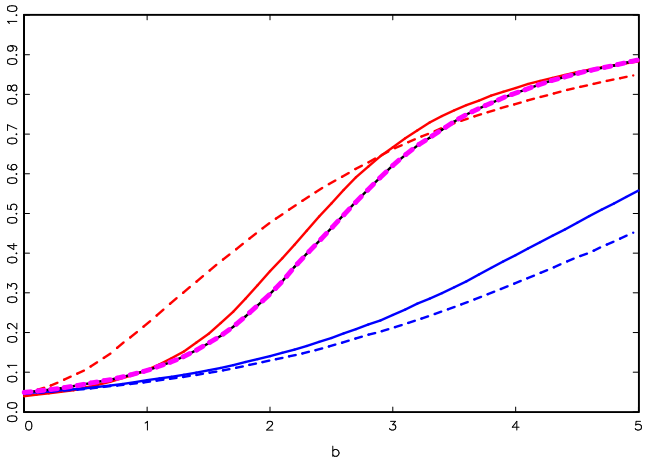

(e) $\kappa = 0.8$

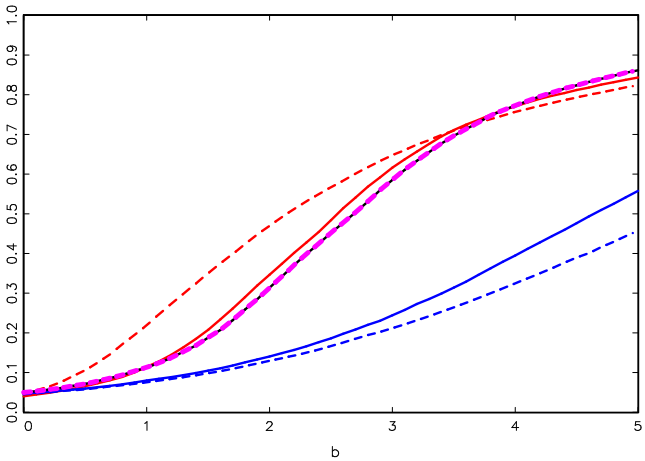

(f) $\kappa = 1.0$

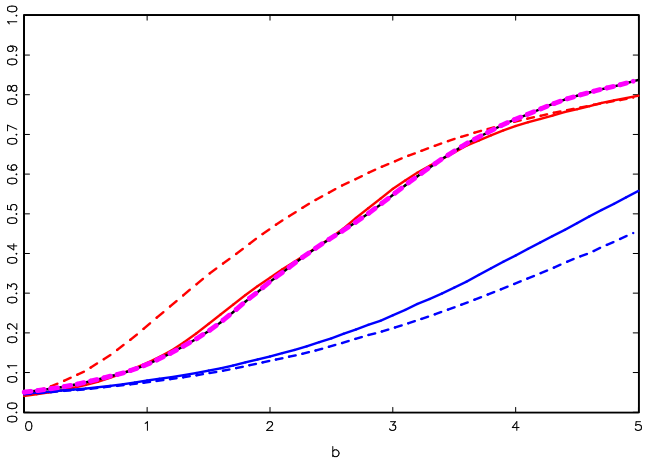

t_{μ}^{OLS}: – –, Q_{μ}^{GLS}: ——, t_{τ}^{OLS}: – –, Q_{τ}^{GLS}: ——, U^{hyb}: ——, S^{hyb}: – –

Figure S.37: Local Asymptotic Power of Left-Tailed Tests. DGP (1)-(3) with $c = 2$, $\delta = -0.95$ and $\kappa = \{0.0, 0.2, 0.4, 0.6, 0.8, 1.0\}$, where c, κ and δ are the local-to-unity AR, local-to-zero trend, and endogeneity correlation parameters, respectively.

(a) $\kappa = 0.0$

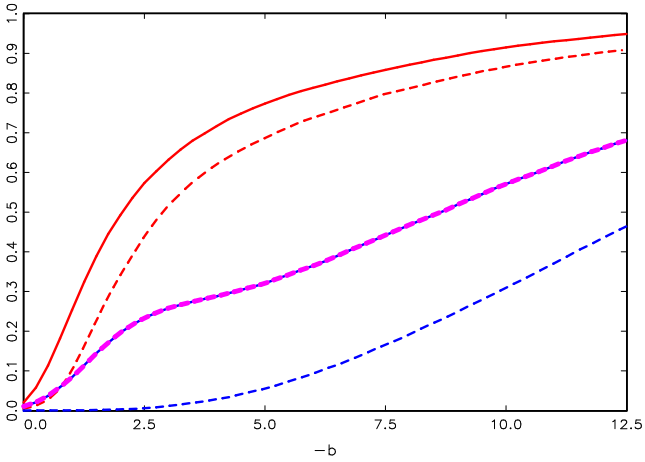

(b) $\kappa = 0.2$

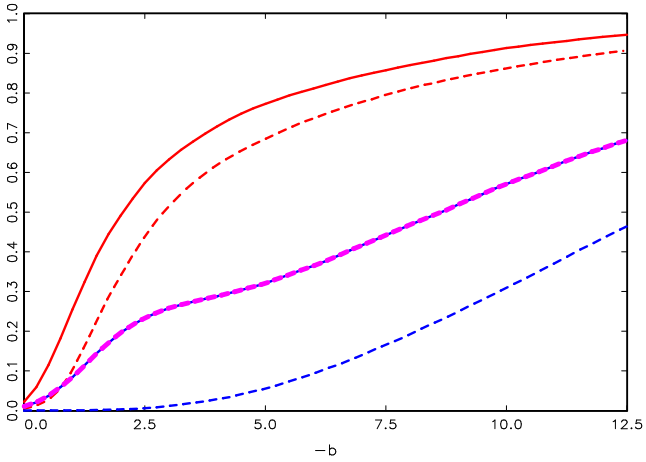

(c) $\kappa = 0.4$

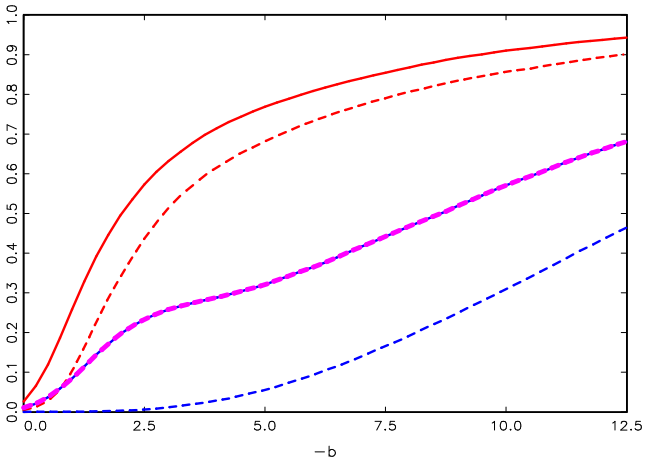

(d) $\kappa = 0.6$

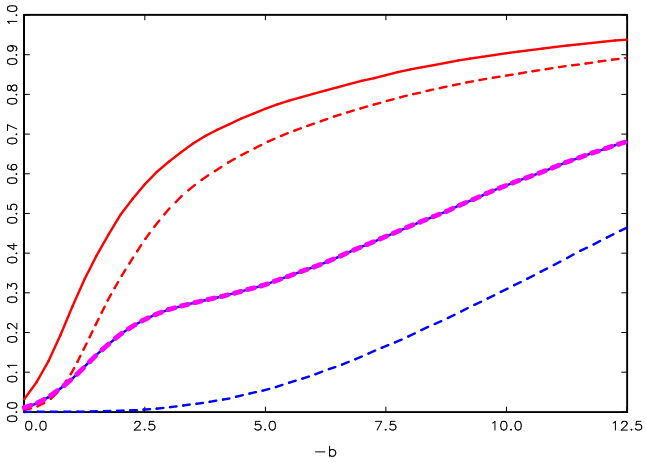

(e) $\kappa = 0.8$

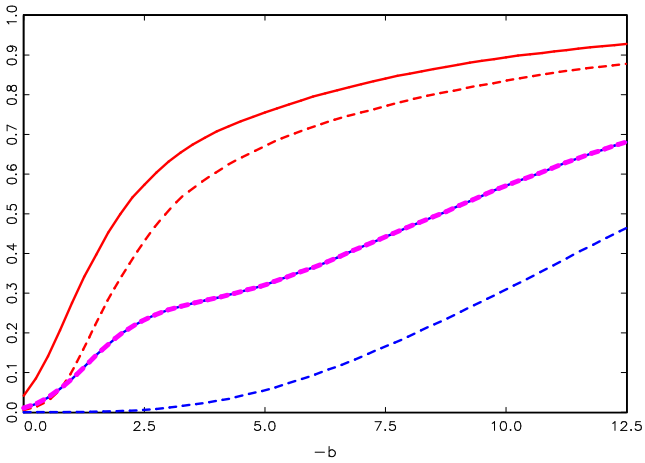

(f) $\kappa = 1.0$

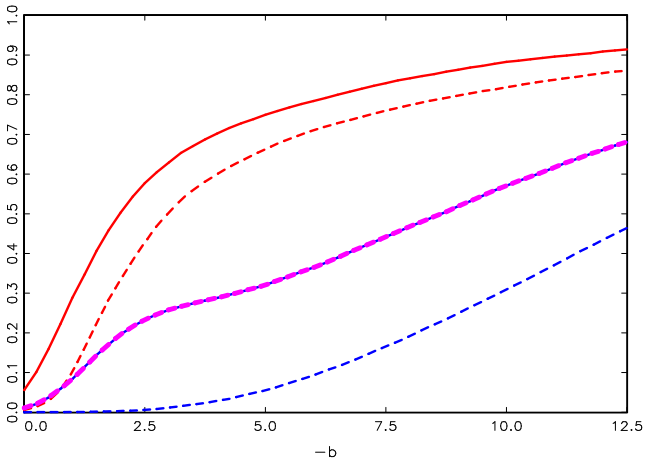

t_μ^{OLS}: – –, Q_μ^{GLS}: ——, t_τ^{OLS}: – –, Q_τ^{GLS}: ——, S^{hyb}: – –

Figure S.38: Local Asymptotic Power of Left-Tailed Tests. DGP (1)-(3) with $c = 2$, $\delta = -0.75$ and $\kappa = \{0.0, 0.2, 0.4, 0.6, 0.8, 1.0\}$, where c, κ and δ are the local-to-unity AR, local-to-zero trend, and endogeneity correlation parameters, respectively.

(a) $\kappa = 0.0$

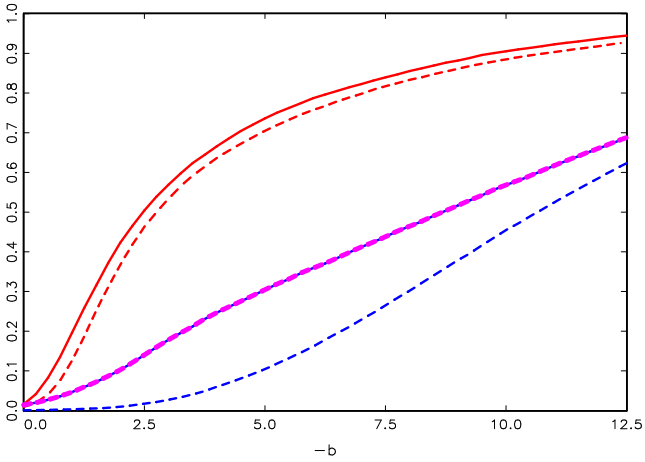

(b) $\kappa = 0.2$

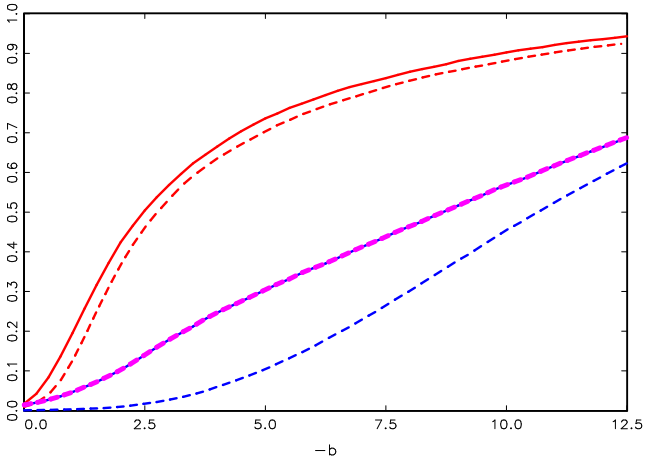

(c) $\kappa = 0.4$

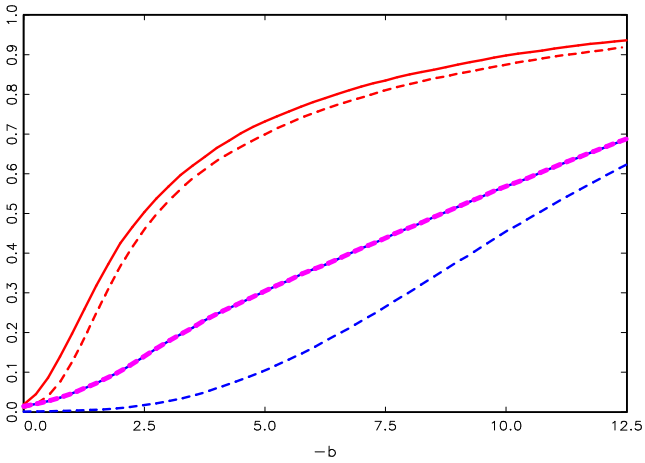

(d) $\kappa = 0.6$

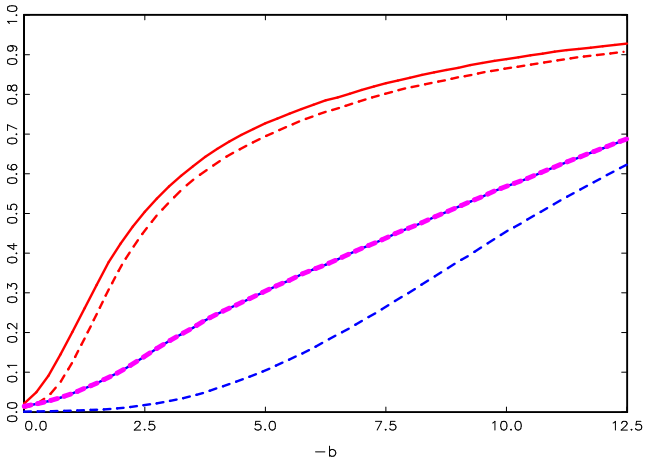

(e) $\kappa = 0.8$

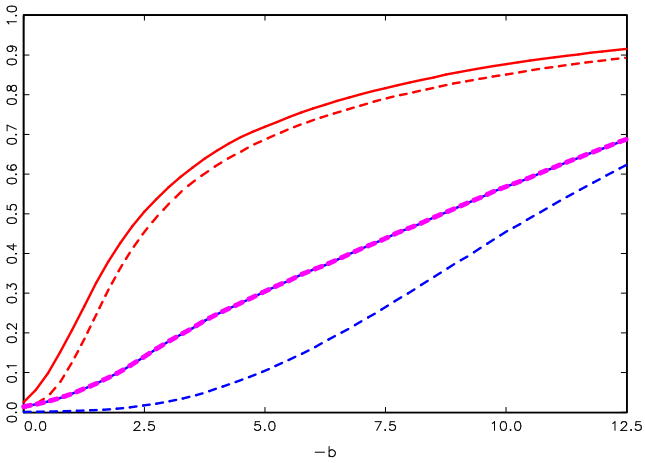

(f) $\kappa = 1.0$

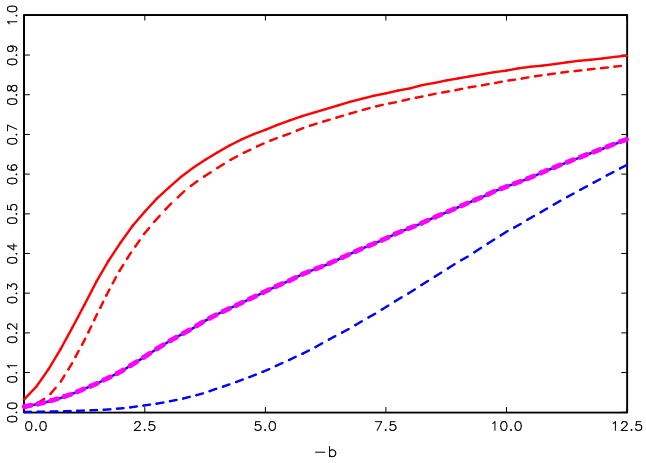

t_μ^{OLS}: – –, Q_μ^{GLS}: ——, t_τ^{OLS}: – –, Q_τ^{GLS}: ——, S^{hyb}: – –

Figure S.39: Local Asymptotic Power of Right-Tailed Bonferroni and Infeasible t_μ and Q_μ tests. DGP (1)-(3) with $\delta = -0.75$ and $\kappa = 0$, where c, κ and δ are the local-to-unity AR, trend, and endogeneity correlation parameters, respectively.

(a) $c = 0$

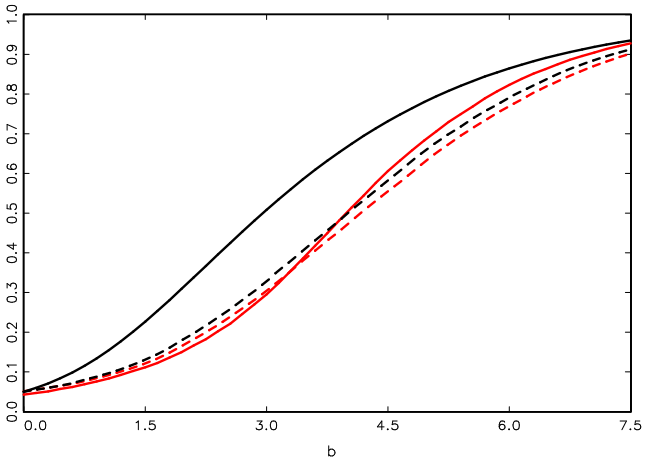

(b) $c = -2$

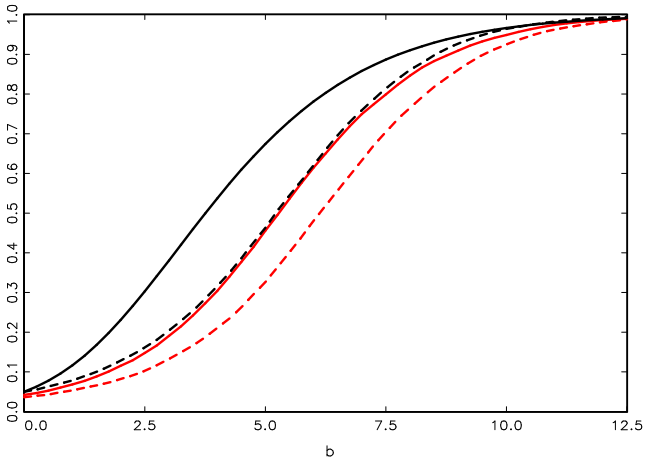

(c) $c = -5$

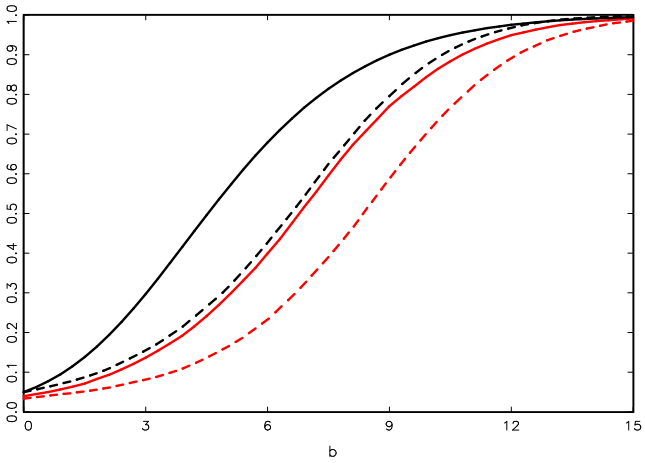

(d) $c = -10$

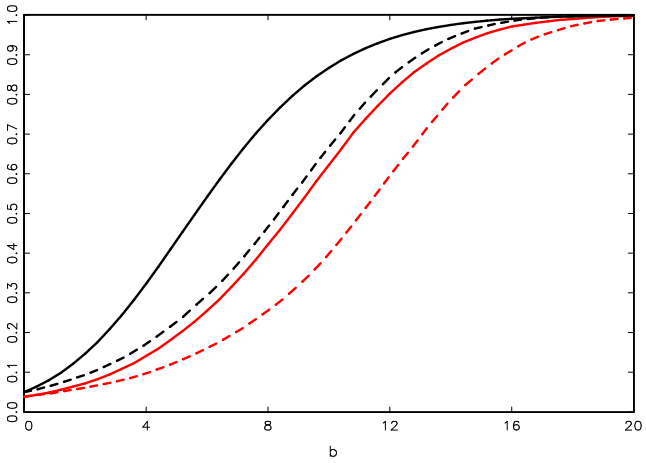

(e) $c = -20$

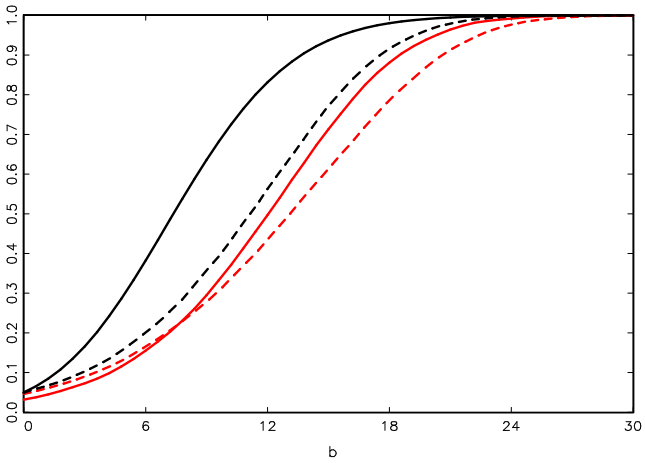

(f) $c = -50$

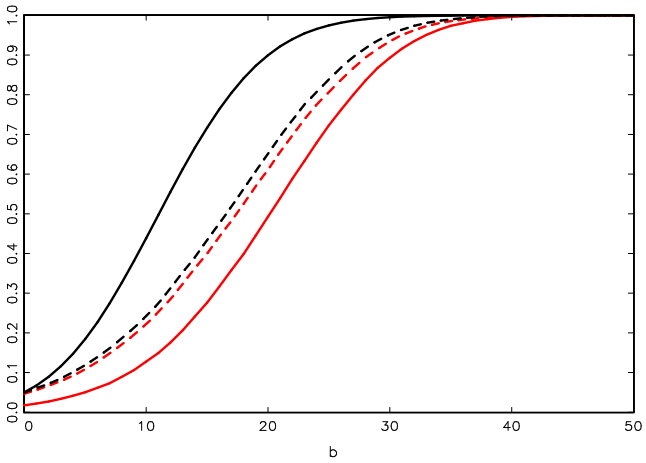

t_μ^{OLS}: – – , Q_μ^{GLS}: ——, t_μ^{IF}: – – , Q_μ^{IF}: ——

Figure S.40: Local Asymptotic Power of Right-Tailed Bonferroni and Infeasible t_τ and Q_τ tests. DGP (1)-(3) with $\delta = -0.75$, where c and δ are the local-to-unity AR and endogeneity correlation parameters, respectively.

(a) $c = 0$

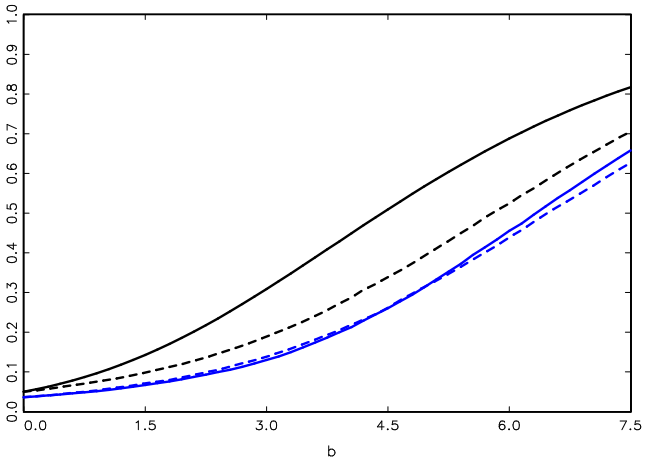

(b) $c = -2$

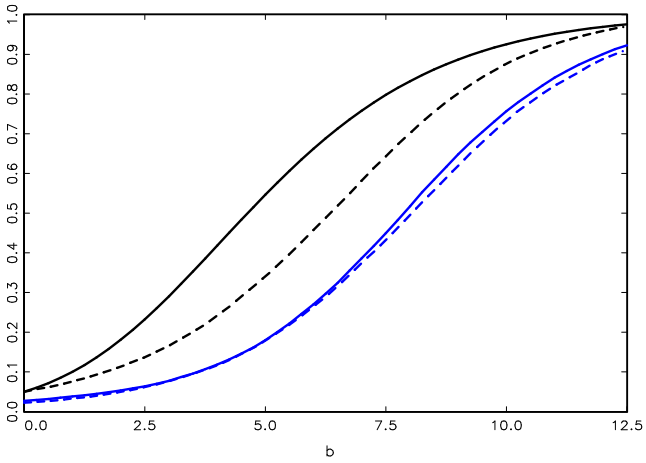

(c) $c = -5$

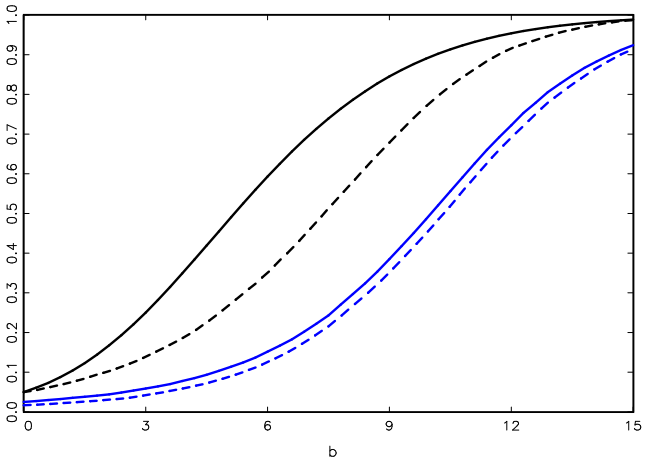

(d) $c = -10$

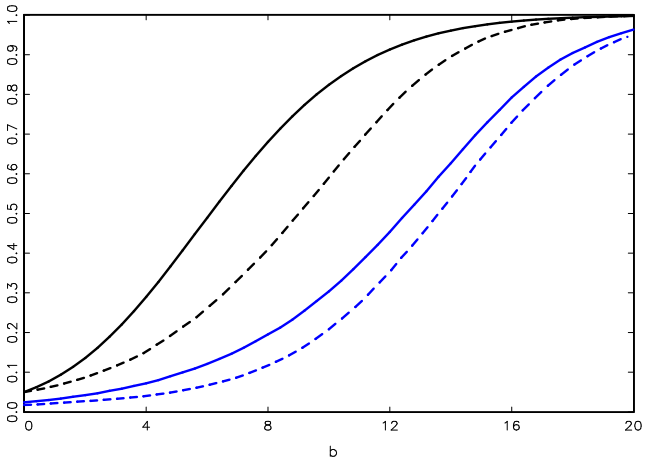

(e) $c = -20$

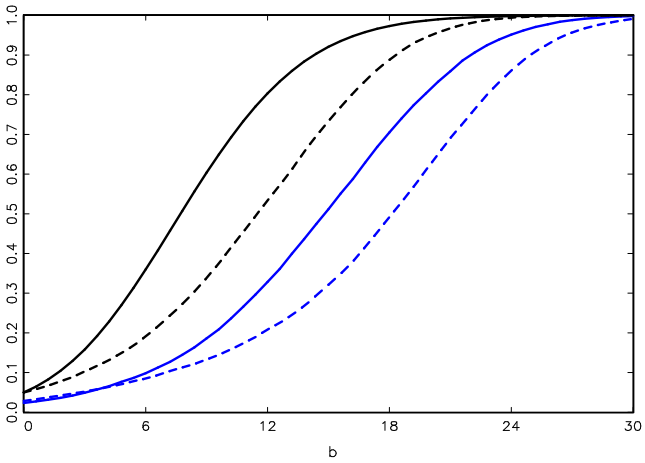

(f) $c = -50$

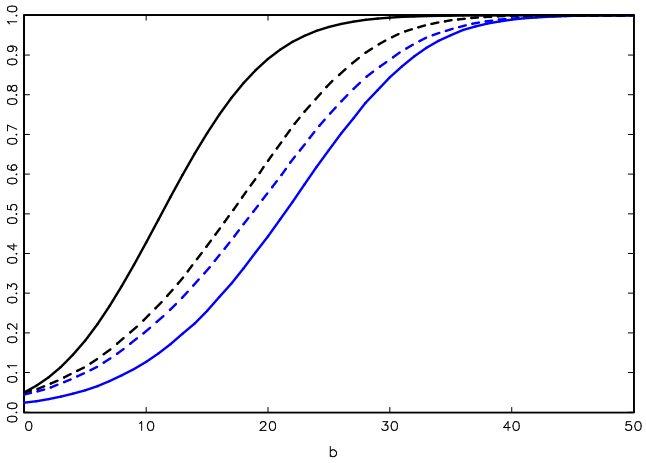

t_τ^{OLS}: – – , Q_τ^{GLS}: ——, t_τ^{IF}: – – , Q_τ^{IF}: ——

S.6 Finite Sample Size and Power

In this section we evaluate the finite sample size and power of tests for predictability discussed in this paper. To do so data were generated according to (1) - (3) with $v_t = \phi v_{t-1} + e_t$ where $e_t \sim NIID(0,1)$, setting $w_1 = v_1 = e_1$. We set $T = 250$ and generate data according to Assumptions 1 and 4.1 such that $\rho = 1 + cT^{-1}$ and $\gamma_T = \kappa\omega_v T^{-1/2}$, noting that for larger negative values of c the predictor will behave more like a weakly stationary process in finite samples. All tests are performed at a nominal level of 0.05. Following CY, lag selection for all of the unit root tests utilised in the test procedures is performed using the Bayes Information Criterion (BIC) with a maximum number of lagged differences of 4. Finally in the context of the diverging critical value $cv_{NB} = -\upsilon T^{1/2}$, we set $\upsilon = 10$ such that our hybrid S^{hyb} and U^{hyb} tests switch into the conventional t-test whenever $NB\text{-}OLS_\tau < -10T^{1/2}$ as we found this choice of υ delivered good finite sample performance across a wide range of DGPs.

S.6.1 Finite Sample Size

We being by examining the finite sample size of the tests. We first report result for $\phi = 0.0$ such that v_t is an i.i.d. process, and for $c = 2, 0, -2, -5, -10, -20, -30, -40, -50, -100, -250$, with the final setting clearly corresponding to weak persistence ($\rho = 0$ when $c = -250$). We report results for $\kappa = 0$ in Table S.2 and $\kappa = 0.5 + 0.5I(c > -20)$ in Table S.3, where we make κ dependent on c in the latter scenario due to the impact of κ on the size of the tests being greater the more negative is the value of c.

Turning first to Table S.2 we see that for right-tailed tests with $\kappa = 0$ and $\phi = 0.0$ all tests are well size controlled for $c > -50$, with this result unsurprising given that all tests are designed to be asymptotically size controlled when ρ is local-to-unity, with the t_μ^{OLS} and t_τ^{OLS} tests retaining size control across all other values of c. As c becomes more negative we do see some size distortions for the Q_d^{GLS} tests, as for these values of c the predictor will be behaving more like a weakly stationary process, in which case these tests are asymptotically invalid. While the Q_μ^{GLS} test displays severe size distortions only for $c = -250$, the Q_τ^{GLS} test also suffers severe size distortions for $c = -100$. As a consequence, the U^{hyb} test does suffer from severe size distortions for $c = -100$ as while U^{hyb} is correctly switching into

the conventional t-test in almost all (99.9%) of replications for $c = -250$, and is therefore correctly sized, this will not be true for $c = -100$ and the oversize of Q_τ^{GLS} in this scenario feeds through into the size of U^{hyb}. This renders the U^{hyb} test potentially unreliable. The size of the S^{hyb} test, on the other hand, is well controlled across all values of c. This is due to the fact for intermediate values of c that span the gap between strongly persistent and weakly persistent predictors this test will be switching into the size controlled t_τ^{OLS} test with very high probability.

For left-tailed tests with $\kappa = 0$ and $\phi = 0.0$ we observe that, with the exception of the Q_μ^{GLS} test for larger negative values of c, all tests display reasonable size control across all values of c. While the tests have very low size for values of c closer to zero this is in line with the asymptotic size of the tests when maximising size at 0.05 across a large range of c. We see that the size of S^{hyb} is identical to that of Q_τ^{GLS} for c close to 0, and to that of t_τ^{OLS} for more negative values of c (with the exception of $c = -250$ where S^{hyb} is almost always switching into conventional t) demonstrating that the switching rule in (20) is effective in finite samples.

We now turn to Table S.3 which reports results for a large positive value of κ. First we observe that the size of the Q_τ^{GLS} and t_τ^{OLS} tests are identical to those in Table S.2 for both right and left-tailed tests due to these tests being invariant to the value of κ. For right (left) tail tests we see that both the Q_μ^{GLS} and t_μ^{GLS} tests can be severely undersized (oversized), with this undersize (oversize) more pronounced the more negative is the value of c for a given value of κ. For right-tailed tests we see that for c close to zero the size of both U^{hyb} and S^{hyb} is slightly lower relative to the case where $\kappa = 0$, and we will see that this translates into a loss of power for these tests relative to when $\kappa = 0$, although the power of these tests for $\kappa \neq 0$ will be shown to still be close to that of the most powerful test in each scenario. For left-tailed tests the S^{hyb} test has identical size to that seen in Table S.2 as this test is a function of two tests that are both invariant to κ.

We now briefly discuss the results for the size of the tests when $\phi = 0.5$ so that the predictor is generated as an AR(2) process. We report results only for $c = 2, 0, -2, -5, -10, -20, -30, -40, -50$ so that the serial correlation induced by the value of $\rho = 1 + cT^{-1}$ remains the dominant driver of the persistence of the predictor.

Table S.4 reports the size of the tests when $\kappa = 0$ and Table S.5 reports results for when $\kappa = 0.5 + 0.5I(c > -20)$. While the size of the tests is not identical to the case when $\phi = 0.0$, the difference in size between $\phi = 0.5$ and $\phi = 0.0$ is minimal in a vast majority of cases. This is likely due to the fact that we are using the BIC to select the AR order for the predictor, which selects the true order in a vast majority of instances.

S.6.2 Finite Sample Power

We now examine the finite sample power properties of all tests. We begin by reporting power for both right and left-tailed tests for $c = 0, -2, -5, -10, -20, -30, -40, -50, -100, -250$ and for $\delta = -0.95, -0.75$, all across various values of κ. We then briefly discuss the relative power performance of the tests for an explosive predictor with $c = 2$.

We first examine the finite sample power of right-tailed tests for predictability when $\delta = -0.95$ reported in Figures S.41 - S.50. The power of the tests when $\kappa = 0$ is reported in panel (a) of each figure, with these results mirroring those found for local asymptotic power in sections 4.1 and 6 where the best overall power performance for c close to zero is displayed by the Q_{μ}^{GLS} test. For the more negative values of $c <= -30$ the best power is displayed by the t_{μ}^{OLS} test. For c close to zero we see that, much like when examining local asymptotic power, the finite sample power of the hybrid U^{hyb} and S^{hyb} tests is very close to that of the best performing Q_{μ}^{GLS} test. For larger negative values of c the power of the U^{hyb} test is less competitive, and for $c = -100$ the test is oversized, as noted above. The S^{hyb} test, on the other hand, is among the better performing tests for all values of c, owing to this test basing inference on the t_{τ}^{OLS} test with increasing probability as c becomes more negative. For the largest value of c considered ($c = -250$), both U^{hyb} and S^{hyb} have switched into the standard t_{τ} test in almost all replications, and consequently display an attractive power profile.

The power of right-tailed tests when $\delta = -0.95$ and $\kappa > 0$ is reported in panels (b) - (f) of Figures S.41 - S.50. Again, these results closely mirror those found for the local asymptotic power of the tests, with the power of the Q_{μ}^{GLS} and t_{μ}^{OLS} tests falling away as the value of κ increases, and the power of Q_{τ}^{GLS} and t_{τ}^{OLS} invariant to the value of κ. For c close to zero the power of the hybrid U^{hyb} and S^{hyb} tests tracks close to the most powerful Q_{μ}^{GLS} test for small κ, while for larger κ, the hybrid tests closely track the power of the

better performing Q_τ^{GLS} test, hence the U^{hyb} and S^{hyb} tests are among the most powerful tests regardless of the value of κ. For larger negative values of c we see that S^{hyb} continues to be among the most powerful tests given that it is increasingly likely to switch into the t_τ^{OLS} test, which performs well in this region, as the value of c decreases.

Results for right-tailed tests with $\delta = -0.75$ are reported in Figures S.51 - S.60, with the relative power of the tests across both c and κ qualitatively similar to that found for $\delta = -0.95$.

Results for left-tailed tests with $\delta = -0.95$ are reported in Figures S.61 - S.70. As with the local asymptotic power results, although the Q_μ^{GLS} and t_μ^{OLS} tests perform well when $\kappa = 0$, these tests suffer from substantial oversize when $\kappa \neq 0$. Among the with-trend tests, the Q_τ^{GLS} test displays the best overall power for c close to zero, and the t_τ^{OLS} test performs best for more negative values of c. With the exception of the case $c = -250$, the U^{hyb} test here reduces to Q_τ^{GLS}, and therefore does not perform well unless c is close to zero. On the other hand, the hybrid S^{hyb} test is able to capture the superior power of the best performing test in each scenario, tracking closely the power of Q_τ^{GLS} for c close to zero, and that of t_τ^{OLS} for other values of c.

Results for left-tailed tests with $\delta = -0.75$ are reported in Figures S.71 - S.80, with the relative power of the tests across both c and κ, again, qualitatively similar to that found for $\delta = -0.95$.

Finally, the finite sample power of the tests for an explosive predictor with $c = 2$ are reported in Figures S.81 - S.84. Figures S.81 and S.82 report power of right-tailed tests for $\delta = -0.95$ and $\delta = -0.75$, respectively. The main differences that we see compared to the previous values of c considered is that in the explosive predictor case the best overall power performance is, in fact, delivered by the t_μ^{OLS} test, with the impact of an omitted trend on the constant-only tests less pronounced than for $c \leq 0$. Figures S.83 and S.84 report power of left-tailed tests for $\delta = -0.95$ and $\delta = -0.75$, respectively. Much like with right-tailed tests with an explosive predictor, the presence of an omitted trend has minimal impact on the constant-only tests such that Q_μ^{GLS} and t_μ^{OLS} are the best performing tests. While for an explosive predictor the constant-only tests appear to remain the better performing tests even for relatively large values of κ, this does not change our recommendation to use

our proposed hybrid tests in practice given that a predictor that is explosive for the entire sample period is extremely unlikely to be observed in empirical practice.

Overall, we have demonstrated that the S^{hyb} test, in particular, is very well suited to testing for predictability when uncertainty exists over the presence of a trend. For both right and left-tailed tests S^{hyb} displays excellent size control, and has power that is never far behind that of the best performing test in each scenario considered across a very wide range of values of c and κ.

Table S.2: Finite Sample Size, $T = 250$, $\phi = 0.0$, $\kappa = 0$.

(a) Right-Tailed Tests

c	δ	Q_μ^{GLS}	t_μ^{OLS}	Q_τ^{GLS}	t_τ^{OLS}	U^{hyb}	S^{hyb}
2	-0.95	0.049	0.048	0.047	0.053	0.055	0.055
	-0.75	0.046	0.049	0.055	0.050	0.056	0.056
	-0.50	0.045	0.050	0.054	0.047	0.052	0.052
	-0.25	0.047	0.049	0.053	0.050	0.053	0.053
0	-0.95	0.049	0.051	0.047	0.036	0.052	0.052
	-0.75	0.052	0.052	0.045	0.038	0.054	0.054
	-0.50	0.055	0.051	0.046	0.040	0.052	0.052
	-0.25	0.057	0.052	0.048	0.046	0.049	0.049
-2	-0.95	0.050	0.044	0.039	0.025	0.044	0.044
	-0.75	0.051	0.038	0.033	0.024	0.044	0.044
	-0.50	0.054	0.041	0.035	0.029	0.041	0.042
	-0.25	0.055	0.045	0.041	0.039	0.041	0.041
-5	-0.95	0.049	0.044	0.036	0.028	0.041	0.042
	-0.75	0.049	0.034	0.031	0.018	0.038	0.038
	-0.50	0.051	0.034	0.031	0.021	0.036	0.036
	-0.25	0.052	0.038	0.036	0.031	0.036	0.036
-10	-0.95	0.045	0.047	0.039	0.039	0.038	0.038
	-0.75	0.044	0.039	0.033	0.020	0.035	0.036
	-0.50	0.047	0.034	0.031	0.018	0.031	0.032
	-0.25	0.047	0.034	0.034	0.026	0.032	0.032
-20	-0.95	0.038	0.049	0.043	0.047	0.034	0.038
	-0.75	0.036	0.045	0.036	0.034	0.031	0.034
	-0.50	0.039	0.042	0.033	0.026	0.028	0.030
	-0.25	0.045	0.042	0.037	0.028	0.030	0.031
-30	-0.95	0.034	0.050	0.053	0.049	0.037	0.047
	-0.75	0.032	0.045	0.041	0.043	0.031	0.040
	-0.50	0.036	0.046	0.037	0.038	0.028	0.037
	-0.25	0.043	0.047	0.039	0.038	0.029	0.036
-40	-0.95	0.032	0.049	0.067	0.050	0.046	0.050
	-0.75	0.030	0.047	0.050	0.046	0.036	0.045
	-0.50	0.034	0.047	0.042	0.044	0.029	0.042
	-0.25	0.042	0.049	0.041	0.044	0.029	0.042
-50	-0.95	0.032	0.049	0.085	0.051	0.060	0.051
	-0.75	0.030	0.048	0.064	0.047	0.046	0.047
	-0.50	0.033	0.049	0.051	0.047	0.033	0.046
	-0.25	0.041	0.051	0.045	0.048	0.030	0.048
-100	-0.95	0.050	0.047	0.316	0.048	0.259	0.048
	-0.75	0.042	0.047	0.248	0.049	0.203	0.049
	-0.50	0.036	0.049	0.161	0.049	0.118	0.049
	-0.25	0.037	0.051	0.085	0.051	0.055	0.051
-250	-0.95	0.281	0.040	0.857	0.036	0.065	0.065
	-0.75	0.274	0.041	0.837	0.038	0.061	0.061
	-0.50	0.207	0.045	0.793	0.041	0.057	0.057
	-0.25	0.099	0.048	0.594	0.047	0.053	0.054

(b) Left-Tailed Tests

c	δ	Q_μ^{GLS}	t_μ^{OLS}	Q_τ^{GLS}	t_τ^{OLS}	U^{hyb}	S^{hyb}
2	-0.95	0.017	0.005	0.009	0.000	0.009	0.009
	-0.75	0.013	0.010	0.013	0.000	0.013	0.013
	-0.50	0.021	0.023	0.018	0.005	0.018	0.018
	-0.25	0.035	0.030	0.029	0.027	0.029	0.029
0	-0.95	0.010	0.004	0.023	0.000	0.023	0.023
	-0.75	0.010	0.010	0.013	0.000	0.013	0.013
	-0.50	0.018	0.021	0.013	0.007	0.013	0.013
	-0.25	0.030	0.028	0.025	0.028	0.025	0.026
-2	-0.95	0.010	0.011	0.024	0.000	0.024	0.024
	-0.75	0.009	0.018	0.019	0.002	0.019	0.019
	-0.50	0.016	0.029	0.019	0.014	0.019	0.019
	-0.25	0.029	0.034	0.029	0.036	0.029	0.030
-5	-0.95	0.013	0.034	0.016	0.001	0.016	0.016
	-0.75	0.010	0.035	0.013	0.007	0.013	0.013
	-0.50	0.015	0.041	0.017	0.026	0.017	0.017
	-0.25	0.028	0.041	0.031	0.043	0.031	0.032
-10	-0.95	0.019	0.046	0.017	0.006	0.017	0.017
	-0.75	0.012	0.045	0.013	0.026	0.013	0.013
	-0.50	0.017	0.045	0.018	0.042	0.018	0.021
	-0.25	0.028	0.045	0.029	0.049	0.029	0.035
-20	-0.95	0.035	0.046	0.017	0.046	0.017	0.026
	-0.75	0.020	0.046	0.014	0.050	0.014	0.033
	-0.50	0.021	0.047	0.017	0.049	0.017	0.040
	-0.25	0.031	0.046	0.029	0.050	0.029	0.047
-30	-0.95	0.067	0.048	0.019	0.048	0.019	0.048
	-0.75	0.035	0.049	0.014	0.049	0.014	0.049
	-0.50	0.028	0.047	0.017	0.049	0.017	0.049
	-0.25	0.036	0.048	0.029	0.051	0.029	0.051
-40	-0.95	0.107	0.049	0.020	0.047	0.020	0.047
	-0.75	0.057	0.048	0.014	0.048	0.014	0.048
	-0.50	0.041	0.049	0.017	0.049	0.017	0.049
	-0.25	0.041	0.048	0.027	0.051	0.027	0.051
-50	-0.95	0.150	0.048	0.022	0.047	0.022	0.047
	-0.75	0.084	0.048	0.016	0.049	0.016	0.049
	-0.50	0.054	0.048	0.017	0.049	0.017	0.049
	-0.25	0.046	0.049	0.028	0.051	0.028	0.051
-100	-0.95	0.315	0.050	0.040	0.052	0.037	0.052
	-0.75	0.232	0.051	0.026	0.052	0.024	0.052
	-0.50	0.148	0.051	0.018	0.051	0.017	0.051
	-0.25	0.079	0.051	0.020	0.052	0.020	0.052
-250	-0.95	0.447	0.065	0.048	0.074	0.039	0.039
	-0.75	0.407	0.062	0.039	0.067	0.042	0.041
	-0.50	0.345	0.059	0.030	0.062	0.044	0.043
	-0.25	0.205	0.053	0.018	0.055	0.046	0.046

Table S.3: Finite Sample Size, $T = 250$, $\phi = 0.0$ $\kappa = 0.5 + 0.5I(c > -20)$.

(a) Right-Tailed Tests

c	δ	Q_μ^{GLS}	t_μ^{OLS}	Q_τ^{GLS}	t_τ^{OLS}	U^{hyb}	S^{hyb}
2	-0.95	0.050	0.048	0.047	0.053	0.055	0.055
	-0.75	0.047	0.047	0.055	0.050	0.057	0.057
	-0.50	0.045	0.047	0.054	0.047	0.053	0.053
	-0.25	0.045	0.047	0.053	0.050	0.051	0.051
0	-0.95	0.030	0.044	0.047	0.036	0.044	0.044
	-0.75	0.034	0.045	0.045	0.038	0.043	0.043
	-0.50	0.039	0.044	0.046	0.040	0.043	0.043
	-0.25	0.046	0.047	0.048	0.046	0.046	0.046
-2	-0.95	0.010	0.029	0.039	0.025	0.027	0.027
	-0.75	0.014	0.028	0.033	0.024	0.027	0.027
	-0.50	0.023	0.032	0.035	0.029	0.030	0.030
	-0.25	0.038	0.041	0.041	0.039	0.039	0.039
-5	-0.95	0.001	0.020	0.036	0.028	0.023	0.023
	-0.75	0.004	0.020	0.031	0.018	0.021	0.021
	-0.50	0.013	0.025	0.031	0.021	0.024	0.024
	-0.25	0.031	0.035	0.036	0.031	0.033	0.033
-10	-0.95	0.000	0.011	0.039	0.039	0.024	0.025
	-0.75	0.002	0.012	0.033	0.020	0.022	0.023
	-0.50	0.010	0.019	0.031	0.018	0.023	0.024
	-0.25	0.027	0.030	0.034	0.026	0.032	0.032
-20	-0.95	0.001	0.029	0.043	0.047	0.027	0.037
	-0.75	0.003	0.027	0.036	0.034	0.023	0.029
	-0.50	0.009	0.027	0.033	0.026	0.022	0.027
	-0.25	0.025	0.034	0.037	0.028	0.031	0.032
-30	-0.95	0.001	0.028	0.053	0.049	0.035	0.047
	-0.75	0.002	0.026	0.041	0.043	0.028	0.040
	-0.50	0.007	0.027	0.037	0.038	0.025	0.036
	-0.25	0.022	0.032	0.039	0.038	0.030	0.037
-40	-0.95	0.001	0.026	0.067	0.050	0.045	0.050
	-0.75	0.002	0.026	0.050	0.046	0.035	0.045
	-0.50	0.006	0.027	0.042	0.044	0.028	0.043
	-0.25	0.020	0.033	0.041	0.044	0.032	0.042
-50	-0.95	0.000	0.024	0.085	0.051	0.060	0.051
	-0.75	0.001	0.024	0.064	0.047	0.046	0.047
	-0.50	0.005	0.027	0.051	0.047	0.033	0.046
	-0.25	0.019	0.033	0.045	0.048	0.034	0.048
-100	-0.95	0.001	0.007	0.316	0.048	0.259	0.048
	-0.75	0.002	0.011	0.248	0.049	0.203	0.049
	-0.50	0.006	0.018	0.161	0.049	0.120	0.049
	-0.25	0.018	0.029	0.085	0.051	0.062	0.051
-250	-0.95	0.000	0.003	0.857	0.036	0.065	0.065
	-0.75	0.000	0.006	0.837	0.038	0.061	0.061
	-0.50	0.002	0.012	0.793	0.041	0.057	0.057
	-0.25	0.012	0.024	0.594	0.047	0.053	0.054

(b) Left-Tailed Tests

c	δ	Q_μ^{GLS}	t_μ^{OLS}	Q_τ^{GLS}	t_τ^{OLS}	U^{hyb}	S^{hyb}
2	-0.95	0.046	0.006	0.009	0.000	0.009	0.009
	-0.75	0.030	0.011	0.013	0.000	0.013	0.013
	-0.50	0.030	0.026	0.018	0.005	0.018	0.018
	-0.25	0.040	0.033	0.029	0.027	0.029	0.029
0	-0.95	0.042	0.011	0.023	0.000	0.023	0.023
	-0.75	0.027	0.017	0.013	0.000	0.013	0.013
	-0.50	0.030	0.029	0.013	0.007	0.013	0.013
	-0.25	0.038	0.033	0.025	0.028	0.025	0.026
-2	-0.95	0.069	0.032	0.024	0.000	0.024	0.024
	-0.75	0.038	0.036	0.019	0.002	0.019	0.019
	-0.50	0.039	0.043	0.019	0.014	0.019	0.019
	-0.25	0.043	0.039	0.029	0.036	0.029	0.030
-5	-0.95	0.161	0.064	0.016	0.001	0.016	0.016
	-0.75	0.077	0.061	0.013	0.007	0.013	0.013
	-0.50	0.058	0.060	0.017	0.026	0.017	0.017
	-0.25	0.055	0.045	0.031	0.043	0.031	0.032
-10	-0.95	0.302	0.101	0.017	0.006	0.017	0.017
	-0.75	0.138	0.085	0.013	0.026	0.013	0.013
	-0.50	0.086	0.074	0.018	0.042	0.018	0.021
	-0.25	0.066	0.052	0.029	0.049	0.029	0.035
-20	-0.95	0.341	0.079	0.017	0.046	0.017	0.026
	-0.75	0.162	0.069	0.014	0.050	0.014	0.033
	-0.50	0.095	0.061	0.017	0.049	0.017	0.040
	-0.25	0.068	0.052	0.029	0.050	0.029	0.047
-30	-0.95	0.460	0.080	0.019	0.048	0.019	0.048
	-0.75	0.229	0.071	0.014	0.049	0.014	0.049
	-0.50	0.125	0.063	0.017	0.049	0.017	0.049
	-0.25	0.079	0.055	0.029	0.051	0.029	0.051
-40	-0.95	0.535	0.081	0.020	0.047	0.020	0.047
	-0.75	0.282	0.072	0.014	0.048	0.014	0.048
	-0.50	0.149	0.064	0.017	0.049	0.017	0.049
	-0.25	0.088	0.057	0.027	0.051	0.027	0.051
-50	-0.95	0.577	0.082	0.022	0.047	0.022	0.047
	-0.75	0.321	0.072	0.016	0.049	0.016	0.049
	-0.50	0.167	0.064	0.017	0.049	0.017	0.049
	-0.25	0.092	0.056	0.028	0.051	0.028	0.051
-100	-0.95	0.609	0.098	0.040	0.052	0.037	0.052
	-0.75	0.377	0.086	0.026	0.052	0.024	0.052
	-0.50	0.200	0.074	0.018	0.051	0.017	0.051
	-0.25	0.105	0.057	0.020	0.052	0.020	0.052
-250	-0.95	0.830	0.158	0.048	0.074	0.039	0.039
	-0.75	0.594	0.125	0.039	0.067	0.042	0.041
	-0.50	0.314	0.101	0.030	0.062	0.044	0.043
	-0.25	0.143	0.062	0.018	0.055	0.046	0.046

Table S.4: Finite Sample Size, $T = 250$, $\phi = 0.5$, $\kappa = 0$.

(a) Right-Tailed Tests

c	δ	Q_μ^{GLS}	t_μ^{OLS}	Q_τ^{GLS}	t_τ^{OLS}	U^{hyb}	S^{hyb}
2	-0.95	0.050	0.050	0.048	0.055	0.054	0.054
	-0.75	0.045	0.051	0.053	0.053	0.056	0.056
	-0.50	0.045	0.049	0.052	0.048	0.052	0.052
	-0.25	0.048	0.049	0.051	0.049	0.053	0.053
0	-0.95	0.048	0.051	0.046	0.038	0.051	0.052
	-0.75	0.051	0.051	0.044	0.040	0.054	0.054
	-0.50	0.055	0.052	0.044	0.042	0.051	0.051
	-0.25	0.055	0.052	0.048	0.047	0.048	0.048
-2	-0.95	0.048	0.043	0.037	0.026	0.042	0.043
	-0.75	0.050	0.040	0.033	0.025	0.043	0.043
	-0.50	0.053	0.042	0.034	0.031	0.043	0.043
	-0.25	0.055	0.045	0.041	0.040	0.042	0.042
-5	-0.95	0.046	0.045	0.033	0.028	0.037	0.037
	-0.75	0.046	0.036	0.029	0.018	0.036	0.036
	-0.50	0.049	0.034	0.031	0.022	0.035	0.036
	-0.25	0.052	0.040	0.037	0.032	0.036	0.036
-10	-0.95	0.040	0.048	0.033	0.035	0.031	0.033
	-0.75	0.040	0.039	0.029	0.019	0.030	0.031
	-0.50	0.043	0.033	0.030	0.019	0.029	0.030
	-0.25	0.047	0.036	0.034	0.027	0.031	0.031
-20	-0.95	0.028	0.049	0.032	0.046	0.027	0.037
	-0.75	0.029	0.045	0.028	0.029	0.026	0.030
	-0.50	0.035	0.041	0.030	0.023	0.025	0.028
	-0.25	0.043	0.039	0.036	0.027	0.028	0.030
-30	-0.95	0.021	0.048	0.034	0.047	0.024	0.045
	-0.75	0.023	0.047	0.028	0.037	0.022	0.036
	-0.50	0.029	0.045	0.030	0.032	0.023	0.034
	-0.25	0.039	0.044	0.036	0.032	0.027	0.033
-40	-0.95	0.016	0.049	0.035	0.049	0.024	0.048
	-0.75	0.019	0.047	0.029	0.042	0.022	0.042
	-0.50	0.025	0.046	0.029	0.037	0.022	0.037
	-0.25	0.037	0.047	0.036	0.038	0.025	0.038
-50	-0.95	0.013	0.050	0.037	0.049	0.024	0.049
	-0.75	0.015	0.047	0.030	0.045	0.021	0.045
	-0.50	0.022	0.046	0.030	0.041	0.020	0.041
	-0.25	0.035	0.049	0.036	0.043	0.025	0.043

(b) Left-Tailed Tests

c	δ	Q_μ^{GLS}	t_μ^{OLS}	Q_τ^{GLS}	t_τ^{OLS}	U^{hyb}	S^{hyb}
2	-0.95	0.000	0.006	0.010	0.000	0.010	0.010
	-0.75	0.005	0.010	0.013	0.000	0.013	0.013
	-0.50	0.015	0.023	0.018	0.005	0.018	0.018
	-0.25	0.033	0.031	0.029	0.027	0.029	0.029
0	-0.95	0.010	0.004	0.021	0.000	0.021	0.021
	-0.75	0.010	0.010	0.011	0.001	0.011	0.011
	-0.50	0.018	0.021	0.013	0.007	0.013	0.013
	-0.25	0.031	0.028	0.026	0.027	0.026	0.026
-2	-0.95	0.010	0.011	0.023	0.000	0.023	0.023
	-0.75	0.009	0.018	0.018	0.002	0.018	0.018
	-0.50	0.016	0.029	0.019	0.014	0.019	0.019
	-0.25	0.029	0.035	0.029	0.034	0.029	0.030
-5	-0.95	0.013	0.033	0.015	0.001	0.015	0.015
	-0.75	0.010	0.034	0.013	0.006	0.013	0.013
	-0.50	0.015	0.040	0.018	0.025	0.018	0.018
	-0.25	0.029	0.041	0.030	0.043	0.030	0.032
-10	-0.95	0.017	0.046	0.017	0.005	0.017	0.017
	-0.75	0.012	0.043	0.013	0.023	0.013	0.014
	-0.50	0.017	0.044	0.019	0.040	0.019	0.022
	-0.25	0.029	0.045	0.031	0.049	0.031	0.036
-20	-0.95	0.033	0.046	0.020	0.036	0.020	0.026
	-0.75	0.020	0.047	0.015	0.047	0.015	0.030
	-0.50	0.022	0.047	0.020	0.048	0.020	0.038
	-0.25	0.033	0.047	0.031	0.049	0.031	0.045
-30	-0.95	0.063	0.047	0.021	0.049	0.021	0.049
	-0.75	0.034	0.047	0.016	0.049	0.016	0.047
	-0.50	0.030	0.047	0.019	0.049	0.019	0.048
	-0.25	0.038	0.049	0.030	0.050	0.030	0.049
-40	-0.95	0.104	0.048	0.023	0.049	0.023	0.049
	-0.75	0.055	0.048	0.016	0.047	0.016	0.047
	-0.50	0.041	0.047	0.019	0.050	0.019	0.050
	-0.25	0.043	0.048	0.030	0.050	0.030	0.050
-50	-0.95	0.150	0.049	0.024	0.049	0.024	0.049
	-0.75	0.081	0.048	0.017	0.048	0.017	0.048
	-0.50	0.055	0.048	0.020	0.049	0.020	0.049
	-0.25	0.048	0.047	0.030	0.050	0.030	0.050

Table S.5: Finite Sample Size, $T = 250$, $\phi = 0.5$ $\kappa = 0.5 + 0.5I(c > -20)$.

(a) Right-Tailed Tests

c	δ	Q_μ^{GLS}	t_μ^{OLS}	Q_τ^{GLS}	t_τ^{OLS}	U^{hyb}	S^{hyb}
2	-0.95	0.049	0.048	0.048	0.055	0.056	0.056
	-0.75	0.046	0.047	0.053	0.053	0.057	0.057
	-0.50	0.045	0.047	0.052	0.048	0.052	0.052
	-0.25	0.045	0.048	0.051	0.049	0.051	0.051
0	-0.95	0.030	0.044	0.046	0.038	0.044	0.044
	-0.75	0.033	0.043	0.044	0.040	0.044	0.044
	-0.50	0.038	0.045	0.044	0.042	0.044	0.044
	-0.25	0.047	0.048	0.048	0.047	0.045	0.045
-2	-0.95	0.009	0.030	0.037	0.026	0.026	0.026
	-0.75	0.012	0.028	0.033	0.025	0.026	0.027
	-0.50	0.023	0.030	0.034	0.031	0.030	0.030
	-0.25	0.038	0.039	0.041	0.040	0.039	0.039
-5	-0.95	0.001	0.020	0.033	0.028	0.020	0.021
	-0.75	0.004	0.019	0.029	0.018	0.020	0.021
	-0.50	0.014	0.024	0.031	0.022	0.024	0.024
	-0.25	0.031	0.034	0.037	0.032	0.035	0.035
-10	-0.95	0.001	0.011	0.033	0.035	0.020	0.022
	-0.75	0.003	0.012	0.029	0.019	0.019	0.021
	-0.50	0.011	0.018	0.030	0.019	0.021	0.023
	-0.25	0.027	0.030	0.034	0.027	0.033	0.033
-20	-0.95	0.000	0.025	0.032	0.046	0.021	0.035
	-0.75	0.002	0.022	0.028	0.029	0.019	0.026
	-0.50	0.008	0.025	0.030	0.023	0.019	0.025
	-0.25	0.025	0.032	0.036	0.027	0.029	0.031
-30	-0.95	0.000	0.020	0.034	0.047	0.021	0.045
	-0.75	0.002	0.018	0.028	0.037	0.019	0.035
	-0.50	0.007	0.020	0.030	0.032	0.020	0.033
	-0.25	0.023	0.030	0.036	0.032	0.030	0.035
-40	-0.95	0.000	0.015	0.035	0.049	0.023	0.048
	-0.75	0.002	0.014	0.029	0.042	0.020	0.042
	-0.50	0.007	0.017	0.029	0.037	0.021	0.037
	-0.25	0.021	0.029	0.036	0.038	0.030	0.039
-50	-0.95	0.001	0.011	0.037	0.049	0.024	0.049
	-0.75	0.002	0.012	0.030	0.045	0.020	0.045
	-0.50	0.007	0.016	0.030	0.041	0.021	0.041
	-0.25	0.021	0.027	0.036	0.043	0.031	0.044

(b) Left-Tailed Tests

c	δ	Q_μ^{GLS}	t_μ^{OLS}	Q_τ^{GLS}	t_τ^{OLS}	U^{hyb}	S^{hyb}
2	-0.95	0.007	0.006	0.010	0.000	0.010	0.010
	-0.75	0.012	0.012	0.013	0.000	0.013	0.013
	-0.50	0.022	0.026	0.018	0.005	0.018	0.018
	-0.25	0.036	0.033	0.029	0.027	0.029	0.029
0	-0.95	0.039	0.011	0.021	0.000	0.021	0.021
	-0.75	0.026	0.016	0.011	0.001	0.011	0.011
	-0.50	0.031	0.030	0.013	0.007	0.013	0.013
	-0.25	0.040	0.033	0.026	0.027	0.026	0.026
-2	-0.95	0.067	0.033	0.023	0.000	0.023	0.023
	-0.75	0.039	0.036	0.018	0.002	0.018	0.018
	-0.50	0.039	0.043	0.019	0.014	0.019	0.019
	-0.25	0.044	0.039	0.029	0.034	0.029	0.030
-5	-0.95	0.155	0.064	0.015	0.001	0.015	0.015
	-0.75	0.077	0.059	0.013	0.006	0.013	0.013
	-0.50	0.058	0.060	0.018	0.025	0.018	0.018
	-0.25	0.054	0.044	0.030	0.043	0.030	0.032
-10	-0.95	0.286	0.098	0.017	0.005	0.017	0.017
	-0.75	0.134	0.084	0.013	0.023	0.013	0.014
	-0.50	0.086	0.073	0.019	0.040	0.019	0.022
	-0.25	0.065	0.051	0.031	0.049	0.031	0.036
-20	-0.95	0.339	0.084	0.020	0.036	0.020	0.026
	-0.75	0.161	0.073	0.015	0.047	0.015	0.030
	-0.50	0.096	0.063	0.020	0.048	0.020	0.038
	-0.25	0.070	0.052	0.031	0.049	0.031	0.045
-30	-0.95	0.452	0.090	0.021	0.049	0.021	0.049
	-0.75	0.222	0.078	0.016	0.049	0.016	0.047
	-0.50	0.122	0.067	0.019	0.049	0.019	0.048
	-0.25	0.079	0.055	0.030	0.050	0.030	0.049
-40	-0.95	0.514	0.095	0.023	0.049	0.023	0.049
	-0.75	0.262	0.082	0.016	0.047	0.016	0.047
	-0.50	0.141	0.071	0.019	0.050	0.019	0.050
	-0.25	0.086	0.057	0.030	0.050	0.030	0.050
-50	-0.95	0.542	0.099	0.024	0.049	0.024	0.049
	-0.75	0.286	0.084	0.017	0.048	0.017	0.048
	-0.50	0.152	0.072	0.020	0.049	0.020	0.049
	-0.25	0.088	0.059	0.030	0.050	0.030	0.050

Figure S.41: Finite Power of Right-Tailed Tests. DGP (1)-(3) with $c = 0$, $\delta = -0.95$ and $\kappa = \{0.0, 0.2, 0.4, 0.6, 0.8, 1.0\}$, where c, κ and δ are the local-to-unity AR, local-to-zero trend, and endogeneity correlation parameters, respectively.

(a) $\kappa = 0.0$

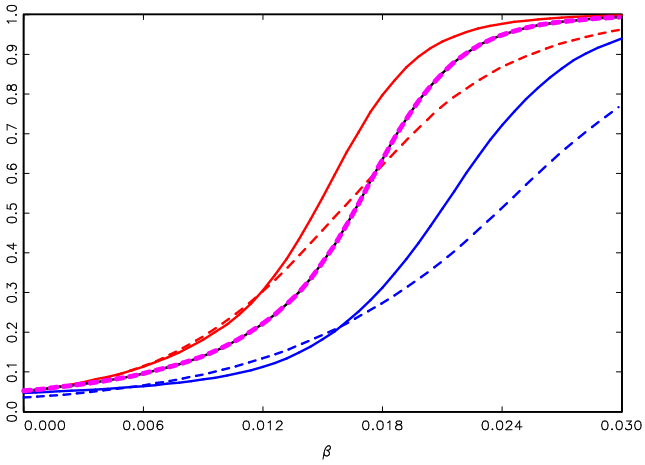

(b) $\kappa = 0.2$

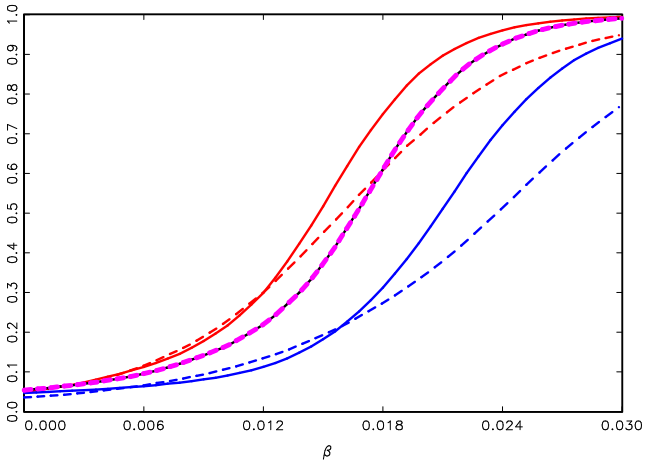

(c) $\kappa = 0.4$

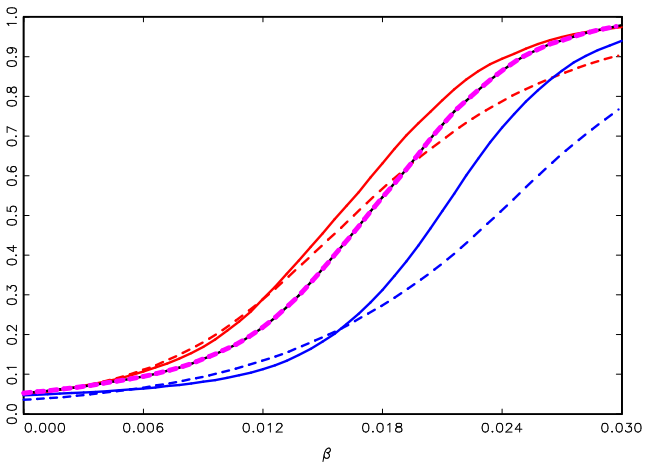

(d) $\kappa = 0.6$

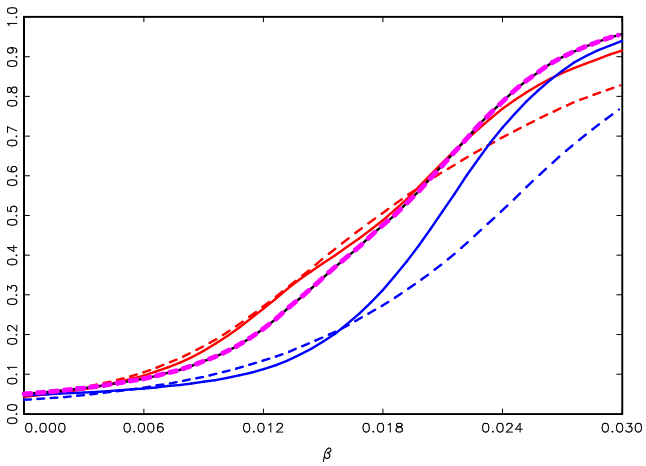

(e) $\kappa = 0.8$

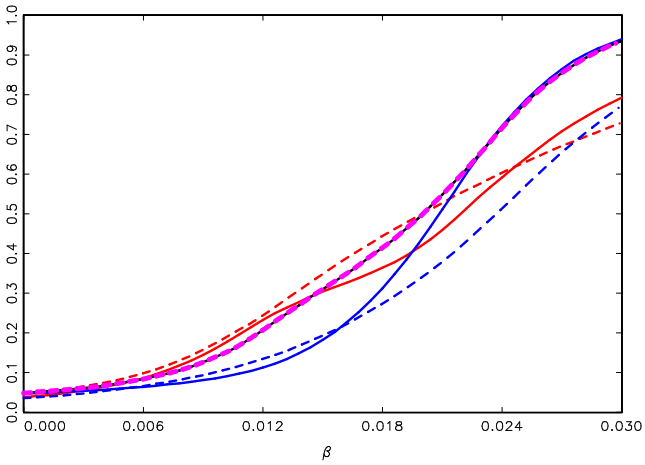

(f) $\kappa = 1.0$

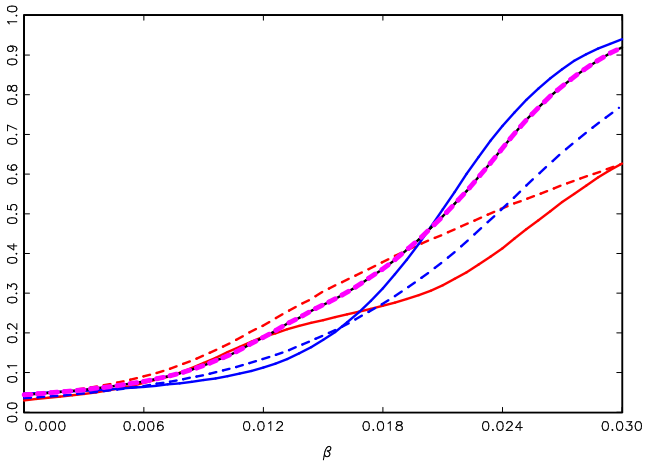

t_μ^{OLS}: – –, Q_μ^{GLS}: ——, t_τ^{OLS}: – –, Q_τ^{GLS}: ——, U^{hyb}: ——, S^{hyb}: – –

Figure S.42: Finite Power of Right-Tailed Tests. DGP (1)-(3) with $c = -2$, $\delta = -0.95$ and $\kappa = \{0.0, 0.2, 0.4, 0.6, 0.8, 1.0\}$, where c, κ and δ are the local-to-unity AR, local-to-zero trend, and endogeneity correlation parameters, respectively.

(a) $\kappa = 0.0$

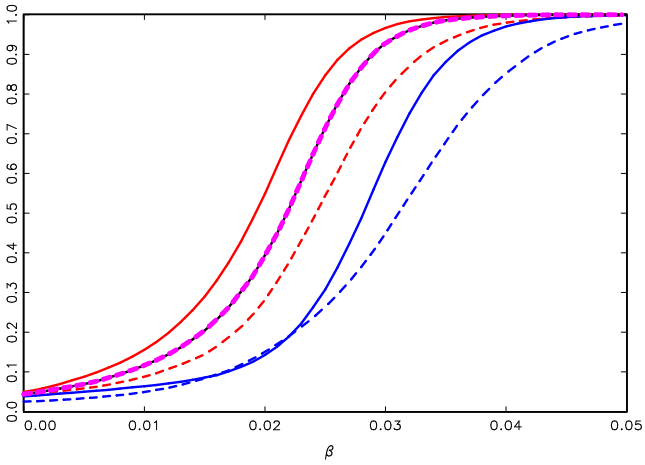

(b) $\kappa = 0.2$

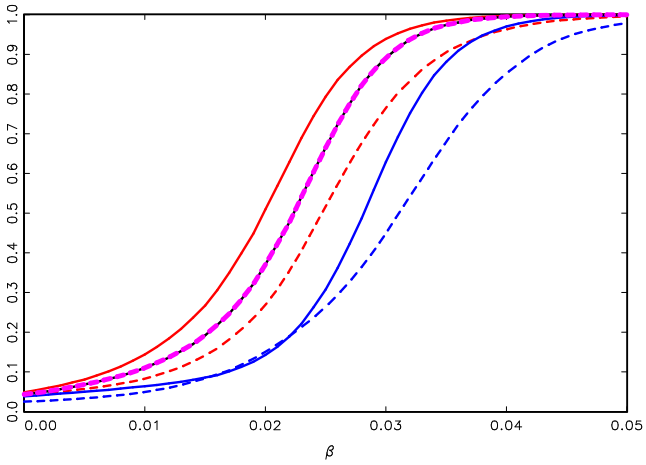

(c) $\kappa = 0.4$

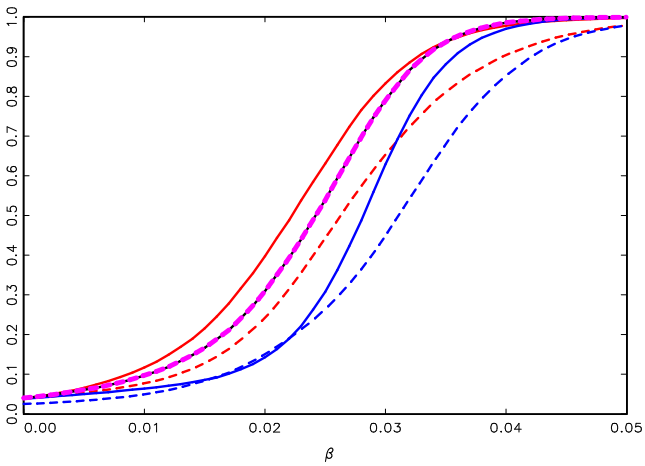

(d) $\kappa = 0.6$

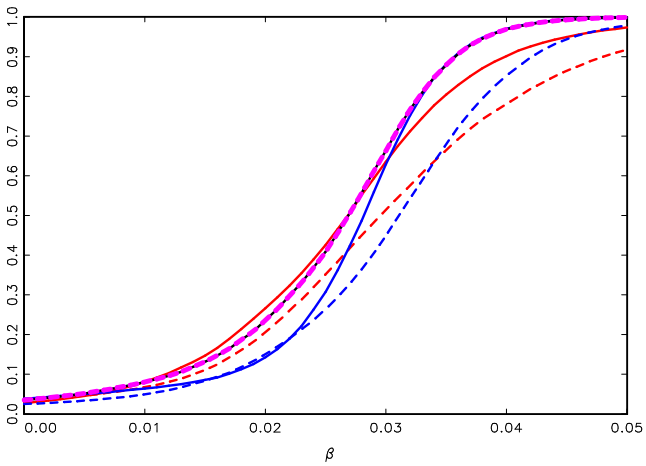

(e) $\kappa = 0.8$

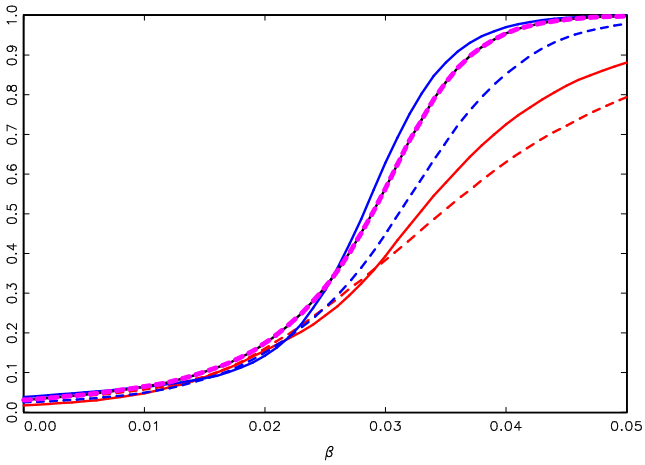

(f) $\kappa = 1.0$

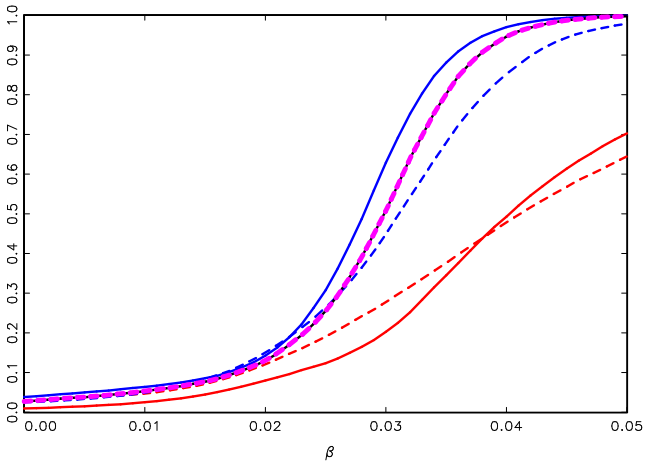

t_μ^{OLS}: – –, Q_μ^{GLS}: ——, t_τ^{OLS}: – –, Q_τ^{GLS}: ——, U^{hyb}: ——, S^{hyb}: – –

Figure S.43: Finite Power of Right-Tailed Tests. DGP (1)-(3) with $c = -5$, $\delta = -0.95$ and $\kappa = \{0.0, 0.2, 0.4, 0.6, 0.8, 1.0\}$, where c, κ and δ are the local-to-unity AR, local-to-zero trend, and endogeneity correlation parameters, respectively.

(a) $\kappa = 0.0$

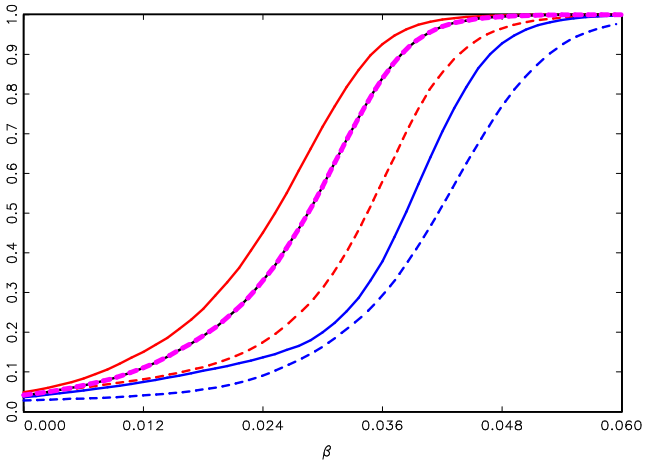

(b) $\kappa = 0.2$

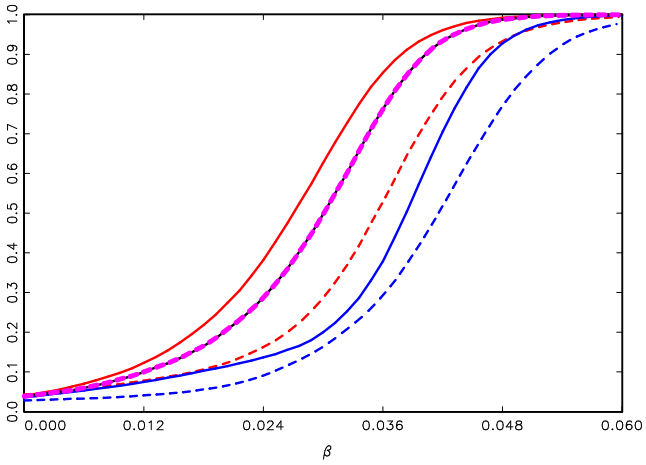

(c) $\kappa = 0.4$

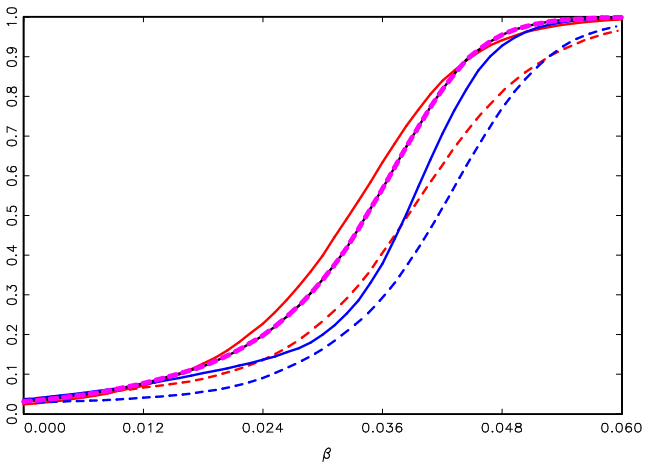

(d) $\kappa = 0.6$

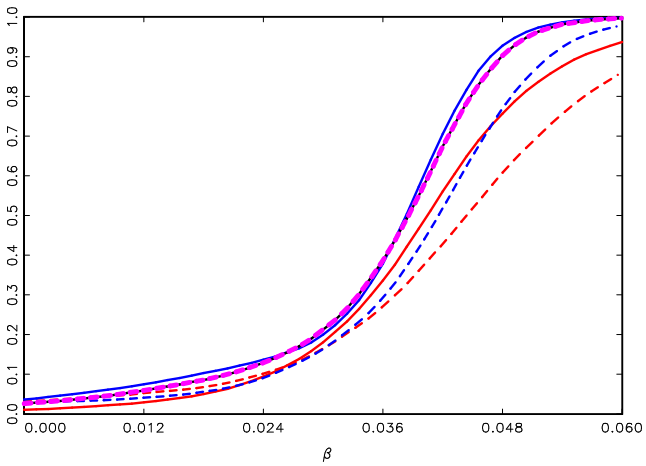

(e) $\kappa = 0.8$

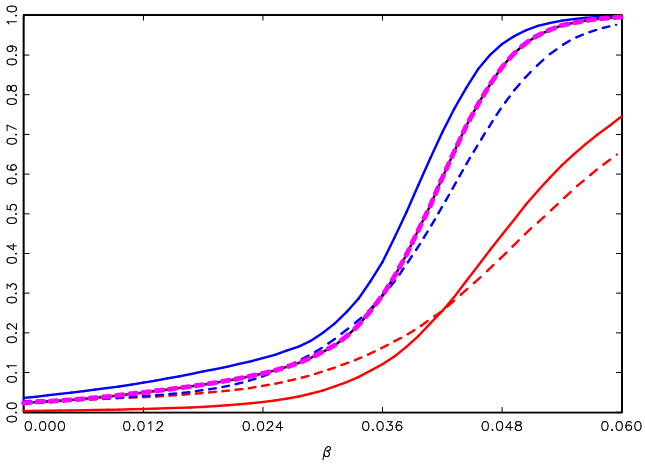

(f) $\kappa = 1.0$

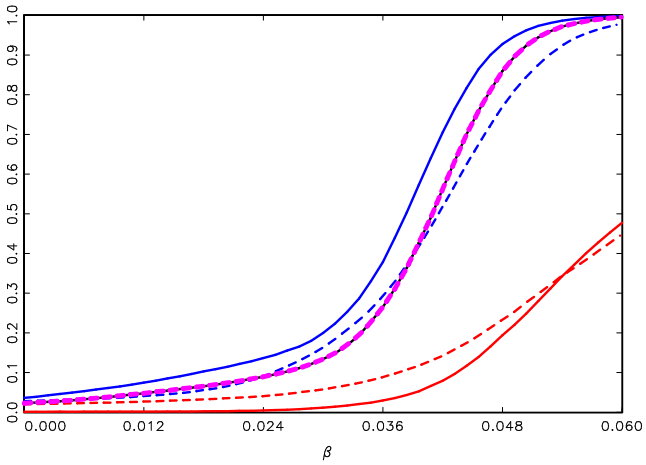

t_{μ}^{OLS}: – –, Q_{μ}^{GLS}: ——, t_{τ}^{OLS}: – –, Q_{τ}^{GLS}: ——, U^{hyb}: ——, S^{hyb}: – –

Figure S.44: Finite Power of Right-Tailed Tests. DGP (1)-(3) with $c = -10$, $\delta = -0.95$ and $\kappa = \{0.0, 0.2, 0.4, 0.6, 0.8, 1.0\}$, where c, κ and δ are the local-to-unity AR, local-to-zero trend, and endogeneity correlation parameters, respectively.

(a) $\kappa = 0.0$

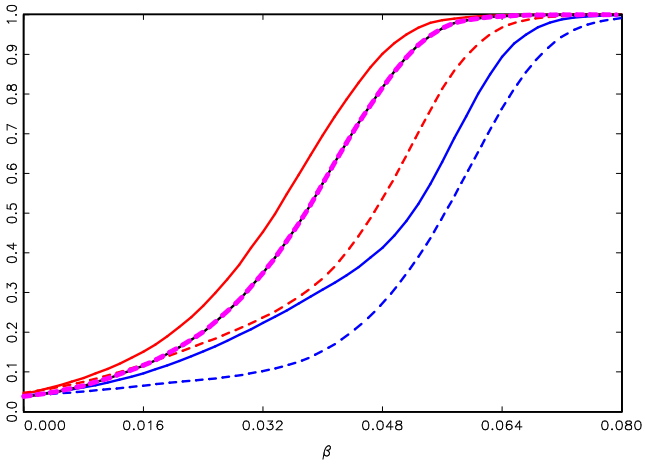

(b) $\kappa = 0.2$

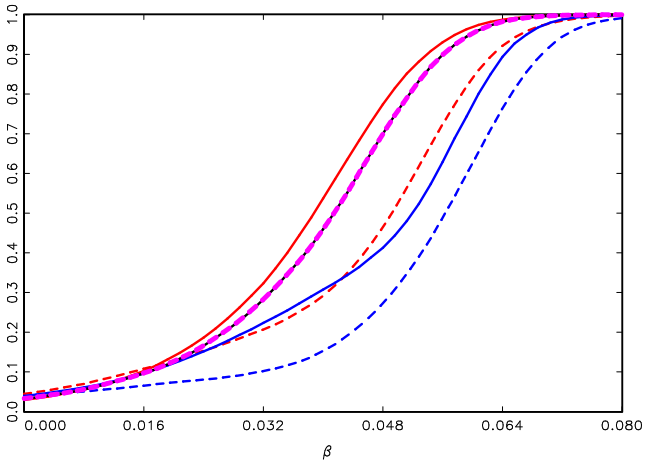

(c) $\kappa = 0.4$

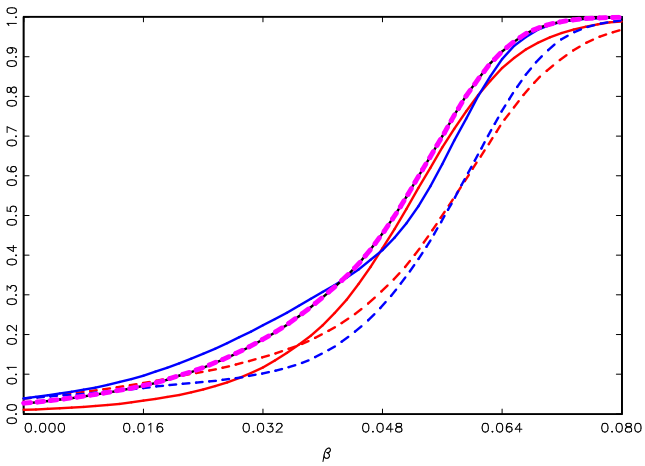

(d) $\kappa = 0.6$

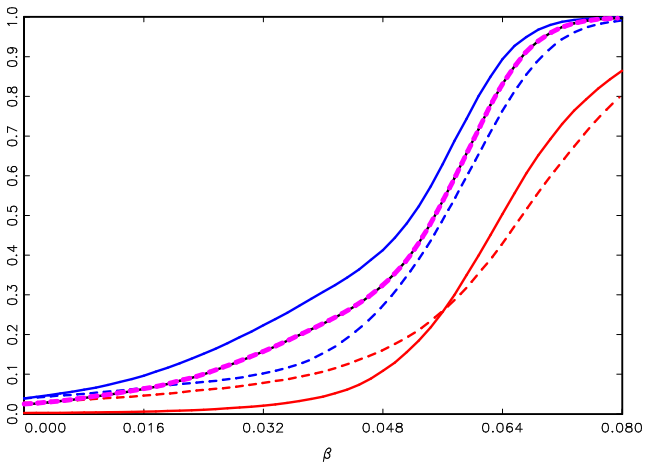

(e) $\kappa = 0.8$

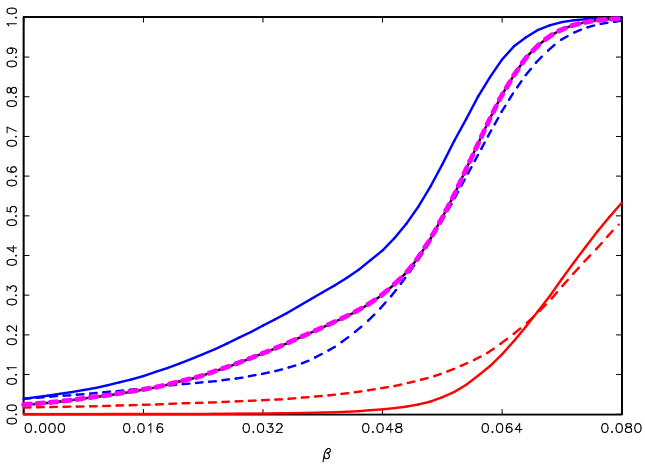

(f) $\kappa = 1.0$

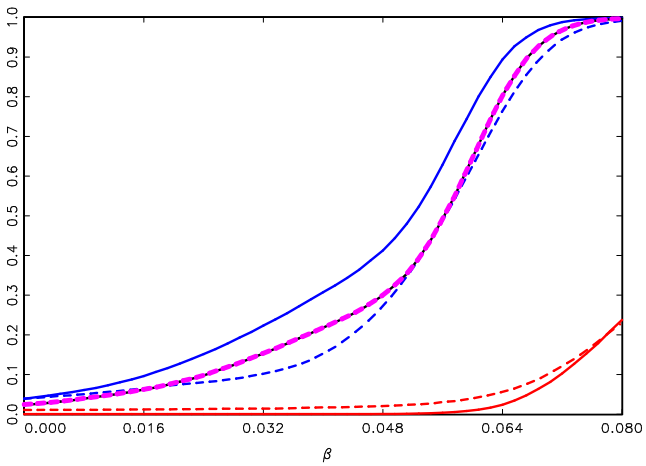

t_μ^{OLS}: – – , Q_μ^{GLS}: ——— , t_τ^{OLS}: – –, Q_τ^{GLS}: ———, U^{hyb}: ———, S^{hyb}: – –

Figure S.45: Finite Power of Right-Tailed Tests. DGP (1)-(3) with $c = -20$, $\delta = -0.95$ and $\kappa = \{0.0, 0.1, 0.2, 0.3, 0.4, 0.5\}$, where c, κ and δ are the local-to-unity AR, local-to-zero trend, and endogeneity correlation parameters, respectively.

(a) $\kappa = 0.0$

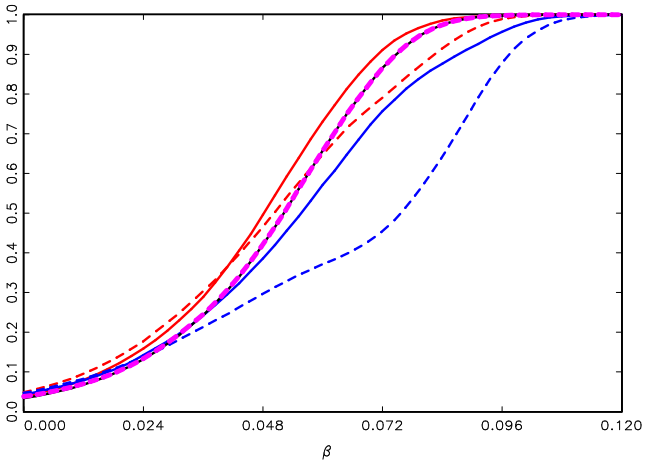

(b) $\kappa = 0.1$

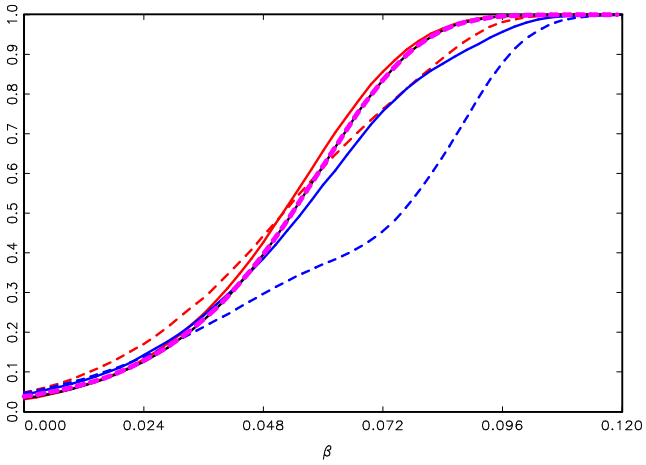

(c) $\kappa = 0.2$

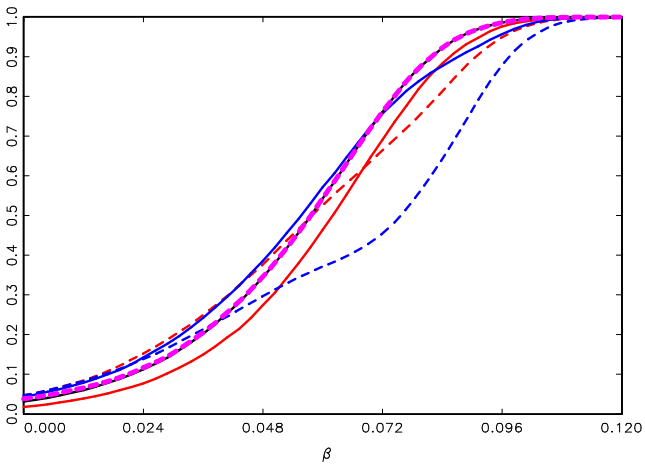

(d) $\kappa = 0.3$

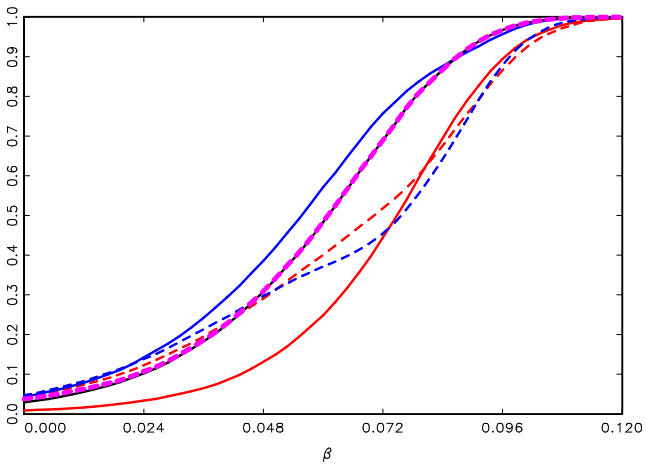

(e) $\kappa = 0.4$

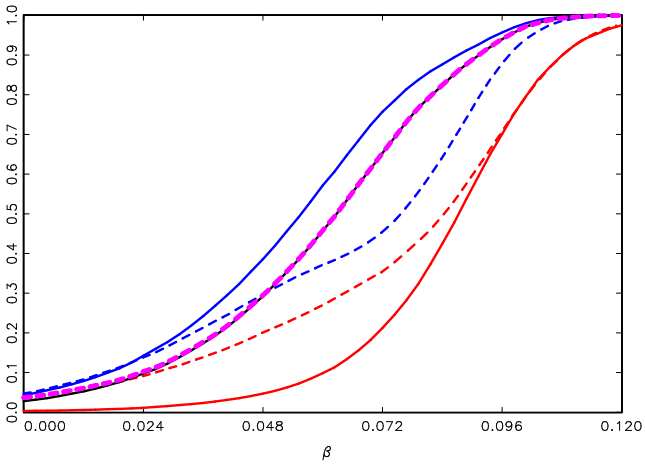

(f) $\kappa = 0.5$

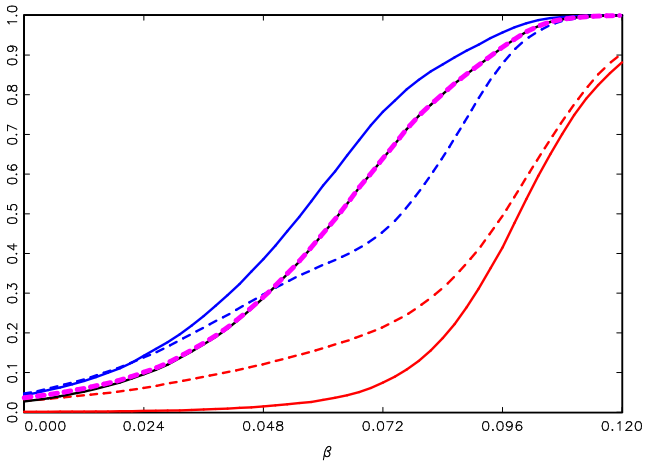

t_μ^{OLS}: – –, Q_μ^{GLS}: ——, t_τ^{OLS}: – –, Q_τ^{GLS}: ——, U^{hyb}: ——, S^{hyb}: – –

Figure S.46: Finite Power of Right-Tailed Tests. DGP (1)-(3) with $c = -30$, $\delta = -0.95$ and $\kappa = \{0.0, 0.1, 0.2, 0.3, 0.4, 0.5\}$, where c, κ and δ are the local-to-unity AR, local-to-zero trend, and endogeneity correlation parameters, respectively.

(a) $\kappa = 0.0$

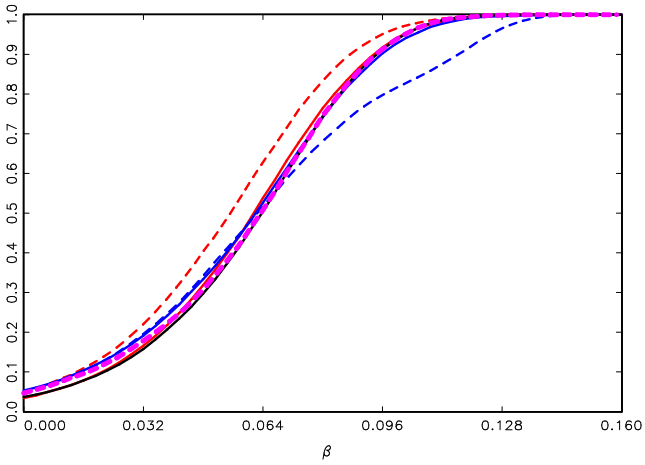

(b) $\kappa = 0.1$

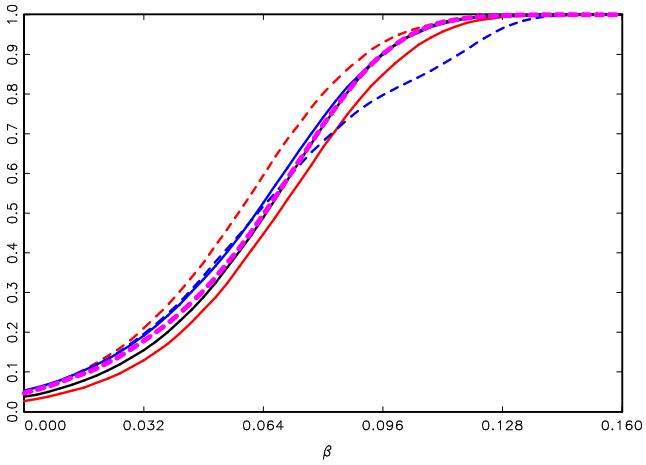

(c) $\kappa = 0.2$

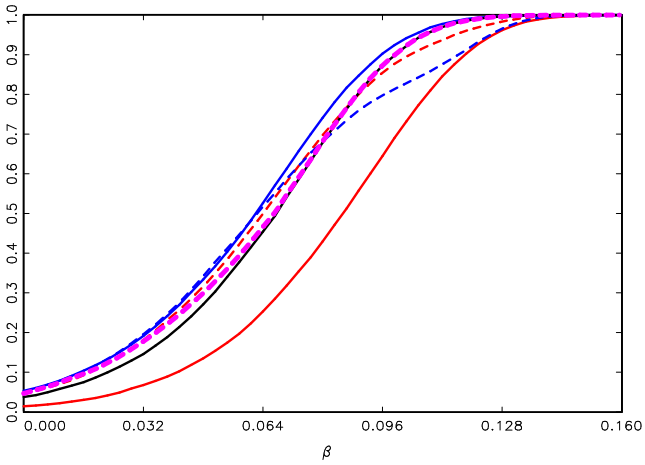

(d) $\kappa = 0.3$

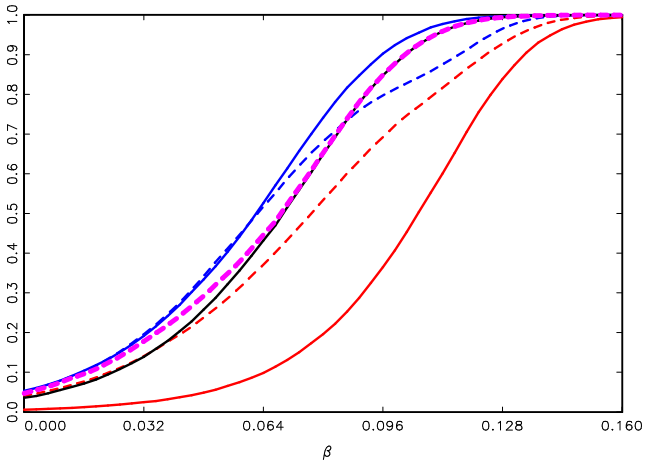

(e) $\kappa = 0.4$

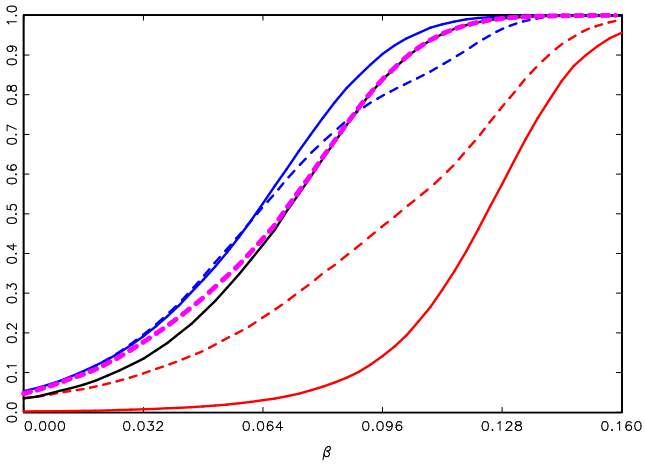

(f) $\kappa = 0.5$

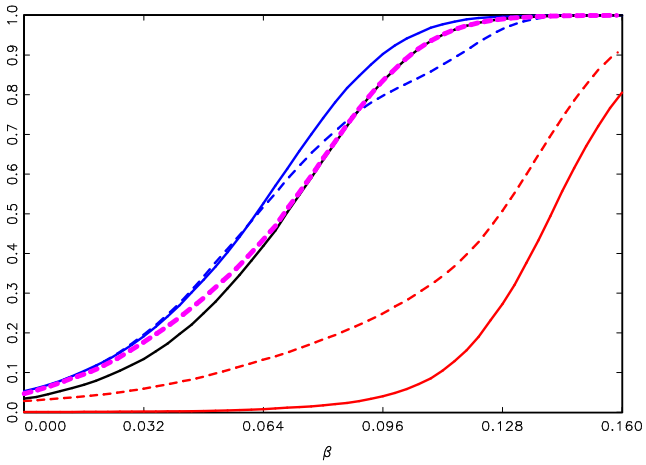

t_μ^{OLS}: – – , Q_μ^{GLS}: ——— , t_τ^{OLS}: – –, Q_τ^{GLS}: ———, U^{hyb}: ———, S^{hyb}: – –

Figure S.47: Finite Power of Right-Tailed Tests. DGP (1)-(3) with $c = -40$, $\delta = -0.95$ and $\kappa = \{0.0, 0.1, 0.2, 0.3, 0.4, 0.5\}$, where c, κ and δ are the local-to-unity AR, local-to-zero trend, and endogeneity correlation parameters, respectively.

(a) $\kappa = 0.0$

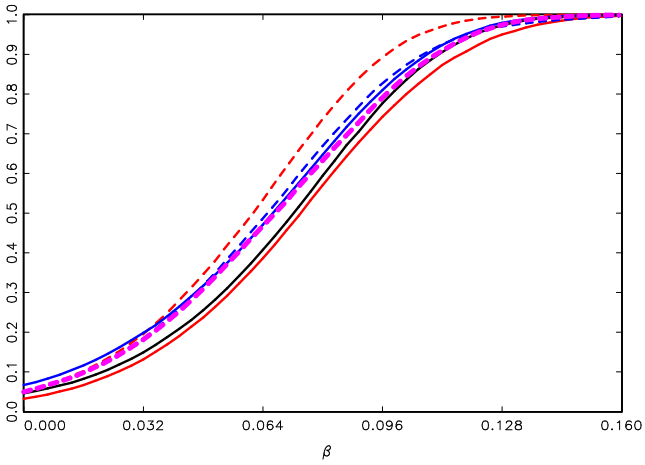

(b) $\kappa = 0.1$

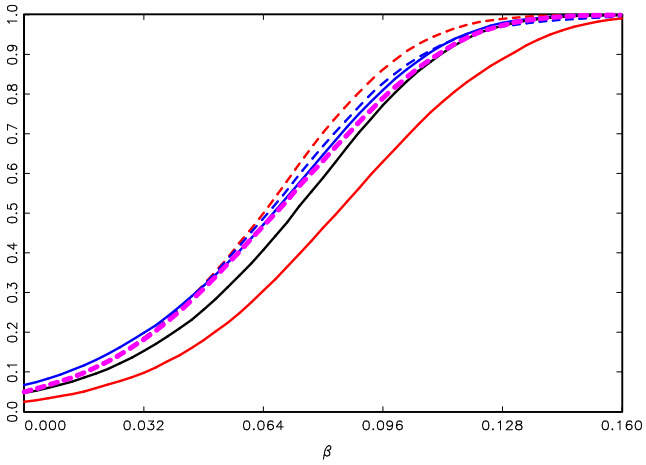

(c) $\kappa = 0.2$

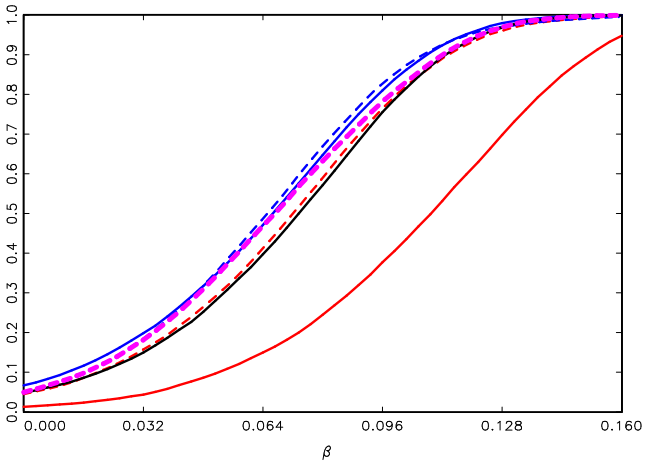

(d) $\kappa = 0.3$

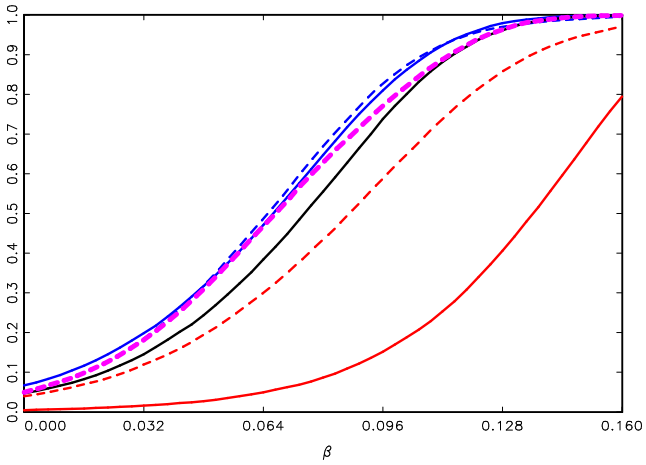

(e) $\kappa = 0.4$

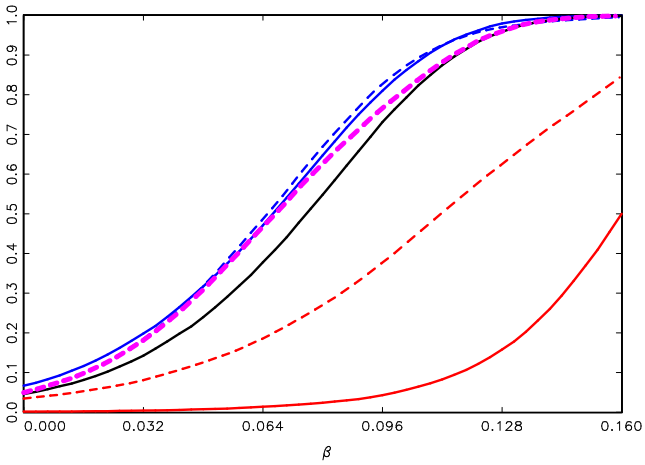

(f) $\kappa = 0.5$

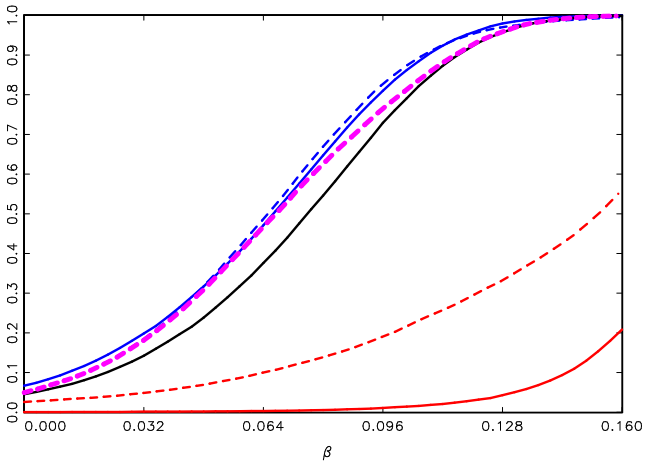

t_μ^{OLS}: – – , Q_μ^{GLS}: ——— , t_τ^{OLS}: – –, Q_τ^{GLS}: ———, U^{hyb}: ———, S^{hyb}: – –

Figure S.48: Finite Power of Right-Tailed Tests. DGP (1)-(3) with $c = -50$, $\delta = -0.95$ and $\kappa = \{0.0, 0.1, 0.2, 0.3, 0.4, 0.5\}$, where c, κ and δ are the local-to-unity AR, local-to-zero trend, and endogeneity correlation parameters, respectively.

(a) $\kappa = 0.0$

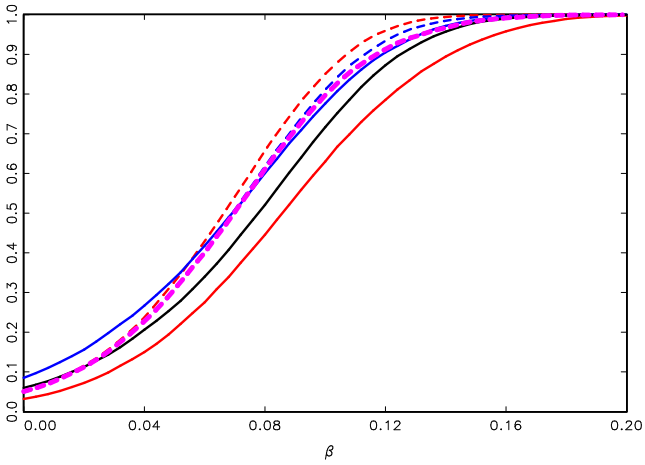

(b) $\kappa = 0.1$

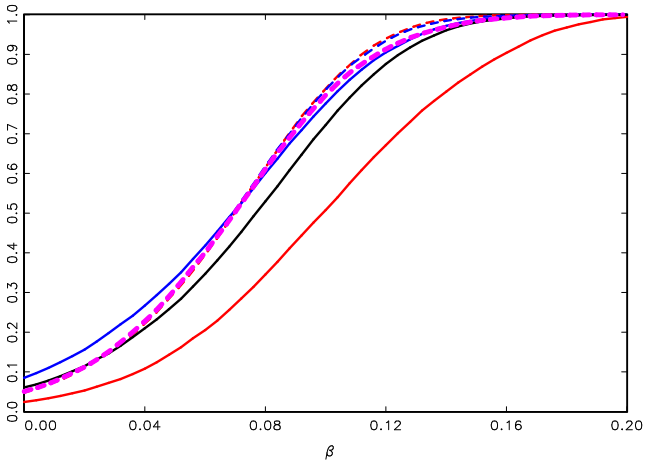

(c) $\kappa = 0.2$

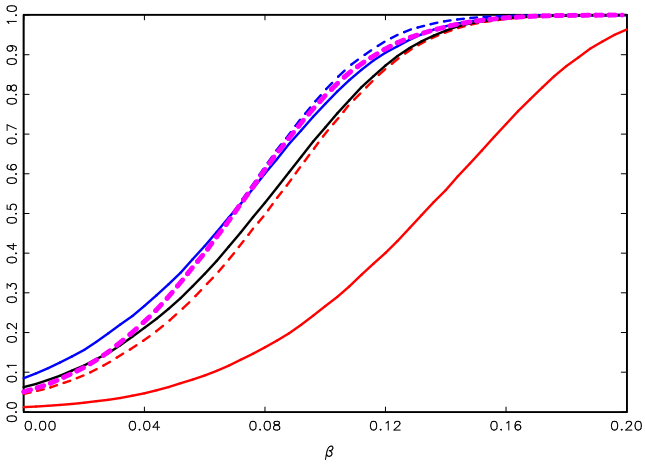

(d) $\kappa = 0.3$

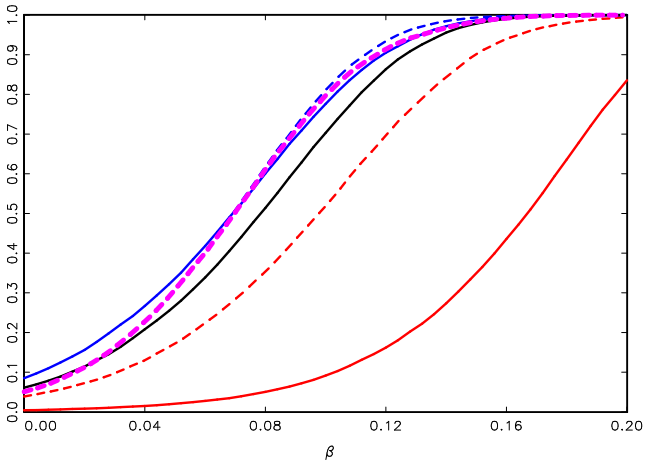

(e) $\kappa = 0.4$

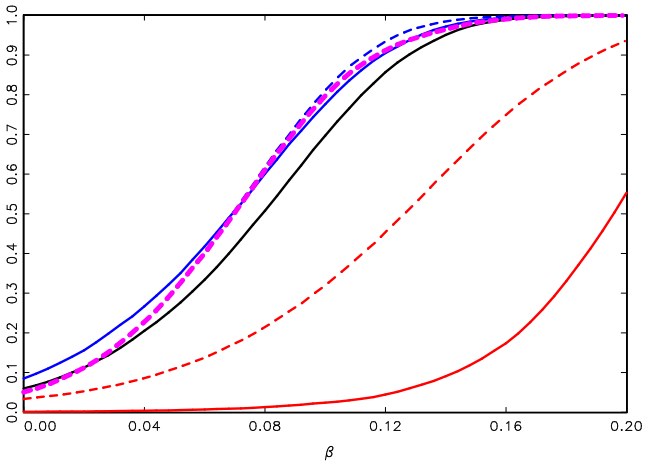

(f) $\kappa = 0.5$

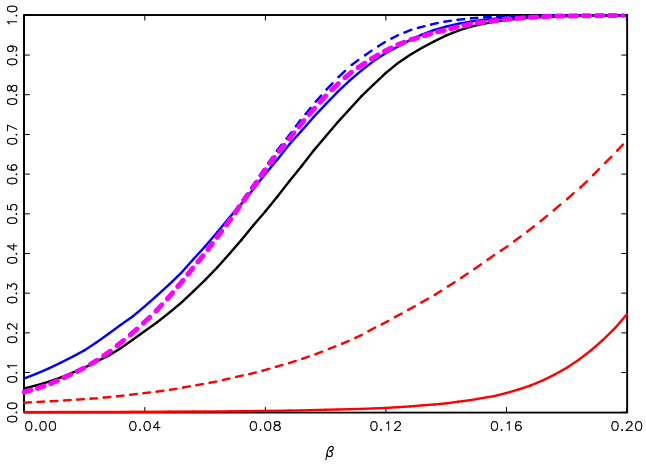

t_{μ}^{OLS}: – – , Q_{μ}^{GLS}: ——— , t_{τ}^{OLS}: – –, Q_{τ}^{GLS}: ———, U^{hyb}: ———, S^{hyb}: – –

Figure S.49: Finite Power of Right-Tailed Tests. DGP (1)-(3) with $c = -100$, $\delta = -0.95$ and $\kappa = \{0.0, 0.1, 0.2, 0.3, 0.4, 0.5\}$, where c, κ and δ are the local-to-unity AR, local-to-zero trend, and endogeneity correlation parameters, respectively.

(a) $\kappa = 0.0$

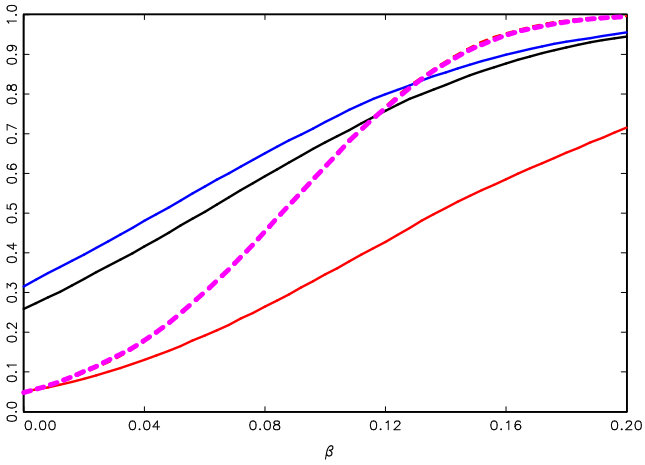

(b) $\kappa = 0.1$

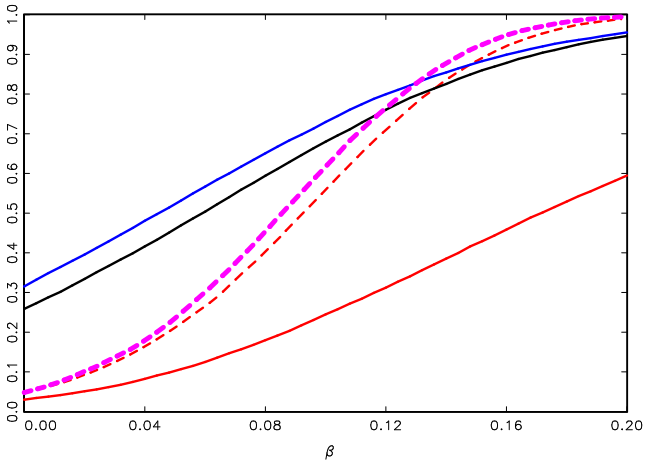

(c) $\kappa = 0.2$

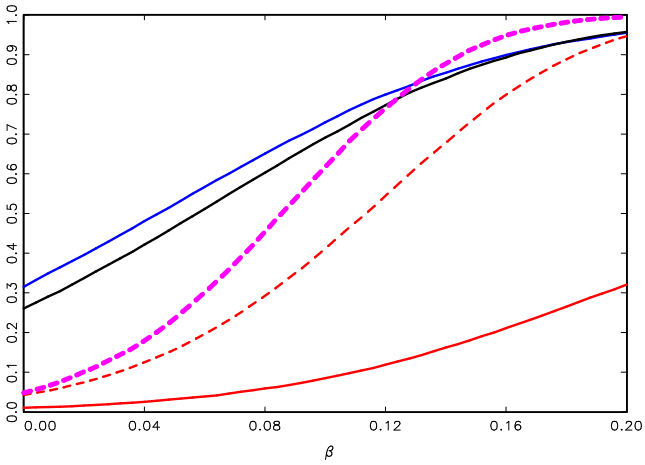

(d) $\kappa = 0.3$

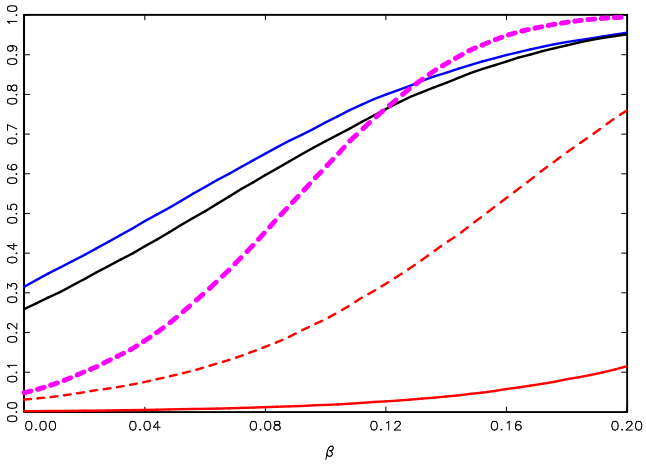

(e) $\kappa = 0.4$

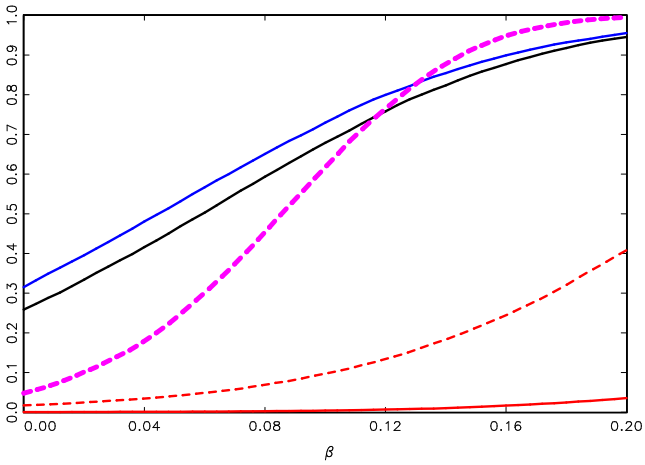

(f) $\kappa = 0.5$

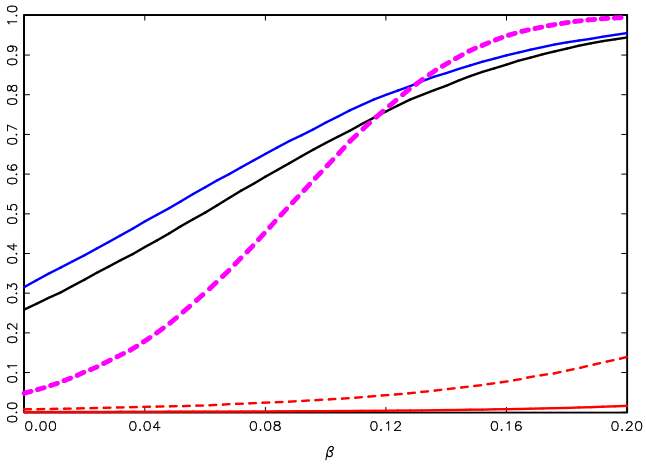

t_{μ}^{OLS}: – – , Q_{μ}^{GLS}: ——— , t_{τ}^{OLS}: – –, Q_{τ}^{GLS}: ———, U^{hyb}: ———, S^{hyb}: – –

Figure S.50: Finite Power of Right-Tailed Tests. DGP (1)-(3) with $c = -250$, $\delta = -0.95$ and $\kappa = \{0.0, 0.1, 0.2, 0.3, 0.4, 0.5\}$, where c, κ and δ are the local-to-unity AR, local-to-zero trend, and endogeneity correlation parameters, respectively.

(a) $\kappa = 0.0$

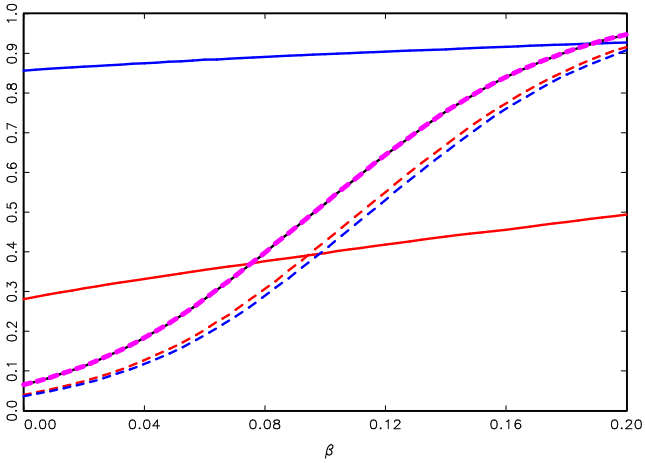

(b) $\kappa = 0.1$

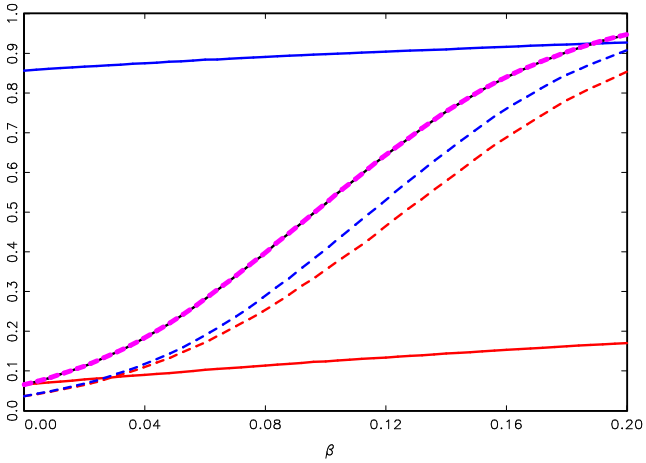

(c) $\kappa = 0.2$

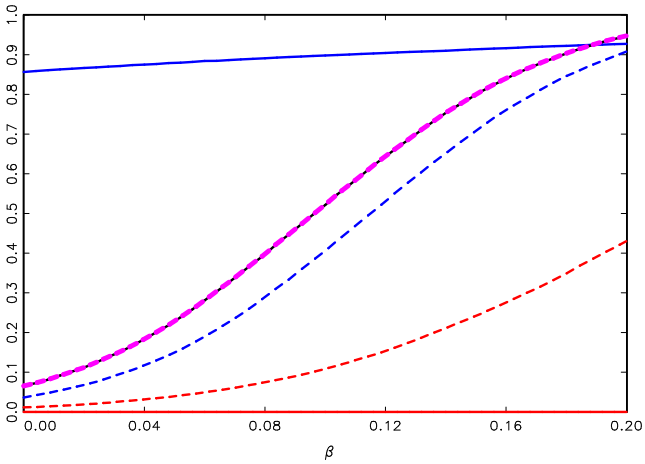

(d) $\kappa = 0.3$

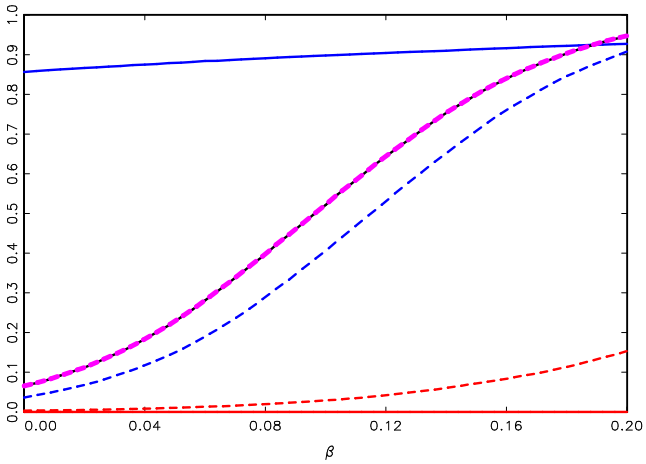

(e) $\kappa = 0.4$

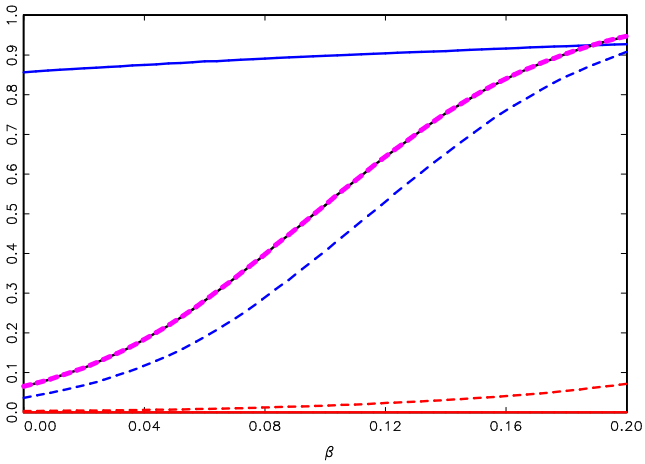

(f) $\kappa = 0.5$

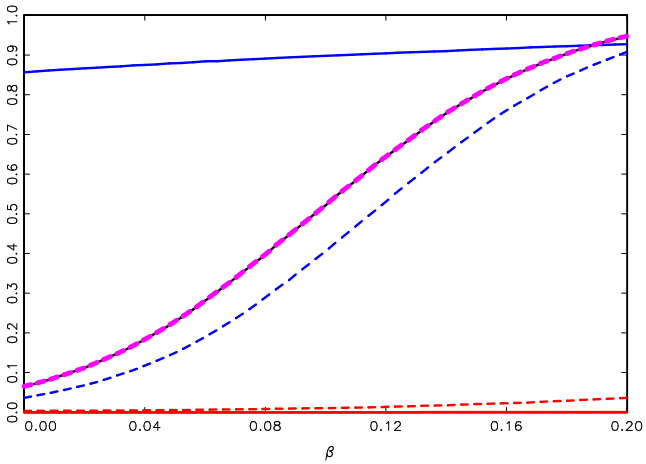

t_μ^{OLS}: – –, Q_μ^{GLS}: ——, t_τ^{OLS}: – –, Q_τ^{GLS}: ——, U^{hyb}: ——, S^{hyb}: – –

Figure S.51: Finite Power of Right-Tailed Tests. DGP (1)-(3) with $c = 0$, $\delta = -0.75$ and $\kappa = \{0.0, 0.2, 0.4, 0.6, 0.8, 1.0\}$, where c, κ and δ are the local-to-unity AR, local-to-zero trend, and endogeneity correlation parameters, respectively.

(a) $\kappa = 0.0$

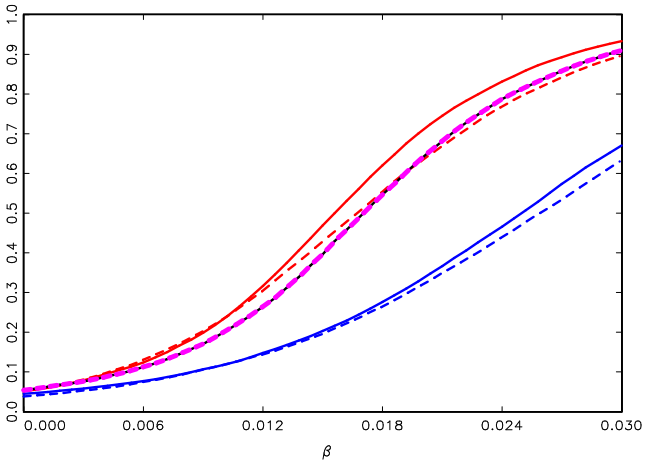

(b) $\kappa = 0.2$

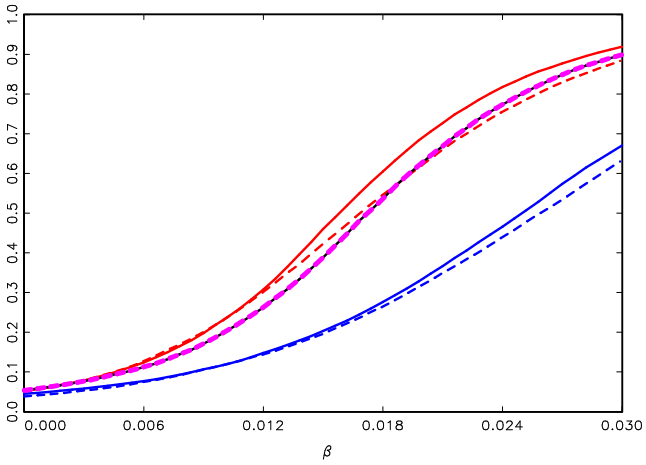

(c) $\kappa = 0.4$

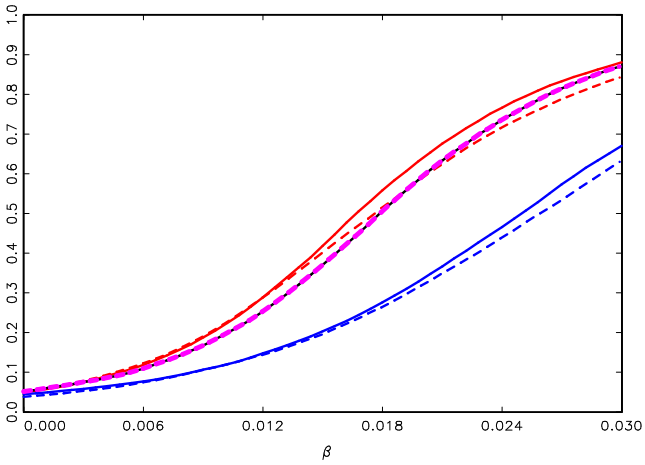

(d) $\kappa = 0.6$

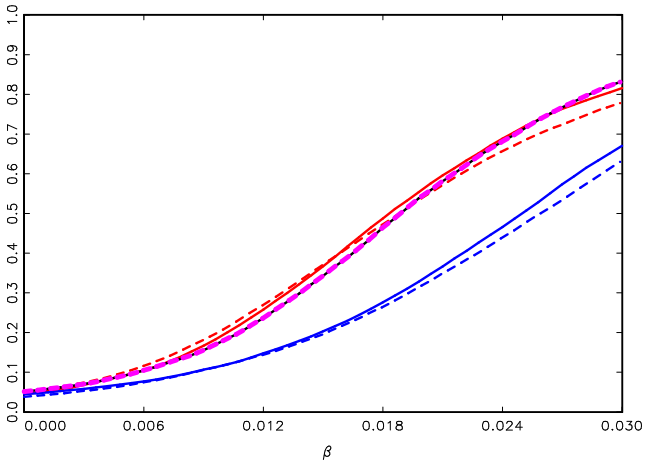

(e) $\kappa = 0.8$

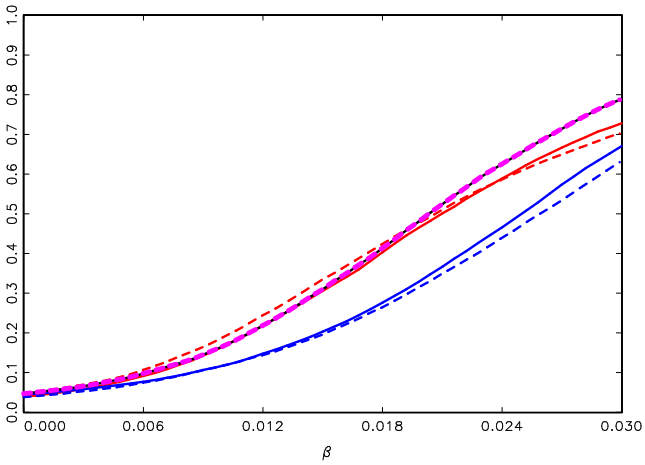

(f) $\kappa = 1.0$

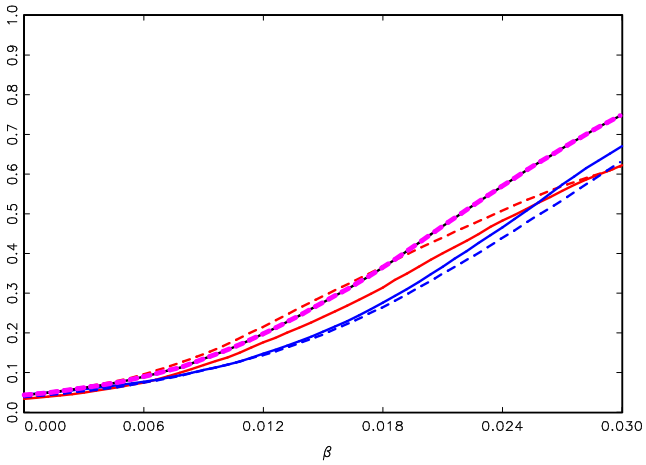

t_μ^{OLS}: – –, Q_μ^{GLS}: ——, t_τ^{OLS}: – –, Q_τ^{GLS}: ——, U^{hyb}: ——, S^{hyb}: – –

Figure S.52: Finite Power of Right-Tailed Tests. DGP (1)-(3) with $c = -2$, $\delta = -0.75$ and $\kappa = \{0.0, 0.2, 0.4, 0.6, 0.8, 1.0\}$, where c, κ and δ are the local-to-unity AR, local-to-zero trend, and endogeneity correlation parameters, respectively.

(a) $\kappa = 0.0$

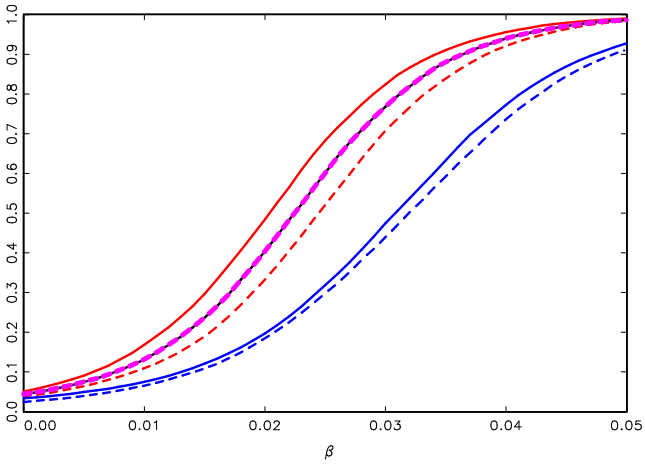

(b) $\kappa = 0.2$

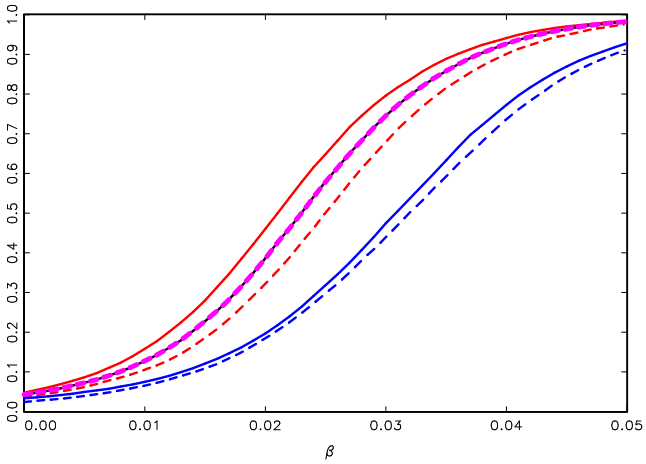

(c) $\kappa = 0.4$

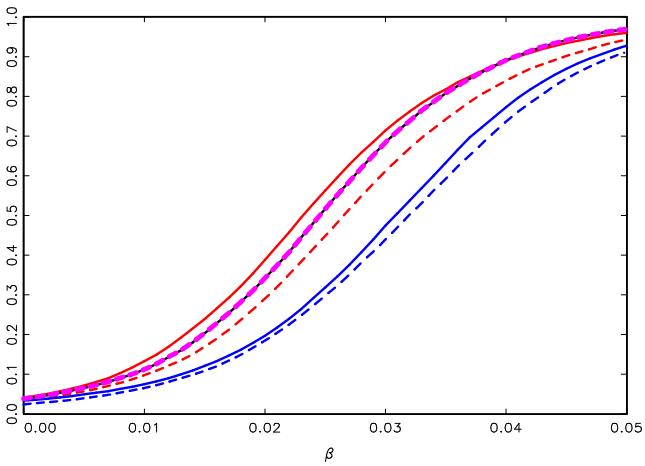

(d) $\kappa = 0.6$

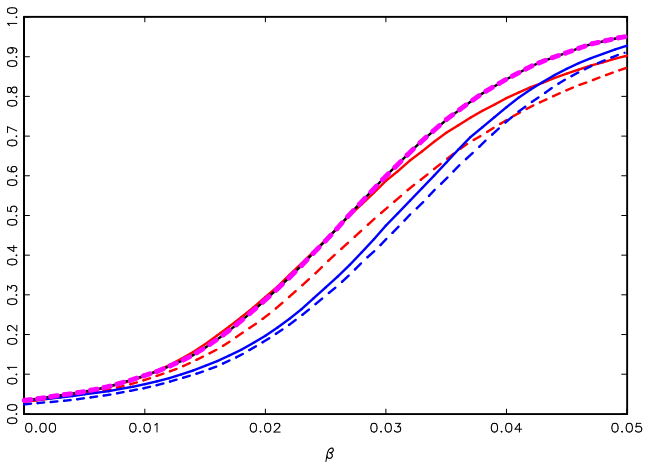

(e) $\kappa = 0.8$

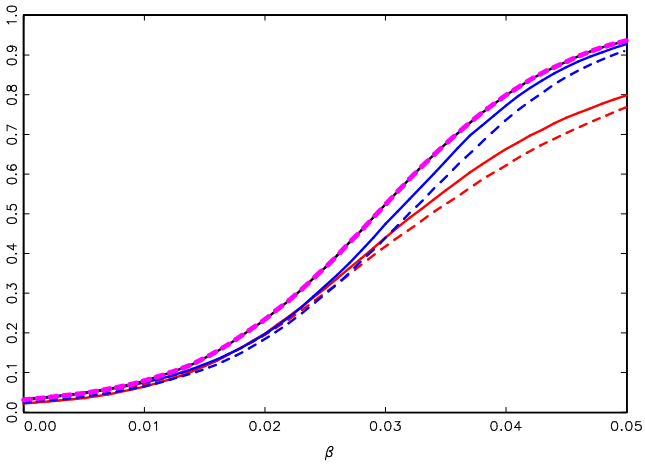

(f) $\kappa = 1.0$

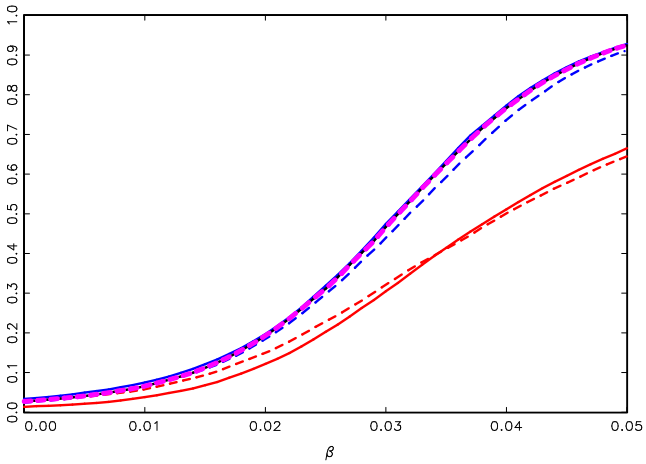

t_μ^{OLS}: – –, Q_μ^{GLS}: ——, t_τ^{OLS}: – –, Q_τ^{GLS}: ——, U^{hyb}: ——, S^{hyb}: – –

Figure S.53: Finite Power of Right-Tailed Tests. DGP (1)-(3) with $c = -5$, $\delta = -0.75$ and $\kappa = \{0.0, 0.2, 0.4, 0.6, 0.8, 1.0\}$, where c, κ and δ are the local-to-unity AR, local-to-zero trend, and endogeneity correlation parameters, respectively.

(a) $\kappa = 0.0$

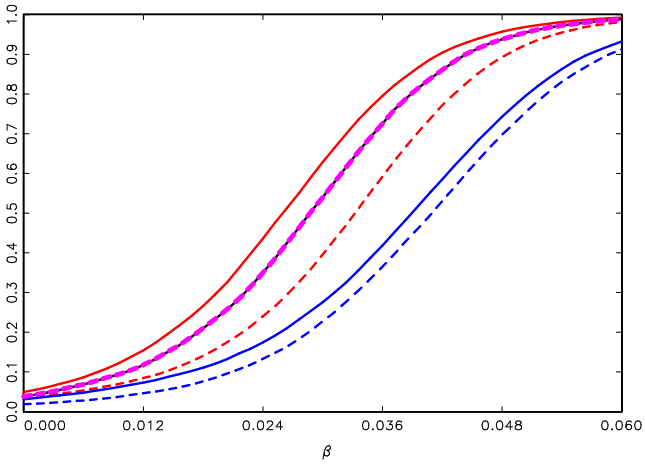

(b) $\kappa = 0.2$

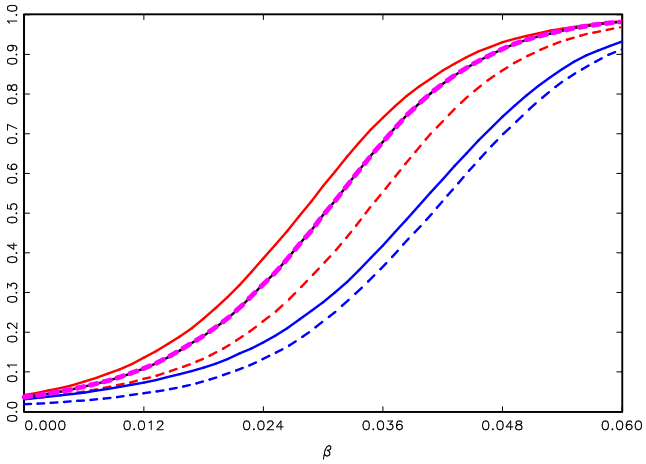

(c) $\kappa = 0.4$

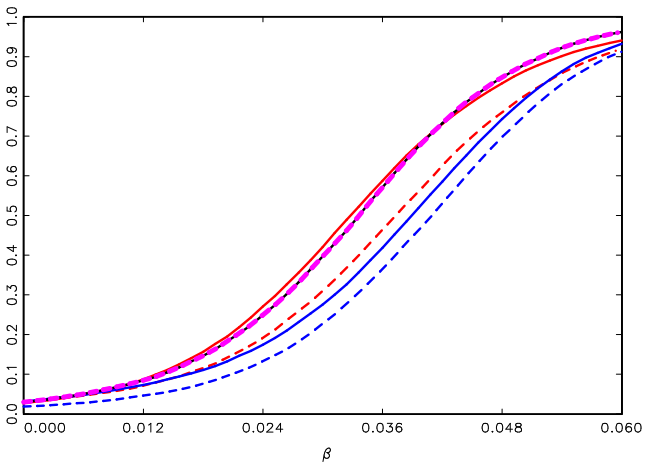

(d) $\kappa = 0.6$

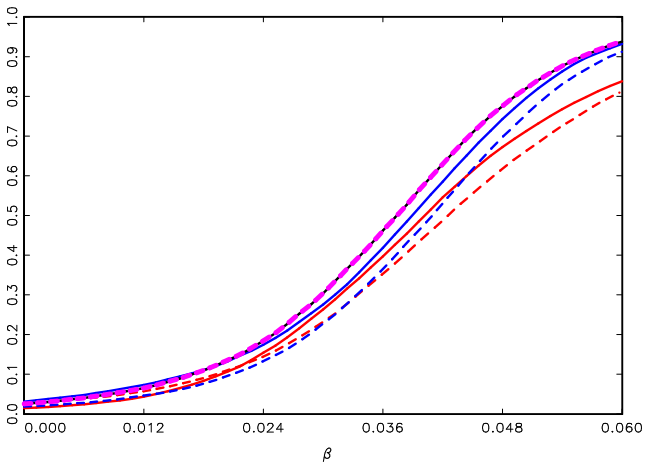

(e) $\kappa = 0.8$

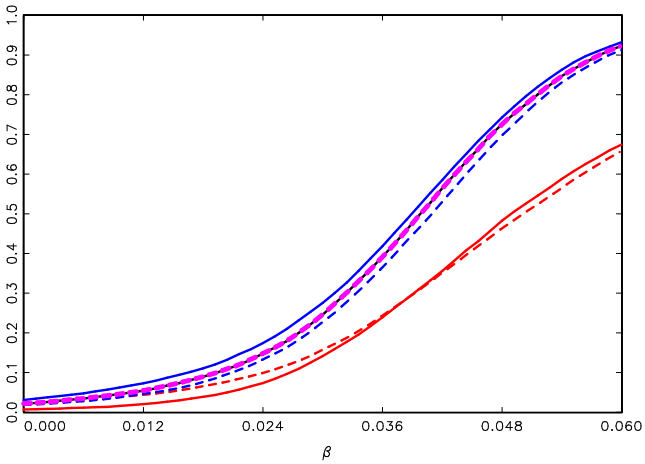

(f) $\kappa = 1.0$

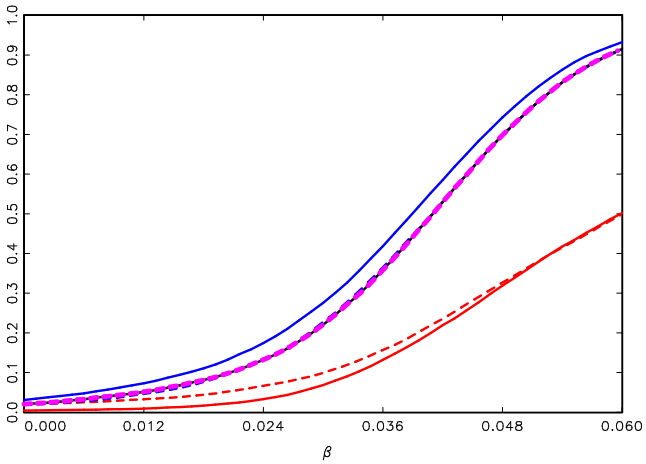

t_{μ}^{OLS}: – –, Q_{μ}^{GLS}: ——, t_{τ}^{OLS}: – –, Q_{τ}^{GLS}: ——, U^{hyb}: ——, S^{hyb}: – –

Figure S.54: Finite Power of Right-Tailed Tests. DGP (1)-(3) with $c = -10$, $\delta = -0.75$ and $\kappa = \{0.0, 0.2, 0.4, 0.6, 0.8, 1.0\}$, where c, κ and δ are the local-to-unity AR, local-to-zero trend, and endogeneity correlation parameters, respectively.

(a) $\kappa = 0.0$

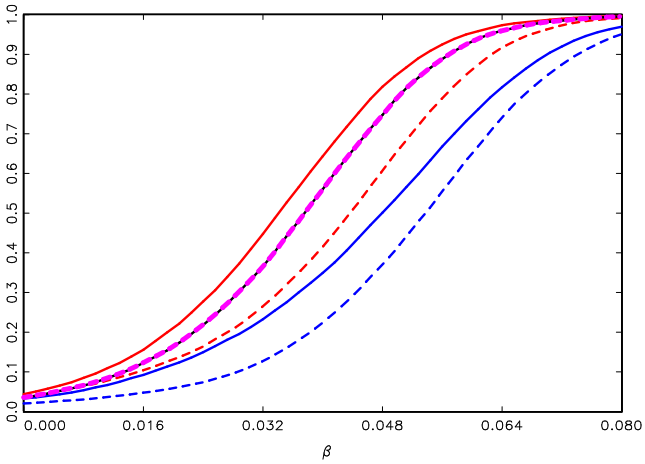

(b) $\kappa = 0.2$

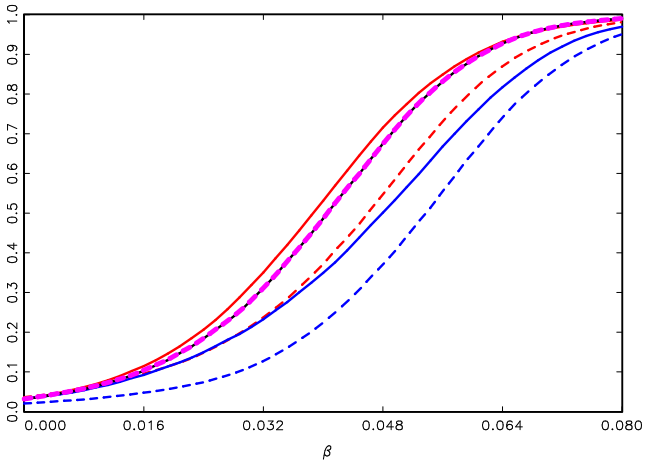

(c) $\kappa = 0.4$

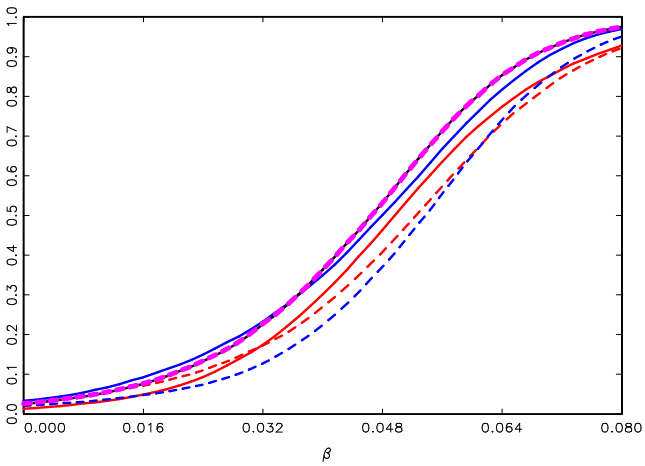

(d) $\kappa = 0.6$

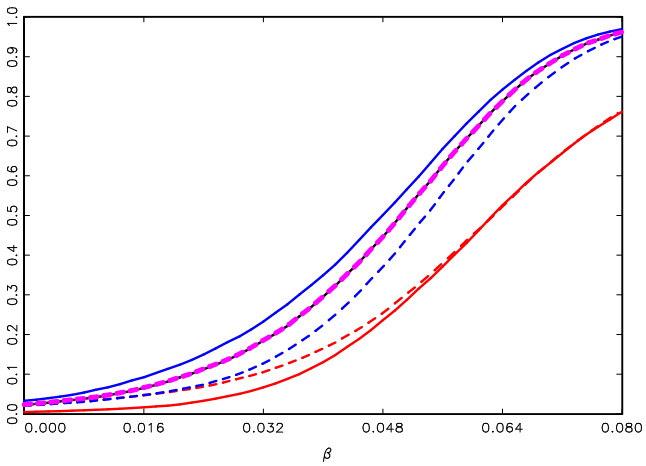

(e) $\kappa = 0.8$

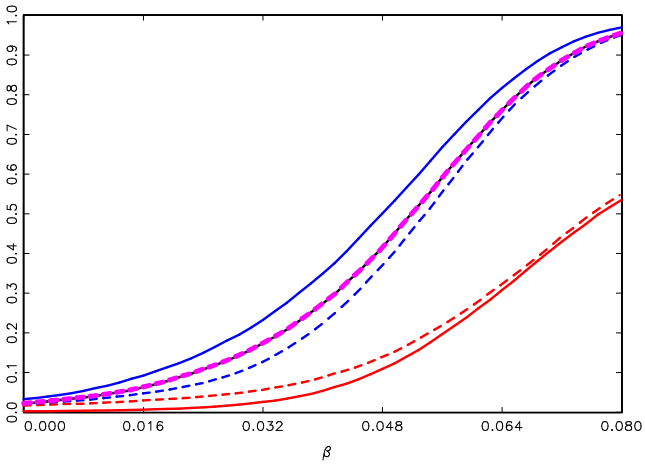

(f) $\kappa = 1.0$

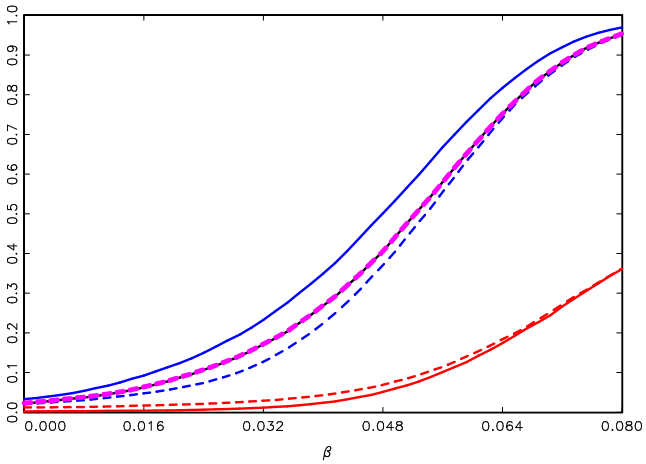

t_μ^{OLS}: – –, Q_μ^{GLS}: ——, t_τ^{OLS}: – –, Q_τ^{GLS}: ——, U^{hyb}: ——, S^{hyb}: – –

Figure S.55: Finite Power of Right-Tailed Tests. DGP (1)-(3) with $c = -20$, $\delta = -0.75$ and $\kappa = \{0.0, 0.1, 0.2, 0.3, 0.4, 0.5\}$, where c, κ and δ are the local-to-unity AR, local-to-zero trend, and endogeneity correlation parameters, respectively.

(a) $\kappa = 0.0$

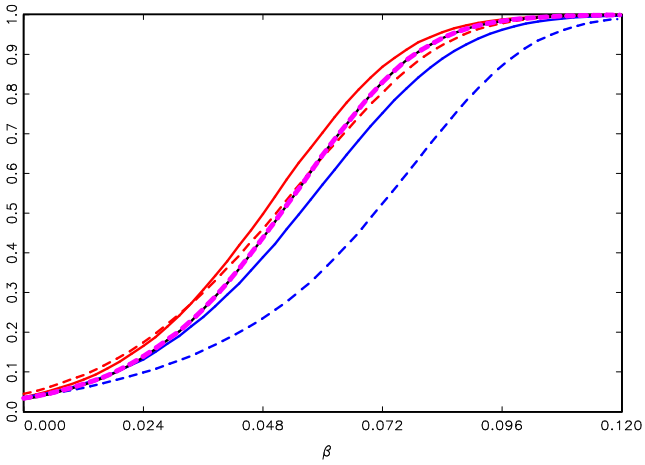

(b) $\kappa = 0.1$

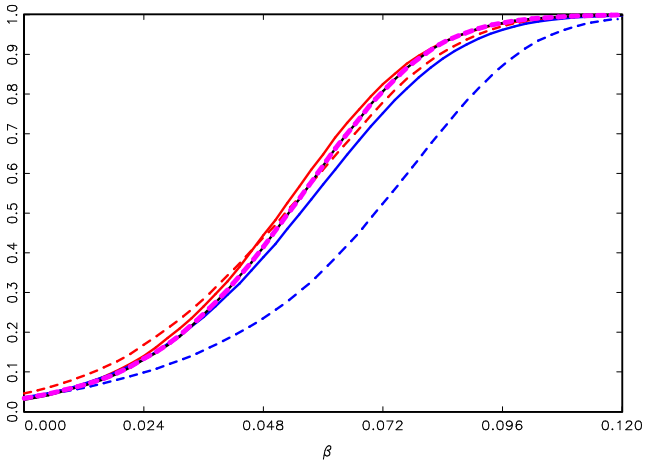

(c) $\kappa = 0.2$

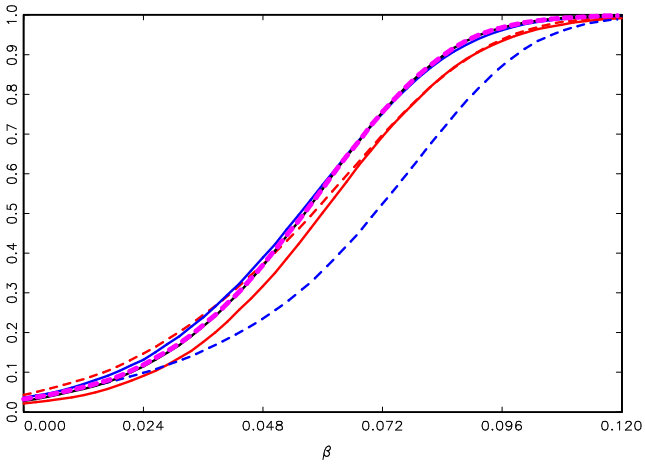

(d) $\kappa = 0.3$

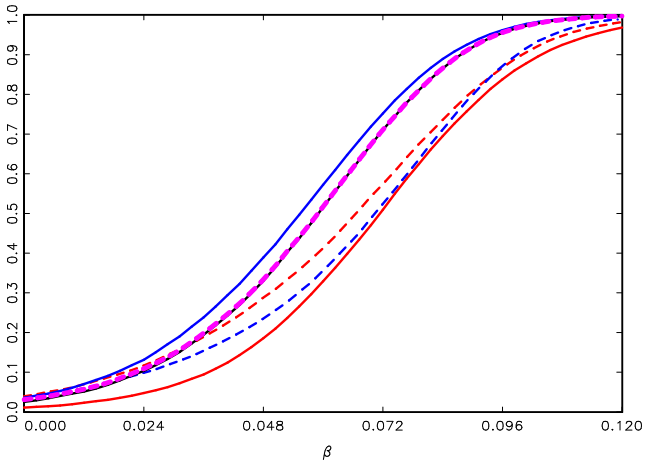

(e) $\kappa = 0.4$

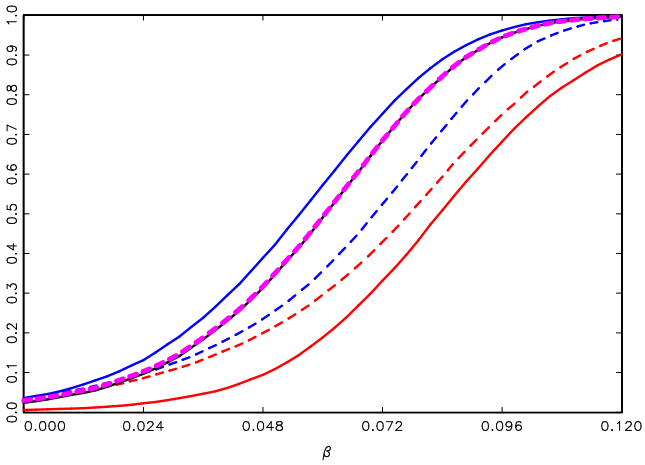

(f) $\kappa = 0.5$

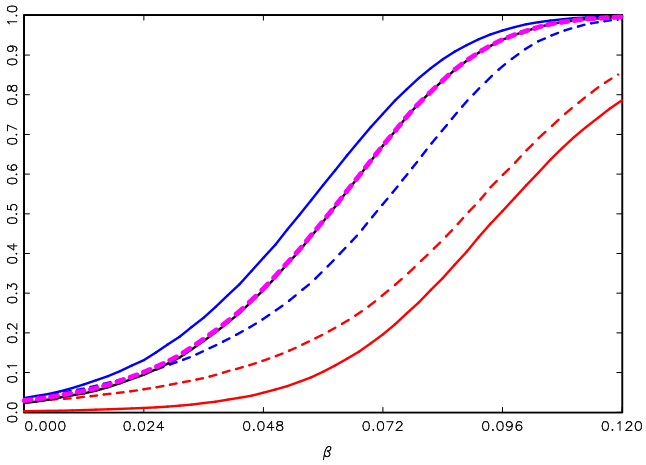

t_μ^{OLS}: – –, Q_μ^{GLS}: ——, t_τ^{OLS}: – –, Q_τ^{GLS}: ——, U^{hyb}: ——, S^{hyb}: – –

Figure S.56: Finite Power of Right-Tailed Tests. DGP (1)-(3) with $c = -30$, $\delta = -0.75$ and $\kappa = \{0.0, 0.1, 0.2, 0.3, 0.4, 0.5\}$, where c, κ and δ are the local-to-unity AR, local-to-zero trend, and endogeneity correlation parameters, respectively.

(a) $\kappa = 0.0$

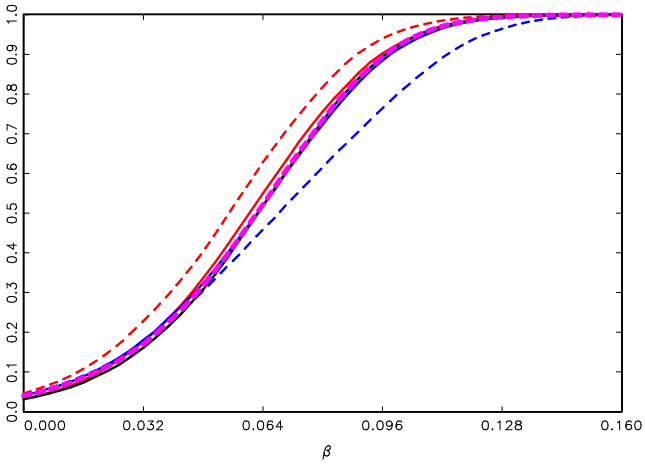

(b) $\kappa = 0.1$

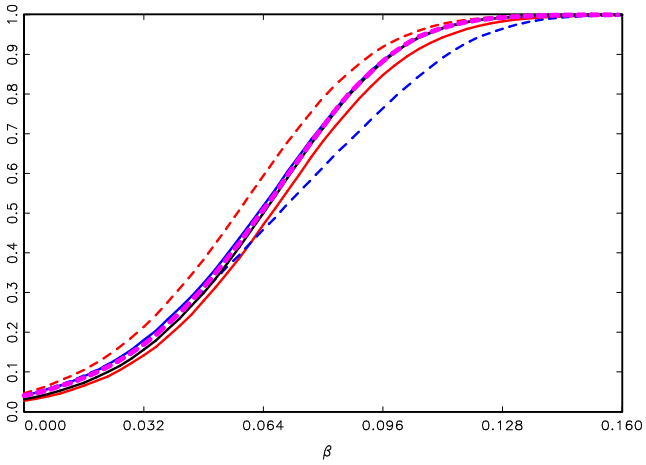

(c) $\kappa = 0.2$

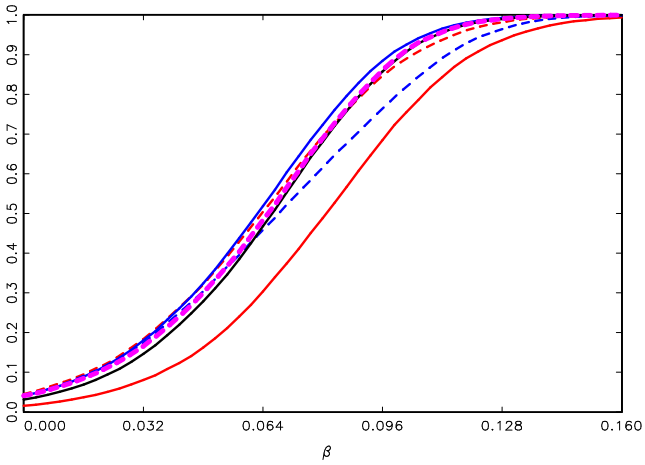

(d) $\kappa = 0.3$

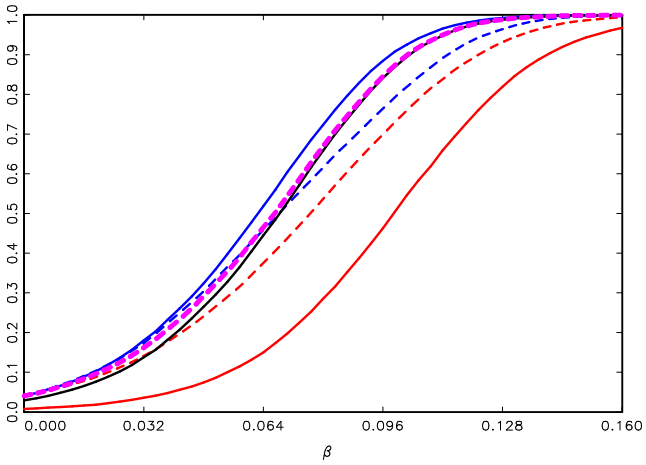

(e) $\kappa = 0.4$

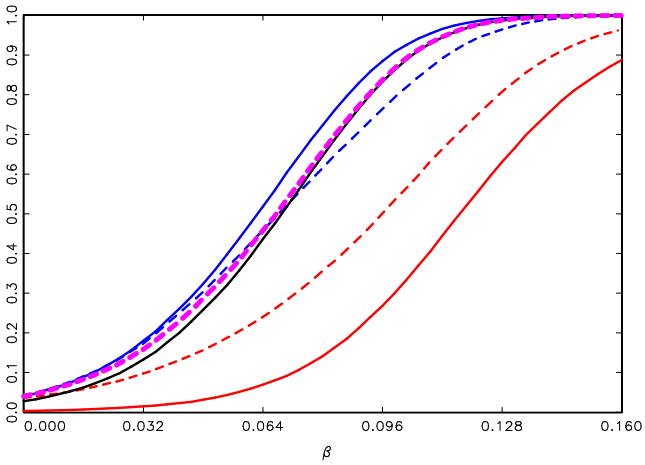

(f) $\kappa = 0.5$

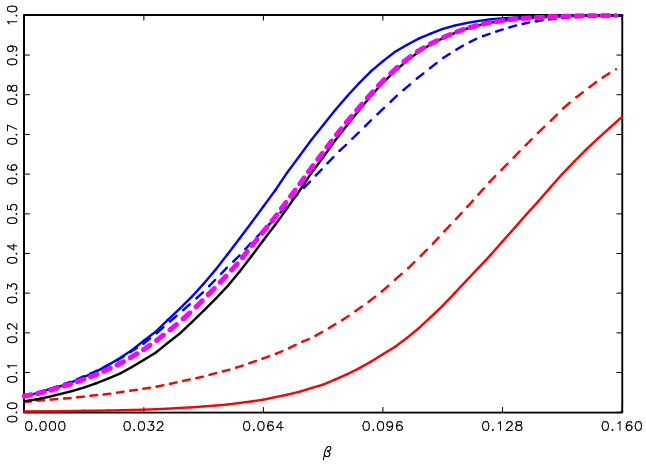

t_μ^{OLS}: – – , Q_μ^{GLS}: ——— , t_τ^{OLS}: – –, Q_τ^{GLS}: ———, U^{hyb}: ———, S^{hyb}: – –

Figure S.57: Finite Power of Right-Tailed Tests. DGP (1)-(3) with $c = -40$, $\delta = -0.75$ and $\kappa = \{0.0, 0.1, 0.2, 0.3, 0.4, 0.5\}$, where c, κ and δ are the local-to-unity AR, local-to-zero trend, and endogeneity correlation parameters, respectively.

(a) $\kappa = 0.0$

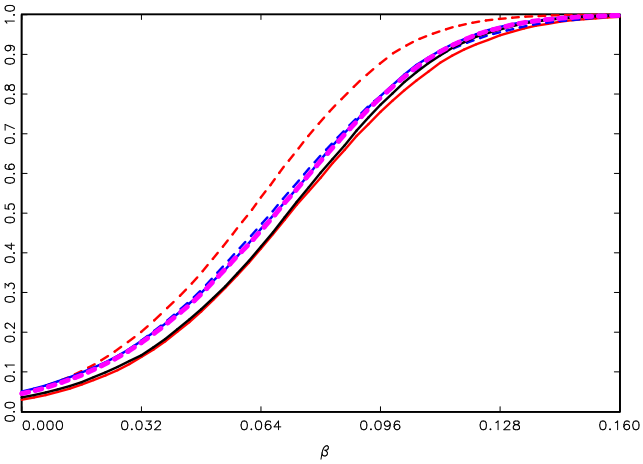

(b) $\kappa = 0.1$

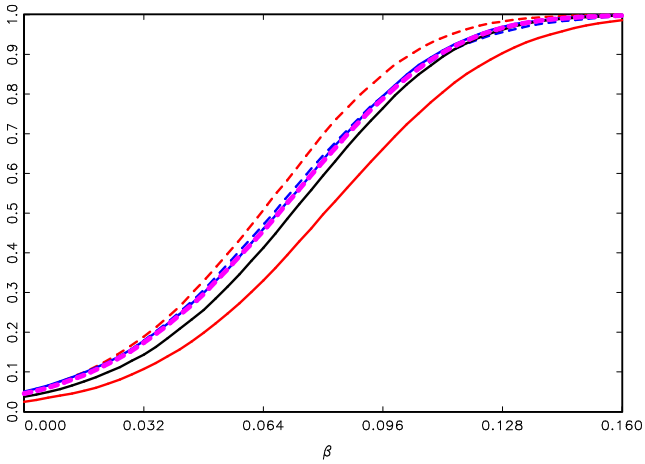

(c) $\kappa = 0.2$

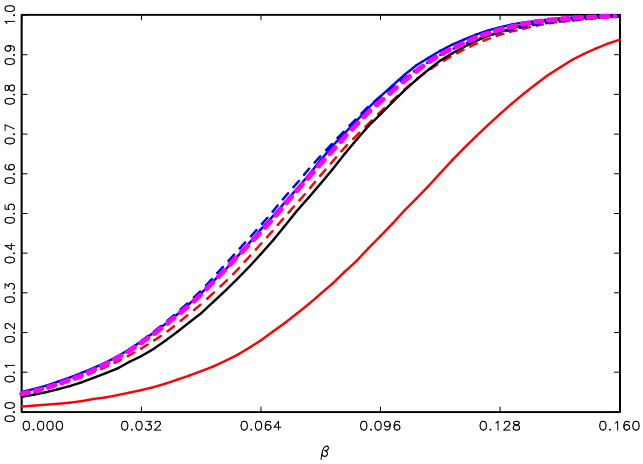

(d) $\kappa = 0.3$

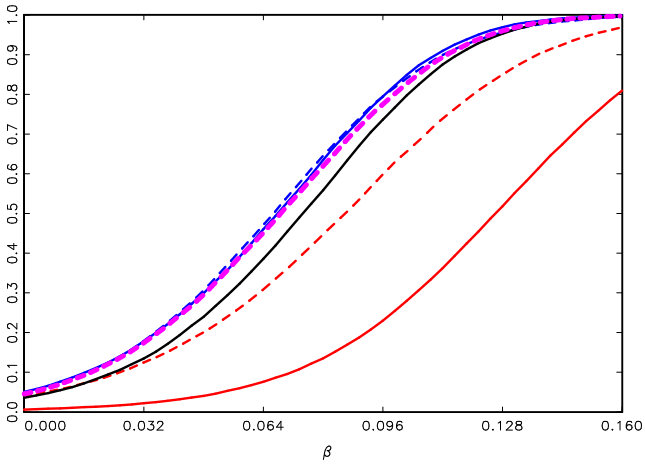

(e) $\kappa = 0.4$

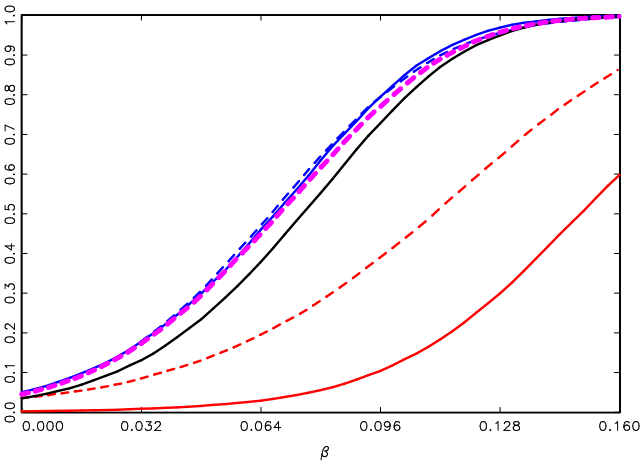

(f) $\kappa = 0.5$

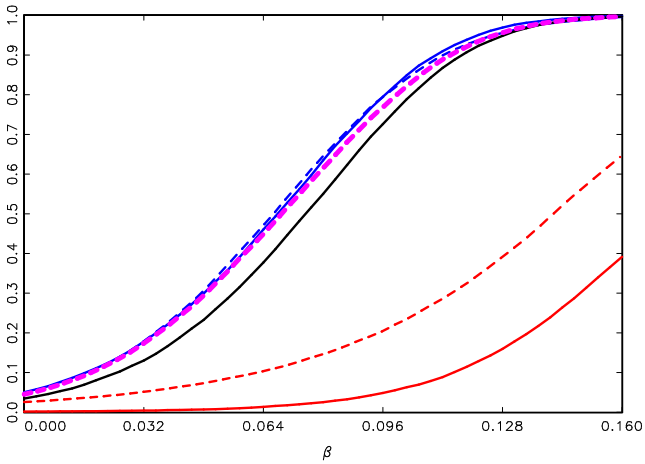

t_μ^{OLS}: – – , Q_μ^{GLS}: ——— , t_τ^{OLS}: – –, Q_τ^{GLS}: ———, U^{hyb}: ———, S^{hyb}: – –

Figure S.58: Finite Power of Right-Tailed Tests. DGP (1)-(3) with $c = -50$, $\delta = -0.75$ and $\kappa = \{0.0, 0.1, 0.2, 0.3, 0.4, 0.5\}$, where c, κ and δ are the local-to-unity AR, local-to-zero trend, and endogeneity correlation parameters, respectively.

(a) $\kappa = 0.0$

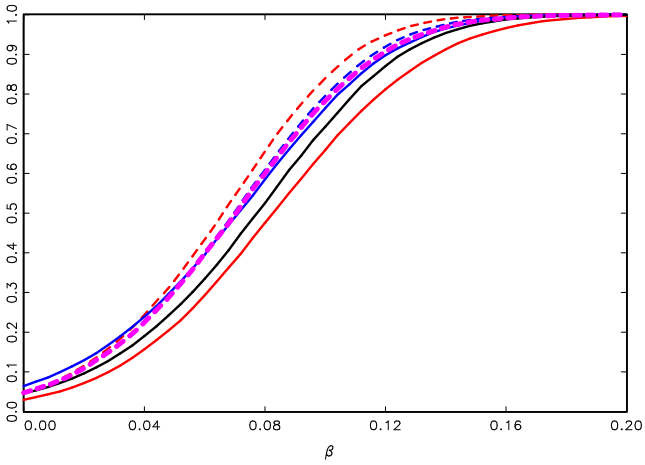

(b) $\kappa = 0.1$

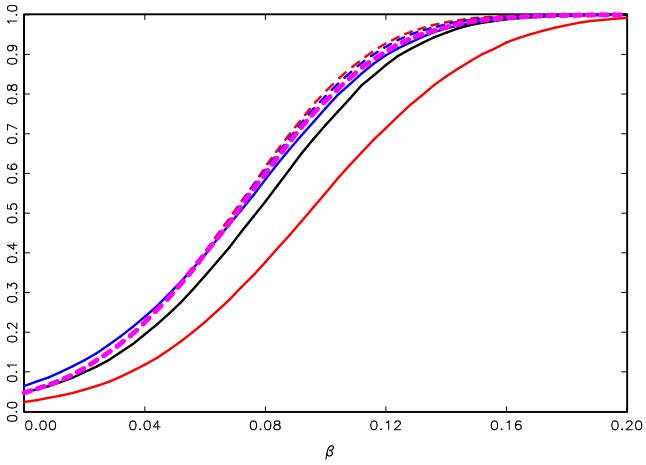

(c) $\kappa = 0.2$

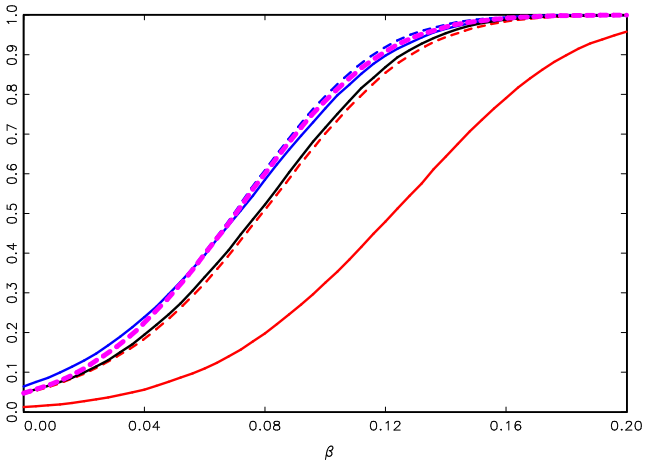

(d) $\kappa = 0.3$

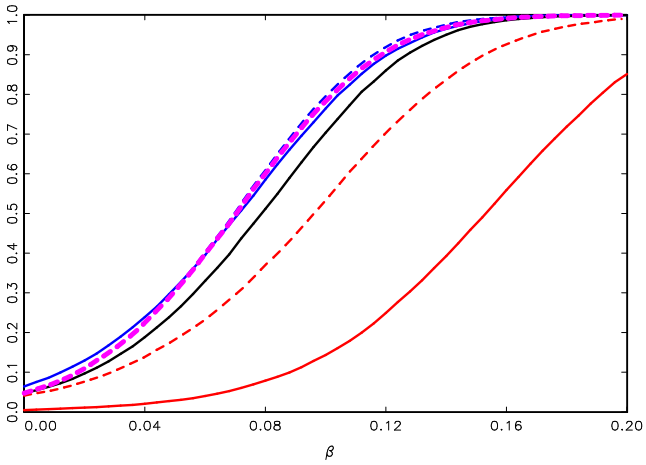

(e) $\kappa = 0.4$

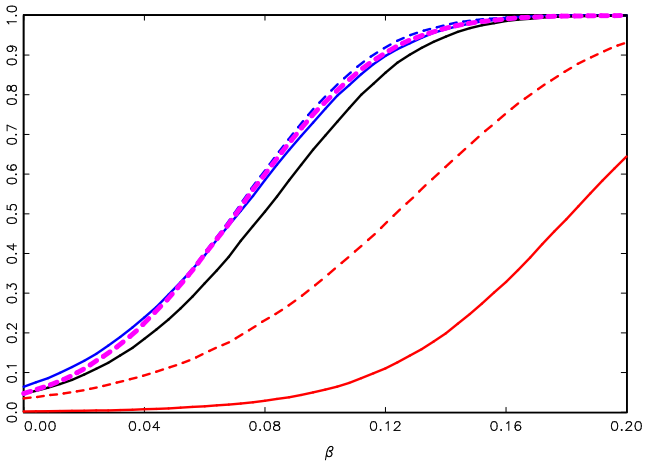

(f) $\kappa = 0.5$

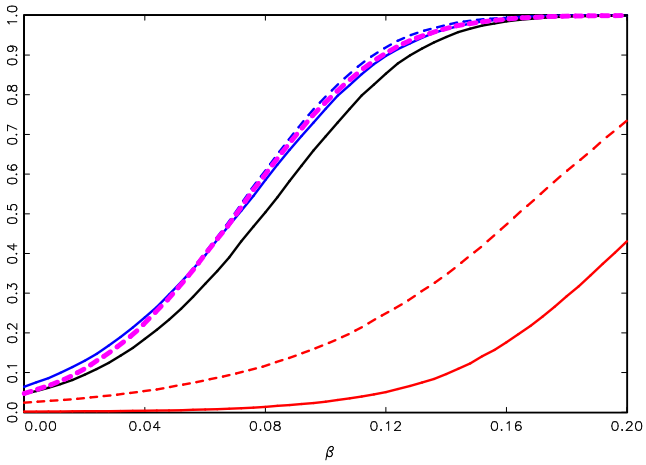

t_{μ}^{OLS}: – –, Q_{μ}^{GLS}: ——, t_{τ}^{OLS}: – –, Q_{τ}^{GLS}: ——, U^{hyb}: ——, S^{hyb}: – –

Figure S.59: Finite Power of Right-Tailed Tests. DGP (1)-(3) with $c = -100$, $\delta = -0.75$ and $\kappa = \{0.0, 0.1, 0.2, 0.3, 0.4, 0.5\}$, where c, κ and δ are the local-to-unity AR, local-to-zero trend, and endogeneity correlation parameters, respectively.

(a) $\kappa = 0.0$

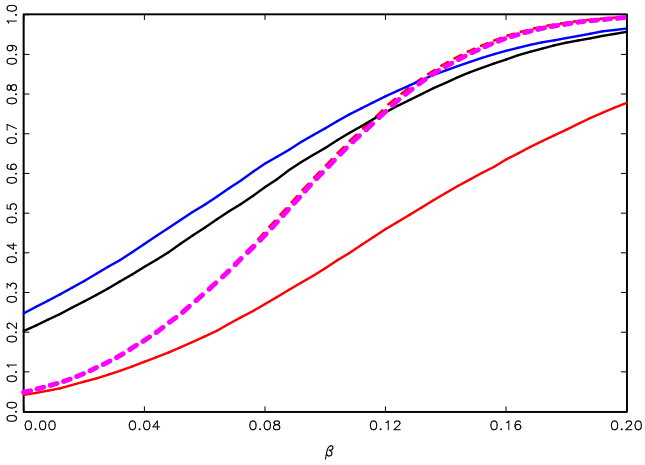

(b) $\kappa = 0.1$

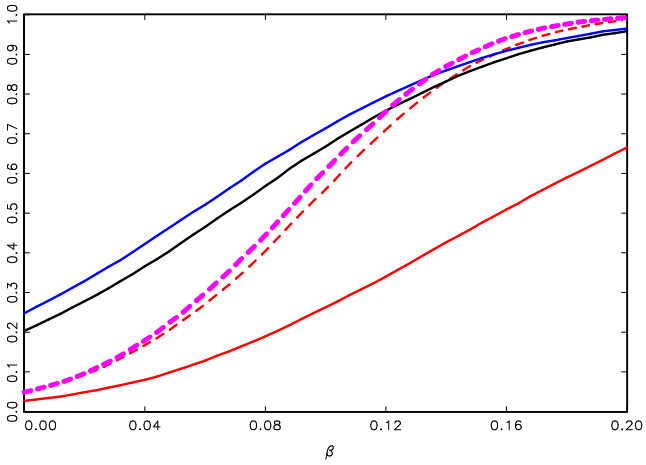

(c) $\kappa = 0.2$

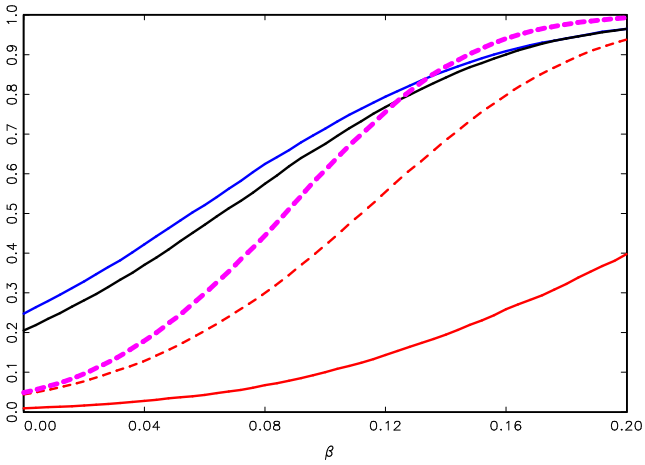

(d) $\kappa = 0.3$

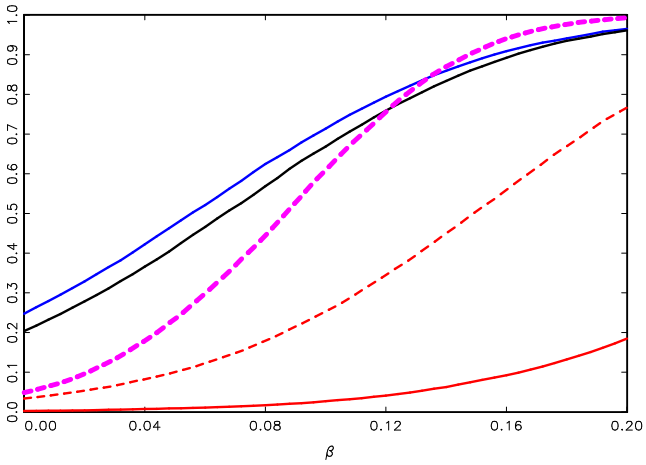

(e) $\kappa = 0.4$

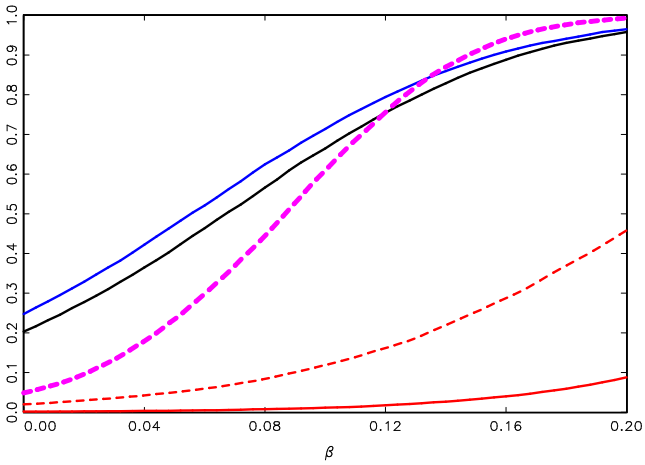

(f) $\kappa = 0.5$

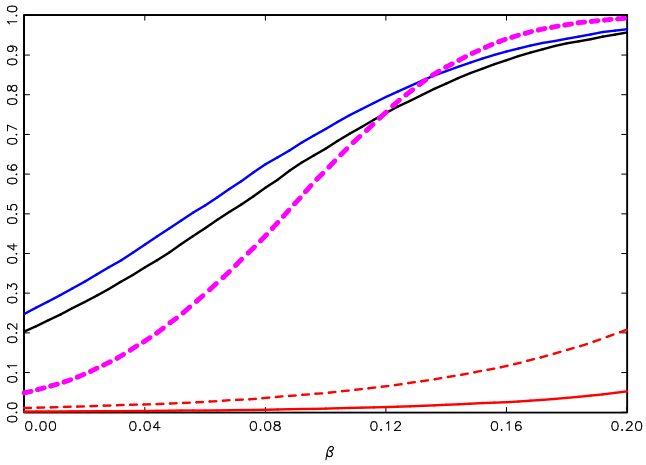

t_{μ}^{OLS}: – – , Q_{μ}^{GLS}: ——— , t_{τ}^{OLS}: – –, Q_{τ}^{GLS}: ———, U^{hyb}: ———, S^{hyb}: – –

Figure S.60: Finite Power of Right-Tailed Tests. DGP (1)-(3) with $c = -250$, $\delta = -0.75$ and $\kappa = \{0.0, 0.1, 0.2, 0.3, 0.4, 0.5\}$, where c, κ and δ are the local-to-unity AR, local-to-zero trend, and endogeneity correlation parameters, respectively.

(a) $\kappa = 0.0$

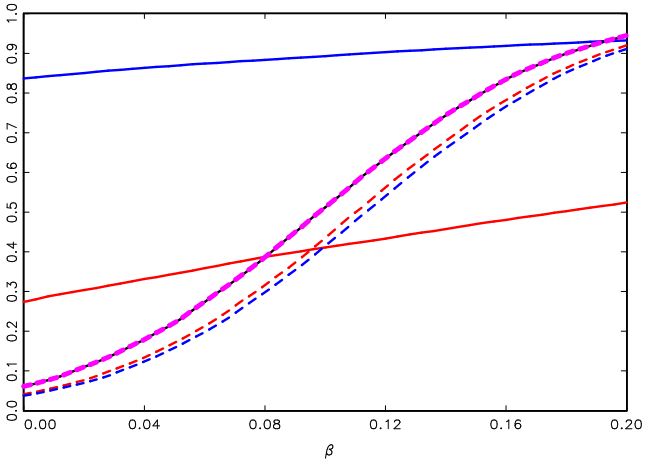

(b) $\kappa = 0.1$

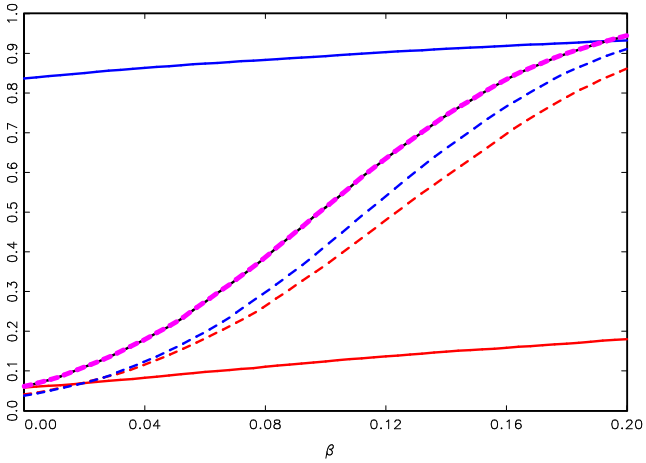

(c) $\kappa = 0.2$

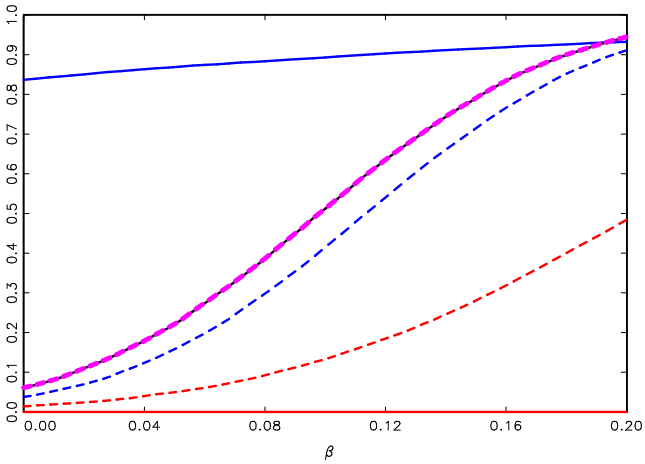

(d) $\kappa = 0.3$

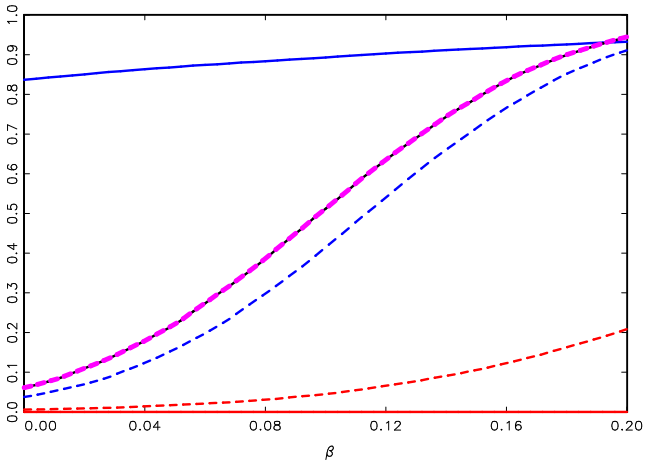

(e) $\kappa = 0.4$

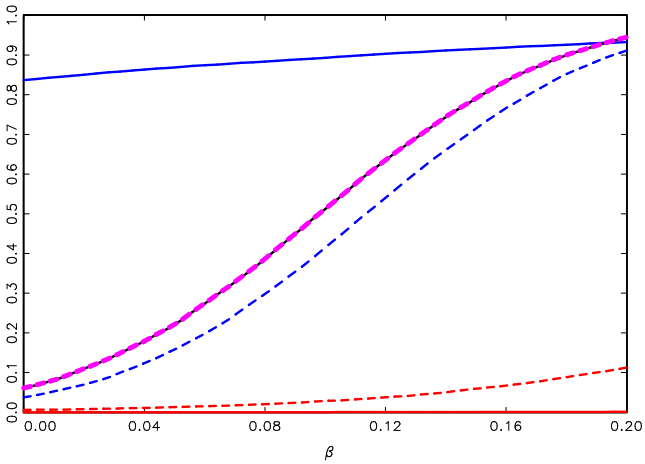

(f) $\kappa = 0.5$

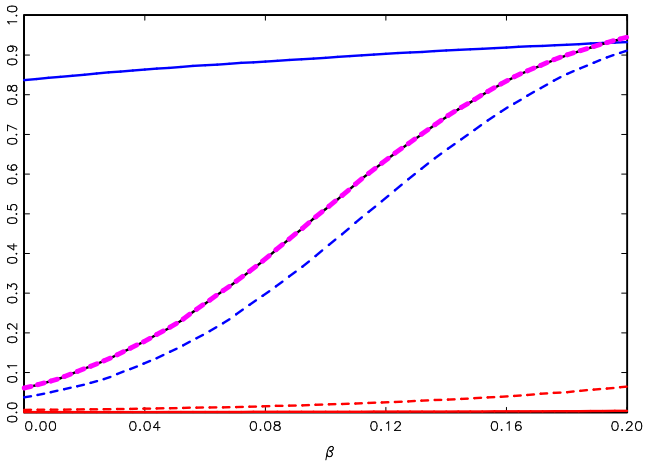

t_μ^{OLS}: – – , Q_μ^{GLS}: ——— , t_τ^{OLS}: – –, Q_τ^{GLS}: ———, U^{hyb}: ———, S^{hyb}: – –

Figure S.61: Finite Power of Left-Tailed Tests. DGP (1)-(3) with $c = 0$, $\delta = -0.95$ and $\kappa = \{0.0, 0.2, 0.4, 0.6, 0.8, 1.0\}$, where c, κ and δ are the local-to-unity AR, local-to-zero trend, and endogeneity correlation parameters, respectively.

(a) $\kappa = 0.0$

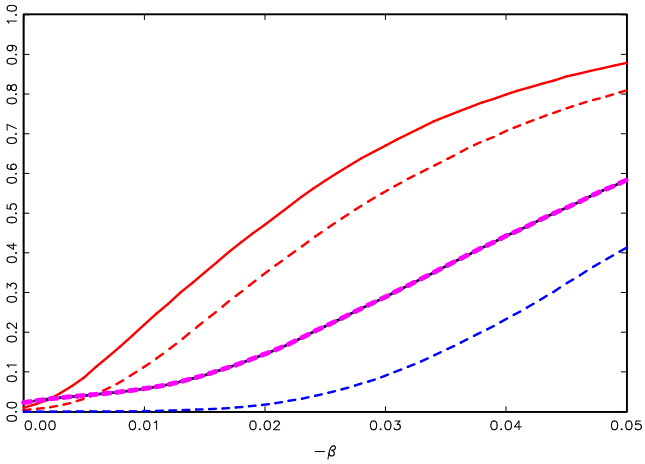

(b) $\kappa = 0.2$

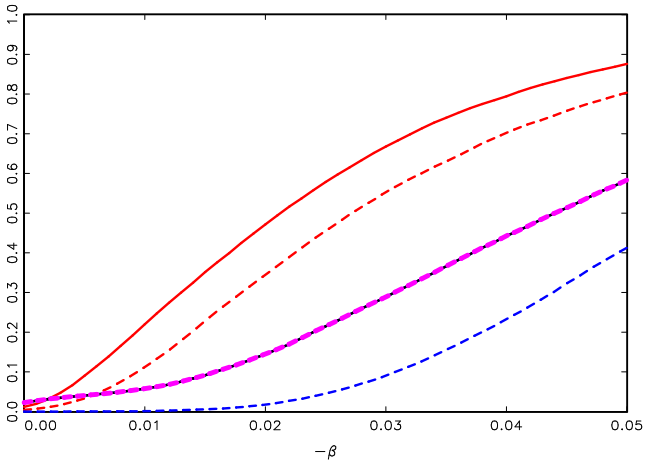

(c) $\kappa = 0.4$

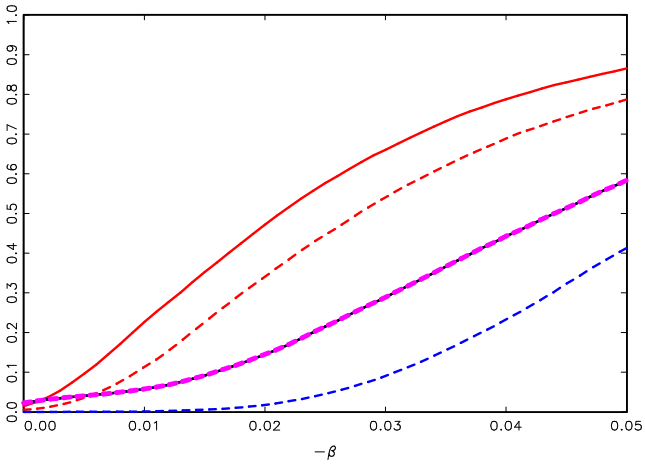

(d) $\kappa = 0.6$

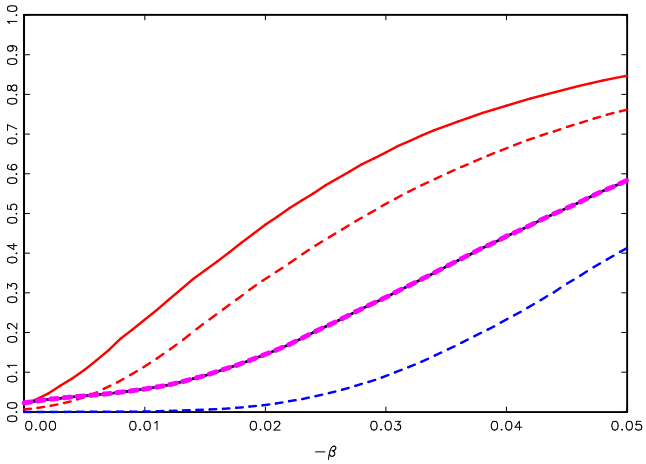

(e) $\kappa = 0.8$

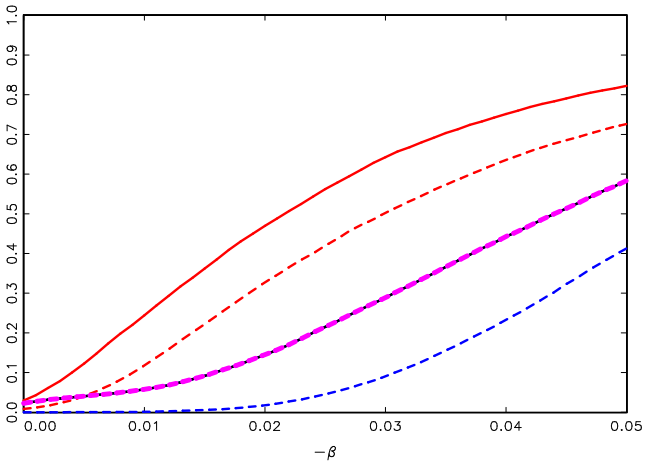

(f) $\kappa = 1.0$

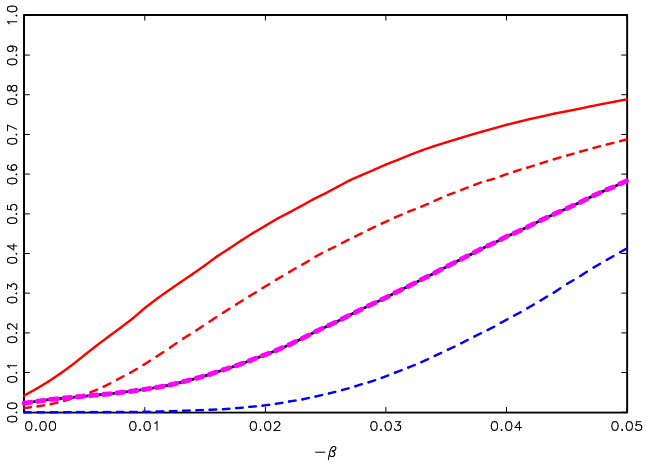

t_{μ}^{OLS}: – –, Q_{μ}^{GLS}: ——, t_{τ}^{OLS}: – –, Q_{τ}^{GLS}: ——, U^{hyb}: ——, S^{hyb}: – –

Figure S.62: Finite Power of Left-Tailed Tests. DGP (1)-(3) with $c = -2$, $\delta = -0.95$ and $\kappa = \{0.0, 0.2, 0.4, 0.6, 0.8, 1.0\}$, where c, κ and δ are the local-to-unity AR, local-to-zero trend, and endogeneity correlation parameters, respectively.

(a) $\kappa = 0.0$

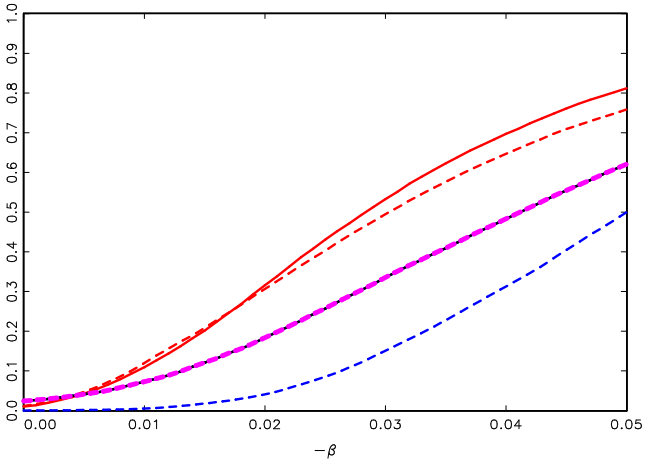

(b) $\kappa = 0.2$

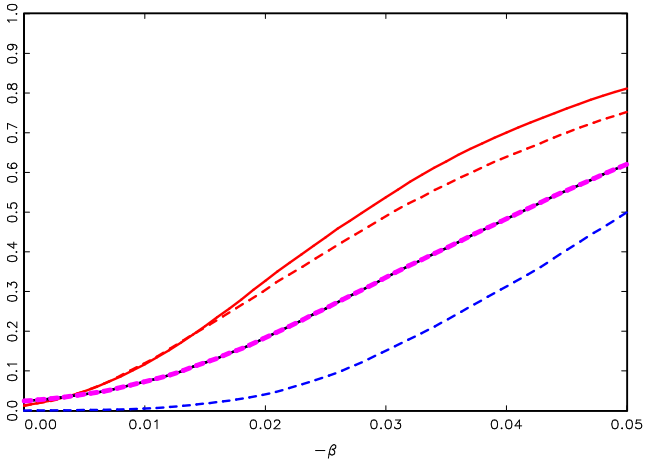

(c) $\kappa = 0.4$

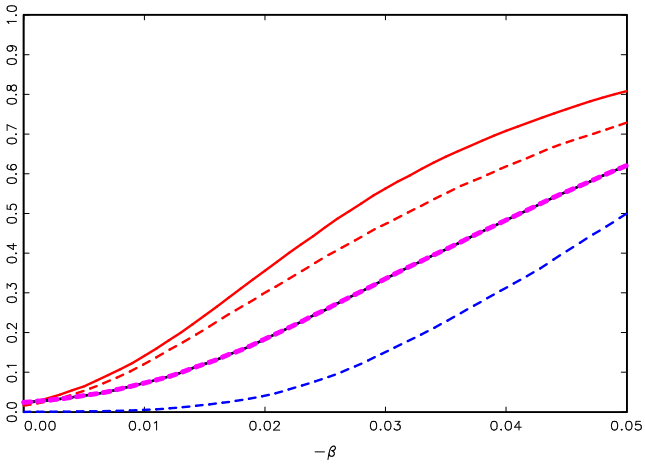

(d) $\kappa = 0.6$

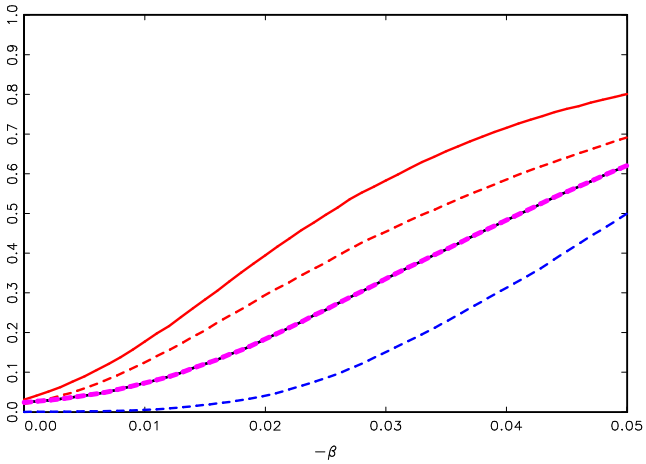

(e) $\kappa = 0.8$

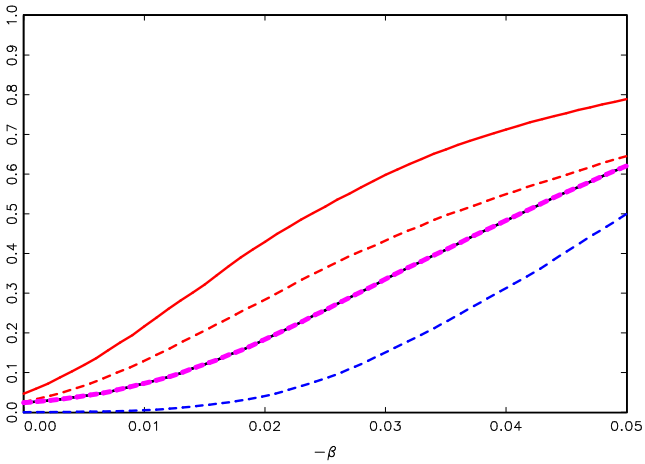

(f) $\kappa = 1.0$

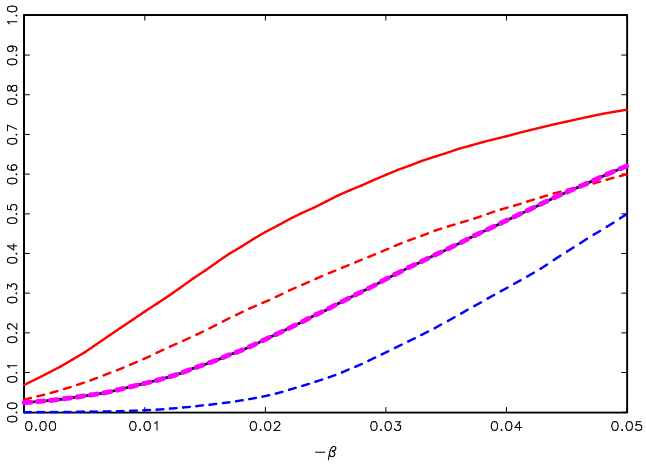

t_{μ}^{OLS}: – –, Q_{μ}^{GLS}: ——, t_{τ}^{OLS}: – –, Q_{τ}^{GLS}: ——, U^{hyb}: ——, S^{hyb}: – –

Figure S.63: Finite Power of Left-Tailed Tests. DGP (1)-(3) with $c = -5$, $\delta = -0.95$ and $\kappa = \{0.0, 0.2, 0.4, 0.6, 0.8, 1.0\}$, where c, κ and δ are the local-to-unity AR, local-to-zero trend, and endogeneity correlation parameters, respectively.

(a) $\kappa = 0.0$

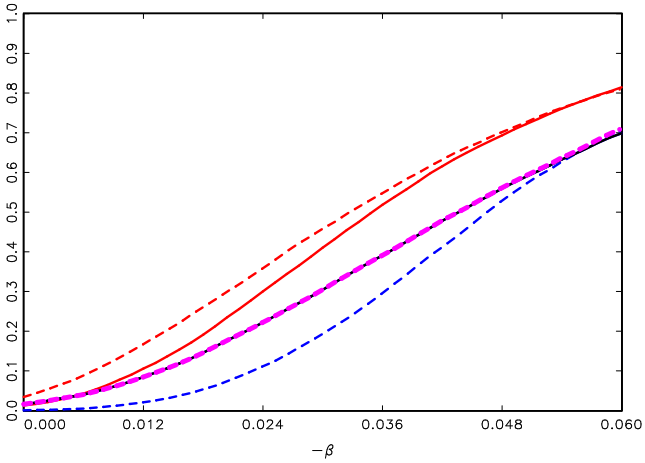

(b) $\kappa = 0.2$

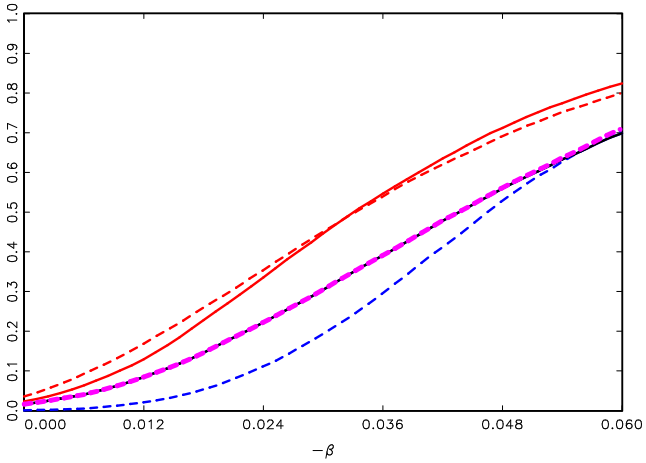

(c) $\kappa = 0.4$

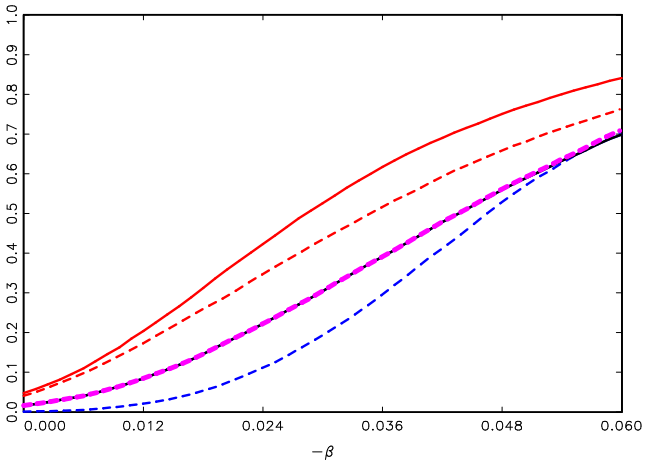

(d) $\kappa = 0.6$

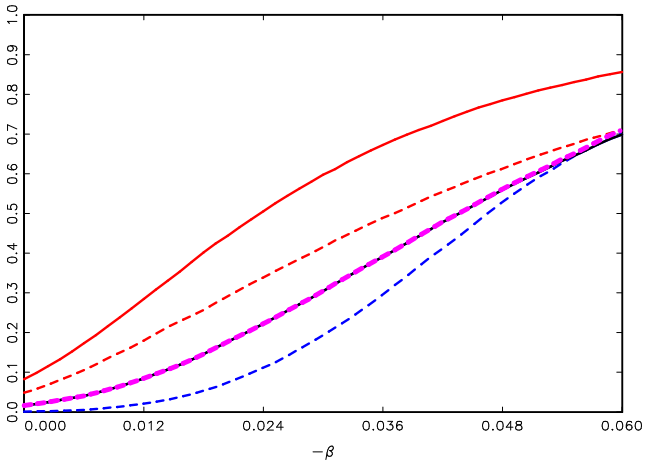

(e) $\kappa = 0.8$

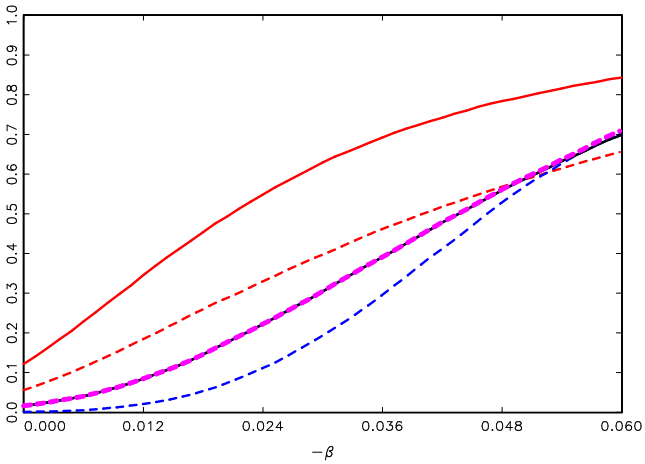

(f) $\kappa = 1.0$

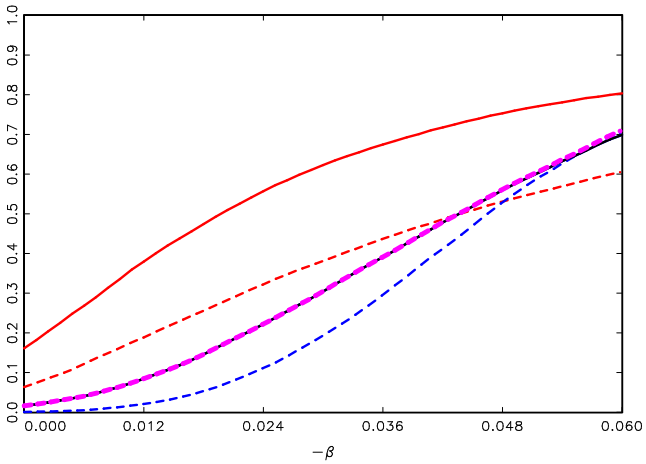

t_{μ}^{OLS}: – –, Q_{μ}^{GLS}: ——, t_{τ}^{OLS}: – –, Q_{τ}^{GLS}: ——, U^{hyb}: ——, S^{hyb}: – –

Figure S.64: Finite Power of Left-Tailed Tests. DGP (1)-(3) with $c = -10$, $\delta = -0.95$ and $\kappa = \{0.0, 0.2, 0.4, 0.6, 0.8, 1.0\}$, where c, κ and δ are the local-to-unity AR, local-to-zero trend, and endogeneity correlation parameters, respectively.

(a) $\kappa = 0.0$

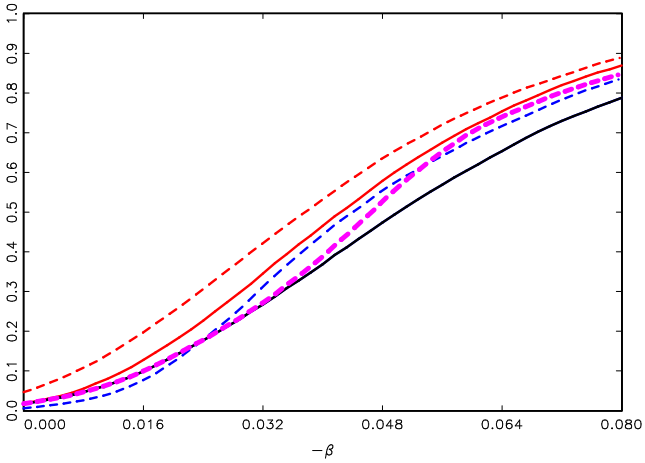

(b) $\kappa = 0.2$

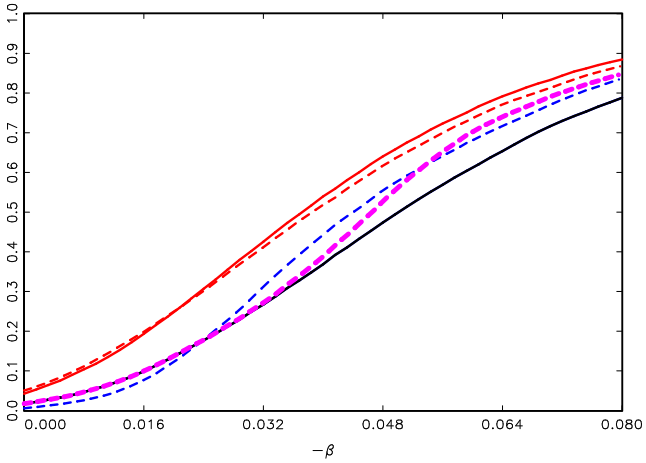

(c) $\kappa = 0.4$

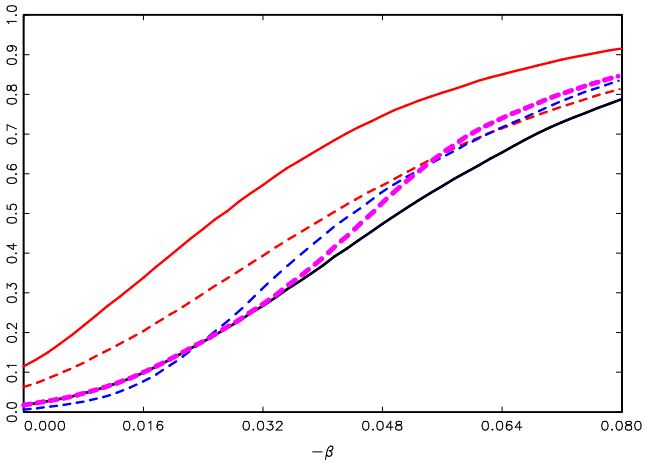

(d) $\kappa = 0.6$

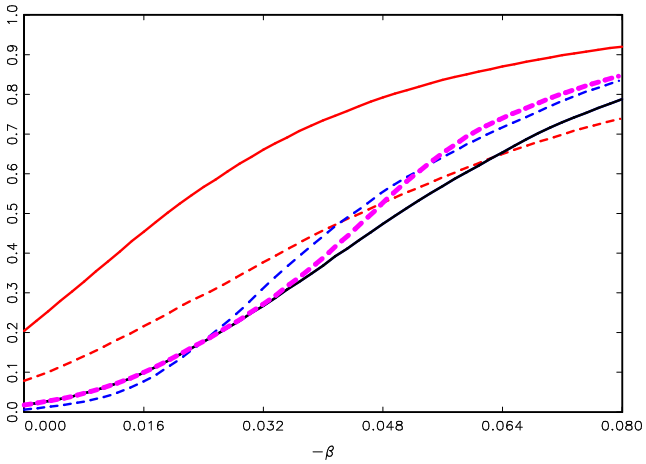

(e) $\kappa = 0.8$

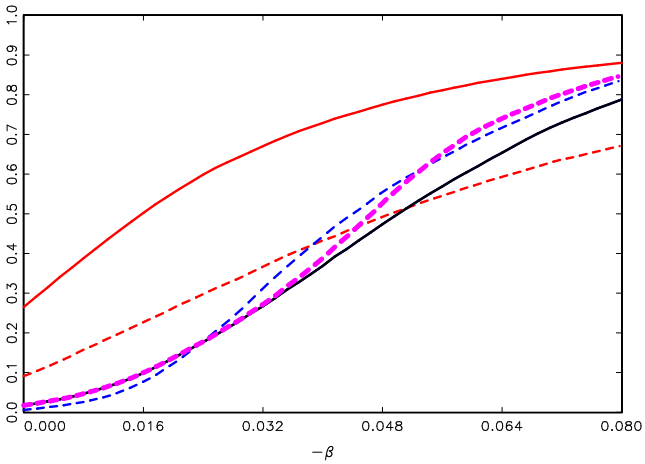

(f) $\kappa = 1.0$

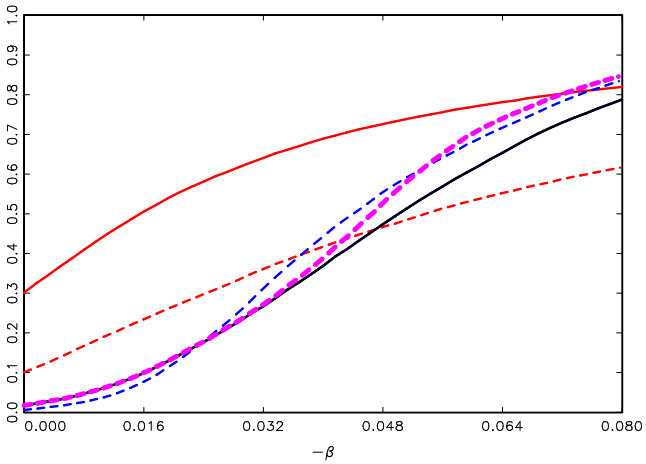

t_μ^{OLS}: – –, Q_μ^{GLS}: ——, t_τ^{OLS}: – –, Q_τ^{GLS}: ——, U^{hyb}: ——, S^{hyb}: – –

Figure S.65: Finite Power of Left-Tailed Tests. DGP (1)-(3) with $c = -20$, $\delta = -0.95$ and $\kappa = \{0.0, 0.1, 0.2, 0.3, 0.4, 0.5\}$, where c, κ and δ are the local-to-unity AR, local-to-zero trend, and endogeneity correlation parameters, respectively.

(a) $\kappa = 0.0$

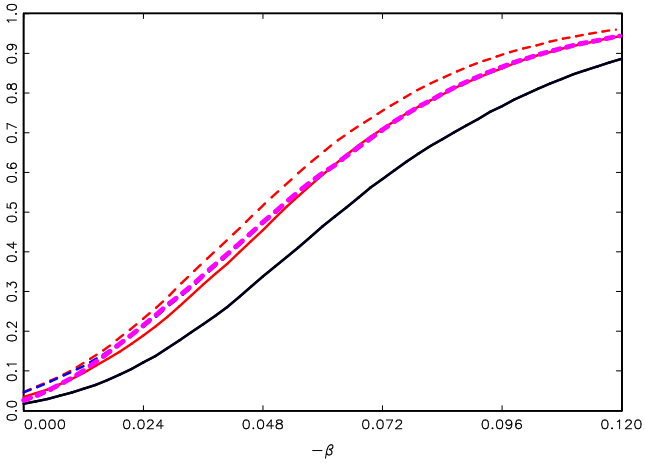

(b) $\kappa = 0.1$

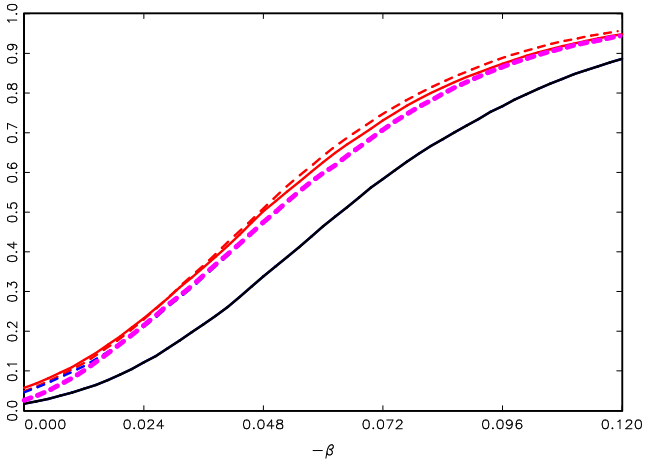

(c) $\kappa = 0.2$

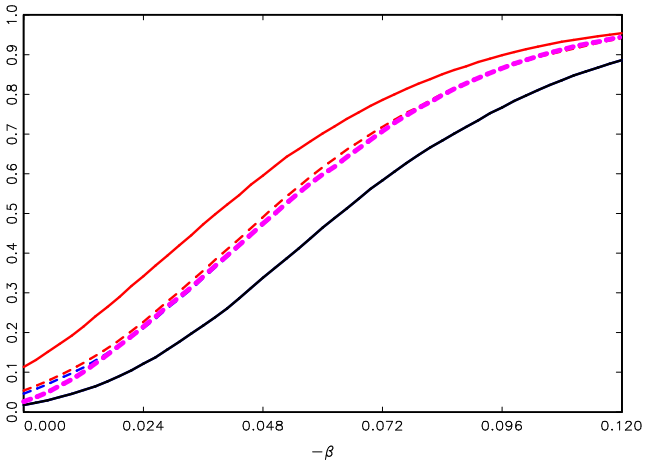

(d) $\kappa = 0.3$

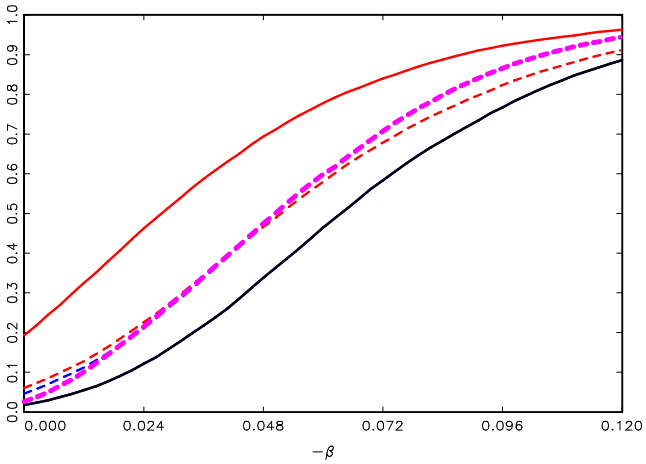

(e) $\kappa = 0.4$

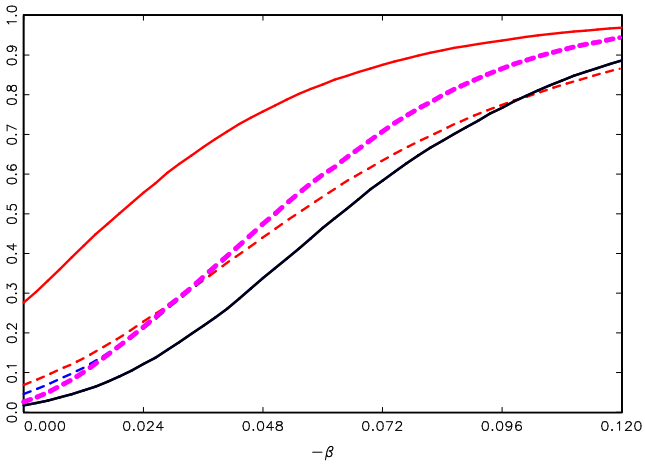

(f) $\kappa = 0.5$

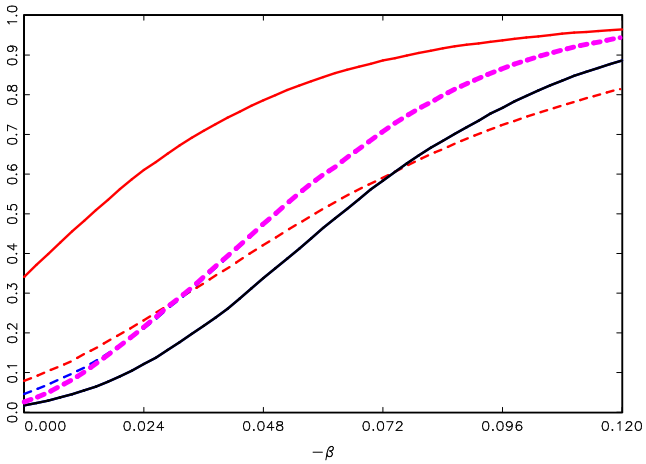

t_{μ}^{OLS}: – –, Q_{μ}^{GLS}: ——, t_{τ}^{OLS}: – –, Q_{τ}^{GLS}: ——, U^{hyb}: ——, S^{hyb}: – –

Figure S.66: Finite Power of Left-Tailed Tests. DGP (1)-(3) with $c = -30$, $\delta = -0.95$ and $\kappa = \{0.0, 0.1, 0.2, 0.3, 0.4, 0.5\}$, where c, κ and δ are the local-to-unity AR, local-to-zero trend, and endogeneity correlation parameters, respectively.

(a) $\kappa = 0.0$

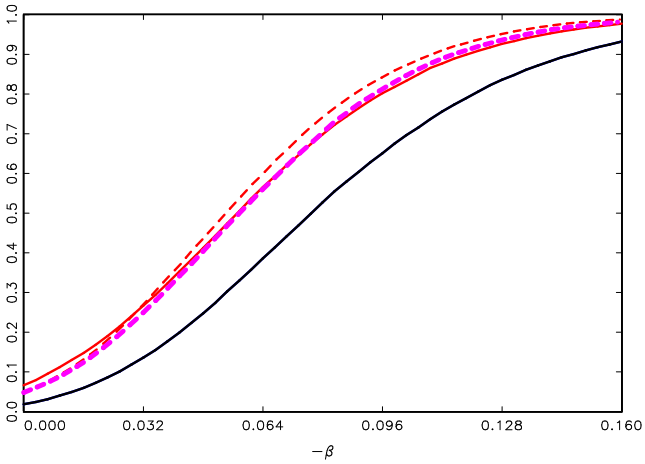

(b) $\kappa = 0.1$

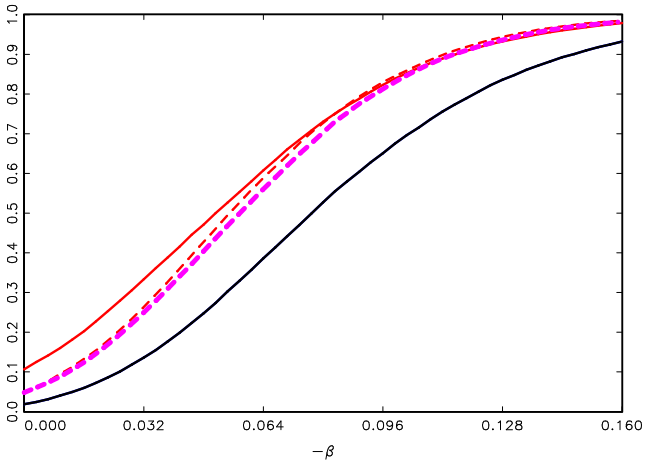

(c) $\kappa = 0.2$

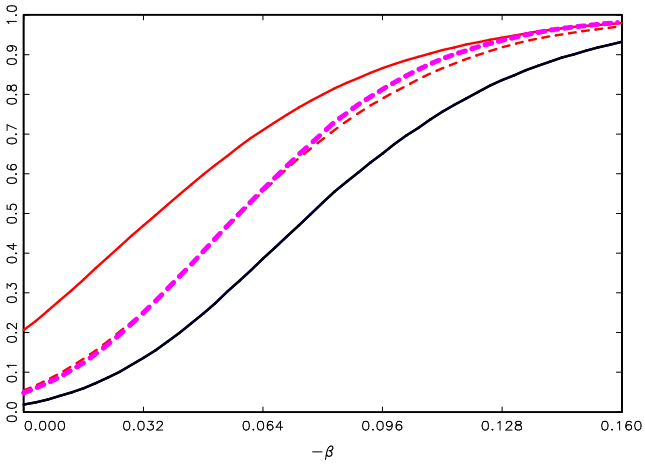

(d) $\kappa = 0.3$

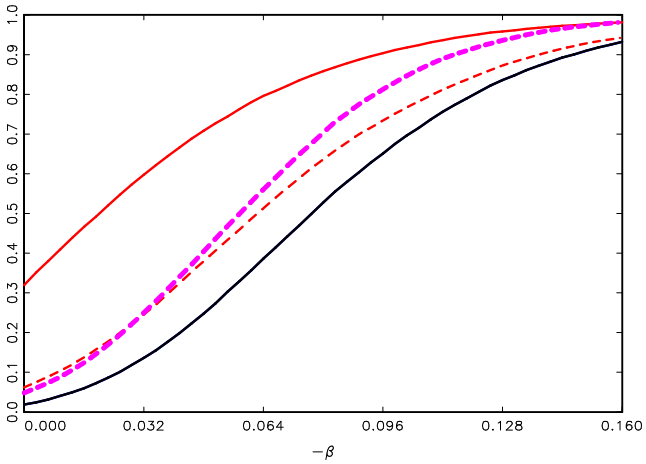

(e) $\kappa = 0.4$

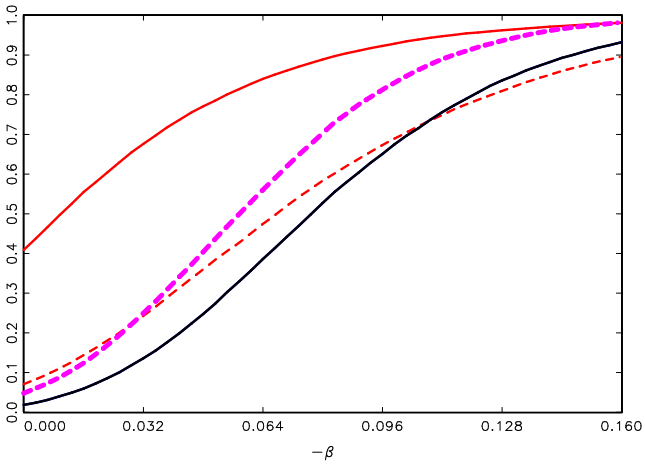

(f) $\kappa = 0.5$

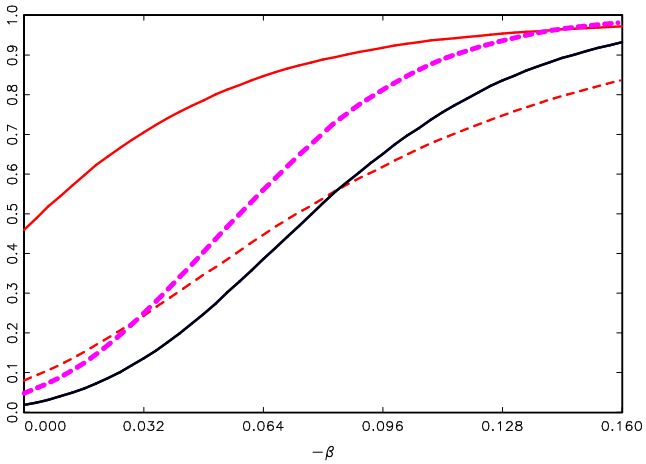

t_{μ}^{OLS}: – – , Q_{μ}^{GLS}: ——— , t_{τ}^{OLS}: – –, Q_{τ}^{GLS}: ———, U^{hyb}: ———, S^{hyb}: – –

Figure S.67: Finite Power of Left-Tailed Tests. DGP (1)-(3) with $c = -40$, $\delta = -0.95$ and $\kappa = \{0.0, 0.1, 0.2, 0.3, 0.4, 0.5\}$, where c, κ and δ are the local-to-unity AR, local-to-zero trend, and endogeneity correlation parameters, respectively.

(a) $\kappa = 0.0$

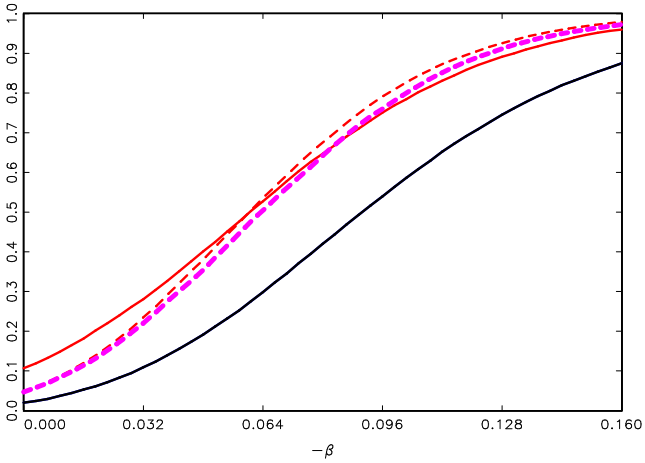

(b) $\kappa = 0.1$

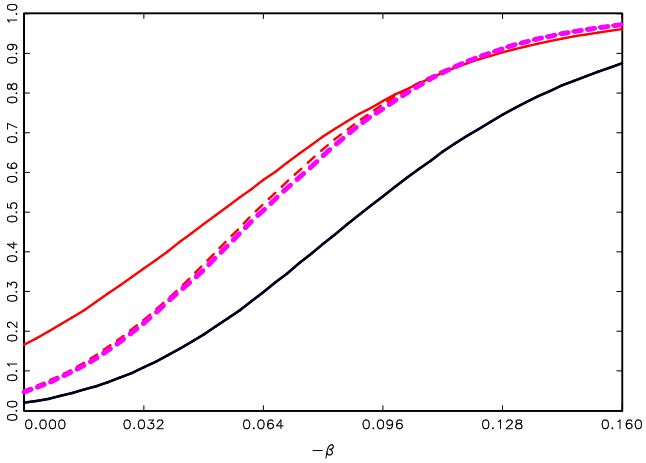

(c) $\kappa = 0.2$

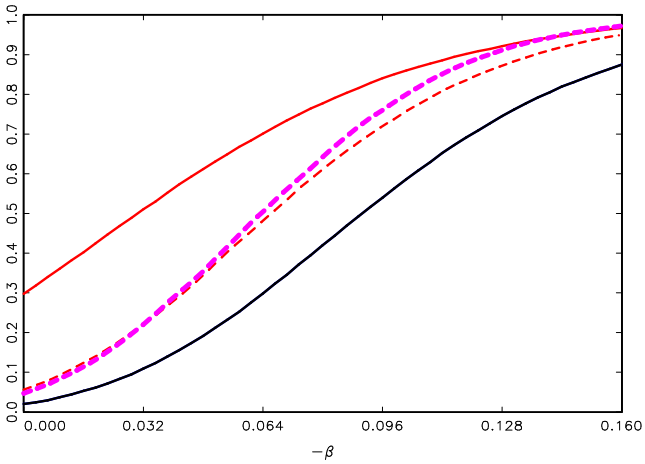

(d) $\kappa = 0.3$

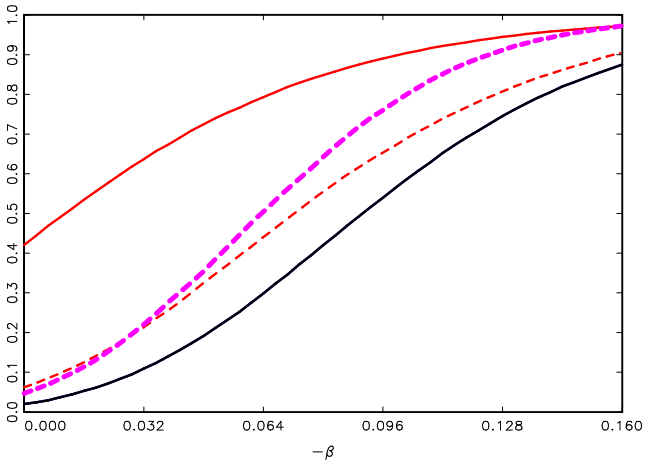

(e) $\kappa = 0.4$

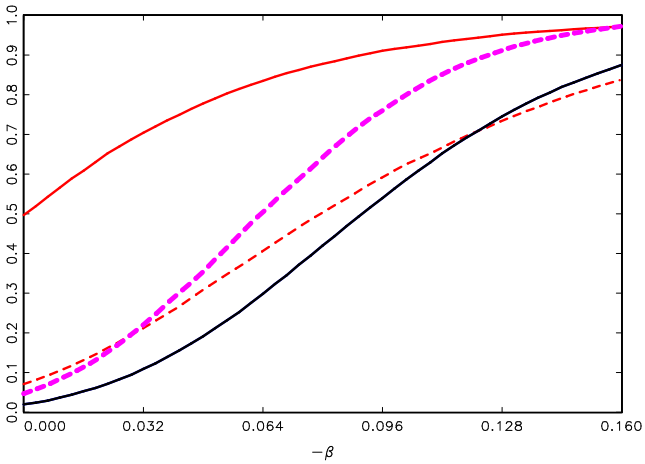

(f) $\kappa = 0.5$

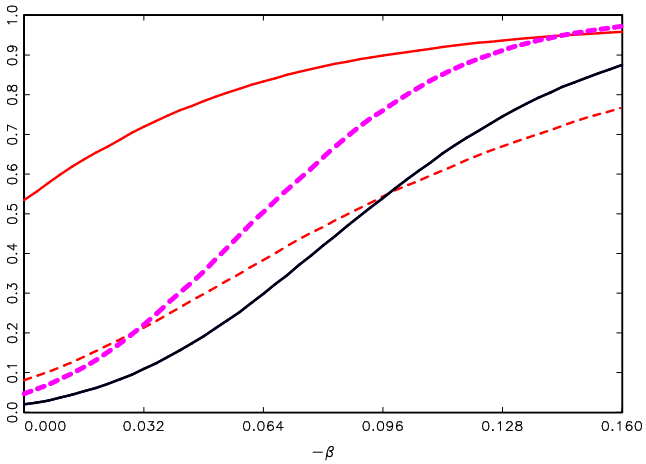

t_{μ}^{OLS}: – –, Q_{μ}^{GLS}: ——, t_{τ}^{OLS}: – –, Q_{τ}^{GLS}: ——, U^{hyb}: ——, S^{hyb}: – –

Figure S.68: Finite Power of Left-Tailed Tests. DGP (1)-(3) with $c = -50$, $\delta = -0.95$ and $\kappa = \{0.0, 0.1, 0.2, 0.3, 0.4, 0.5\}$, where c, κ and δ are the local-to-unity AR, local-to-zero trend, and endogeneity correlation parameters, respectively.

(a) $\kappa = 0.0$

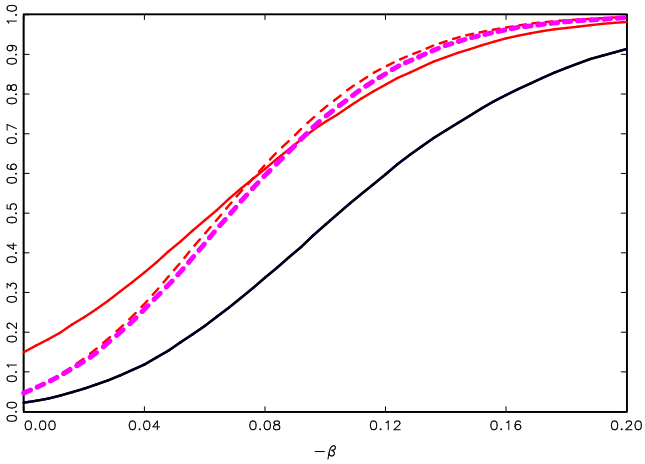

(b) $\kappa = 0.1$

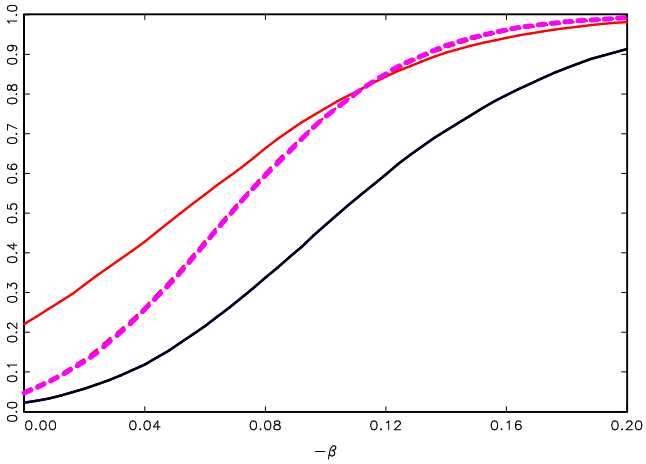

(c) $\kappa = 0.2$

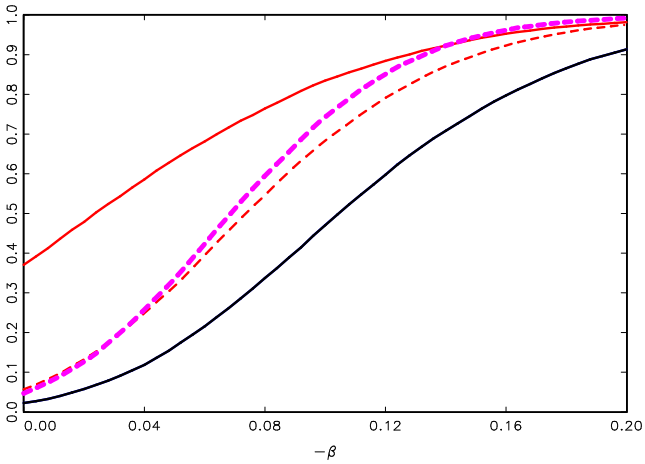

(d) $\kappa = 0.3$

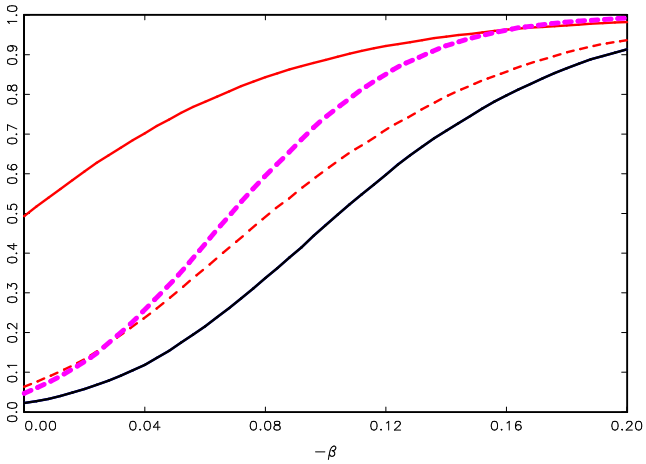

(e) $\kappa = 0.4$

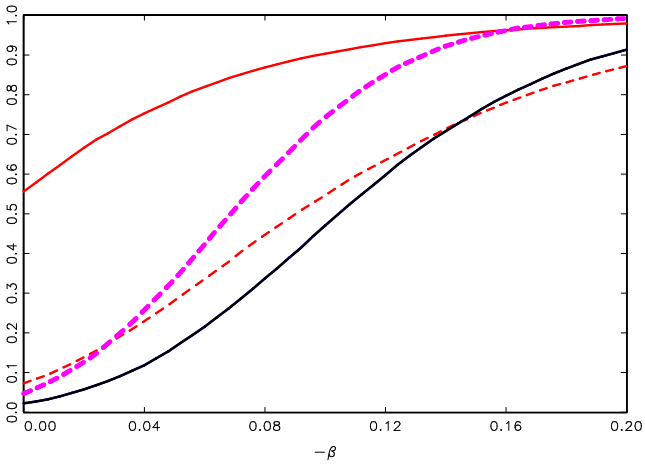

(f) $\kappa = 0.5$

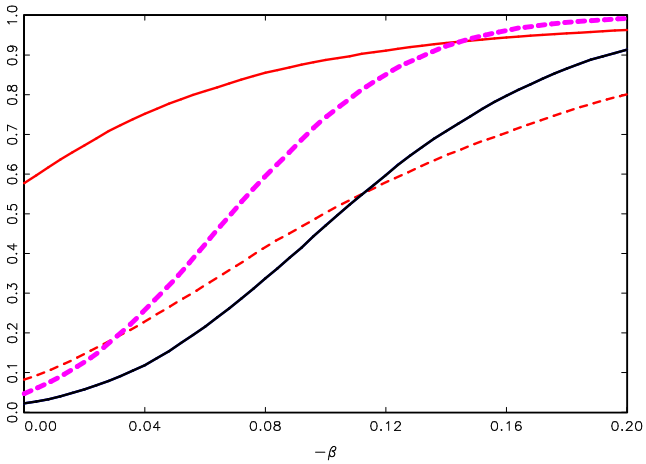

t_{μ}^{OLS}: – – , Q_{μ}^{GLS}: ——— , t_{τ}^{OLS}: – –, Q_{τ}^{GLS}: ———, U^{hyb}: ———, S^{hyb}: – –

Figure S.69: Finite Power of Left-Tailed Tests. DGP (1)-(3) with $c = -100$, $\delta = -0.95$ and $\kappa = \{0.0, 0.1, 0.2, 0.3, 0.4, 0.5\}$, where c, κ and δ are the local-to-unity AR, local-to-zero trend, and endogeneity correlation parameters, respectively.

(a) $\kappa = 0.0$

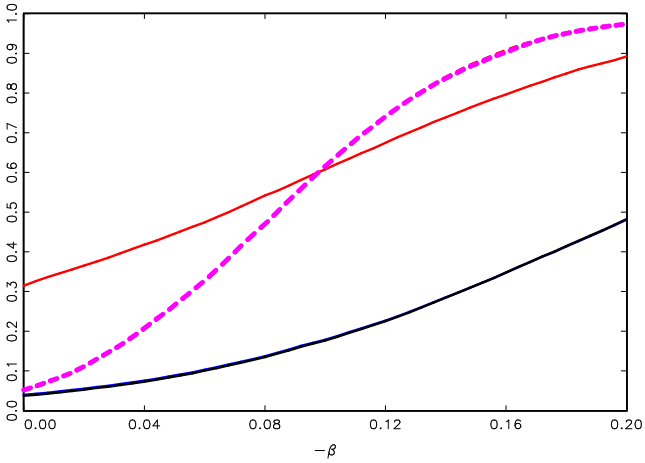

(b) $\kappa = 0.1$

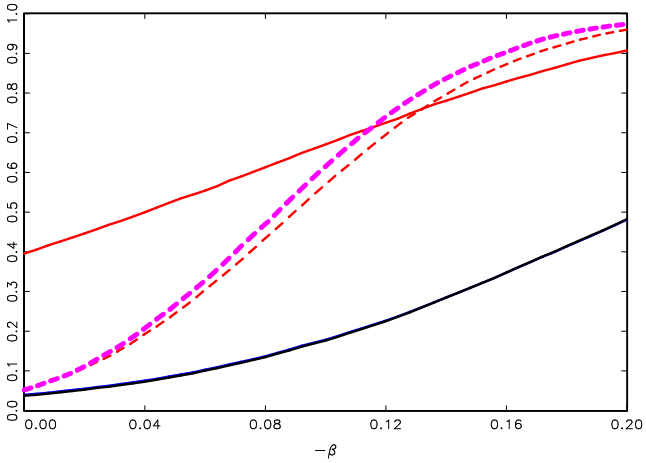

(c) $\kappa = 0.2$

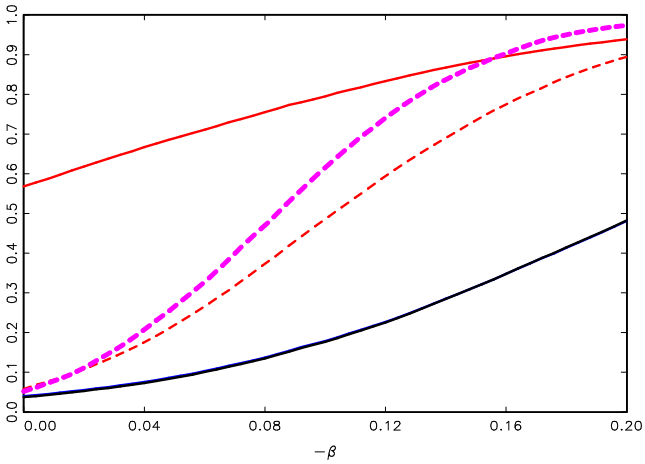

(d) $\kappa = 0.3$

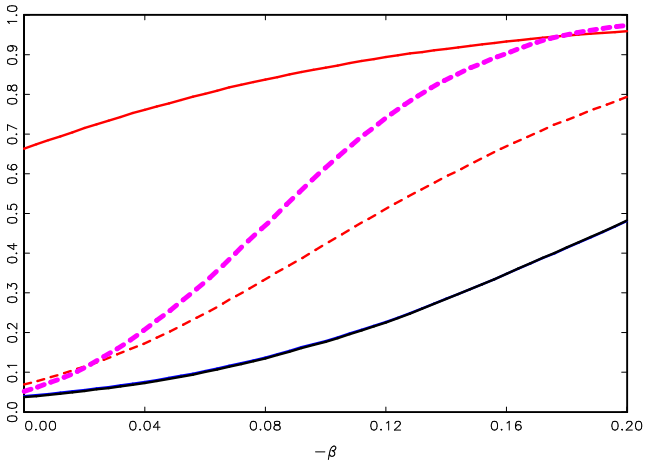

(e) $\kappa = 0.4$

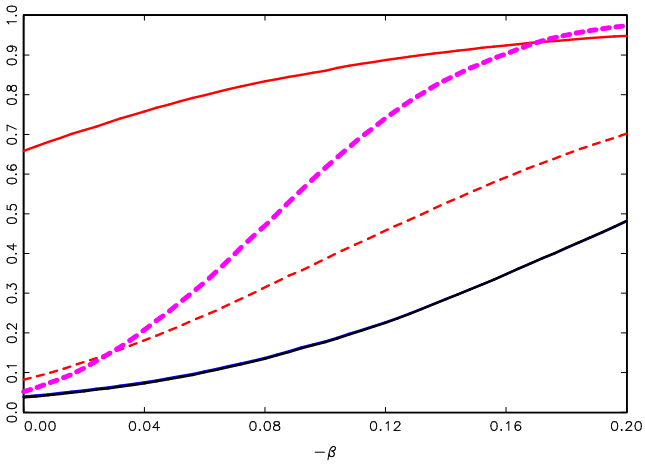

(f) $\kappa = 0.5$

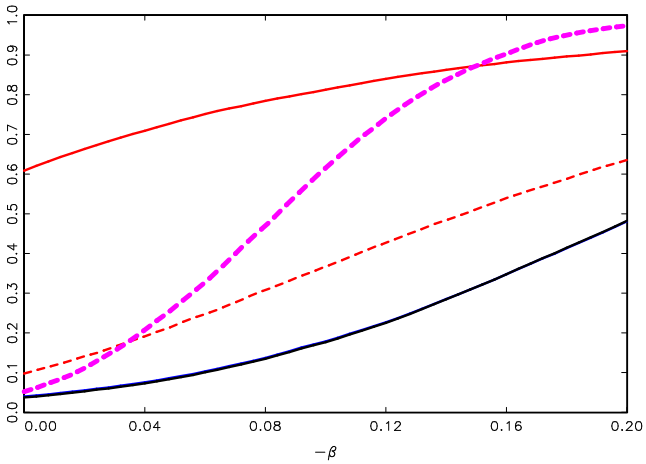

t_{μ}^{OLS}: – – , Q_{μ}^{GLS}: ——— , t_{τ}^{OLS}: – –, Q_{τ}^{GLS}: ———, U^{hyb}: ———, S^{hyb}: – –

Figure S.70: Finite Power of Left-Tailed Tests. DGP (1)-(3) with $c = -250$, $\delta = -0.95$ and $\kappa = \{0.0, 0.1, 0.2, 0.3, 0.4, 0.5\}$, where c, κ and δ are the local-to-unity AR, local-to-zero trend, and endogeneity correlation parameters, respectively.

(a) $\kappa = 0.0$

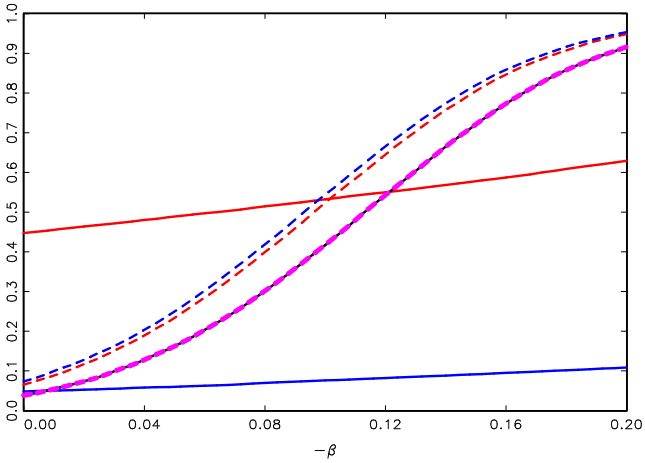

(b) $\kappa = 0.1$

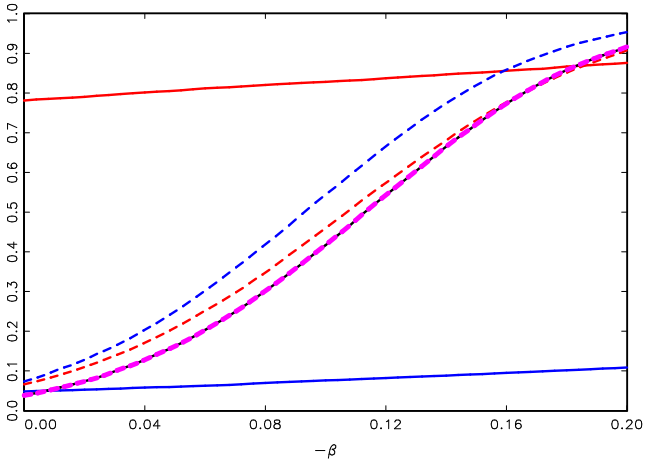

(c) $\kappa = 0.2$

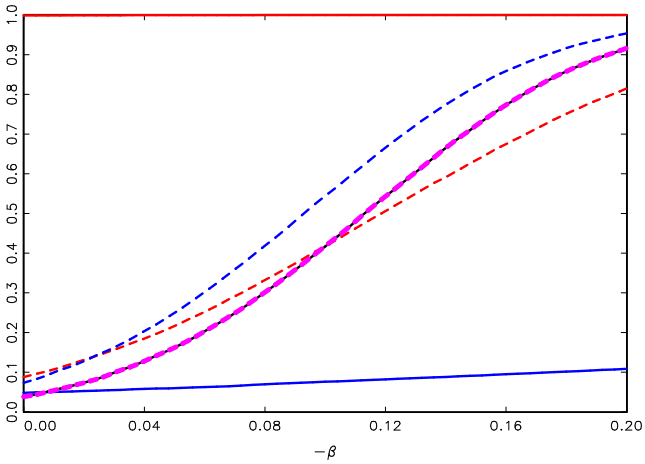

(d) $\kappa = 0.3$

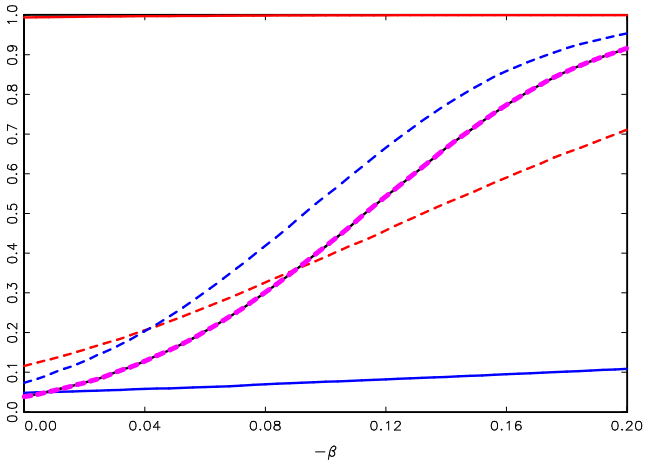

(e) $\kappa = 0.4$

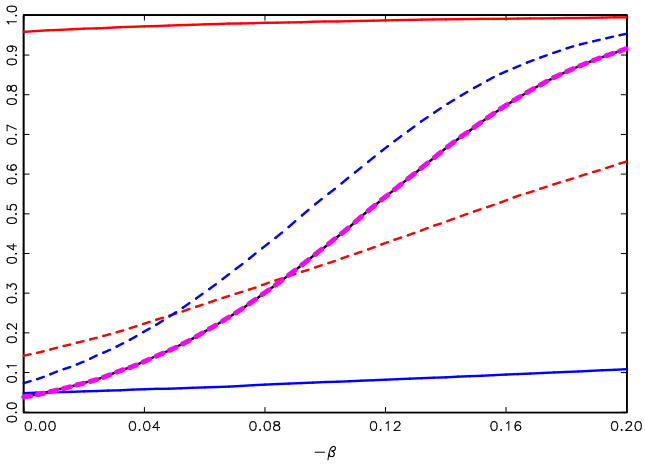

(f) $\kappa = 0.5$

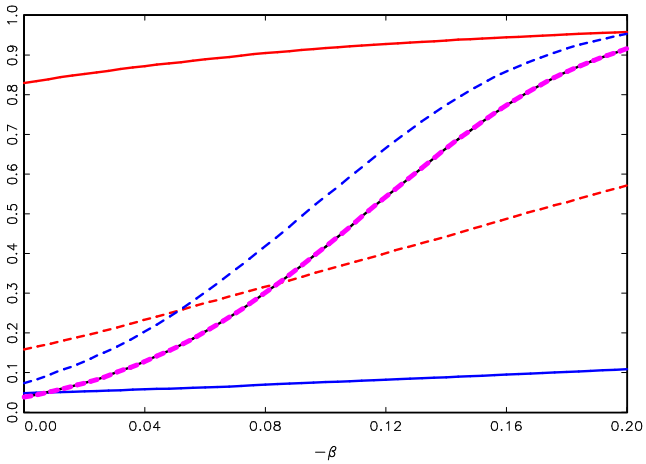

t_{μ}^{OLS}: – – , Q_{μ}^{GLS}: ——— , t_{τ}^{OLS}: – –, Q_{τ}^{GLS}: ———, U^{hyb}: ———, S^{hyb}: – –

Figure S.71: Finite Power of Left-Tailed Tests. DGP (1)-(3) with $c = 0$, $\delta = -0.75$ and $\kappa = \{0.0, 0.2, 0.4, 0.6, 0.8, 1.0\}$, where c, κ and δ are the local-to-unity AR, local-to-zero trend, and endogeneity correlation parameters, respectively.

(a) $\kappa = 0.0$

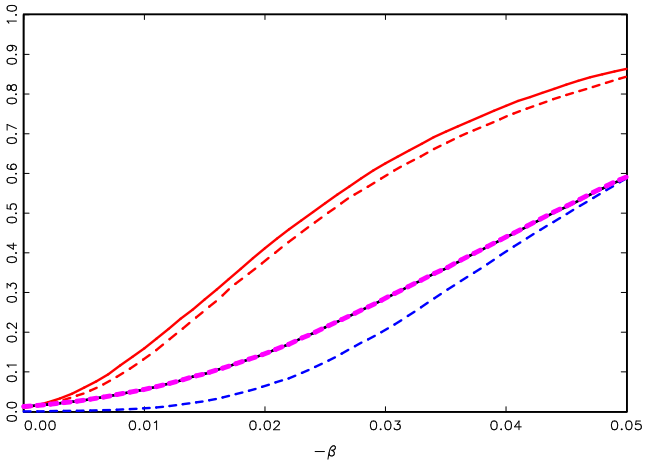

(b) $\kappa = 0.2$

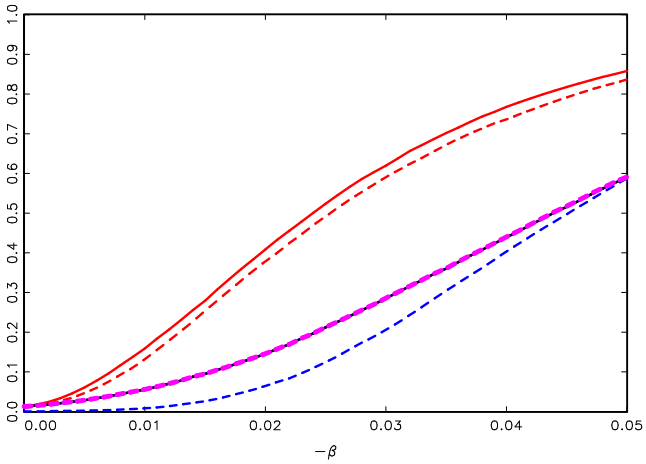

(c) $\kappa = 0.4$

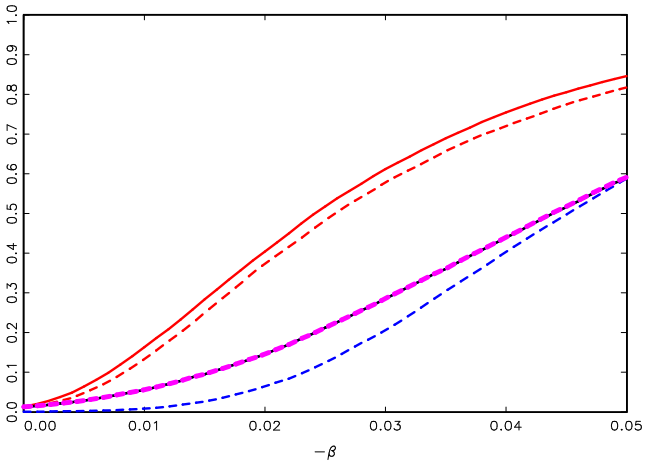

(d) $\kappa = 0.6$

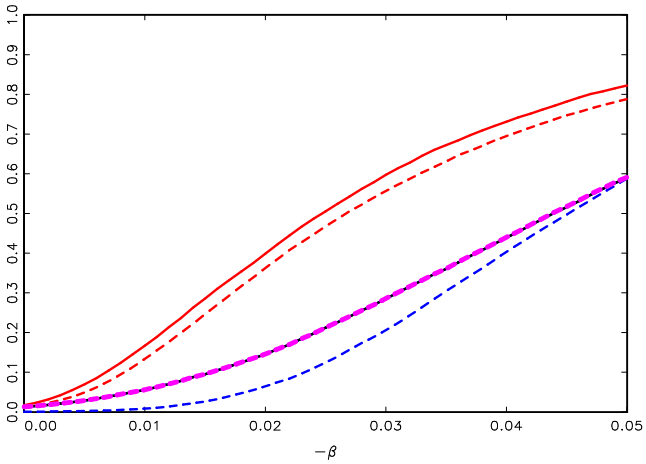

(e) $\kappa = 0.8$

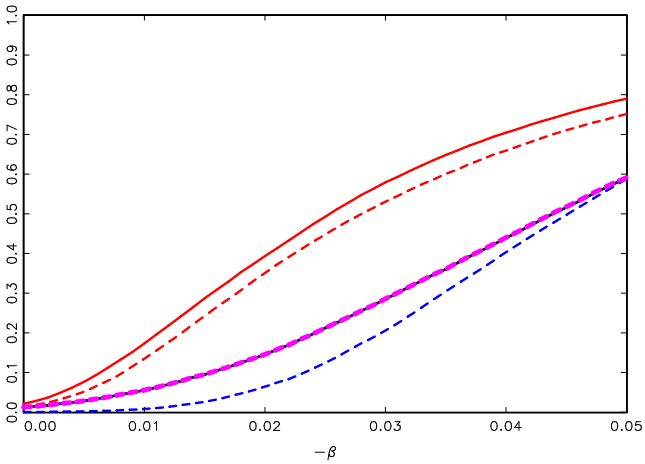

(f) $\kappa = 1.0$

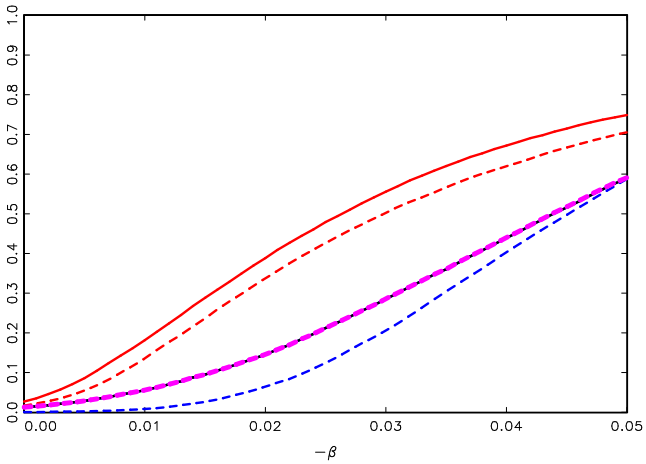

t_{μ}^{OLS}: – –, Q_{μ}^{GLS}: ——, t_{τ}^{OLS}: – –, Q_{τ}^{GLS}: ——, U^{hyb}: ——, S^{hyb}: – –

Figure S.72: Finite Power of Left-Tailed Tests. DGP (1)-(3) with $c = -2$, $\delta = -0.75$ and $\kappa = \{0.0, 0.2, 0.4, 0.6, 0.8, 1.0\}$, where c, κ and δ are the local-to-unity AR, local-to-zero trend, and endogeneity correlation parameters, respectively.

(a) $\kappa = 0.0$

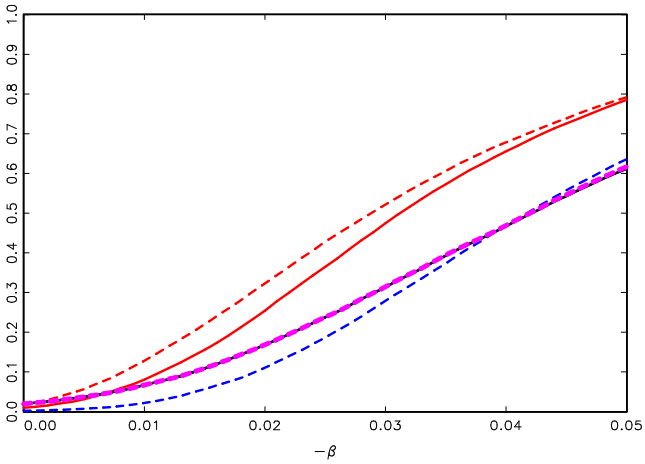

(b) $\kappa = 0.2$

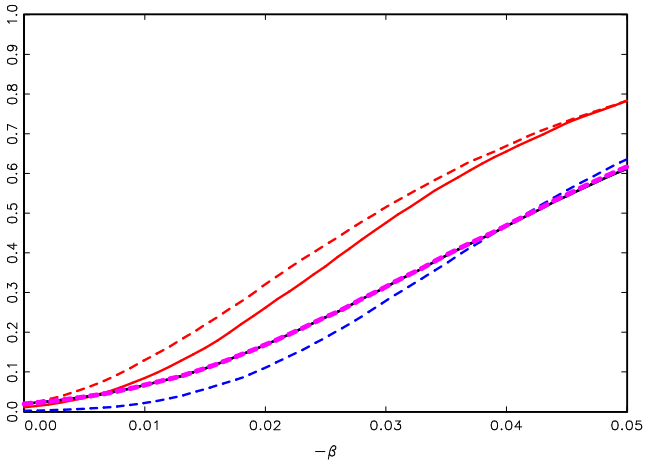

(c) $\kappa = 0.4$

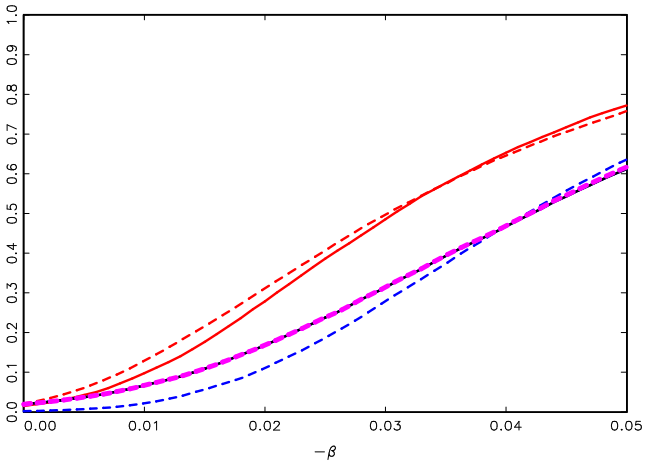

(d) $\kappa = 0.6$

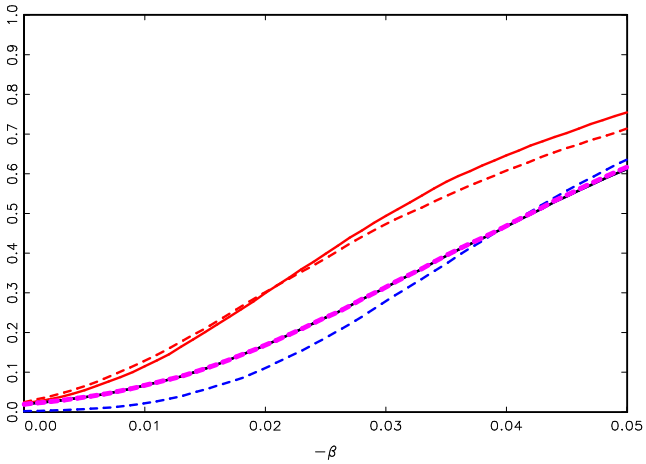

(e) $\kappa = 0.8$

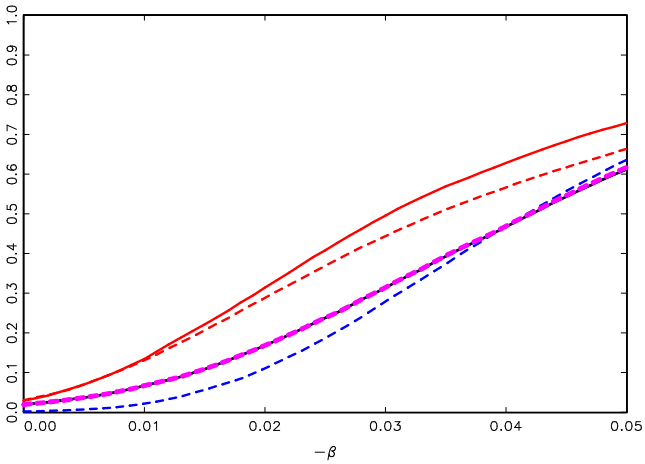

(f) $\kappa = 1.0$

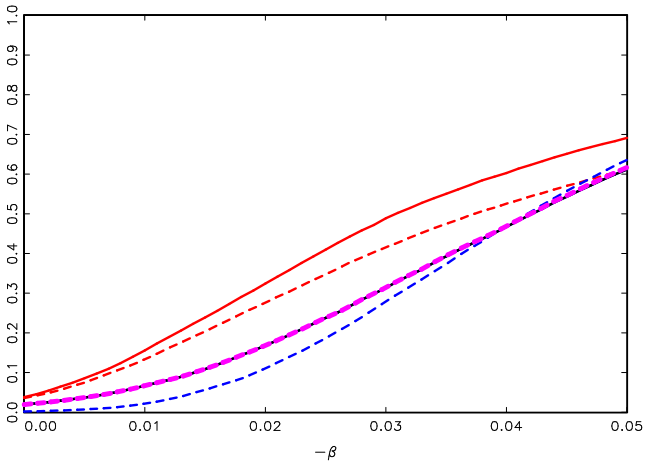

t_{μ}^{OLS}: – –, Q_{μ}^{GLS}: ——, t_{τ}^{OLS}: – –, Q_{τ}^{GLS}: ——, U^{hyb}: ——, S^{hyb}: – –

Figure S.73: Finite Power of Left-Tailed Tests. DGP (1)-(3) with $c = -5$, $\delta = -0.75$ and $\kappa = \{0.0, 0.2, 0.4, 0.6, 0.8, 1.0\}$, where c, κ and δ are the local-to-unity AR, local-to-zero trend, and endogeneity correlation parameters, respectively.

(a) $\kappa = 0.0$

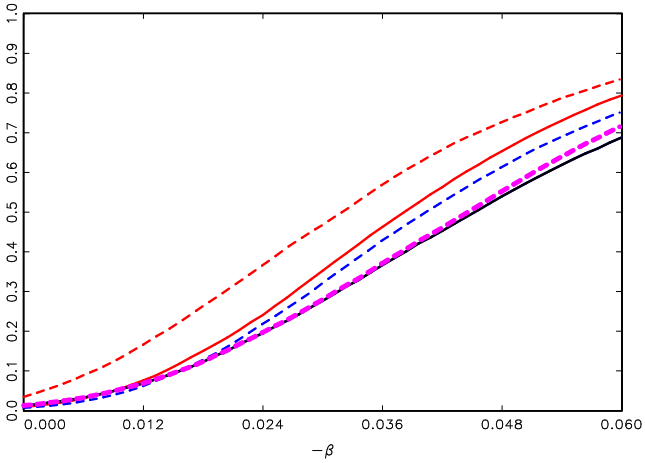

(b) $\kappa = 0.2$

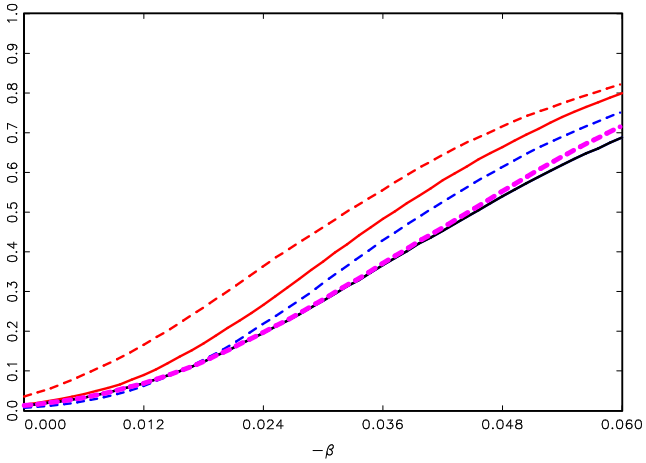

(c) $\kappa = 0.4$

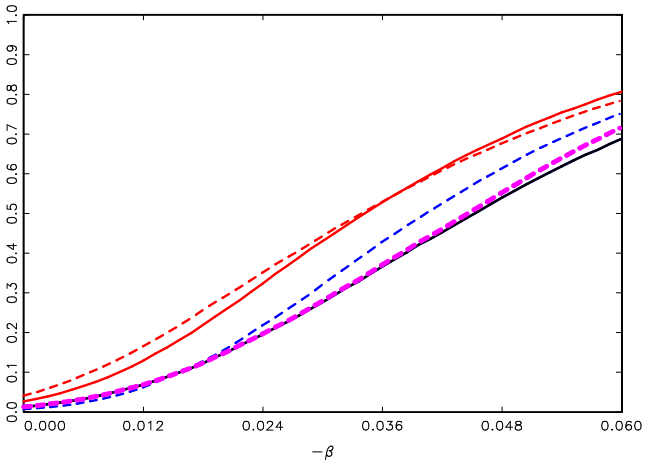

(d) $\kappa = 0.6$

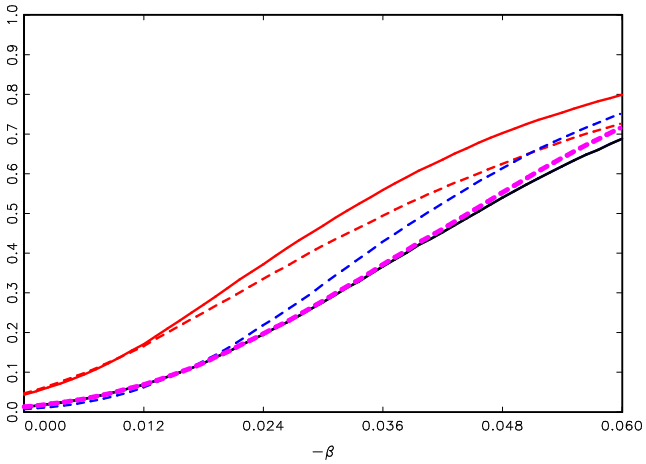

(e) $\kappa = 0.8$

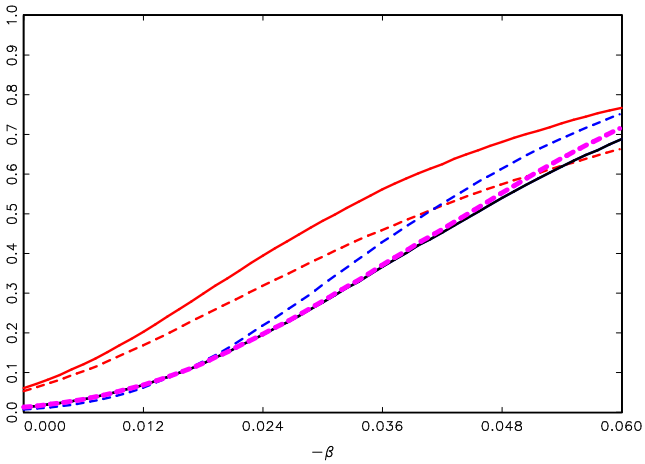

(f) $\kappa = 1.0$

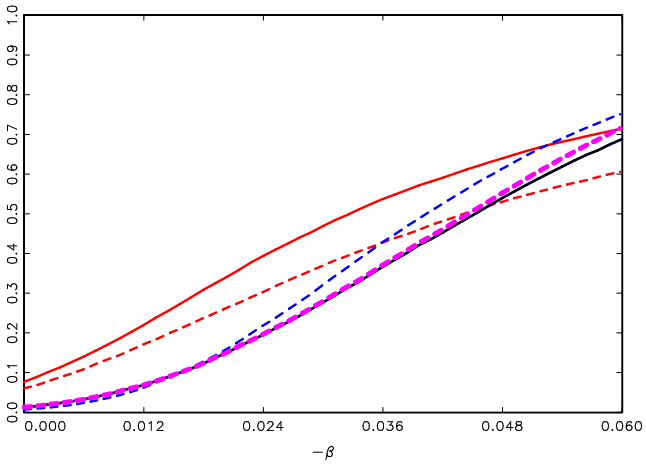

t_{μ}^{OLS}: – –, Q_{μ}^{GLS}: ——, t_{τ}^{OLS}: – –, Q_{τ}^{GLS}: ——, U^{hyb}: ——, S^{hyb}: – –

Figure S.74: Finite Power of Left-Tailed Tests. DGP (1)-(3) with $c = -10$, $\delta = -0.75$ and $\kappa = \{0.0, 0.2, 0.4, 0.6, 0.8, 1.0\}$, where c, κ and δ are the local-to-unity AR, local-to-zero trend, and endogeneity correlation parameters, respectively.

(a) $\kappa = 0.0$

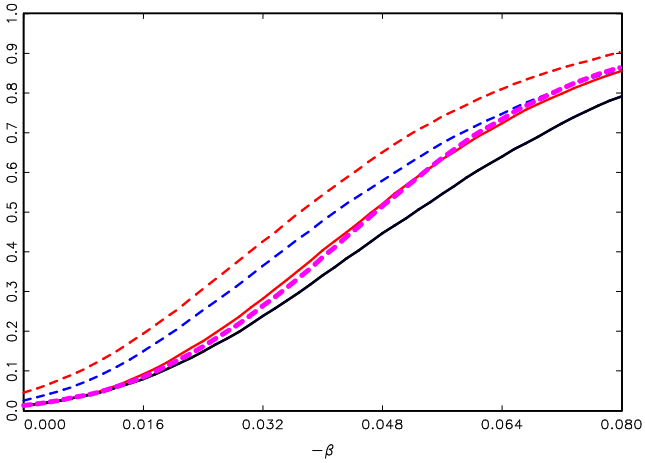

(b) $\kappa = 0.2$

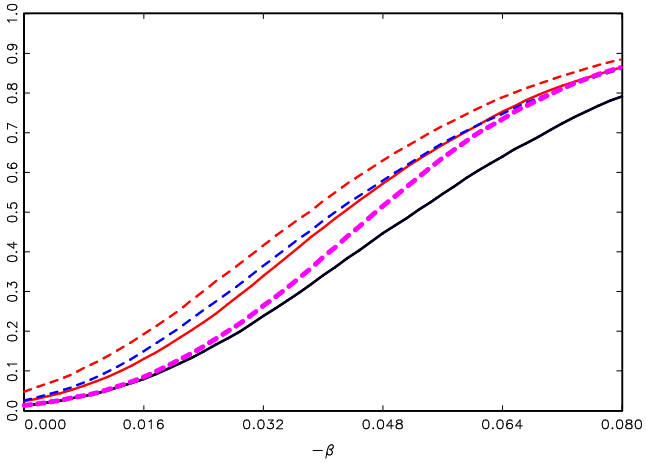

(c) $\kappa = 0.4$

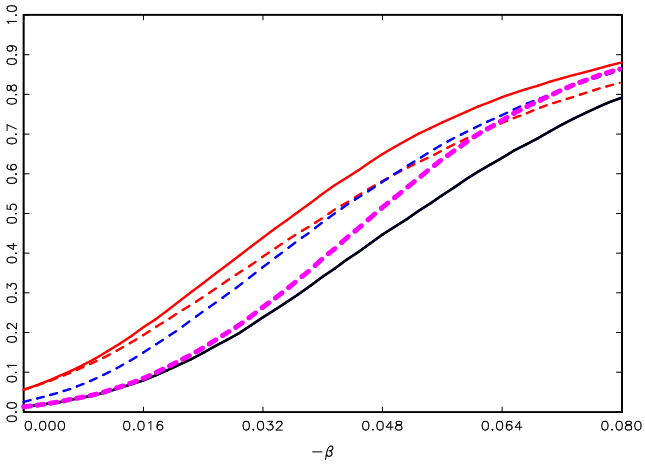

(d) $\kappa = 0.6$

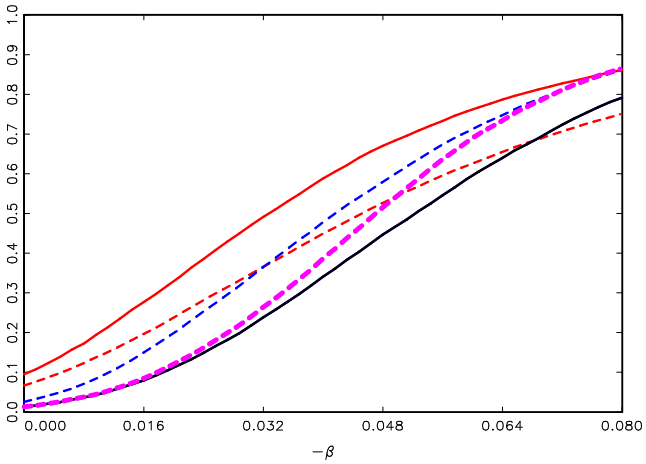

(e) $\kappa = 0.8$

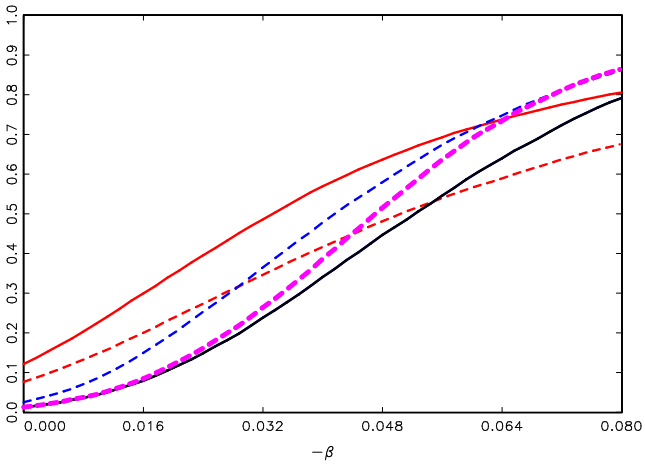

(f) $\kappa = 1.0$

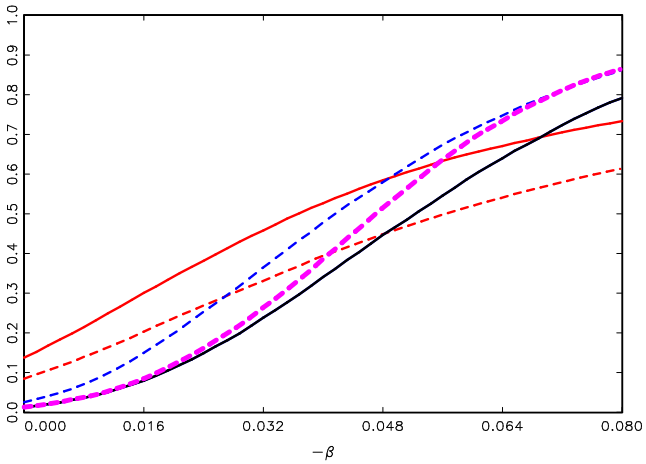

t_{μ}^{OLS}: – –, Q_{μ}^{GLS}: ——, t_{τ}^{OLS}: – –, Q_{τ}^{GLS}: ——, U^{hyb}: ——, S^{hyb}: – –

Figure S.75: Finite Power of Left-Tailed Tests. DGP (1)-(3) with $c = -20$, $\delta = -0.75$ and $\kappa = \{0.0, 0.1, 0.2, 0.3, 0.4, 0.5\}$, where c, κ and δ are the local-to-unity AR, local-to-zero trend, and endogeneity correlation parameters, respectively.

(a) $\kappa = 0.0$

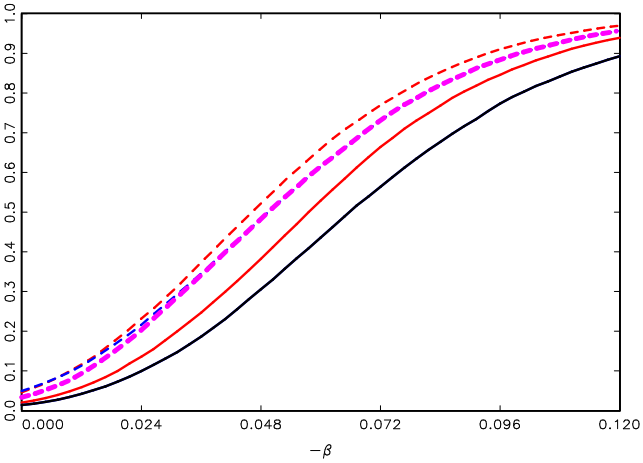

(b) $\kappa = 0.1$

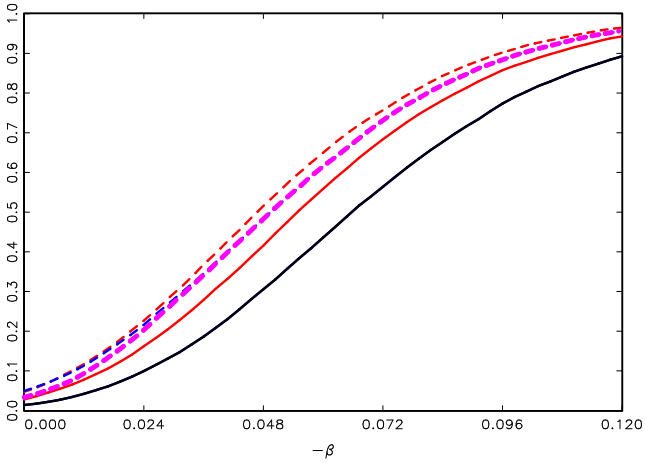

(c) $\kappa = 0.2$

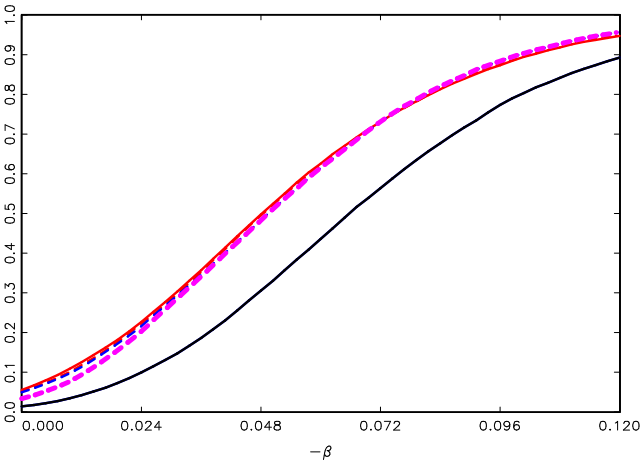

(d) $\kappa = 0.3$

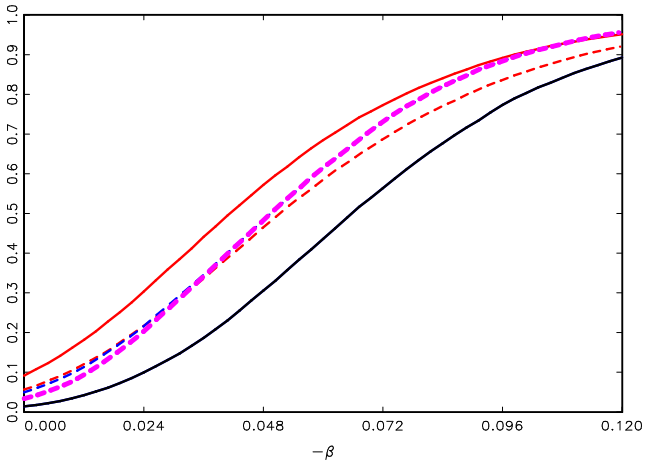

(e) $\kappa = 0.4$

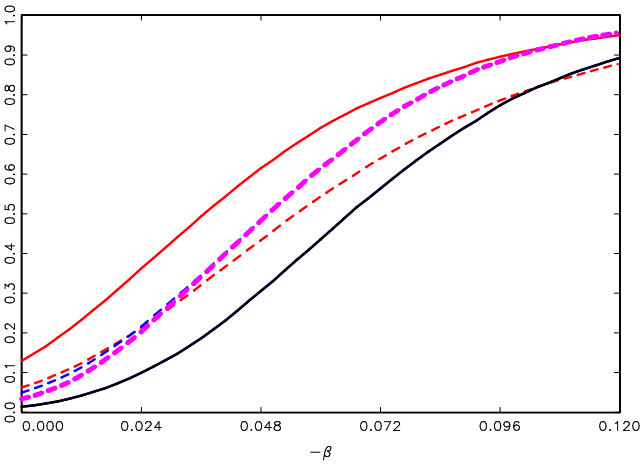

(f) $\kappa = 0.5$

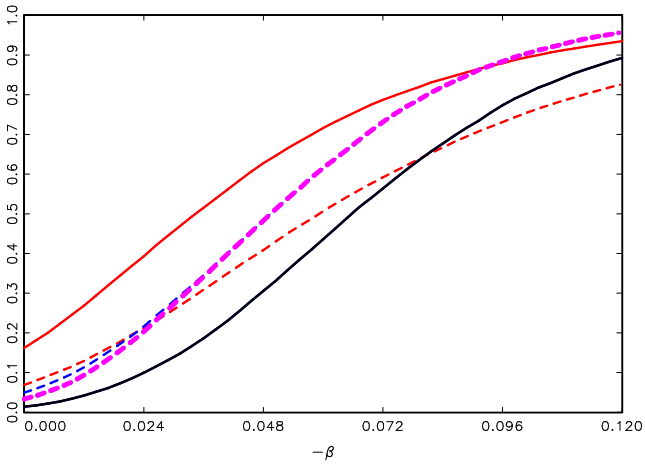

t_μ^{OLS}: – –, Q_μ^{GLS}: ——, t_τ^{OLS}: – –, Q_τ^{GLS}: ——, U^{hyb}: ——, S^{hyb}: – –

Figure S.76: Finite Power of Left-Tailed Tests. DGP (1)-(3) with $c = -30$, $\delta = -0.75$ and $\kappa = \{0.0, 0.1, 0.2, 0.3, 0.4, 0.5\}$, where c, κ and δ are the local-to-unity AR, local-to-zero trend, and endogeneity correlation parameters, respectively.

(a) $\kappa = 0.0$

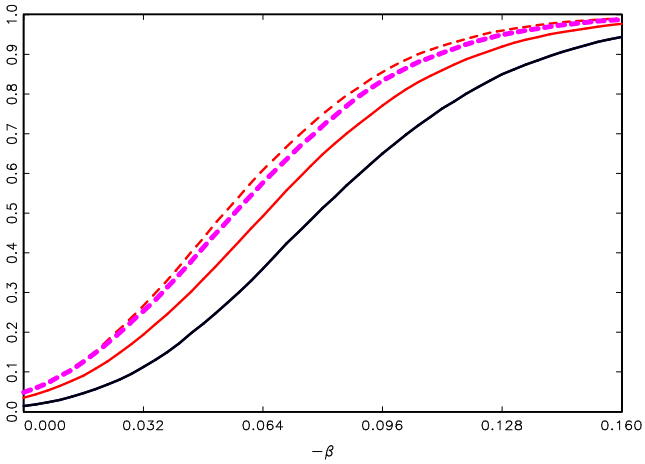

(b) $\kappa = 0.1$

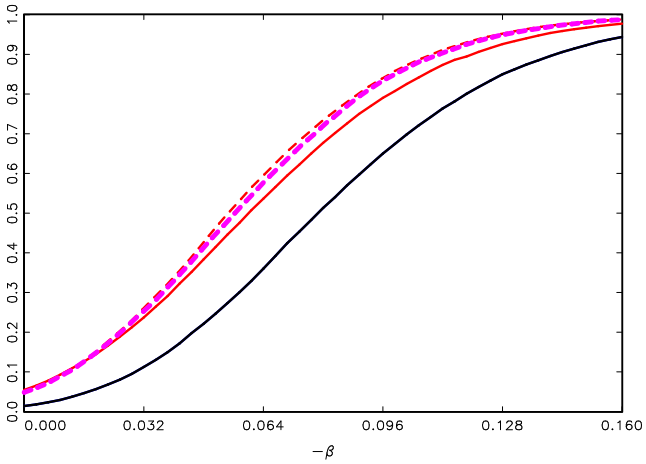

(c) $\kappa = 0.2$

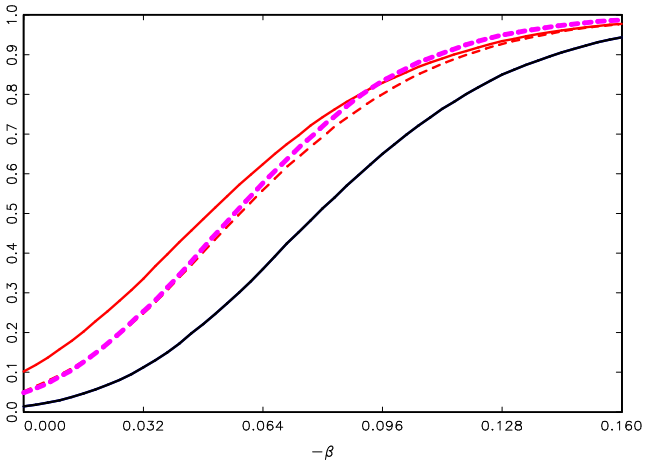

(d) $\kappa = 0.3$

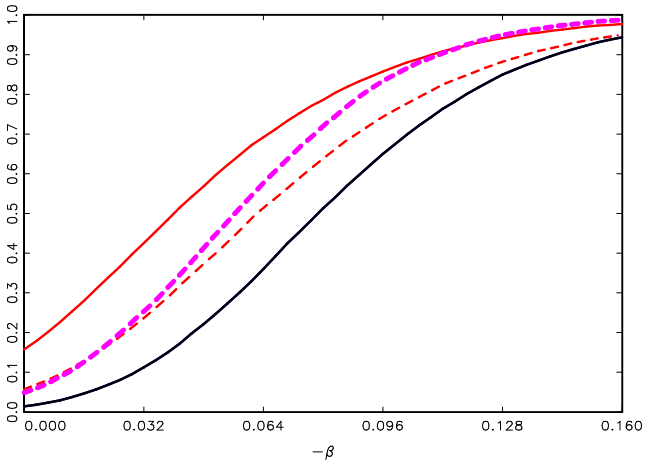

(e) $\kappa = 0.4$

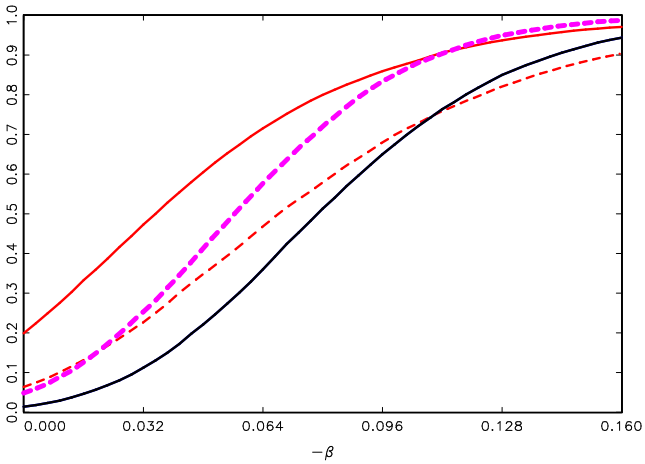

(f) $\kappa = 0.5$

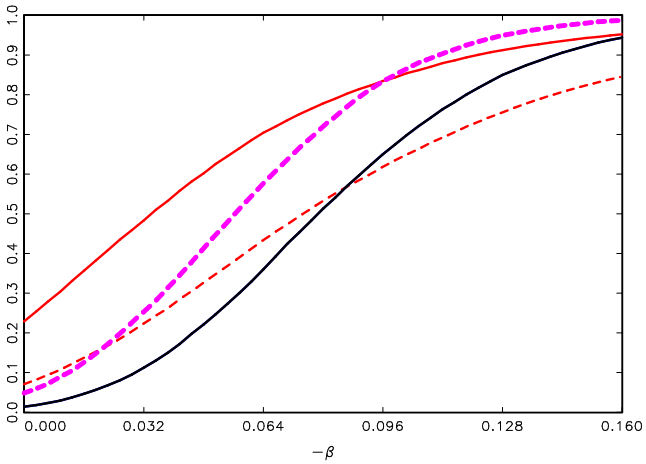

t_{μ}^{OLS}: – –, Q_{μ}^{GLS}: ——, t_{τ}^{OLS}: – –, Q_{τ}^{GLS}: ——, U^{hyb}: ——, S^{hyb}: – –

Figure S.77: Finite Power of Left-Tailed Tests. DGP (1)-(3) with $c = -40$, $\delta = -0.75$ and $\kappa = \{0.0, 0.1, 0.2, 0.3, 0.4, 0.5\}$, where c, κ and δ are the local-to-unity AR, local-to-zero trend, and endogeneity correlation parameters, respectively.

(a) $\kappa = 0.0$

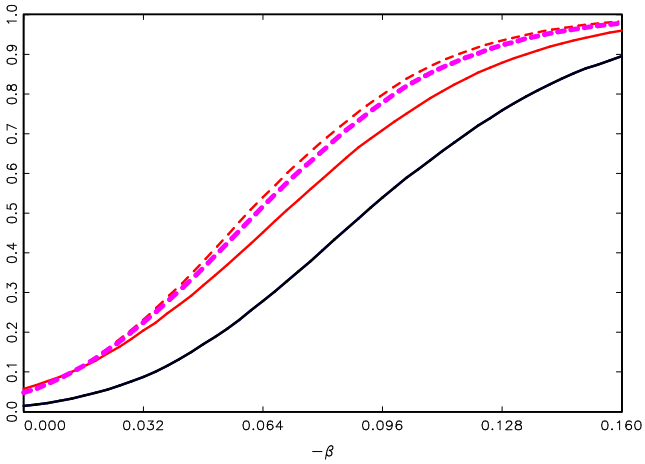

(b) $\kappa = 0.1$

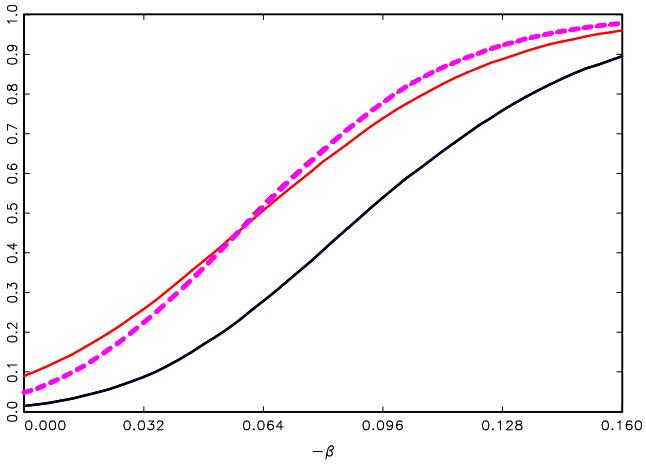

(c) $\kappa = 0.2$

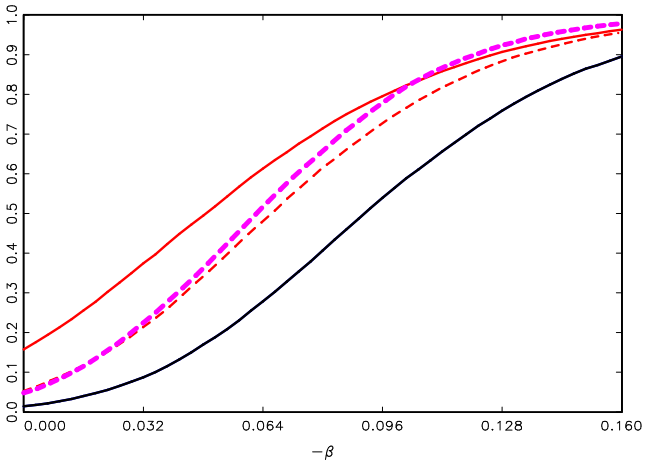

(d) $\kappa = 0.3$

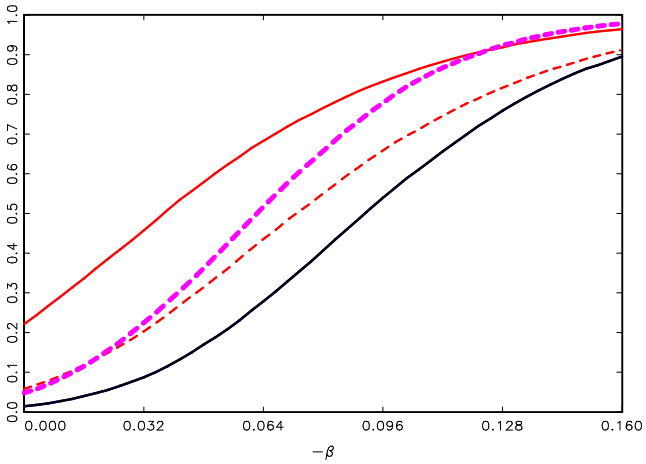

(e) $\kappa = 0.4$

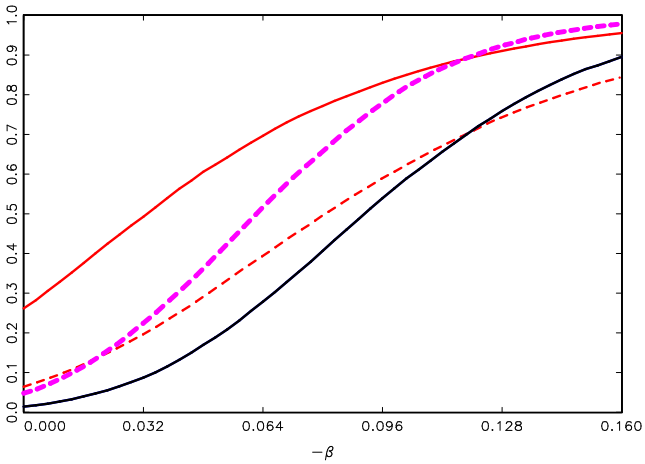

(f) $\kappa = 0.5$

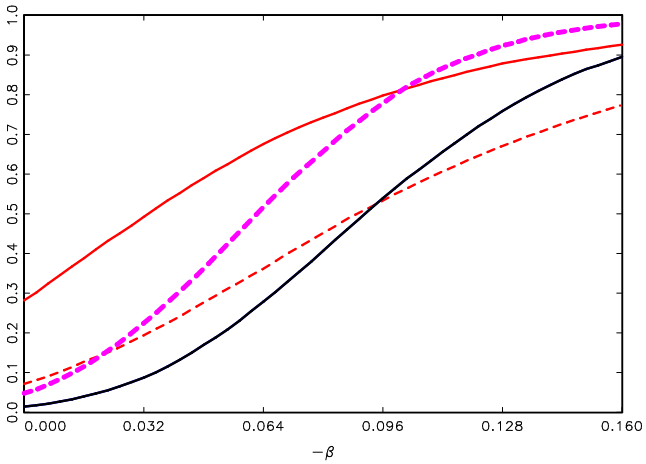

t_{μ}^{OLS}: – –, Q_{μ}^{GLS}: ——, t_{τ}^{OLS}: – –, Q_{τ}^{GLS}: ——, U^{hyb}: ——, S^{hyb}: – –

Figure S.78: Finite Power of Left-Tailed Tests. DGP (1)-(3) with $c = -50$, $\delta = -0.75$ and $\kappa = \{0.0, 0.1, 0.2, 0.3, 0.4, 0.5\}$, where c, κ and δ are the local-to-unity AR, local-to-zero trend, and endogeneity correlation parameters, respectively.

(a) $\kappa = 0.0$

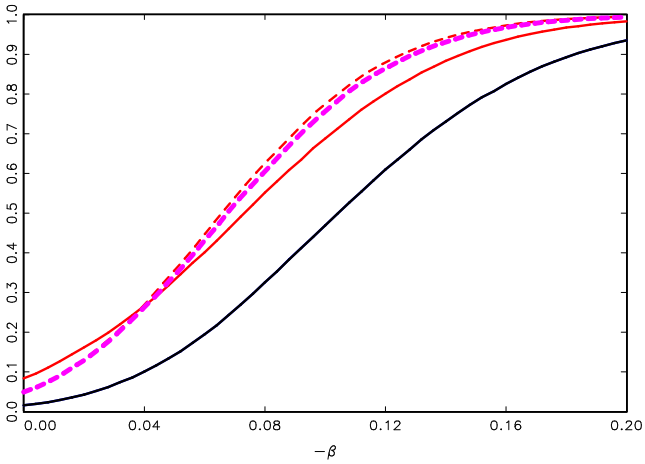

(b) $\kappa = 0.1$

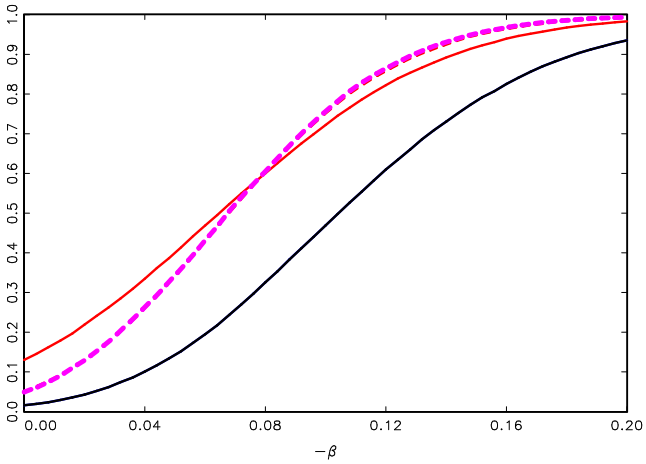

(c) $\kappa = 0.2$

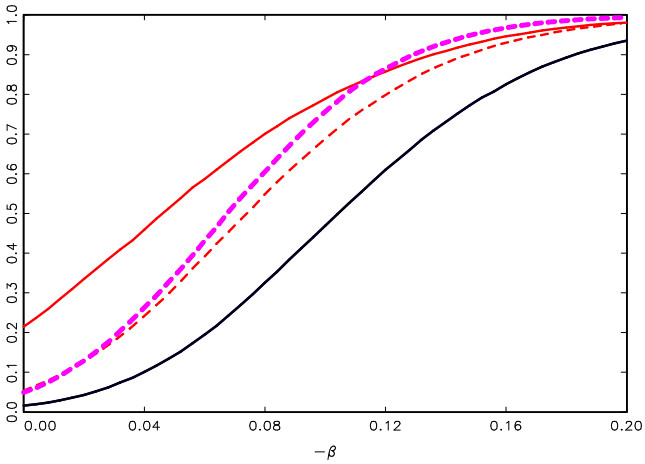

(d) $\kappa = 0.3$

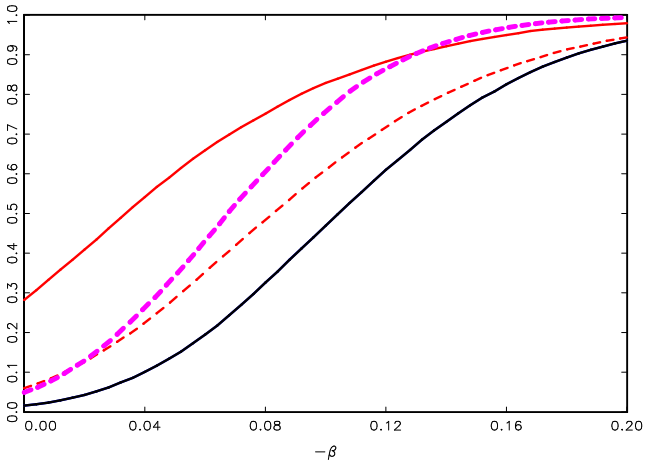

(e) $\kappa = 0.4$

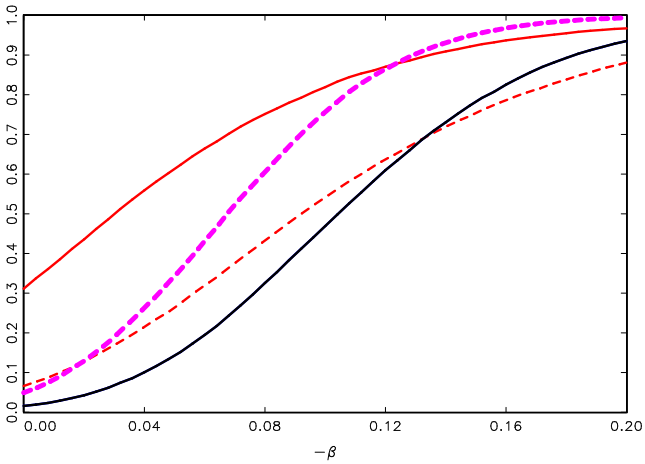

(f) $\kappa = 0.5$

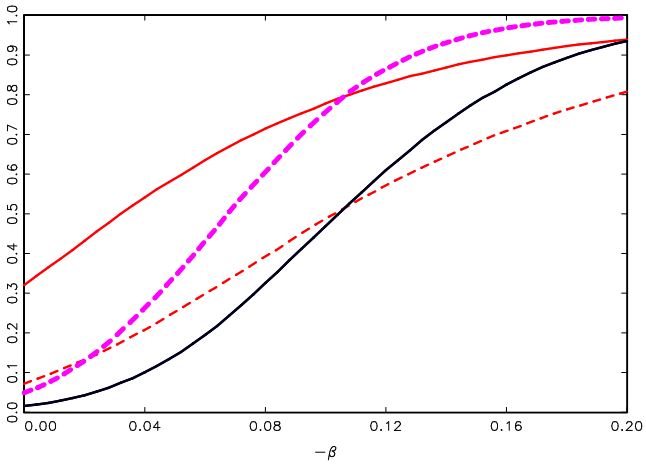

t_{μ}^{OLS}: – – , Q_{μ}^{GLS}: ——— , t_{τ}^{OLS}: – –, Q_{τ}^{GLS}: ———, U^{hyb}: ———, S^{hyb}: – –

Figure S.79: Finite Power of Left-Tailed Tests. DGP (1)-(3) with $c = -100$, $\delta = -0.75$ and $\kappa = \{0.0, 0.1, 0.2, 0.3, 0.4, 0.5\}$, where c, κ and δ are the local-to-unity AR, local-to-zero trend, and endogeneity correlation parameters, respectively.

(a) $\kappa = 0.0$

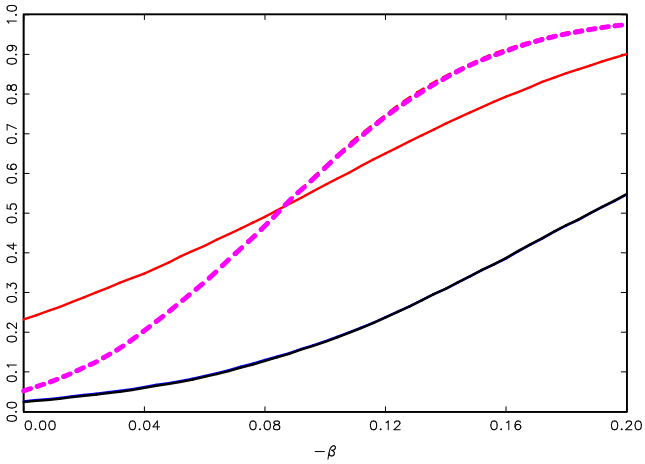

(b) $\kappa = 0.1$

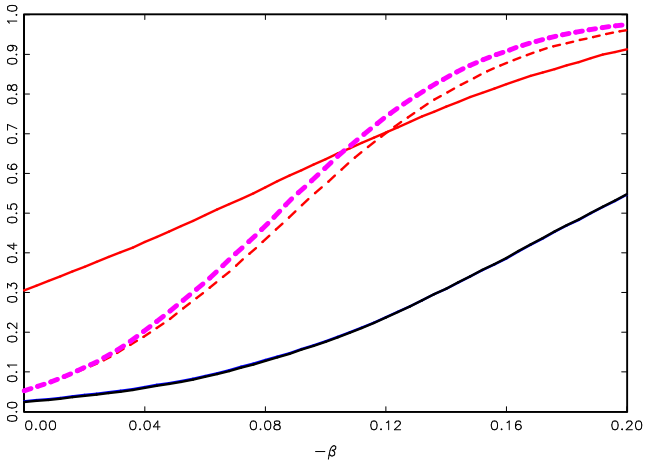

(c) $\kappa = 0.2$

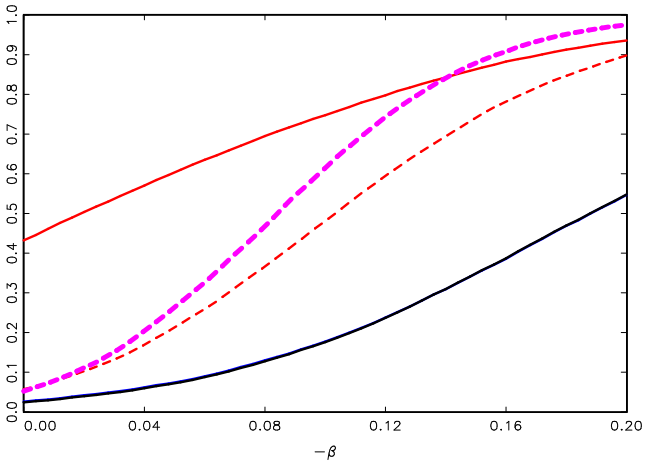

(d) $\kappa = 0.3$

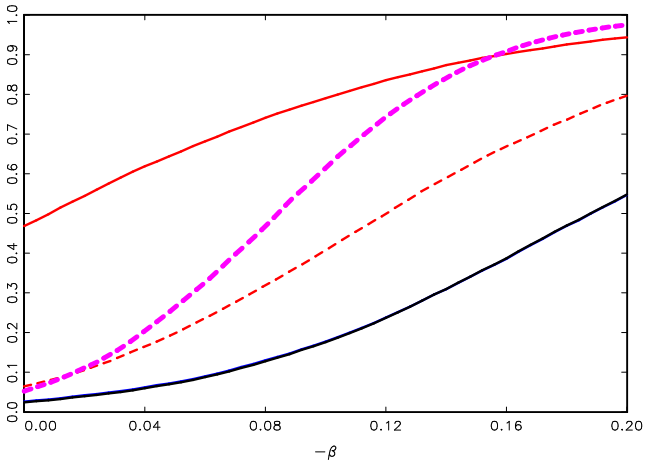

(e) $\kappa = 0.4$

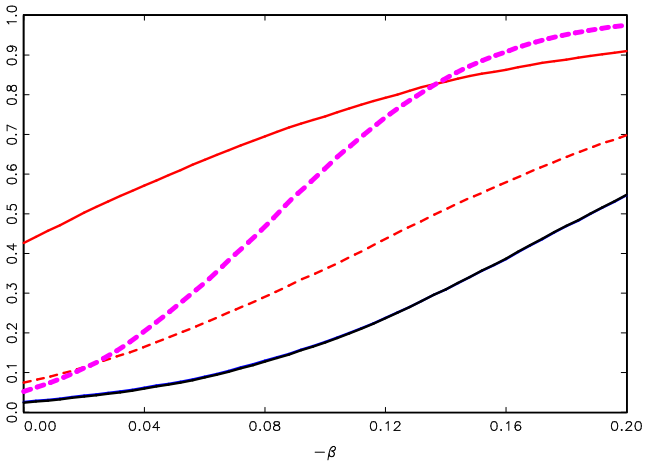

(f) $\kappa = 0.5$

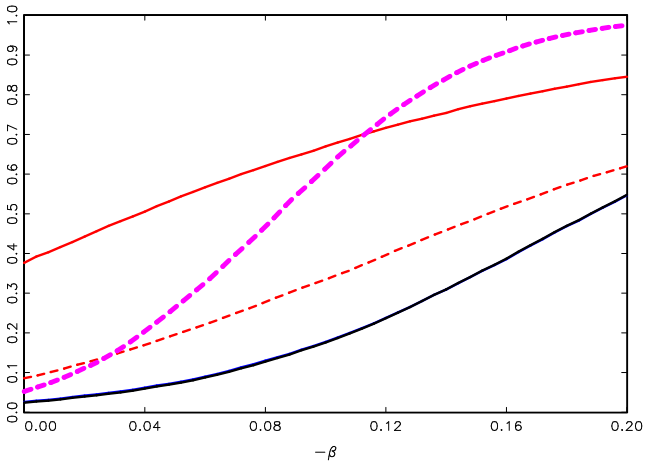

t_{μ}^{OLS}: – – , Q_{μ}^{GLS}: ——— , t_{τ}^{OLS}: – –, Q_{τ}^{GLS}: ———, U^{hyb}: ———, S^{hyb}: – –

Figure S.80: Finite Power of Left-Tailed Tests. DGP (1)-(3) with $c = -250$, $\delta = -0.75$ and $\kappa = \{0.0, 0.1, 0.2, 0.3, 0.4, 0.5\}$, where c, κ and δ are the local-to-unity AR, local-to-zero trend, and endogeneity correlation parameters, respectively.

(a) $\kappa = 0.0$

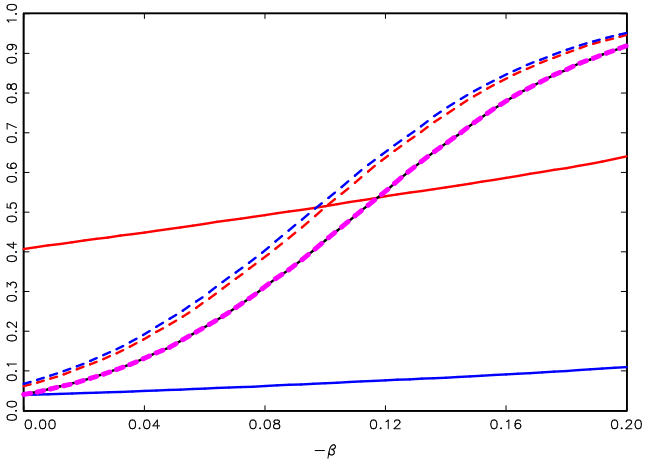

(b) $\kappa = 0.1$

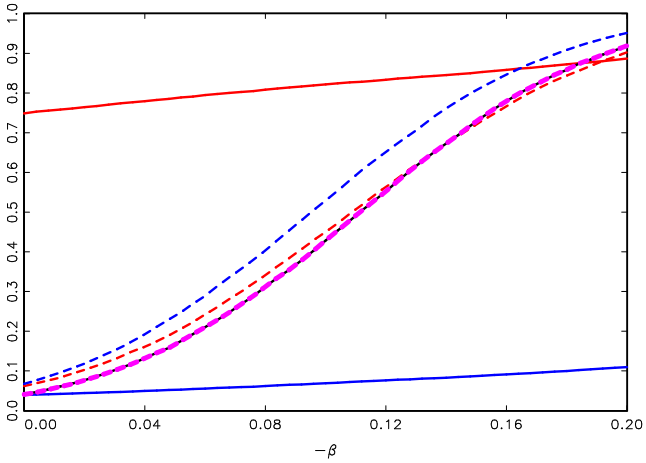

(c) $\kappa = 0.2$

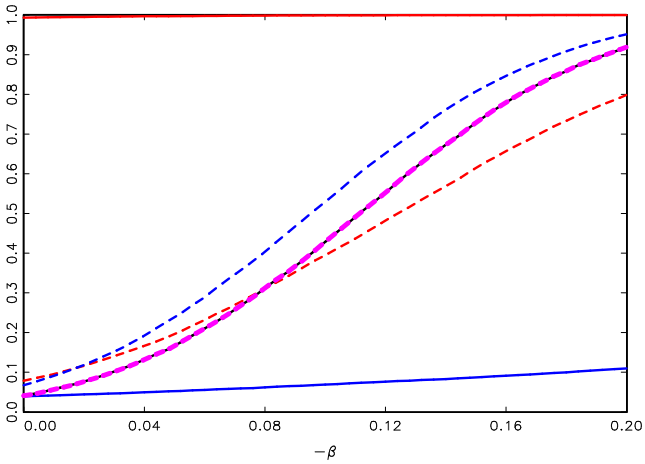

(d) $\kappa = 0.3$

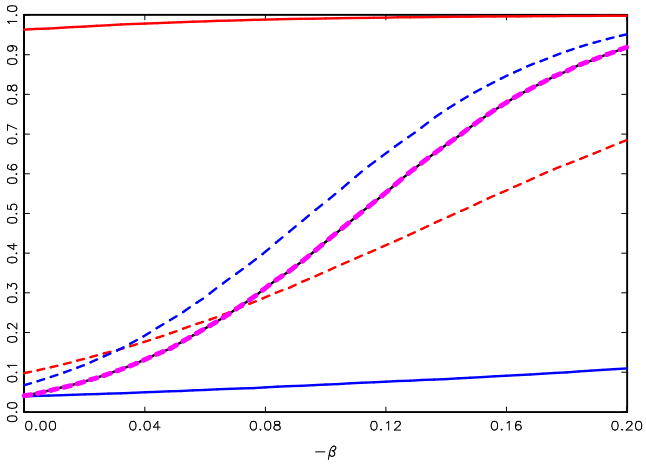

(e) $\kappa = 0.4$

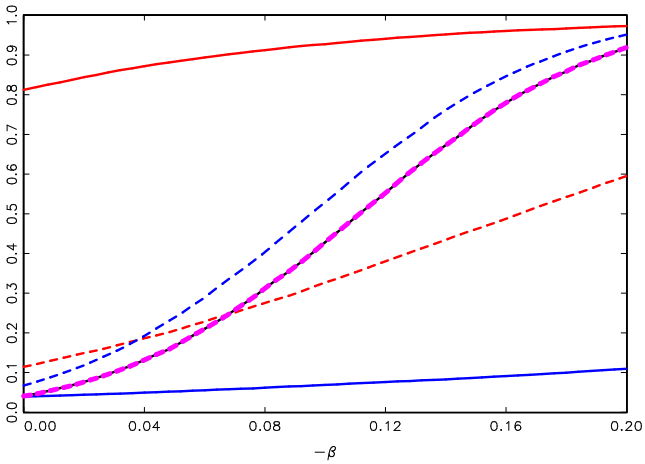

(f) $\kappa = 0.5$

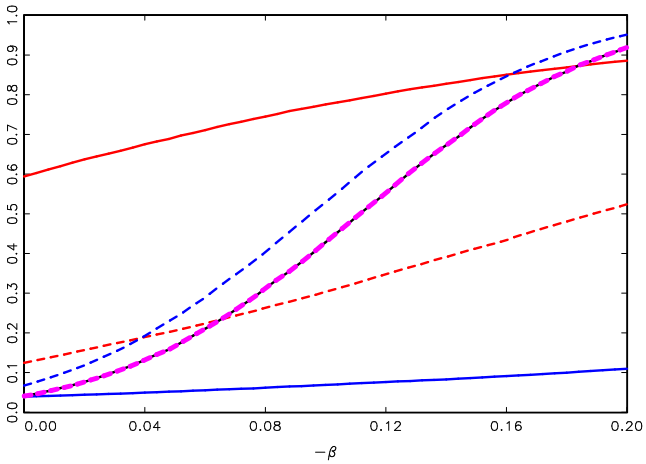

t_{μ}^{OLS}: – – , Q_{μ}^{GLS}: ——— , t_{τ}^{OLS}: – –, Q_{τ}^{GLS}: ———, U^{hyb}: ———, S^{hyb}: – –

Figure S.81: Finite Power of Right-Tailed Tests. DGP (1)-(3) with $c = 2$, $\delta = -0.95$ and $\kappa = \{0.0, 0.2, 0.4, 0.6, 0.8, 1.0\}$, where c, κ and δ are the local-to-unity AR, local-to-zero trend, and endogeneity correlation parameters, respectively.

(a) $\kappa = 0.0$

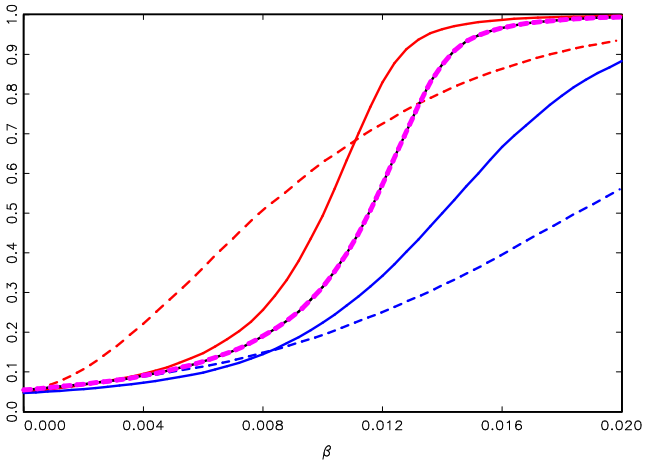

(b) $\kappa = 0.2$

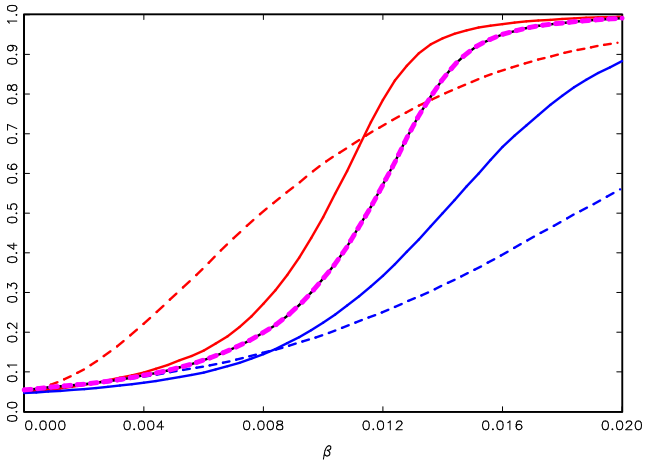

(c) $\kappa = 0.4$

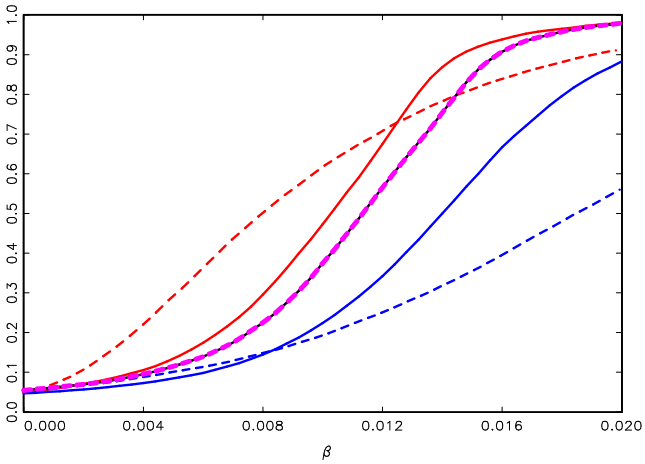

(d) $\kappa = 0.6$

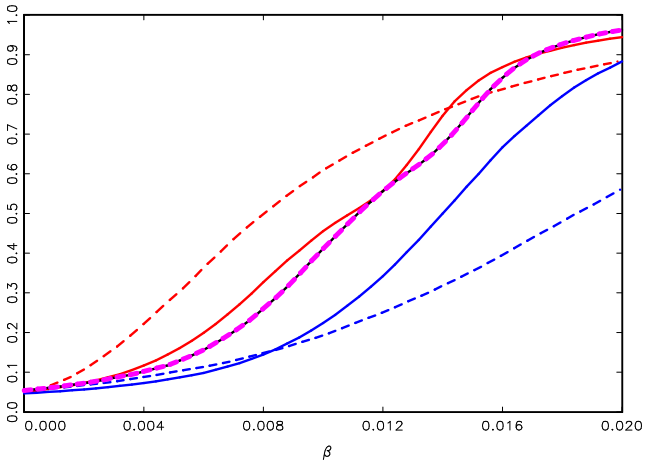

(e) $\kappa = 0.8$

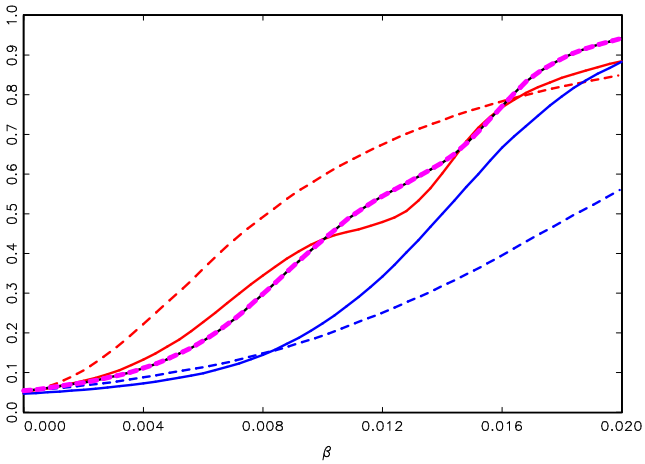

(f) $\kappa = 1.0$

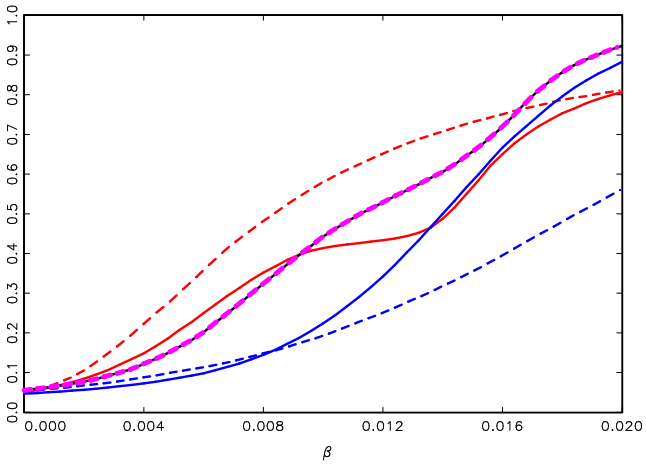

t_{μ}^{OLS}: – –, Q_{μ}^{GLS}: ——, t_{τ}^{OLS}: – –, Q_{τ}^{GLS}: ——, U^{hyb}: ——, S^{hyb}: – –

Figure S.82: Finite Power of Right-Tailed Tests. DGP (1)-(3) with $c = 2$, $\delta = -0.75$ and $\kappa = \{0.0, 0.2, 0.4, 0.6, 0.8, 1.0\}$, where c, κ and δ are the local-to-unity AR, local-to-zero trend, and endogeneity correlation parameters, respectively.

(a) $\kappa = 0.0$

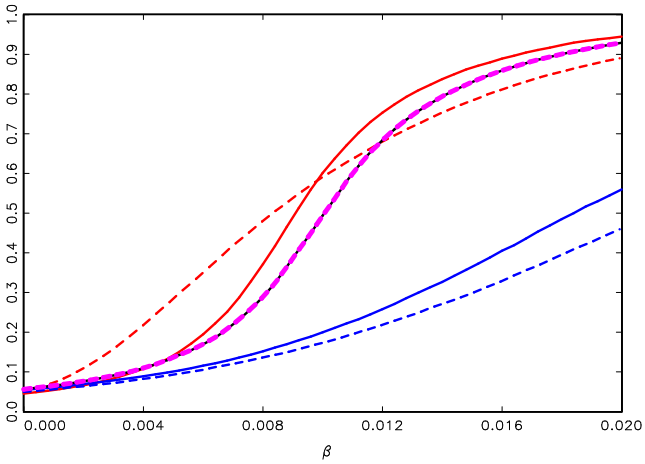

(b) $\kappa = 0.2$

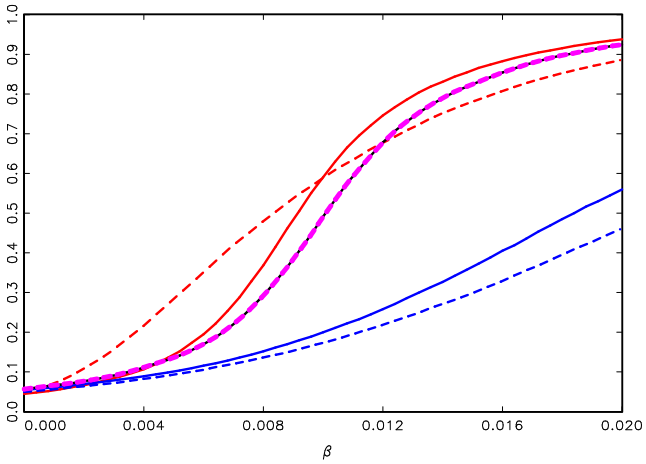

(c) $\kappa = 0.4$

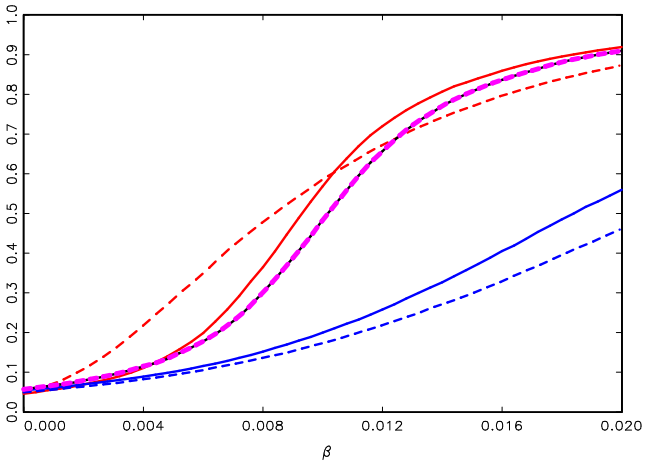

(d) $\kappa = 0.6$

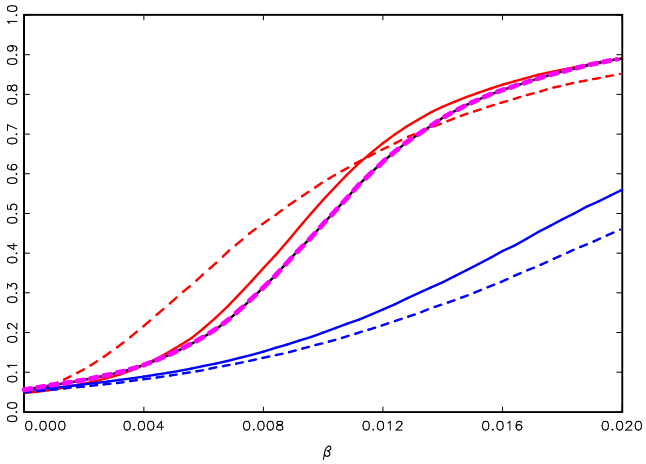

(e) $\kappa = 0.8$

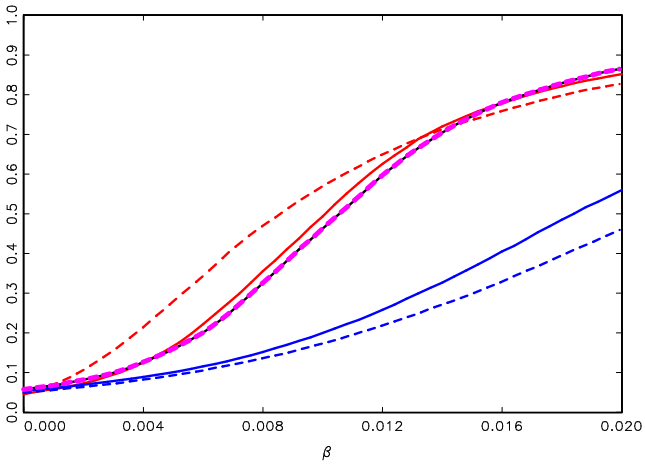

(f) $\kappa = 1.0$

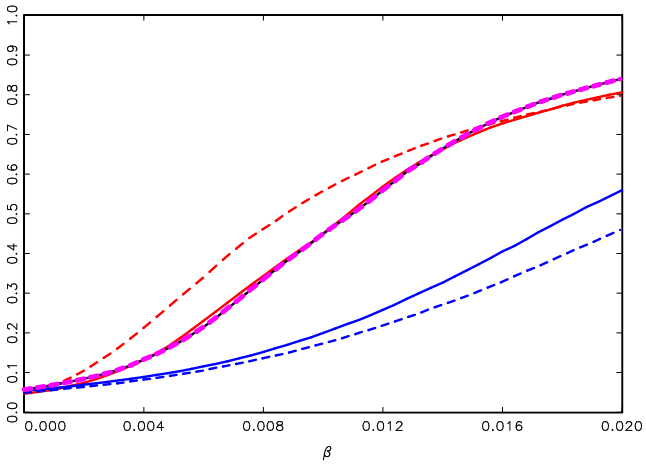

t_{μ}^{OLS}: – –, Q_{μ}^{GLS}: ——, t_{τ}^{OLS}: – –, Q_{τ}^{GLS}: ——, U^{hyb}: ——, S^{hyb}: – –

Figure S.83: Finite Power of Left-Tailed Tests. DGP (1)-(3) with $c = 2$, $\delta = -0.95$ and $\kappa = \{0.0, 0.2, 0.4, 0.6, 0.8, 1.0\}$, where c, κ and δ are the local-to-unity AR, local-to-zero trend, and endogeneity correlation parameters, respectively.

(a) $\kappa = 0.0$

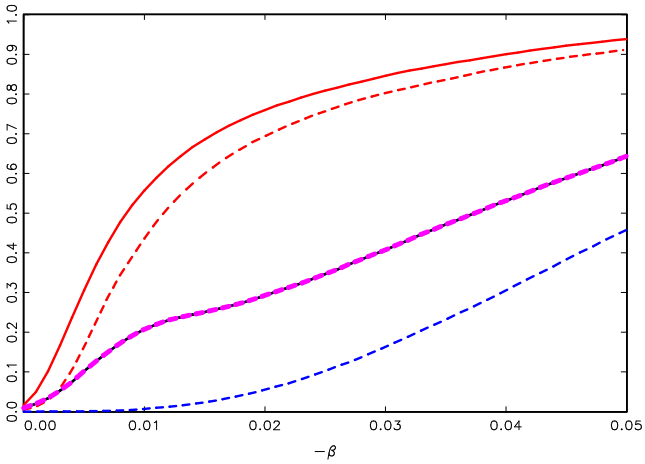

(b) $\kappa = 0.2$

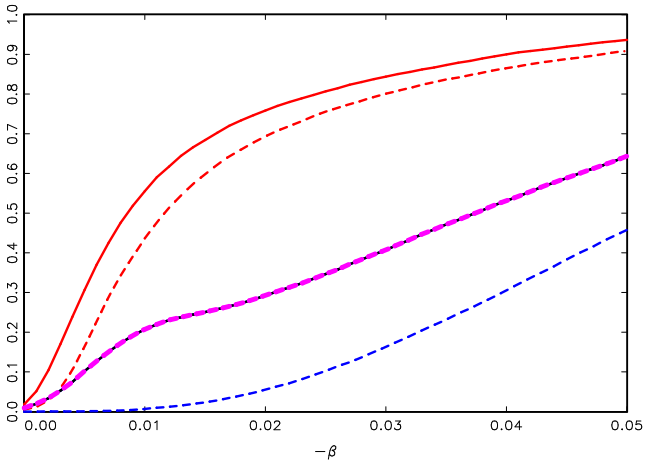

(c) $\kappa = 0.4$

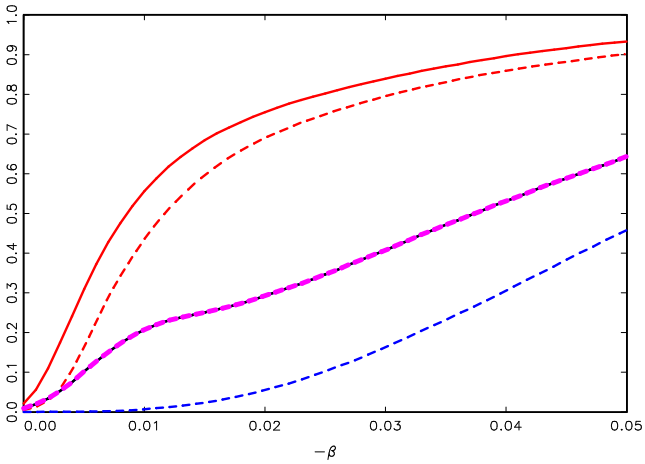

(d) $\kappa = 0.6$

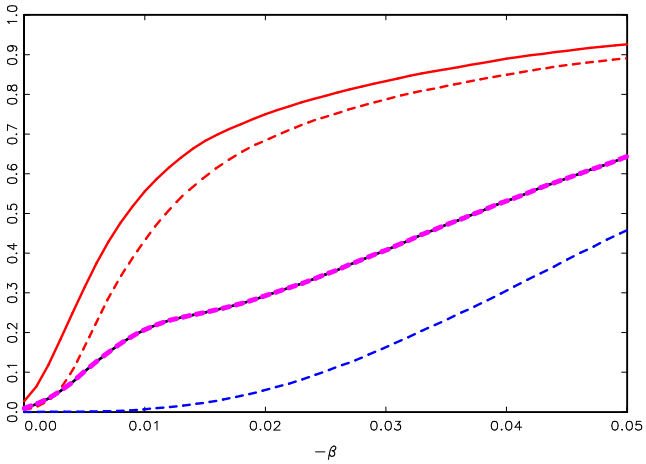

(e) $\kappa = 0.8$

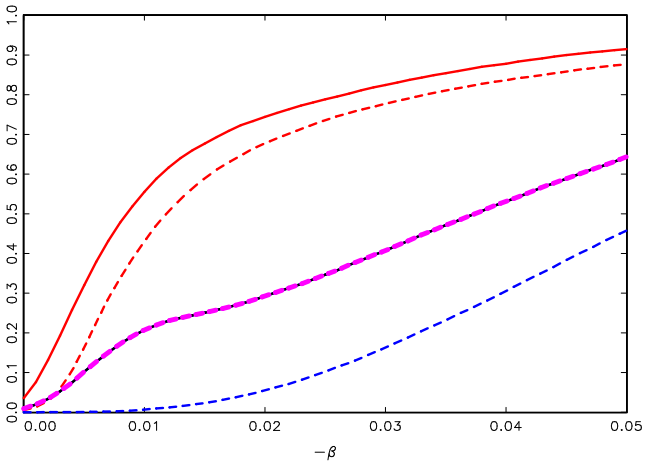

(f) $\kappa = 1.0$

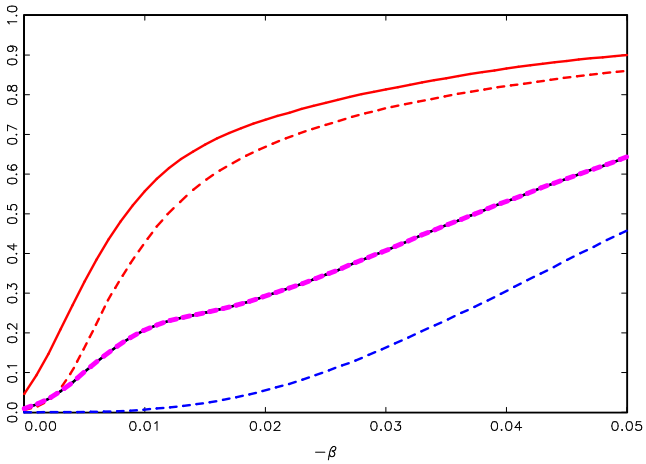

t_{μ}^{OLS}: – –, Q_{μ}^{GLS}: ——, t_{τ}^{OLS}: – –, Q_{τ}^{GLS}: ——, U^{hyb}: ——, S^{hyb}: – –

Figure S.84: Finite Power of Left-Tailed Tests. DGP (1)-(3) with $c = 2$, $\delta = -0.75$ and $\kappa = \{0.0, 0.2, 0.4, 0.6, 0.8, 1.0\}$, where c, κ and δ are the local-to-unity AR, local-to-zero trend, and endogeneity correlation parameters, respectively.

(a) $\kappa = 0.0$

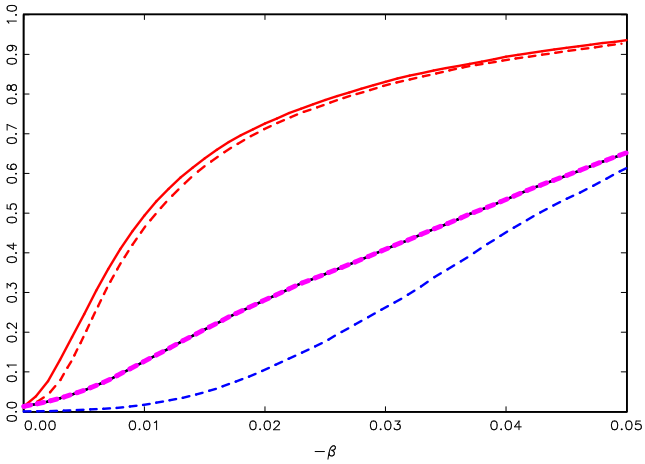

(b) $\kappa = 0.2$

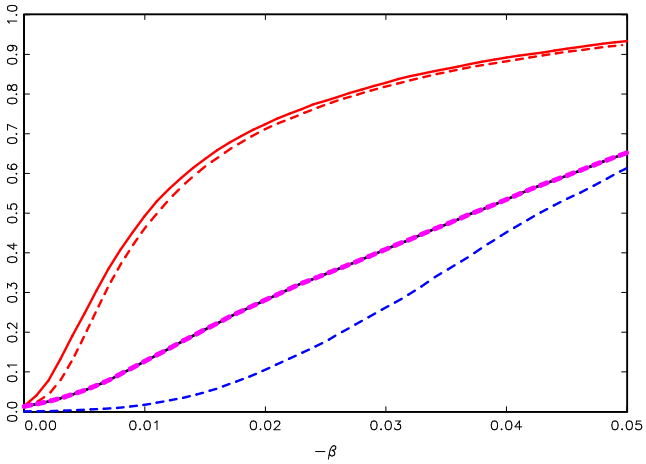

(c) $\kappa = 0.4$

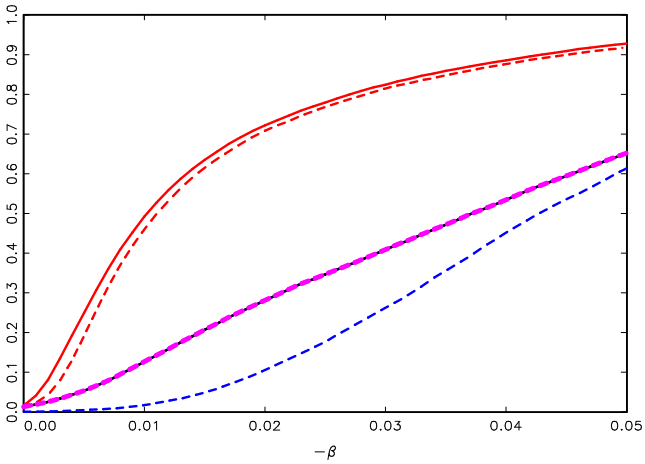

(d) $\kappa = 0.6$

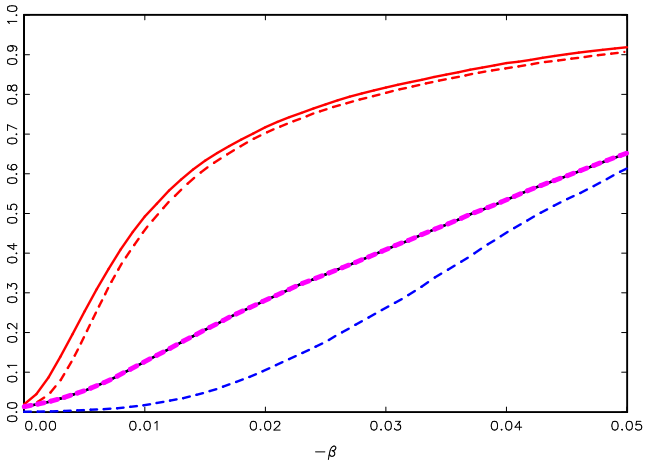

(e) $\kappa = 0.8$

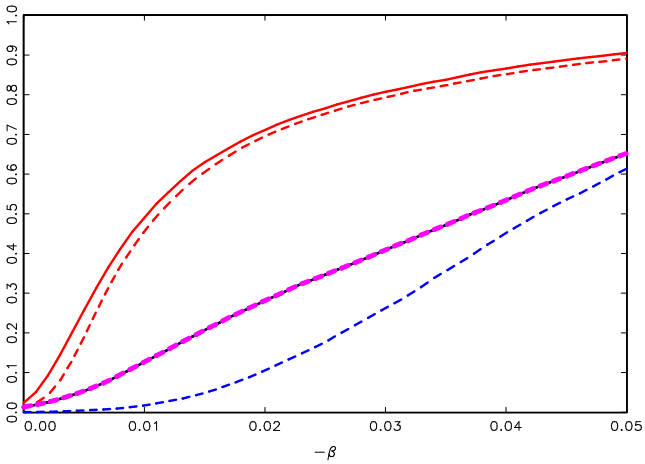

(f) $\kappa = 1.0$

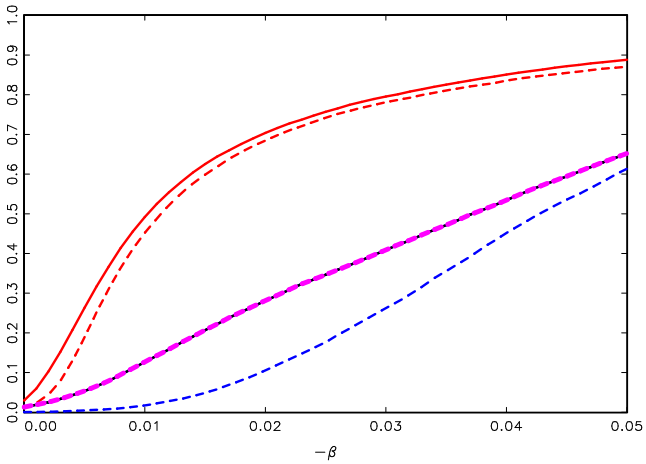

t_{μ}^{OLS}: – –, Q_{μ}^{GLS}: ——, t_{τ}^{OLS}: – –, Q_{τ}^{GLS}: ——, U^{hyb}: ——, S^{hyb}: – –